

Effect of Rotational Base Stiffness on the Behaviour of Loadbearing Masonry Walls

by

Clayton Edward James Pettit

A thesis submitted in partial fulfillment of the requirements for the degree of

Master of Science

in

STRUCTURAL ENGINEERING

Department of Civil and Environmental Engineering
University of Alberta

© Clayton Edward James Pettit, 2020

ABSTRACT

Slender, loadbearing masonry walls are typically used in low-rise commercial and industrial settings, as they are an efficient system to resist out-of-plane (OOP) and gravity loads. Masonry walls are usually built upon concrete footings, with their first course mortared upon the concrete surface, and their reinforcement is spliced to dowels cast into the foundation. Despite the inherent rotational stiffness of this type of connection, when the walls are slender (height-to-thickness ratio > 30) North American codes instruct the designer to assume a pinned condition at the base, neglecting any rotational stiffness provided by the foundation. This results in an underestimation of the capacity of the wall. The goal of this research is to (1) quantify the reactive rotational stiffness at the support for typical foundations used in masonry construction, (2) assess the increase in loadbearing capacity provided by the foundation stiffness, and (3) determine the effect of the foundation stiffness on critical aspects of the structural response of the walls, such as stiffness, ultimate capacity, and failure modes. Overall, it is expected that this research will lead to a better understanding of the OOP behaviour of slender masonry walls accounting for the presence of the foundation in a rational manner.

To achieve these goals, the research was divided into two steps. The first step comprised a full-scale experimental program in which a total of four identical wall specimens were tested under a combination of OOP and gravity loads. Each specimen featured a unique rotational support stiffness, determined through the evaluation of common foundation geometries and soil properties. Data acquired from the experimental program was then

used to evaluate the effect of rotational support stiffness on the flexural stiffness, the failure modes, and the ultimate load capacity of the walls.

The second step of the research consisted of the numerical modelling of all four wall specimens and of experimental results obtained from similar studies. An analysis model based on the differential equation that governs the displacement of elastic beam-columns subjected to axial and distributed lateral loads was used to investigate the response of the walls including the presence of the foundation. The model accounts for material and geometric nonlinearities through a fibre-section approach. Specimens from multiple experimental programs were simulated using the model with the predicted results showing a good agreement with experimental findings in terms of load-displacement response, failure modes and load capacity. Applications of the model are presented, and the limitations discussed.

To all who come to this happy place; welcome.

- Walt Disney

DEDICATION

To my loving parents, Ron and Marie Pettit:

Thank you for all of the support you have given me throughout the years. I would not be where I am today without your unconditional love and kindness.

ACKNOWLEDGEMENTS

I would like to thank my supervisor, Dr. Lobo, whose support and friendship guided me throughout this research project. I would like to also thank Dr. Mark Hagel, whose technical guidance proved invaluable.

A special thanks to the University of Alberta lab technicians Greg Miller and Cameron West, whose help in the Structural Lab was invaluable throughout the project.

Funding for this research has been provided in part by Mitacs, Alberta Masonry Council (AMC), the Masonry Contractors Association of Alberta (MCAA), Mirko Ambrozic, Norman and Tess Reid, and the University of Alberta.

TABLE OF CONTENTS

1	INTRODUCTION	1
1.1	Background	1
1.2	Problem Statement	3
1.3	Objectives, Methods, and Scope	4
1.4	Organization of Thesis	5
2	LITERATURE REVIEW	7
2.1	Introduction	7
2.2	Experimental Programs	9
2.3	Numerical and Finite Element Modelling	17
2.4	Flexural Rigidity	24
3	EXPERIMENTAL PROGRAM.....	30
3.1	Introduction.....	30
3.2	Numerical Estimation of Rotational Support Stiffness.....	30
3.2.1	OpenSEES Finite Element Model for Strip Footing Foundations.....	31
3.2.2	Support Stiffness Assessment.....	32
3.3	Test Specimens	34
3.4	Material Properties	37
3.4.1	Mortar	37
3.4.2	Grout	38
3.4.3	Masonry Assemblage.....	38
3.4.4	Reinforcing Steel	43
3.4.5	Predicted Ultimate Moment Capacity	43

3.5	Experimental Setup	44
3.5.1	Lateral Bracing System.....	46
3.5.2	Gravity and Lateral Load Application.....	48
3.5.3	Simulation of Base Rotational Stiffness	49
3.6	Instrumentation	51
3.7	Testing Procedure	53
3.8	Results and Observations	55
3.8.1	Test 1 (Rotational Stiffness = 0 kNm/rad).....	56
3.8.2	Test 2 (Rotational Stiffness = 2,300 kNm/rad).....	60
3.8.3	Test 3 (Rotational Stiffness = 5,000 kNm/rad).....	63
3.8.4	Test 4 (Rotational Stiffness = 9,500 kNm/rad).....	66
3.9	Discussion of Results	69
3.9.1	Lateral Load–Midspan Displacement.....	69
3.9.2	Lateral Load–Base Rotation	74
3.9.3	Second-Order Effects.....	75
3.9.4	Moment Magnification Factor.....	78
3.9.5	Total Moment Profile	79
3.9.6	Deflection Profile.....	87
3.9.7	Summary.....	92
4	MECHANICS-BASED ANALYSIS MODEL FOR LOADBEARING MASONRY WALLS	94
4.1	Introduction.....	94
4.2	Formulation.....	94
4.3	Moment–Curvature Relationship.....	98

4.4	Material Models	99
4.4.1	Masonry	99
4.4.2	Reinforcing Steel	100
4.5	Failure Modes	101
4.6	Model Implementation.....	101
4.7	Model Limitations.....	103
4.8	Validation.....	104
4.8.1	Study 1: Slender walls without a base stiffness subjected to a monotonic lateral load (SEASC 1982)	104
4.8.1.1	Experimental Setup	104
4.8.1.2	Masonry properties.....	105
4.8.1.3	Results	106
4.8.2	Study 2: Slender walls with a base stiffness subjected to a monotonic gravity load (Mohsin 2003)	115
4.8.2.1	Experimental Setup	115
4.8.2.2	Masonry Assemblage	116
4.8.2.3	Results	117
4.8.3	Study 3: Non-slender walls with a base stiffness subjected to a cyclic lateral load	122
4.9	Discussion	125
4.10	Application – Slenderness Interaction Diagrams.....	126
4.11	Summary	129
5	CONCLUSIONS AND RECOMMENDATIONS	130
5.1	Summary	130

5.2	Conclusions.....	131
5.3	Recommendations and Future Research.....	132
	REFERENCES	134
	APPENDIX A: ROTATIONAL SUPPORT STIFFNESS PROVIDED BY A VARIETY OF FOUNDATIONS.....	137
	APPENDIX B: MECHANICS-BASED MODEL MATLAB CODE.....	182

LIST OF TABLES

Table 3.1 – Modulus of Subgrade for Various Soils	32
Table 3.2 – Numerically Determined Support Stiffness.....	33
Table 3.3 – Mortar Cube Data	38
Table 3.4 – Grout Cylinder Data	38
Table 3.5 – 2-Course Hollow Prism Data.....	41
Table 3.6 – 2-Course Grouted Prism Data.....	41
Table 3.7 – 5-Course Hollow Prism Data.....	42
Table 3.8 – 5-Course Grouted Prism Data.....	42
Table 3.9 – Single 20-cm Unit Data	42
Table 3.10 – Masonry Assemblage Properties Summary.....	43
Table 3.11 – Steel Rebar Properties	43
Table 3.12 – Ultimate Moment Capacity of the Wall Specimens	44
Table 3.13 – Simulated Rotational Stiffness	51
Table 3.14 – LVDT Locations.....	52
Table 3.15 – Lateral Loading Protocol	54
Table 3.16 – Summary of Test Results.....	55
Table 3.17 – Relative Increase in Lateral Load Capacity.....	72
Table 3.18 – Midspan Moment Composition at Failure.....	76
Table 3.19 – Moment Magnification Factor.....	79
Table 4.1 – Masonry Wall Panel Summary (SEASC 1982).....	105
Table 4.2 – Masonry Material Properties (SEASC 1982)	105
Table 4.3 – Reinforcing Steel Properties (SEASC 1982).....	106

Table 4.4 – Test Specimen Summary (Mohsin 2003)	117
Table 4.5 – Masonry Material Properties (Mohsin 2003)	117
Table 4.6 – Reinforcing Steel Properties (Mohsin 2003)	117
Table 4.7 – Peak Lateral Load Comparison	123
Table 4.8 – Example Wall Section Properties	126
Table 4.9 – Maximum Applied Moment for a Standard Wall.....	127
Table 4.10 – Comparison of Moment Magnification Factors	128

LIST OF FIGURES

Figure 2.1 – Reinforced Masonry Wall (Minaie et al. 2009)	7
Figure 2.2 – Wall Test Specimens (Cranston and Roberts 1976).....	11
Figure 2.3 – Simulated Support Stiffness (Mohsin 2005)	15
Figure 2.4 – Experimental Setup (Liu and Hu 2007)	16
Figure 2.5 – Newmark’s Numerical Procedure (Muqtadir 1991).....	19
Figure 2.6 – Homogenization of Masonry Material (Ma et al. 2001)	21
Figure 2.7 – Stress Distribution on a Wall Cross-Section (Liu and Dawe 2003).....	22
Figure 3.1 – Shallow Strip Footing Foundation	31
Figure 3.2 – Finite Element Foundation Model a) Prior to Analysis b) During Analysis	32
Figure 3.3 – Specimen Cross-Section.....	34
Figure 3.4 – Specimen Profile	35
Figure 3.5 – Specimen Construction (Bond Beams)	35
Figure 3.6 – Specimen Construction (Bed Joint Reinforcement).....	36
Figure 3.7 – Completed Specimens	37
Figure 3.8 – 5-Course (Hollow and Grouted) and 2-Course Grouted Masonry Prisms .	40
Figure 3.9 – 2 Course Hollow Masonry Prisms	40
Figure 3.10 – Out-of-Plane Experimental Setup (Without Rotational Stiffness).....	44
Figure 3.11 – Out-of-Plane Experimental Setup (With Rotational Stiffness).....	45
Figure 3.12 – In-Plane Experimental Setup.....	45
Figure 3.13 – Experimental Setup	46
Figure 3.14 – Bottom Lateral Bracing Fixture	47

Figure 3.15 – Top Lateral Bracing Fixture	47
Figure 3.16 – Adjustable Threaded Rods	48
Figure 3.17 – Gravity Load Application.....	48
Figure 3.18 – Lateral Load Application	49
Figure 3.19 – Simulation of Base Rotational Stiffness.....	50
Figure 3.20 – Simulated Support Stiffness FE Model.....	50
Figure 3.21 – Instrumentation.....	52
Figure 3.22 – Strain Gauge Locations	53
Figure 3.23 – Cyclic Loading Protocol.....	54
Figure 3.24 – Effective Specimen Height.....	56
Figure 3.25 – Lateral Load–Midspan Displacement Response (Specimen 1).....	57
Figure 3.26 – Lateral Load–Base Rotation Response (Specimen 1)	57
Figure 3.27 – Total Moment Profiles (Specimen 1)	58
Figure 3.28 – Deflection Profiles (Specimen 1)	58
Figure 3.29 – First Signs of Failure (Specimen 1).....	59
Figure 3.30 – Failure (Specimen 1)	59
Figure 3.31 – Lateral Load–Midspan Displacement Response (Specimen 2).....	60
Figure 3.32 – Lateral Load–Base Rotation Response (Specimen 2)	61
Figure 3.33 – Total Moment Profiles (Specimen 2)	61
Figure 3.34 – Deflection Profiles (Specimen 2)	62
Figure 3.35 – Failure (Specimen 2)	62
Figure 3.36 – Lateral Load–Midspan Displacement Response (Specimen 3).....	63
Figure 3.37 – Lateral Load–Base Rotation Response (Specimen 3)	64

Figure 3.38 – Total Moment Profiles (Specimen 3)	64
Figure 3.39 – Deflection Profiles (Specimen 3)	65
Figure 3.40 – Failure (Specimen 3)	65
Figure 3.41 – Lateral Load–Midspan Displacement Response (Specimen 4).....	66
Figure 3.42 – Lateral Load–Base Rotation Response (Specimen 4).....	67
Figure 3.43 – Total Moment Profiles (Specimen 4)	67
Figure 3.44 – Deflection Profiles (Specimen 4)	68
Figure 3.45 – Failure (Specimen 4)	68
Figure 3.46 – Backbone Lateral Load–Midspan Displacement Comparison.....	70
Figure 3.47 – Moment Redistribution of a Point Lateral Load	70
Figure 3.48 – Moment Redistribution of an Eccentric Axial Load	71
Figure 3.49 – Total Moment Profile of the Wall Specimens at the Same Lateral Load (35 kN)	71
Figure 3.50 – Typical Specimen Response to Cyclic Loading.....	74
Figure 3.51 – Base Rotation Comparison.....	75
Figure 3.52 – Total Moment Composition at Failure (Specimen 1).....	76
Figure 3.53 – Total Moment Composition at Failure (Specimen 2).....	77
Figure 3.54 – Total Moment Composition at Failure (Specimen 3).....	77
Figure 3.55 – Total Moment Composition at Failure (Specimen 4).....	78
Figure 3.56 – Total Moment Profile (5-mm Cycle)	79
Figure 3.57 – Total Moment Profiles (10-mm Cycle).....	80
Figure 3.58 – Total Moment Profile (15-mm Cycle)	80
Figure 3.59 – Total Moment Profiles (20-mm Cycle).....	81
Figure 3.60 – Total Moment Profile (30-mm Cycle)	81

Figure 3.61 – Total Moment Profile (40-mm Cycle)	82
Figure 3.62 – Total Moment Profile (50-mm Cycle)	82
Figure 3.63 – Total Moment Profiles (Failure)	83
Figure 3.64 – Effect of Base Stiffness on Total Moment Profile	84
Figure 3.65 – Moment Profile Development of Specimen 2 (Pre-Peak Load)	86
Figure 3.66 – Moment Profile Development of Specimen 2 (Peak Load)	86
Figure 3.67 – Moment Profile Development of Specimen 2 (Failure).....	87
Figure 3.68 – Deflection Profiles (5-mm Cycle).....	88
Figure 3.69 – Deflection Profiles (10-mm Cycle).....	89
Figure 3.70 – Deflection Profiles (15-mm Cycle).....	89
Figure 3.71 – Deflection Profiles (20-mm Cycle).....	90
Figure 3.72 – Deflection Profiles (30-mm Cycle).....	90
Figure 3.73 – Deflection Profiles (40-mm Cycle).....	91
Figure 3.74 – Deflection Profiles (50-mm Cycle).....	91
Figure 3.75 – Deflection Profiles (Failure).....	92
Figure 4.1 – Deflection Curves for Masonry Walls	95
Figure 4.2 – a) External and b) Internal Moments.....	97
Figure 4.3 – Moment and Curvature at Failure	99
Figure 4.4 – Behaviour of Masonry under Compression	100
Figure 4.5 – Behaviour of Masonry under Tension (Wahalathantri et al. 2011).....	100
Figure 4.6 – Behaviour of Reinforcing Steel.....	101
Figure 4.7 – Iteration of Initial Slope	102
Figure 4.8 – Analysis Model Process	103

Figure 4.9 – ACI-SEASC Experimental Setup (ACI-SEASC 1982)	104
Figure 4.10 – Analysis Model Force Equilibrium (Axial Load < Masonry Tensile Force)	107
Figure 4.11 – Analysis Model Moment Composition (Axial Load < Masonry Tensile Force).....	108
Figure 4.12 – Analysis Model Force Equilibrium (Axial Load > Masonry Tensile Force)	108
Figure 4.13 – Analysis Model Moment Composition (Axial Load > Masonry Tensile Force).....	109
Figure 4.14 – Moment-Curvature Response.....	110
Figure 4.15 – Comparison of Analytical Model Prediction to Results of SEASC Experiment (Panel 1, $h/t = 31$, Base Stiffness = 0 kNm/rad)	111
Figure 4.16 – Comparison of Analytical Model Prediction to Results of SEASC Experiment (Panel 2, $h/t = 31$, Base Stiffness = 0 kNm/rad)	111
Figure 4.17 – Comparison of Analytical Model Prediction to Results of SEASC Experiment (Panel 3, $h/t = 31$, Base Stiffness = 0 kNm/rad)	112
Figure 4.18 – Comparison of Analytical Model Prediction to Results of SEASC Experiment (Panel 4, $h/t = 39$, Base Stiffness = 0 kNm/rad)	112
Figure 4.19 – Comparison of Analytical Model Prediction to Results of SEASC Experiment (Panel 5, $h/t = 39$, Base Stiffness = 0 kNm/rad)	113
Figure 4.20 – Comparison of Analytical Model Prediction to Results of SEASC Experiment (Panel 6, $h/t = 39$, Base Stiffness = 0 kNm/rad)	113
Figure 4.21 – Comparison of Analytical Model Prediction to Results of SEASC Experiment (Panel 7, $h/t = 51$, Base Stiffness = 0 kNm/rad)	114
Figure 4.22 – Comparison of Analytical Model Prediction to Results of SEASC Experiment (Panel 8, $h/t = 51$, Base Stiffness = 0 kNm/rad)	114

Figure 4.23 – Comparison of Analytical Model Prediction to Results of SEASC Experiment (Panel 9, $h/t = 51$, Base Stiffness = 0 kNm/rad)	115
Figure 4.24 – Mohsin Experimental Setup (Mohsin 2003)	116
Figure 4.25 – Specimen Cross-Section (Mohsin 2003).....	116
Figure 4.26 – Comparison of Analytical Model Prediction to Results of Mohsin Experiment (W1, $h/t = 29$, Base Stiffness = 0 kNm/rad)	118
Figure 4.27 – Comparison of Analytical Model Prediction to Results of Mohsin Experiment (W2, $h/t = 29$, Base Stiffness = 1,000 kNm/rad)	119
Figure 4.28 – Comparison of Analytical Model Prediction to Results of Mohsin Experiment (W3, $h/t = 29$, Base Stiffness = 5,000 kNm/rad)	119
Figure 4.29 – Comparison of Analytical Model Prediction to Results of Mohsin Experiment (W4, $h/t = 29$, Base Stiffness = 10,000 kNm/rad)	120
Figure 4.30 – Comparison of Analytical Model Prediction to Results of Mohsin Experiment (W5, $h/t = 34$, Base Stiffness = 0 kNm/rad)	120
Figure 4.31 – Comparison of Analytical Model Prediction to Results of Mohsin Experiment (W6, $h/t = 34$, Base Stiffness = 1,000 kNm/rad)	121
Figure 4.32 – Comparison of Analytical Model Prediction to Results of Mohsin Experiment (W7, $h/t = 34$, Base Stiffness = 5,000 kNm/rad)	121
Figure 4.33 – Comparison of Analytical Model Prediction to Results of Mohsin Experiment (W8, $h/t = 34$, Base Stiffness = 10,000 kNm/rad)	122
Figure 4.34 – Comparison of Analytical Model Prediction to Results of Chapter 3 Experiment (Specimen 1, $h/t = 12$, Base Support Stiffness = 0 kNm/rad).....	123
Figure 4.35 – Comparison of Analytical Model Prediction to Results of Chapter 3 Experiment (Specimen 2, $h/t = 12$, Base Stiffness = 2,300 kNm/rad).....	124
Figure 4.36 – Comparison of Analytical Model Prediction to Results of Chapter 3 Experiment (Specimen 3, $h/t = 12$, Base Stiffness = 5,000 kNm/rad).....	124

Figure 4.37 – Comparison of Analytical Model Prediction to Results of Chapter 3
Experiment (Specimen 4, $h/t = 12$, Base Stiffness = 9,500 kNm/rad)..... 125

LIST OF SYMBOLS AND ABBREVIATIONS

A_s	Area of Tensile Steel
A_s'	Area of Compressive Steel
b_i	Width of Fibre i
C_m	The ratio of End Moments on a Member
C_{mi}	Compressive Force in the Masonry at Fibre i
CMU	Concrete Masonry Unit
CV	Coefficient of Variation
CSA	Canadian Standards Association
d_c	Tensile Steel Depth of Cover
d_c'	Compressive Steel Depth of Cover
d_i	Distance from the Centroid of a Fibre to the Midpoint of the Wall
e	Axial Load Eccentricity
e_k	Kern Eccentricity
E'	Instantaneous Tangent Elastic Modulus
E_i	Initial Tangent Modulus of Elasticity
E_m	Elastic Modulus of Masonry
EI	Flexural Rigidity
EI_{eff}	Effective Flexural Rigidity
$\{F\}$	Force Vector
f_c'	Compressive Strength of Concrete
f_m'	Compressive Strength of Masonry
F_{si}	Force in the Reinforcing Steel at Node i

FE	Finite Element
G'	Shear Modulus Related to a Particular State of Stress
h	Masonry Wall Height
H	Total Height of a Masonry Wall
I_{cr}	Cracked Moment of Inertia of the Masonry Cross-Section
I_n	Nominal Moment of Inertia of the Masonry Cross-Section
I_o	Moment of Inertia of the Uncracked Effective Section of Masonry
k	Effective Length Coefficient
$[k]$	Stiffness Matrix
l	Unsupported Length of a Member
M_{cr}	Cracking Moment
$M_{ext,i}$	External Moment at Node i
$M_{int,i}$	Internal Moment at Node i
$M_{o,i}$	First-Order Moment at Node i
M_p	Maximum Primary Bending Moment of a Member
M_T	Maximum Total Bending Moment of a Member
M_u	Total Applied Moment on a Wall
n	Number of Fibres
$N. A.$	Depth of the Neutral Axis
OOP	Out-of-Plane
P	Compressive Axial Load Placed on a Wall
P_o	Cross-Sectional Axial Load Capacity
P_1	Estimated Axial Load
P_{cr}	Euler (Critical) Buckling Load

$q(h)$	Lateral Load Acting on a Wall
R	Rotational Stiffness at the Base of a Wall
RBS	Rotational Base Stiffness
RVE	Representative Volume Element
SEASC	Structural Engineers Association of Southern California
SW_i	Self-Weight at Node i
t	Masonry Wall Thickness
t_m	Thickness of a Mortar Joint
T	Thickness of a Wall
T_{mi}	Tensile Force of the Masonry in Fibre i
TMS	The Masonry Society
$u(a)$	Value of the Deflection Function at Point a
$u(x)$	Value of the Deflection Function at Point x
$u'(a)$	Value of the Deflection Functions First Derivative at Point a
$u''(a)$	Value of the Deflection Functions Second Derivative at Point a
u_i	Deflection at Node i
u_{i-1}	Deflection at Node $i - 1$
$\{w\}$	Displacement Vector
X	Depth of the Neutral Axis
$y(x)$	Lateral Displacement of a Wall at Distance x from the Base
$\alpha(x)$	Slope at Point x
α_i	Slope at Node i
α_{i-1}	Slope at Node $i - 1$
δh	Distance Between Nodes i and $i - 1$

ε	Strain in the Outmost Compressive Masonry Fibre
ε_1	Strain in the Tension Face of Masonry
ε_2	Strain in the Compression Face of Masonry
ε_c	Compressive Strain of Masonry
ε_x	Strain at the Outermost Compressive Fibre
θ	Rotation at the Base of a Wall
ϕ	Curvature
$\phi(x)$	Curvature at Point x
ϕ_{i-1}	Curvature at Node $i - 1$
σ_i	Stress in the Masonry at Fibre i
σ_m	Compressive Stress of Masonry
σ_s	Stress in the Tensile Steel
σ_s'	Stress in the Compressive Steel
ψ	Moment Magnification Factor

1 INTRODUCTION

1.1 Background

Masonry is one of the earliest building materials known to humankind and has played a significant role in sheltering civilizations throughout history. Today, masonry is commonly seen in the residential, commercial, and industrial sectors due to its inherent durability, notable thermal performance, sound and fire protection, and ease of construction. Although masonry consists of many different forms, such as clay brick or natural stone, concrete masonry unit (CMU) blocks are typical for structural applications in Canada.

Current Canadian standards for masonry design (Canadian Standards Association (CSA) S304-14 2014) define a slender masonry wall as that having an effective height-to-thickness (kh/t) ratio greater than 30. Due to the inherent difficulties in studying the experimental response walls with high slenderness ratios through full-scale testing, North American code provisions for slender masonry walls have traditionally relied on a small set of testing conducted in a few universities and research centres (Yokel et al. 1970; Hatzinikolas et al. 1980; SEASC 1982). Due to the scarcity of test data, the design of these structural elements often is conducted using overly conservative code requirements. Such requirements include limiting the axial load placed on the wall to 10% (CSA S304) or 5% (TMS 402) of its gross section capacity, restricting raked joints, specifying a minimum block thickness of 140 mm, limiting the amount of flexural steel reinforcement to less than the balanced ratio, and assuming pinned end conditions.

Of the listed standard requirements for slender masonry walls, the most restrictive is the assumption of pinned end conditions and the limitation of flexural reinforcement. During the design of slender masonry walls, special attention must be given to second-order effects (i.e. the additional moment created when lateral deflections caused by the primary moment create an eccentricity with the gravity load). The determination of second-order effects is often conducted using the moment magnification method, a method in which a moment magnification factor amplifies the primary moment to account for the additional

moments created by second-order effects. Determination of this moment magnification factor heavily relies upon an effective flexural rigidity (EI_{eff}) and effective length factor (k) term. An underestimation of the effective flexural rigidity and the required assumption of pinned end conditions ($k = 1.0$), greatly increases the moment magnification factor, resulting in a large amplification in design moment of the wall. Additional flexural steel reinforcement is then required to meet this design moment; however, the additional steel may then violate the standards required condition that the wall must yield at the ultimate limit state. If violated, designers are then forced to use a larger masonry unit, resulting in an uneconomical design.

Improvement of the current design procedure and moment magnification method for slender masonry walls has proven a challenging task, as many researchers (Colville 1979; Hatzinikolas et al. 1980; Hamid and Drysdale 1980; Sulwaski and Drysdale 1986) have concluded that a proper design procedure for loadbearing masonry walls is difficult without the consideration of the material and geometric nonlinearities present in masonry. Despite an attempt at quantifying material nonlinearity into the design of slender masonry walls into the effective flexural rigidity (EI_{eff}) parameter, research (Liu et al. 1998) has shown that the current Canadian code is overly conservative when attempting to predict the effective rigidity of such walls due to a limited understanding of the nonlinear behaviour of the masonry, cracking mechanisms, and the interaction between flexure and axial load.

When most of the available studies for over 40 years consisting of walls tested with pinned-pinned boundary conditions, Mohsin (2005) was one of the first who investigated the role of non-zero rotational base stiffness on loadbearing masonry walls. The study comprised of an experimental program in which 8 slender masonry wall specimens with varying base stiffness were tested under an eccentric axial load. Results from the study showed the presence of a base rotational stiffness significantly reduced second-order effects by limiting the OOP deflections and increased the loadbearing capacity of the walls as much as 87.5%. Comparisons of the effective flexural rigidity obtained during the experimental program to those calculated using the Canadian standard (CSA S304)

indicated vast conservatism in the code as experimental values were up to 5.1 times greater than those calculated using the standard. However, the study is limited as the presence of lateral load (often the governing load in slender masonry wall design) is absent.

1.2 Problem Statement

Although slender loadbearing masonry walls are a common structural solution for low to mid rise construction, the behaviour of these walls is still relatively uncertain. The Canadian standard for masonry design (CSA S304-14) calls for stringent design procedures which recent research (Liu and Dawe 2001; Mohsin 2005; Liu and Hu 2007; Isfeld et al. 2019) has found to be overly conservative, and not being reflective of the performance of these walls, measured during experiments or calculated with sophisticated finite-element models.

One of the most significant design provisions in the current code is the assumption of a pinned base for walls with slenderness ratios greater than 30. This provision neglects the effect of the rotational support stiffness provided at the base of the wall, which has been proven to both increase the loadbearing capacity and limit OOP deflections of slender loadbearing walls (Mohsin 2005). It could be argued that the pinned base assumption might have validity under realistic loading conditions: these would impose cyclic force demands at the base, causing degradation of the masonry and the steel reinforcement at the connection – eventually, turning it into a hinge.

To test the validity of this assumption, this study aims to provide experimental and analytical evidence on the influence that the rotational base stiffness has on key structural parameters, such as strength, stiffness, and energy dissipation, on walls subjected to cyclic loads. These results could be used to develop more rational design procedures for loadbearing masonry walls.

1.3 Objectives, Methods, and Scope

The outcome of this study is to determine the behaviour of loadbearing masonry walls with support stiffness. To achieve this outcome, the following specific objectives are identified. The tasks required to complete each objective are also presented.

1. Experimental investigation of the response of loadbearing masonry walls with a rotational support stiffness at the base.

- Design a series of masonry wall test specimens to reflect current design provisions commonly found in the Canadian industry
- Estimate the reactive rotational support stiffness provided by typical foundations by developing a numerical model based upon foundation geometry and soil properties
- Test 4 moderately slender loadbearing masonry walls of varying base rotational stiffness under a combination of gravity and OOP loads
- Assessment of experimental results in terms of load-displacement response, loadbearing capacity, base rotation, moment profiles, and failure modes

2. Development of a mechanics-based analysis model to predict the behaviour of loadbearing masonry walls, including the effect of the rotational stiffness at the base.

- Develop an analysis model based on the governing differential equation describing the deflection of elastic beam-columns subjected to axial and lateral distributed loads
- Validate the model with experimental results from objective (1) in addition to other experimental programs involving slender masonry walls with and without a base rotational stiffness
- Show how the model can be used to develop design tools (e.g., interaction diagrams that account for slenderness effects) for slender loadbearing masonry walls.

It is noted that the wall specimens in the study were limited to a slenderness ratio (kh/t) of 12 which is defined by CSA S304 as moderately slender. For these walls, CSA S304 permits the inclusion of the base stiffness in the determination of the flexural rigidity of the wall. The moderately slender walls used in this study ($kh/t < 30$) constitute a first step towards investigating slender walls ($kh/t > 30$), which will be addressed in future studies. This is because there are several novel aspects in this study, the implications of which could impact or influence the design of the next experimental phase. For instance, to the knowledge of the authors this is the first study that incorporates the effects of a cyclic lateral load. The degradation of the connection at the base, and related rotational mechanics are factors that will be important to take into account when taller walls are tested, as an unintended (brittle) failure at the connection could hinder the experiments and present serious safety concerns.

The simulated wind load in the study was limited to a point load due to experimental constraints. As wind loads could be better modeled as uniform loads, it is acknowledged that the results obtained in this study will not be directly applicable to walls subjected to wind load. However, inclusion of lateral load has not been done, to the knowledge of the author, in any of the studies that have addressed the influence of the rigidity of the support.

Due to experimental constraints, only one wall geometry and reinforcing layout were considered in the experimental program. The block size, wall width, wall height, reinforcing bar sizes, and reinforcing bar location were fixed. The rotational base support stiffness was assumed to have been provided by a strip footing. Shear failures of flexural walls are also not considered in this study as all wall specimens were designed to be flexural critical. A single axial load was considered in the experimental program of this study.

1.4 Organization of Thesis

This thesis is organized into five chapters. In Chapter 1, the problem statement is presented, and the objectives and scope are discussed. In Chapter 2, the literature review

is presented, including previous masonry wall testing and numerical modelling of loadbearing masonry walls.

In Chapter 3, the experimental methodology used in the research study is presented. Aspects such as specimen details, estimation, and simulation of support stiffness, test setup, loading protocol, and experimental results are presented and discussed.

In Chapter 4, the development of a simple, mechanics-based analysis model for determining the behaviour of loadbearing masonry walls is presented. Effects of rotational support stiffness, material nonlinearity, and tensile cracking are included in the model. The theory, methodology, and accuracy of the analysis model is presented in detail.

In Chapter 5, the results and conclusions of the study in addition to providing recommendations for future research work are presented.

2 LITERATURE REVIEW

2.1 Introduction

Loadbearing masonry walls are a common structural solution to resist a combination of gravity and OOP loads. Historically, these walls were built without reinforcing steel (often referred to as plain masonry walls), and builders relied on their monolithic nature to provide the necessary moment resistance. Loadbearing masonry walls today are typically designed to contain reinforcing steel (referred to as reinforced masonry walls), which is placed and grouted into the cells of the masonry (Fig. 2.1).

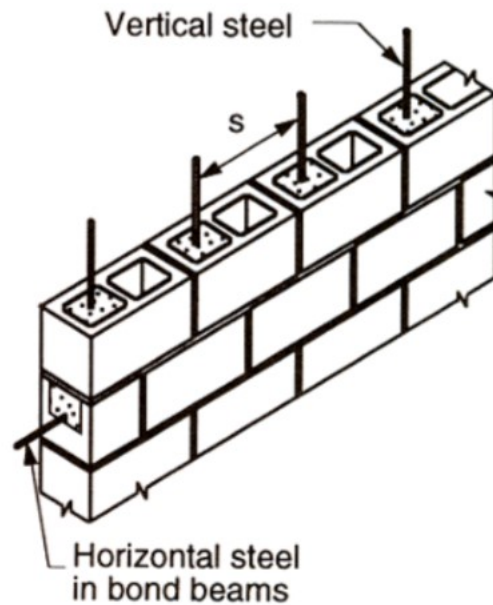


Figure 2.1 – Reinforced Masonry Wall (Minaie et al. 2009)

Perhaps most critical to the design of loadbearing masonry walls is the determination of the second-order effects. The determination of second-order effects is done by determining the total applied moment on the wall. This applied moment is composed of two components – namely, the primary and secondary moments. Primary moments for masonry walls typically come in the form of gravity loads acting at an eccentricity, applied lateral loads, or a combination of the two. The secondary moment arises as the lateral deflection of the wall caused by the primary moment creates an eccentricity

between the wall and applied gravity load. The addition of the secondary moment, in turn, increases the lateral deflection, which then increases the secondary moment. This phenomenon is referred to as second-order, or P- Δ , effects. Slender masonry walls (defined by CSA and The Masonry Society (TMS) as having a slenderness ratio greater than 30) are particularly sensitive to second-order effects due to the large lateral deflections they experience during loading.

North American design provisions currently have two methods to account for these P- Δ effects: P- Δ method and the moment magnifier method. The P- Δ method relies on the calculation of the second-order moment through iteration until convergence is reached, while the moment magnifier method is able to capture the effect in a single calculation, making it the more popular choice among designers. Derived on the basis of an elastic beam-column in single curvature (having the radius in one plane), the moment magnification method was first introduced and applied to slender concrete columns (MacGregor et al. 1970). The method involves the magnification of the maximum primary bending moment by a factor ψ to produce an accurate estimation of the maximum total bending moment (combination of primary and secondary moments) experienced by a member (Eq. 2.1). The method is valid for members in single curvature with the location of the primary maximum bending moment coinciding with the location of the total maximum bending moment.

$$M_T = \psi M_p \quad (2.1)$$

$$\psi = \frac{C_m}{1 - \left(\frac{P}{P_{cr}}\right)} \quad (2.2)$$

$$P_{cr} = \frac{\pi^2 EI}{(kl)^2} \quad (2.3)$$

where M_T = maximum total bending moment of the member,

ψ = moment magnification factor,

- M_p = maximum primary bending moment of the member,
- C_m = ratio of end moments on the member,
- P_{cr} = Euler bucking (critical) load of the member,
- k = effective length coefficient, and
- l = unsupported length of the member.

Challenges associated with the moment magnification factor are the accurate prediction of both the flexural rigidity (EI) and the effective length of the wall (kl). The estimation of the flexural rigidity for masonry walls is rather complex, as phenomena such as tensile cracking and plastic strains result in the flexural rigidity degrading at a nonlinear rate throughout the loading history of the wall. Although the influence of boundary conditions may be accounted for indirectly through the effective length coefficient (k) present in Eq. 2.3, a realistic prediction of k is challenging as the boundary condition associated at the base of a loadbearing masonry wall is neither fixed (complete restriction of rotation, $k = 0.7$) nor pinned (no restriction of rotation, $k = 1.0$), but somewhere in between. Compensating for these challenges, North American standards are rather conservative, as they underestimate the true flexural rigidity of the wall and assume a pinned based for slender walls in the Canadian standard and for all walls (both slender and non-slender) in the American standard.

This chapter presents a review of all the available literature covering the topics related to experimental testing and analytical investigations related to loadbearing masonry walls, and it discusses their findings in relation to the determination of second-order effects of loadbearing masonry walls.

2.2 Experimental Programs

Experimental programs dealing with loadbearing masonry walls largely began in the early 1970s when 60 loadbearing masonry walls (32 reinforced and 28 plain) under an eccentric axial load were tested (Yokel et al. 1970). Each wall specimen was 1.2 m wide and

ranged from 3 m to 6 m in height. The slenderness ratio of the specimens varied between 15 and 40. Boundary conditions of the walls were designed to allow for free rotation at the top of the wall while restricting the rotation at the base. Results from the test suggested an increase in flexural compressive strength with increased levels of strain gradient (eccentricity). Interaction diagram curves derived from both the axial compressive strength and the flexural compressive strength were presented. Because the latter curve showed better agreement with experimental results, it was suggested that the accuracy of the interaction diagram may be improved by considering strain gradient effects. Slenderness effects computed with the moment magnification method were found to provide a conservative prediction of the slenderness effects observed during testing.

Yokel et al. (1971) later tested an additional 90 plain brick and plain block masonry walls under a combination of axial and OOP loads. Concrete block wall specimens were 1.2 m wide and measured 2.4 m in height. The slenderness ratio of the walls was 12. All specimens were fixed at the base and pinned at the top. As in previous tests, results indicated that under large eccentricities the flexural compressive strength of masonry significantly exceeds the axial compressive strength as determined through prism testing. It was also determined that when tensile cracking of the masonry cross-section was accounted for, the predicted slenderness effects computed with the moment magnification factor were in reasonable agreement with those observed during testing.

With vertical reinforcement becoming a more prominent feature in the design of loadbearing masonry walls, research was conducted to determine whether the behaviour of reinforced masonry walls can be accurately predicted by the British standard (CP 111: 1970) (Cranston and Roberts 1976). A total of 38 concrete block masonry walls were tested with OOP loading. Both the height and width of the specimens ranged from 0.2 m to 3.0 m (Fig. 2.2). The upper and lower points of the walls were secured to a steel frame during testing. Comparing the load-deflection response of the specimens with predicted values from the British standard (CP 111: 1970), it was shown the standard tends to overestimate the true deflection of the walls, resulting in a conservative prediction. A

new procedure to predict the ultimate load capacity of reinforced concrete masonry walls through stress-eccentricity-rotation curves was also proposed (discussed in a later section).

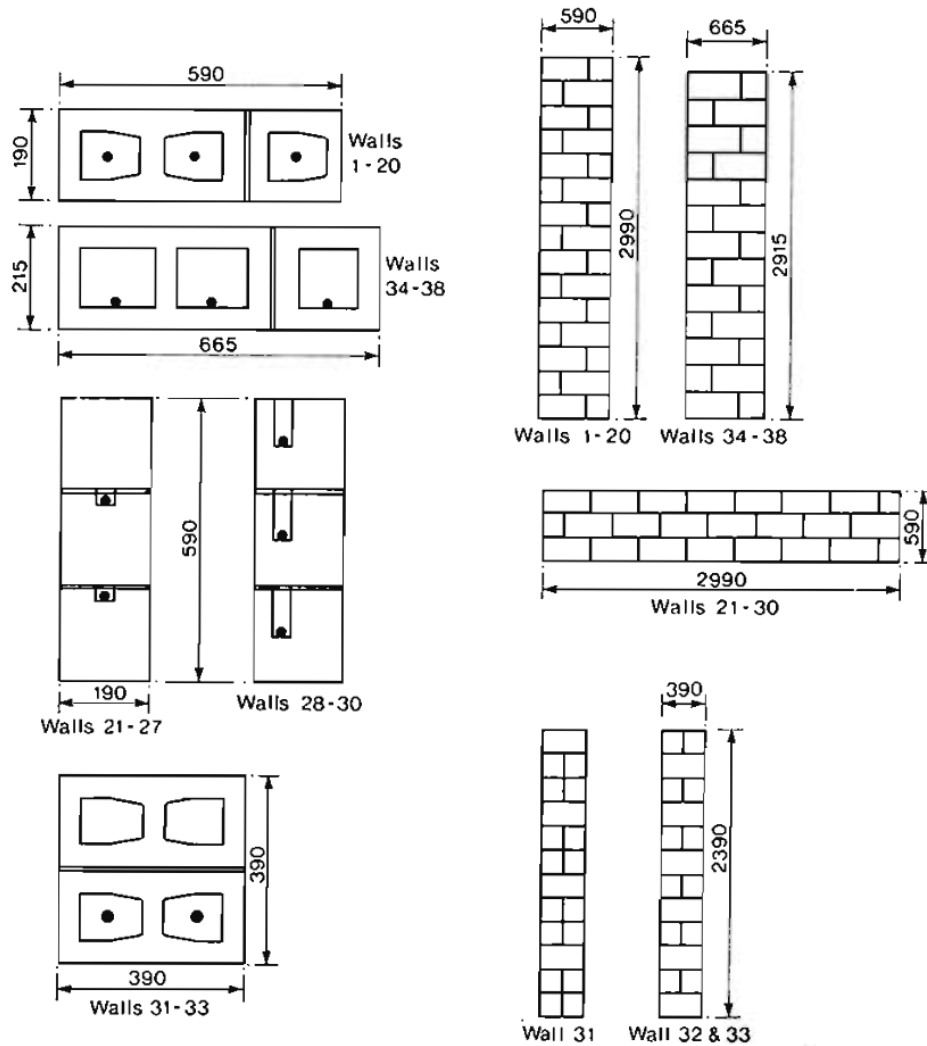


Figure 2.2 – Wall Test Specimens (Cranston and Roberts 1976)

To determine the effect of slenderness and load eccentricity and their implications on the moment magnification method, a comprehensive testing program with 68 concrete masonry walls was conducted (Hatzinikolas et al. 1978a; b). Plain and reinforced specimens were tested, with some of the specimens additionally containing joint reinforcement. Walls measured 1 m wide and varied between 2.4 m and 4.4 m in height.

Slenderness ratios of the specimens varied between 12 and 22. Pinned end conditions with adjustable load were specified at the top and bottom of the wall specimens, allowing for both single and double curvature. It was found the presence of joint reinforcement reduces the axial capacity of the masonry due to stress concentrations arising from the difference in elastic modulus of the steel reinforcement and the mortar bedding. Results also indicated an increased capacity from walls tested in double curvature over single curvature. Comparison of the slenderness effects observed during testing compared to those computed through the moment magnification method suggested the effects of loading conditions, tensile bond strength, and type of wall (plain or reinforced) play important roles and must be accounted for to produce accurate predictions.

Slenderness effects became an increasing concern in the 1980s as the demand for taller walls grew. In an attempt to analyze the behaviour of tall masonry walls and produce effective design provisions, the American Concrete Institute (ACI) and Structural Engineers Association of Southern California (SEASC) (1982) tested 9 reinforced concrete masonry walls under combined axial and lateral loading. All specimens were 1.2 m wide and measured 7.3 m in height. The range of slenderness ratios for the walls consisted of 29, 36, and 48. The ends of the specimens were simply supported. Although none of the specimens were loaded until failure, no lateral instability was reported during the testing. Slenderness effects were described to be more prominent in the thinner walls, with second-order effects contributing approximately 20% of the total moment when the steel reinforcement began to yield. Design provisions arising from this research included a minimum and maximum reinforcement clause, midspan deflection limits, and limitations on applied axial loads.

As the moment magnification method came into common use in North American design standards, research focusing on the accurate evaluation of the effective flexural rigidity (a key parameter in the moment magnification method) began. Liu and Dawe (2001) tested 36 reinforced masonry walls under combined axial and lateral loads. Specimens measured 0.8 m wide and 1.2 m in height. The slenderness ratio for all walls was 8, and each wall was tested with pinned end conditions. Strain measurements were recorded on

both the tension and compression faces at the midspan of each specimen to determine the effective flexural rigidity. Comparing values of effective flexural rigidity obtained from the experiment to those computed using the Canadian standard CSA S304.1-04, the researchers suggested that standard is unconservative in predicting the effective flexural rigidity for very low levels of axial load and begins to become overly conservative as the applied axial load increases. The research also produced a design expression for the effective flexural rigidity of a masonry wall with eccentric loading (discussed in a later section).

Research in determining the true effective flexural rigidity of concrete masonry walls was taken a step further when Mohsin (2005) conducted 8 tests of large-scale slender reinforced masonry walls subjected to an eccentric axial load. Unfortunately, the presence of lateral loads was not accounted for in the experimental program. Walls were 1.2 m wide, with 4 walls 5.4 m in height and the remaining 4 walls 6.4 m. The slenderness ratio of the two groups of walls was 29 and 34. The research attempted to provide realistic boundary conditions by adding a rotational stiffness to the base of each specimen (used to simulate the effects of the strip footing foundation that loadbearing masonry walls are typically constructed on). This rotational stiffness was simulated during the experiment by attaching a steel moment arm to the base of the wall specimens during testing (Fig. 2.3). Rotational stiffnesses specified for the tests were 0 kNm/rad, 1,000 kNm/rad, 5,000 kNm/rad, and 10,000 kNm/rad. Results indicated that as the level of rotational stiffness provided at the base of the walls increased (i.e., foundation became larger), the axial load capacity increased and slenderness effects decreased. The study also found that at a constant slenderness and load eccentricity, the effective flexural rigidity would increase when the rotational stiffness was increased from 0 kNm/rad to 1,000 kNm/rad but would then decrease with additional rotational stiffness, as the cross-section would begin to experience more plastic strain. Using the differential equation for beam-columns (Eq. 2.4) with specified boundary conditions (Eq. 2.5a–2.5d), a transcendental equation for flexural rigidity throughout the load history was determined (Eq. 2.6a–2.6b). Comparing the effective flexural rigidity of the specimens to values calculated with CSA S304.1-04, Mohsin found experimental values of EI_{eff} were on

average 4.6 and 4.4 times larger those calculated using the standard for walls with and without a base support stiffness respectively. Mohsin concluded the standard is overly conservative and does not account for base fixity.

$$\frac{\partial^2}{\partial h^2} \left(EI \frac{\partial^2 u(x)}{\partial h^2} \right) + P \frac{\partial^2 u(x)}{\partial h^2} = q(x) \quad (2.4)$$

$$y(0) = 0 \quad (2.5a)$$

$$y(H) = 0 \quad (2.5b)$$

$$y''(0) = \frac{Pe}{EI} \quad (2.5c)$$

$$y''(H) = \frac{R\theta}{EI} \quad (2.5d)$$

$$y(h) = \frac{1}{EI k^2} \left[R\theta \left\{ -\frac{\sin(kh)}{\sin(kH)} + \frac{h}{H} \right\} + Pe \left\{ 1 + \frac{\sin(kh) \cos(kH)}{\sin(kH)} - \cos(kh) - \frac{h}{H} \right\} \right] \quad (2.6a)$$

$$k = \sqrt{\frac{P}{EI}} \quad (2.6b)$$

where EI = flexural rigidity of the wall,
 $u(x)$ = lateral displacement of the wall at a distance x from the base,
 P = compressive axial load placed upon the wall,
 $q(x)$ = lateral load placed upon the wall,
 H = total height of the wall,

- e = eccentricity of the axial load,
- R = rotational stiffness at the base of the wall, and
- θ = rotation at the base of the wall.

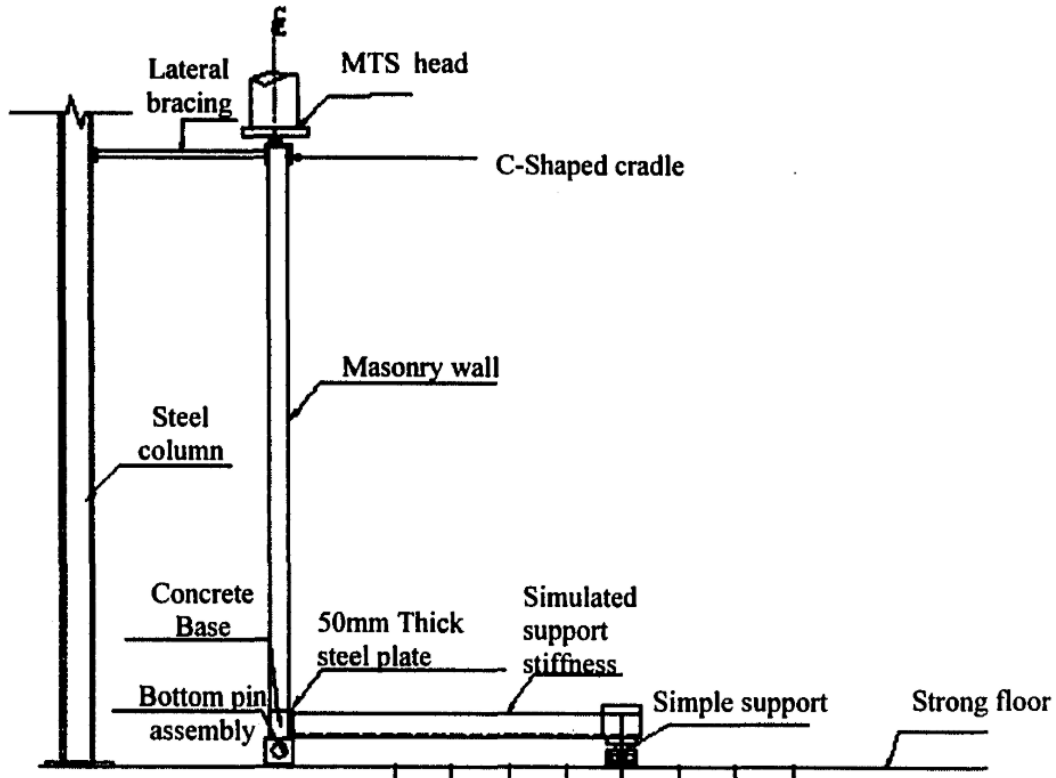


Figure 2.3 – Simulated Support Stiffness (Mohsin 2005)

Liu and Hu (2007) also compared experimental effective flexural rigidity results to values obtained with the Canadian standard, by testing 12 reinforced masonry walls under eccentric axial loading. Specimens in their study measured 0.8 m wide and 2.4 m in height. The slenderness ratio of the walls was 16, and the ends of the walls were simply supported. Results indicated that as the level of eccentricity increased, the axial load capacity of the walls tended to decrease, while the lateral deflection at the midspan increased. A comparison of results to the values predicted by CSA S304.1-04 indicated the standard tends to underestimate the true effective flexural rigidity of walls by as much as 52% and 48% for $e_1/e_2 = 1.0$ and -1.0 respectively.

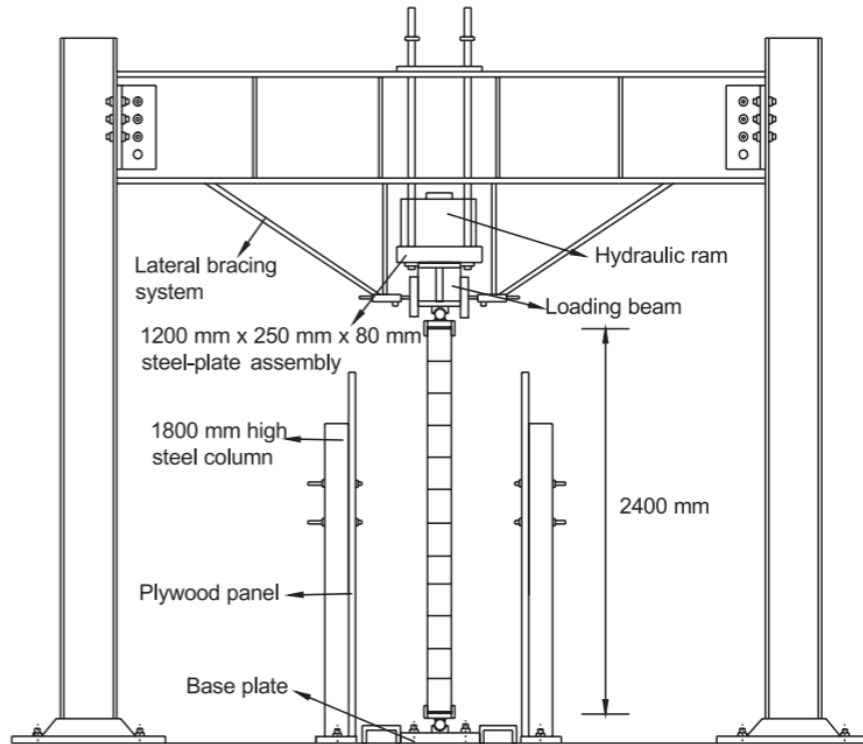


Figure 2.4 – Experimental Setup (Liu and Hu 2007)

The accuracy of the moment magnification methods present in North American design standards for walls with initial imperfections or large eccentricities was investigated when Bean Popehn et al. (2009) tested 4 unreinforced concrete block masonry walls under a combined eccentric axial and lateral load. Walls measured 0.8 m in width and 3.5 m in height. The slenderness ratio of the specimens was 39, and the boundary conditions of the walls were simply supported. The moment magnifications observed from the tests were compared to the moment magnification procedure outlined in the American (TMS 402-08) standard. It was observed that the standard produced conservative values for moment magnification, as the ratio of moment magnification calculated using the standard to moment magnification experimentally determined reaching values as large as 1.85.

A further study of the accuracy of the moment magnification method used in the Canadian standard for walls with unique boundary conditions was conducted by Isfeld et al. (2019) using 3 reinforced concrete masonry walls tested under combined axial and lateral

loading. Test specimens measured 1.2 m wide and 2.4 m in height. The slenderness ratio of the walls was 12. Boundary conditions for the specimens varied between pinned-pinned and fixed-pinned. Comparing observed OOP deflections with simplified calculations defined in CSA S304, it was observed the standard overestimates the OOP displacements for fixed-pinned walls by a factor of 2 and 26 for walls subjected to axial loading alone, and a combination of axial and OOP loads respectively.

2.3 Numerical and Finite Element Modelling

Finite element (FE) modelling of masonry walls can be generally divided into two categories: macro-models and micro-models. Macro-models tend to treat the masonry assemblage as a single homogeneous unit. This allows for a more efficient computation time as compared to micro-models, in which each of the materials, along with the interactions between them, must be independently modelled. Macro-models have been found to be effective in investigating the global behaviour of loadbearing masonry walls but are unable to capture the local behaviour as a micro-model can.

FE micro-models for masonry structures were used by Page in a model for clay brick walls subjected to in-plane loading was presented (Page 1978). The work featured the masonry units modelled as 8-node plane stress continuum elements with isotropic elastic properties. The mortar joints connecting these bricks were defined as nonlinear linkage elements. The displacement matrix for these elements was defined in terms of the relative displacement vector in the normal and shear directions for the top and bottom movement of the joints. The equilibrium equation for the linkage elements is defined below:

$$\{F\} = [k]\{w\} \quad (2.7)$$

where $\{F\} = \begin{Bmatrix} F_s \\ F_n \end{Bmatrix}$, force vector;

$[k] = \begin{bmatrix} k_s & 0 \\ 0 & k_n \end{bmatrix}$, stiffness matrix; and

$$\{w\} = \begin{Bmatrix} w_s(top) - w_s(bottom) \\ w_n(top) - w_n(bottom) \end{Bmatrix}, \text{ displacement vector.}$$

Values for the shear and normal stiffnesses (k_s and k_n , respectively) were suggested as follows:

$$k_s = \frac{G'T}{t_m} \quad (2.8)$$

$$k_n = \frac{E'T}{t_m} \quad (2.9)$$

where G' = shear modulus related to a particular state of stress,
 T = thickness of the wall,
 t_m = thickness of the mortar joint, and
 E' = instantaneous tangent elastic modulus.

Failure criteria for the masonry were not defined, resulting in the inability to predict the ultimate load capacity of the wall. The solver of the model would use an iterative procedure until convergence was reached. The model was deemed useful only for the working stress design method.

Ali et al. (1986) later implemented a local failure criterion for both the joint and brick masonry elements of nonlinear FE models. The model itself was constructed with 2D plane stress elements with the stress–strain relationship of the brick and joint elements obtained through separate experimental investigations. The FE model defined three failure criteria: failure of the bond between the brick and joint element, fracture of the mortar under a biaxial tension–compression or tension–tension state of stress and crushing failure of the brick under biaxial compression. The researchers reported that to aid in computational efficiency, they segmented the element mesh, with a denser mesh being applied to areas of concentrated load. A brick wall subjected to in-plane loads was

simulated using the model, and the results were compared to those from experimental investigations.

As an alternative to FE models, an analytical model based on load-moment-curvature relationships was developed to analyze the behaviour of slender masonry walls (Muqtadir 1991). Based on a combination of the column deflection curve (CDC) method and Newmark's numerical method (Fig. 2.5), in which the differential equation governing elastic beam-column behaviour (Eq. 2.4 above) is approximated, the model accounts for both material nonlinearity and the cracking of the cross-section under tensile loads. The model was deemed suitable for slender masonry walls subjected to in-plane compression and OOP bending. Results from the model were compared to experimental results and showed good agreement.

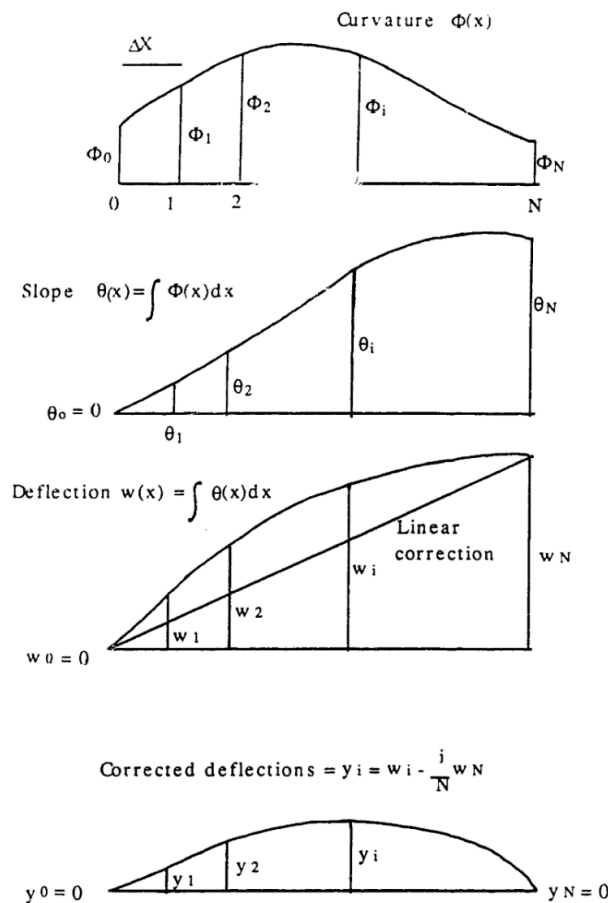


Figure 2.5 – Newmark's Numerical Procedure (Muqtadir 1991)

The progressive cracking of a face-shell bedded masonry wall subjected to in-plane loads was later included in a nonlinear FE model developed by Sayed-Ahmed and Shrive (1994, 1996). The authors proposed the use of shell elements as an alternative to 3D continuum elements, as they were reported to be more computationally efficient while still being able to capture phenomena such as web splitting. Simulation of 7-course high wallettes subjected to concentrated loads was conducted, with the analytical behaviour compared to previously completed experimental investigations.

Interface elements were later introduced in FE models to define the mortar joints of masonry structures (Lotfi and Shing 1994). This allowed the model to effectively capture the true shear behaviour of the mortar joints. Crack initiation and propagation were also included in the model through the material constitutive model employed in the model. It was concluded the use of interface elements is a viable method to predict both the load-carrying capacity of masonry walls and the locations of local failure during loading.

Wang et al. (1997) created an FE macro-model for slender masonry cavity walls in which the wall was treated as a single homogeneous unit. The model was constructed with beam-column elements in the commercially available software ABAQUS. A predefined model for concrete with the ability to capture tensile cracking was employed in the model. Results from prism tests were used to define the compressive behaviour of the elements, while the tensile behaviour was modelled using the bond strength between the block and mortar joints. A tension stiffening model was implemented post cracking. Analysis of the walls was done in two stages, the first stage being a Newton–Raphson iterative procedure in which the applied load was increased in load control until peak load was reached. Upon reaching peak load, the analysis would shift into a modified Riks algorithm to capture the softening behaviour of the wall. The authors reported the model correlated well with experimental results.

A homogeneous masonry element that accounts for the anisotropic nature of masonry was proposed by Lopez et al. (1999). They used the theory of mapped spaces to transform the anisotropic space of the masonry into a fictitious isotropic space in which a modified Mohr–Coulomb criterion could be used to evaluate the plastic flow. Although the

element was unable to identify the fracture mechanisms of the masonry, it could identify the location of localized damage. An FE model using the proposed element showed a good correlation to both experimental results and other FE micro-models. The researchers reported that the use of the element can considerably reduce the time required for mesh generation and computation, making it a viable option for large-scale masonry structures for which micro-models are deemed impractical.

Also attempting to develop a homogenized constitutive model for masonry, Ma et al. (2001) developed a representative volume element (RVE) that captures the equivalent elastic properties, strength envelope, and failure patterns of the masonry assembly (Fig. 2.6). Three failure modes are defined for the element: tensile failure of the mortar, shear failure of the mortar or combined shear failure of the brick and mortar, and the compressive failure of the brick. Various stress–strain curves for compression–tension states of stress were implemented in the numerical simulations. The authors suggested that an RVE significantly smaller than the whole masonry structure be used to avoid edge effects. The element was reported to be unable to capture micro-cracking and was not applicable for walls in which the stress and strain fields vary widely.

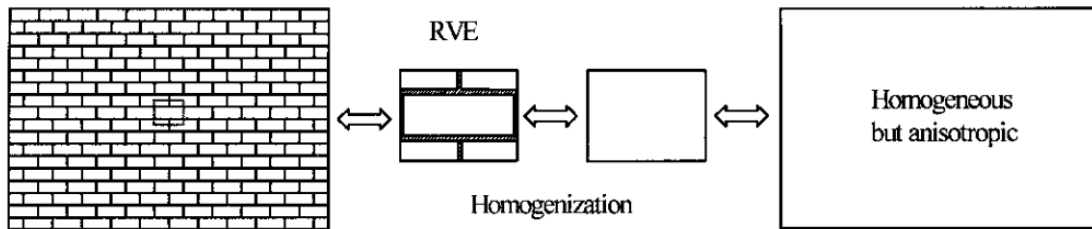


Figure 2.6 – Homogenization of Masonry Material (Ma et al. 2001)

Creazza et al. (2002) developed a 3D FE model for masonry vaults. Homogenization was applied to cut down the severe computational cost associated with the model. The proposed model used two independent internal damage parameters (d^+ and d^-) as functions of the equivalent effective tensile and compressive stresses ($\bar{\tau}^+$ and $\bar{\tau}^-$, respectively). A comparison of experimental and analytical results indicated that a

homogenized model is a viable method for analyzing the behaviour of 3D anisotropic masonry structures.

An FE model to study the behaviour of flexural loadbearing masonry walls was developed by Liu and Dawe (2003). The model consisted of 2-node, 4-degrees-of-freedom (DOF) beam-column elements in which the material nonlinearity and stiffness degradation were accounted for by conducting a moment–curvature analysis over the cross-section of the wall (Fig. 2.7). Assuming both strain compatibility and the depth of the neutral axis, the stresses at each fibre throughout the cross-section were calculated with a stress–strain relation defined by Eq. 2.10. Axial equilibrium was then used to determine an estimate of the axial load (P_1) subjected to the cross-section (Eq. 2.11). If this estimated axial load was greater or less than the true axial load (P), the depth of the neutral axis would be modified, and the analysis reiterated until the estimated axial load was within a reasonable tolerance of the true axial load. With the correct neutral axis determined, the moment (Eq. 2.12) and curvature (Eq. 2.13) were then calculated. The moment–curvature relationship would then be used to determine the reduction in stiffness within the local stiffness matrices of the FE model. Failure modes were incorporated into the model by routinely checking to see whether the applied moment exceeded the maximum moment capacity calculated with the moment–curvature analysis (i.e., crushing of the masonry) and whether the applied axial load exceeded the critical buckling load (i.e., stability failure). The model was compared with experimental results, and a good correlation was reported.

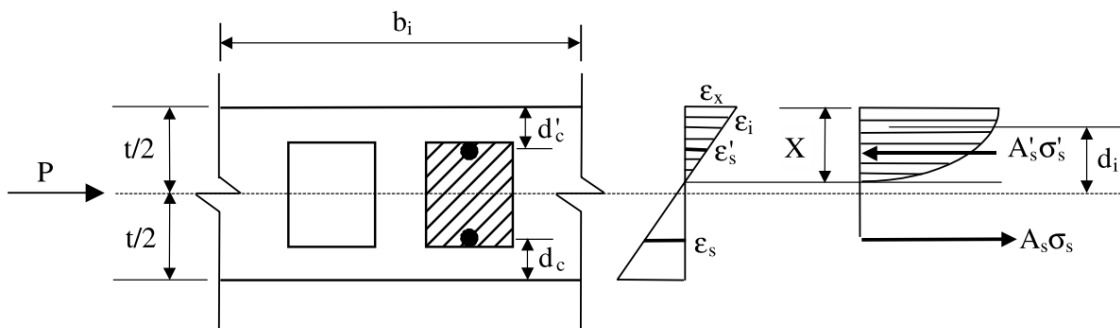


Figure 2.7 – Stress Distribution on a Wall Cross-Section (Liu and Dawe 2003)

$$\sigma_m = 1.067 f'_m \left[\frac{2\varepsilon_c}{0.002} - \left(\frac{\varepsilon_c}{0.002} \right)^2 \right] \quad (2.10)$$

where σ_m = compressive stress of the masonry,
 f'_m = compressive strength of the masonry, and
 ε_c = compressive strain of the masonry.

$$P_1 = \left(\sum_{i=1}^n \sigma_i b_i \right) \frac{X}{n} + A'_s \sigma'_s - A_s \sigma_s \quad (2.11)$$

$$M = \left(\sum_{i=1}^n \sigma_i b_i d_i \right) \frac{X}{n} + A'_s \sigma'_s \left(\frac{t}{2} - d'_c \right) + A_s \sigma_s \left(\frac{t}{2} - d_c \right) \quad (2.12)$$

$$\phi = \frac{\varepsilon_x}{X} \quad (2.13)$$

where P_1 = estimated axial load,
 σ_i = stress in the masonry at fibre i ,
 b_i = width of fibre i ,
 X = depth of the neutral axis,
 n = number of fibres,
 A'_s = area of compressive steel,
 σ'_s = stress in the compressive steel,
 A_s = area of tensile steel,
 σ_s = stress in the tensile steel,

d_i = distance from the centroid of the fibre to the midpoint of the wall,

t = thickness of the wall,

d_c' = compressive steel depth of cover,

d_c = tensile steel depth of cover,

ϕ = curvature, and

ε_x = strain at the outermost compressive fibre.

Entz et al. (2017) developed a finite-element model using the open-source program OpenSEES. The model was constructed using nonlinear beam-column elements. A fibre section approach was used to incorporate material nonlinearity. Comparing results produced from the model with results of experimental tests conducted on prisms subjected to eccentric axial loads, researchers found a good correlation, indicating the validity of using a fibre section approach in the modelling of masonry elements.

2.4 Flexural Rigidity

In the current Canadian masonry design standard CSA S304-14 (CSA 2014) and American masonry design standard TMS 402/602-16 (MSJC 2016), expressions for effective flexural rigidity are given by Eq. 2.14 and Eq. 2.15, respectively:

$$EI_{eff} = E_m \left[0.25I_o - (0.25I_o - I_{cr}) \left(\frac{e - e_k}{e_k} \right) \right] \quad (2.14)$$

$$E_m I_{eff} = \begin{cases} 0.75E_m I_n & \text{for } M_u < M_{cr} \\ E_m I_{cr} & \text{for } M_u \geq M_{cr} \end{cases} \quad (2.15)$$

where EI_{eff} = effective flexural rigidity of the masonry wall,

E_m = elastic modulus of the masonry,

I_o = moment of inertia of the uncracked effective section of the masonry,

I_{cr} = moment of inertia of the cracked masonry cross-section,

e_k = kern eccentricity,

I_n = nominal moment of inertia of the masonry cross-section,

M_{cr} = cracking moment for the masonry cross-section, and

M_u = total applied moment on the wall.

Referring to Eq. 2.14 and Eq. 2.15, both design standards acknowledge the decrease in effective flexural rigidity as load increases, but they do so in different manners. CSA S304 introduces a virtual eccentricity factor that produces lower values of effective flexural rigidity as the loads increase. TMS 402/602-16 (MSJC 2016) accounts for the decrease with a piecewise function, in which the calculation for effective stiffness shifts once the cracking moment is reached. The upper limit of $0.25E_mI_o$ in CSA S304-14 (CSA 2014), has been found to be conservative by Mohsin (2005). TMS 402/602-16 (MSJC 2016) acknowledges this by increasing this limit to $0.75E_mI_o$ prior to the cracking moment but decreases the effective flexural rigidity to E_mI_{cr} (most conservative case) after the cracking moment is reached.

Absent in both expressions is the influence of boundary conditions. Introducing a support moment at the base of the wall results in both a decrease in deflection and moment distribution along the wall. Smaller deflections, in turn, lead to smaller $P\Delta$ effects, a significant advantage when designing slender masonry walls. One issue is accurately assessing the support moment provided by a real foundation – that is, the foundations on which the walls are built. This stiffness would range somewhere between pinned and fixed. The exact value is difficult to determine, as it depends on both the foundation size and soil parameters.

Expressions to estimate the flexural rigidity of masonry walls largely began with the experimental testing of loadbearing masonry walls. Yokel (1971) described flexural rigidity as a function of the level of stress and the cracking of the wall cross-section under the influence of vertical and transverse loading. For walls with eccentric loading, approximate equations were suggested to estimate their flexural rigidity, as shown in Eq. 2.16a and Eq. 2.16b for reinforced and unreinforced masonry walls, respectively.

$$EI = \frac{E_i I_n}{2.5} \quad (2.16a)$$

$$EI = \frac{E_i I_n}{3.5} \quad (2.16b)$$

where E_i = initial tangent modulus of elasticity and

I_n = moment of inertia of the uncracked cross-section.

For a wall subjected to excessive cracking, another approximate equation was suggested:

$$EI = E_i I_n \left(0.2 + \frac{P}{P_o} \right) \leq 0.7 E_i I_n \quad (2.17)$$

where P_o = cross-sectional axial load capacity of the masonry.

The inclusion of a $\left(0.2 + \frac{P}{P_o} \right)$ factor was an attempt to consider the effect of stresses in the cross-section of the wall and cracking effects. Other factors such as load eccentricity and slenderness effect are not directly included.

Realizing that the moment of inertia for loadbearing masonry walls is dependent on both mortar penetration and unit type, Hatzinikolas et al. (1978) suggested experimental testing to more accurately determine the flexural rigidity of loadbearing masonry walls. The authors proposed using factors such as those recommended for concrete design to incorporate the effect of load eccentricity and time-dependent effects on the flexural rigidity of concrete masonry. They suggested a conservative approach for estimating

flexural rigidity that would be valid for both reinforced and plain concrete masonry walls with and without time-dependent effects:

$$EI = E_m I_o \left[0.5 - \frac{e}{t} \right] \geq 0.1 E_m I_o \quad (2.18)$$

The effects of reinforcement ratio, load eccentricity ratio, and slenderness ratio on the flexural rigidity of masonry walls were later evaluated through experimental testing of grouted and ungrouted masonry walls (Aridru and Dawe 1995). They reported that the measurement of strain at the surface of the short wall could be an effective tool for estimating flexural rigidity. The bending moment and flexural rigidity were found to be exponentially related to each other.

Liu et al. (1998) conducted comprehensive testing of 72 full-scale concrete masonry wall specimens subjected to eccentric axial loads. To assess the flexural rigidity of the walls, they measured the strain at the tension and compression faces of each wall's cross-section to determine the curvature. Using the moment–curvature relationship, the flexural rigidity could be evaluated. Based on their experimental data, the authors proposed two equations for estimating flexural rigidity:

$$EI_{eff} = 0.7 E_m I_o \quad \text{for} \quad 0 \leq \frac{e}{t} \leq 0.18 \quad (2.19a)$$

$$EI_{eff} = 2.7 E_m I_o e^{-7.5 \left(\frac{e}{t} \right)} \geq E_m I_{cr} \quad \text{for} \quad \frac{e}{t} > 0.18 \quad (2.19b)$$

Liu and Dawe (2001) tested another set of 36 reinforced concrete masonry walls. Using the strain values recorded experimentally at the tension and compression faces of wall cross-sections, they employed the moment-curvature relationship shown in Eq. 2.20 to estimate the effective flexural rigidity of the wall specimens.

$$EI = \frac{M}{\phi} \quad (2.20)$$

$$\phi = \frac{\varepsilon_1 - \varepsilon_2}{t} \quad (2.21)$$

where ε_1 = strain in the tension face of the masonry and
 ε_2 = strain in the compression face of the masonry.

Analytical studies were later used to determine the flexural rigidity of masonry walls, as Liu and Dawe (2003) performed a computer-based study of effective flexural rigidity of loadbearing masonry walls. They used the numerical model they developed to determine a wall's effective flexural rigidity considering the effects of various parameters, such as reinforcement ratio, load eccentricity ratio, end eccentricities, and the slenderness effect. The equations from the study are displayed below.

$$\frac{EI_{eff}}{EI_o} = 0.8 - 1.95 \left(1 - 0.01 \frac{h}{t}\right) \left(\frac{e}{t}\right) \quad for \quad 0 \leq \frac{e}{t} \leq 0.4 \quad (2.22a)$$

$$\frac{EI_{eff}}{EI_o} = 0.022 \left(1.00 + 0.35 \frac{h}{t}\right) \quad for \quad \frac{e}{t} > 0.4 \quad (2.22b)$$

Mohsin (2003) performed an extensive parametric study on slender masonry walls subjected to eccentric axial loads. Using a database of over 300 specimens, he conducted a nonlinear regression analysis to determine expressions for the effective flexural rigidity of masonry walls with a base rotational stiffness. Key parameters identified when creating the expression were the base rotational stiffness ratio, load eccentricity ratio, and slenderness ratio. Expressions produced from the study and the data ranges they are considered valid over are presented below:

$$\frac{EI_{eff}}{EI_o} = \left[\left\{ 5 + 0.32 \left(\frac{h}{t}\right) - 0.0039 \left(\frac{h}{t}\right)^2 \right\} \left\{ 0.0158 e^{-0.0158 \left(\frac{e}{t}\right)} \right\} \left\{ 5 + 2.9r - 12r^2 \right\} \right] \quad (2.23a)$$

Valid for $e/t < 0.33$, $h/t \leq 42$, and $r \leq 0.26$.

$$\frac{EI_{eff}}{EI_o} = \left[\left\{ 0.01 + 0.12 \left(\frac{h}{t} \right) - 0.00094 \left(\frac{h}{t} \right)^2 \right\} \left\{ 0.0787 e^{-0.0787 \left(\frac{e}{t} \right)} \right\} \left\{ 3 + 1.836r - 12r^2 \right\} \right] \quad (2.23b)$$

Valid for $0.33 \leq e/t < 0.42$, $30 \leq h/t \leq 42$, and $0 \leq r \leq 0.26$.

$$\frac{EI_{eff}}{EI_o} = \left[\left\{ 1 - 0.05 \left(\frac{h}{t} \right) - 0.000892 \left(\frac{h}{t} \right)^2 \right\} \left\{ 1.7024 e^{-0.0133 \left(\frac{e}{t} \right)} \right\} \left\{ 1 + 2.2r - 12r^2 \right\} \right] \quad (2.23c)$$

Valid for $0.33 \leq e/t < 0.42$, $30 \leq h/t \leq 36$, and $0 \leq r \leq 0.051$.

It is evident from the available literature that scarce research has been performed on the incorporation of actual boundary condition effects on the behaviour of loadbearing masonry walls. And of the research performed on base fixity, no studies have attempted to incorporate the effects of lateral loads, a critical factor in the design of slender masonry walls. Thus, it is necessary to conduct the current research to determine the effect of rotational base stiffness on the behaviour of loadbearing walls subjected to gravity and OOP loads.

3 EXPERIMENTAL PROGRAM

3.1 Introduction

This chapter presents the experimental program developed to test loadbearing masonry walls with a reactive rotational support condition and their material properties (masonry assemblage, grout, mortar, masonry units, and reinforcing steel). Based on the literature available, it is evident that few experimental programs have been conducted involving loadbearing masonry walls subjected to both gravity and OOP loads or walls with reactive rotational support stiffness. In this study, four moderately slender masonry walls with typical reinforcing details were tested under a combination of gravity and OOP loads. To determine the effect of base fixity, each wall specimen featured a unique rotational support stiffness at the base to simulate the effect of a strip footing foundation. Walls were tested in a cyclic fashion to determine the effects of base degradation. Results from each wall test, including their load-deflection histories, load-moment histories, moment profiles, and deflection profiles, are discussed and presented.

3.2 Numerical Estimation of Rotational Support Stiffness

Prior to beginning the experimental program, a numerical simulation using the open-source FE program OpenSEES was conducted to determine the rotational support stiffness provided by typical shallow strip footing foundations (Fig. 3.1). Strip footings were selected in this study as they are commonly used for masonry walls due to their continuous spans and ability to spread the gravity loads within the wall across an area of soil. Soil piles were excluded as loadbearing masonry walls are often lightly loaded axially and do not require the additional bearing capacity. The magnitude of rotational restraint these foundations provide at the base of the wall is a function of the soil properties and foundation geometry. An FE model capable of analyzing the behaviour of strip footing foundations is developed in this section, and it is later used to determine the rotational support stiffness values to be used in the experimental program. The simulation of the rotational support stiffness in the experimental setup is discussed in a later section.

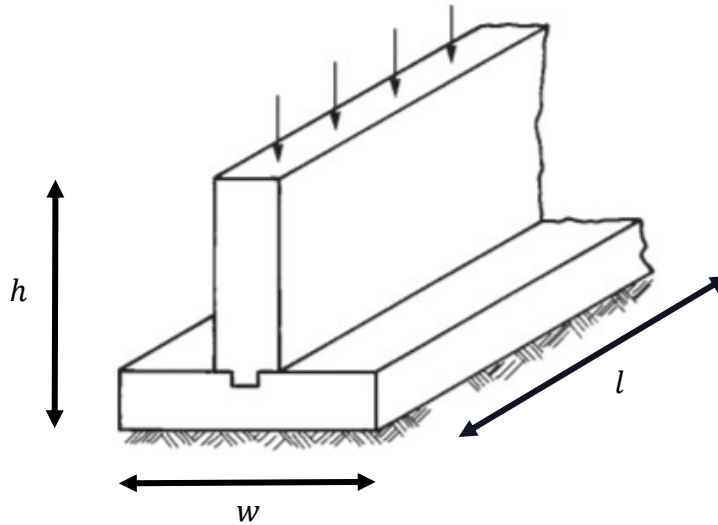


Figure 3.1 – Shallow Strip Footing Foundation

3.2.1 OpenSEES Finite Element Model for Strip Footing Foundations

Foundations were modelled as a 2D series of nodes connected by nonlinear beam-column elements (Fig. 3.2a). The constitutive material behaviour of the elements was defined using the pre-defined Concrete02 material model. The model is a Kent and Park (1971) concrete model with degrading linear unloading/reloading stiffness as per the work of Karsan and Jirsa (1969). A concrete compressive strength (f'_c) of 30 MPa was specified for all elements in the model. A linear response for the soil was assumed, and the soil-foundation interaction was captured by defining elastic springs along the bottom edge of the foundation. The stiffness of each spring was calculated to correspond to the modulus of subgrade reaction of the soil multiplied by the base area of the footing (calculated as $l \times w$ in Fig. 3.1). Typical values for modulus of subgrade reactions for different soil types are presented in Table 3.1.

Since the objective was to calculate the rotational stiffness of the foundation, an applied moment was specified at the top of the foundation for the analysis. This moment was increased throughout the analysis until the rotation at the top of the foundation (Fig. 3.2b) reached a value of 1 radian. The corresponding moment to cause this rotation was taken as the rotational support stiffness (units of kNm/radian). The soil was assumed elastic

and the rotational support stiffness of the foundation was assumed to be a function of the foundation's geometry and the modulus of subgrade solely for the underlying soil (the effect of side soil is neglected). It is assumed that the top of the footing does not move laterally under the applied moment.

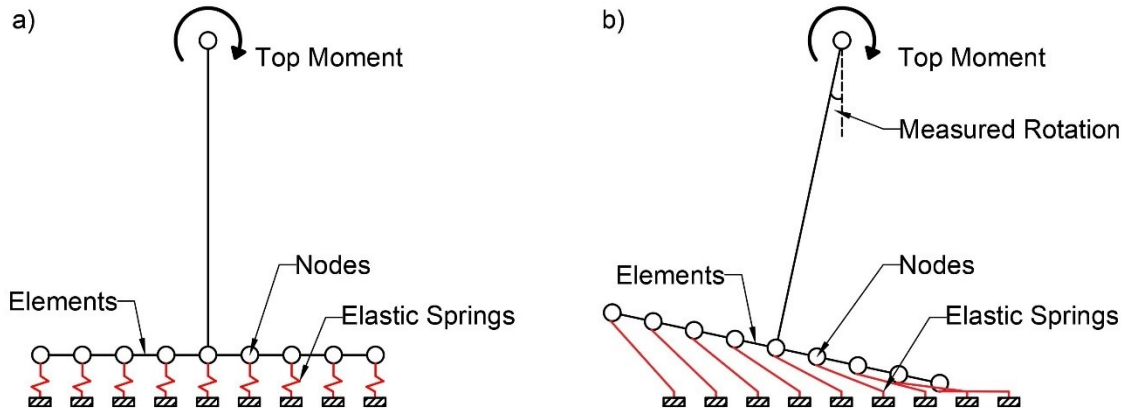


Figure 3.2 – Finite Element Foundation Model a) Prior to Analysis b) During Analysis

Table 3.1 – Modulus of Subgrade for Various Soils

Soil Type	Modulus of Subgrade (kN/m ³)
Loose Sand	4,800–16,000
Medium Dense Sand	9,600–80,000
Dense Sand	64,000–128,000
Clayey Medium Dense Sand	32,000–80,000
Silty Dense Sand	24,000–48,000
Clay Soil	12,000–48,000

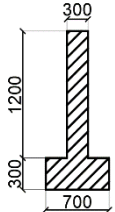
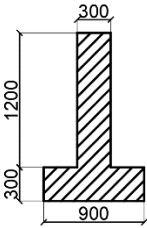
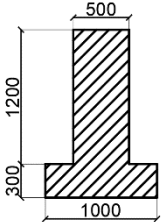
Reference: Foundation Analysis and Design by Joseph E. Bowles

3.2.2 Support Stiffness Assessment

Two wall types were considered in the calculation of rotation stiffness: slender, single-story masonry walls and multi-story, non-slender masonry walls. Slender, single-story masonry walls are typically subjected to lighter gravity loads (often just a roof load) than their multi-story counterparts but are much more susceptible to OOP bending due to their

longer unsupported spans. The foundation design of slender walls is often governed by overturning moment, which results in a smaller foundation length than that of a non-slender wall, whose design is often governed by bearing capacity due to the large gravity loads present in the wall (a large foundation area is required to adequately distribute the loads). Table 3.2 below presents the strip footing dimensions and soil type associated with these values of rotational stiffness.

Table 3.2 – Numerically Determined Support Stiffness

Support Stiffness (kNm/rad)	Strip Footing Dimensions (mm)	Soil Type
2,300		Clayey Medium Dense Sand
5,000		Medium and Dense Sand
9,500		Dense Sand

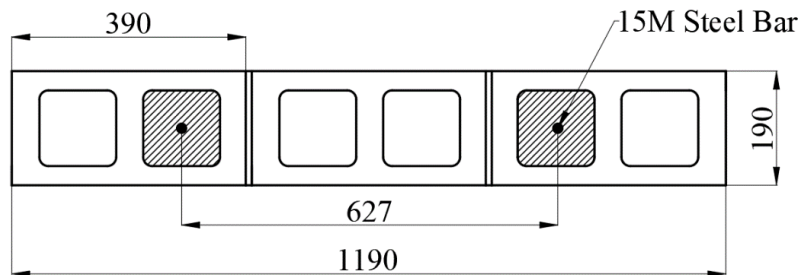
Analyzing the foundations of slender masonry walls, the rotational stiffness provided ranges from 1,500 kNm/rad to 3,500 kNm/rad depending on the soil type. Foundations of non-slender multi-story masonry walls provide much larger rotational stiffnesses, ranging from 9,000 kNm/rad to 12,000 kNm/rad. Data relating different foundation geometry and soil type to rotational stiffness can be found in Appendix A.

Based on the results presented above, and experimental constraints (such as the practical length of the foundation beam used in the experimental test, Fig. 3.11) three values of rotational stiffness were chosen for this investigation: 2,300 kNm/rad, 5,000 kNm/rad, and 9,500 kNm/rad. It is assumed that these cover a practical range of foundation rotational stiffnesses found in practice.

3.3 Test Specimens

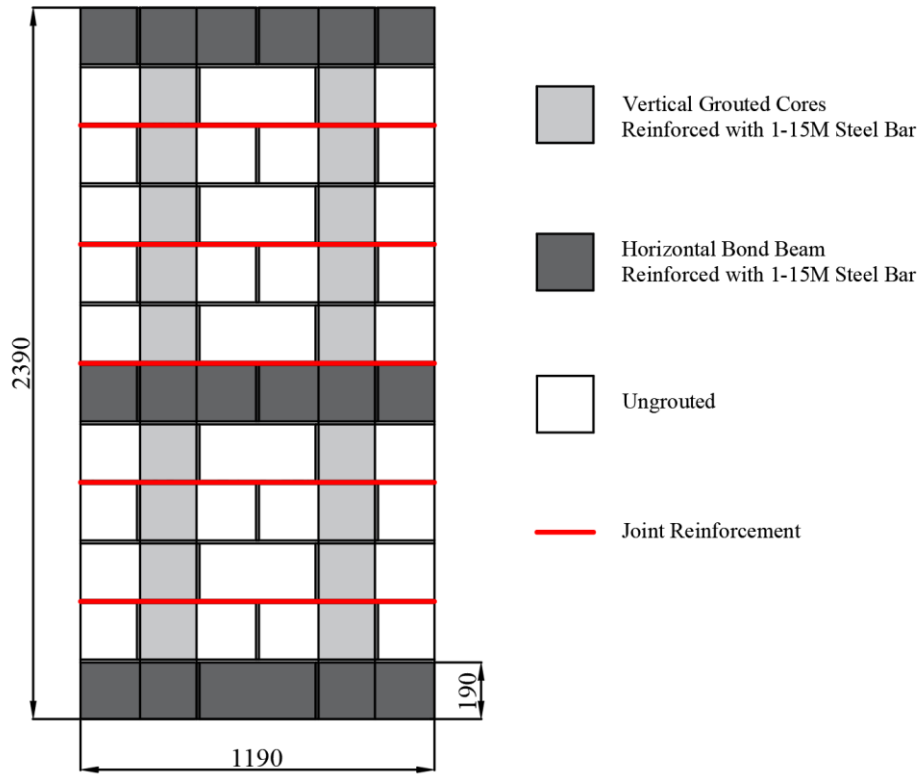
Four wall specimens were constructed with standard 20-cm hollow concrete masonry units with a specified compressive strength of 15 MPa. Each specimen measured 12 courses (2.4 m) in height and 3 courses (1.2 m) wide. Specimens were constructed in running bond pattern by certified masons. All specimens were constructed on 1 in (25.4 mm) thick steel plates to accommodate the handling and transportation of the walls before and after testing.

Reinforcement detailing was designed to reflect typical masonry wall block design practices. Vertical reinforcement consisted of two 15M steel reinforcing bars located in the second cell from each end of the specimen (600 mm on centre). Each bar was welded to the steel plate. Bond beams and bed joint reinforcement were used for horizontal reinforcement. Standard ladder joint reinforcement was placed every second course, while bond beams consisting of a single 15M steel reinforcing bar were located at the 1st, 6th, and 12th courses. All cells containing reinforcing steel were grouted with standard course grout. Reinforcing details can be found in Fig. 3.4.



* dimensions in mm

Figure 3.3 – Specimen Cross-Section



** dimensions in mm*

Figure 3.4 – Specimen Profile



Figure 3.5 – Specimen Construction (Bond Beams)



Figure 3.6 – Specimen Construction (Bed Joint Reinforcement)



Figure 3.7 – Completed Specimens

3.4 Material Properties

3.4.1 Mortar

Type S mortar was used for all joints during the wall and prism construction. The mortar was mixed on-site by certified masons. The specified compressive strength of the mortar was determined by crushing six 2-in (51-mm) mortar cubes under a concentric axial load as per CSA A179. Each cube mold had been filled with mortar used directly in the construction of the walls. Results from the tests indicated a specified compressive strength of 13.8 MPa. Data from the mortar cube tests are presented in Table 3.3.

Table 3.3 – Mortar Cube Data

Specimen	Peak Axial Load (kN)	Compressive Strength (MPa)
1	37.6	14.6
2	33.7	13.1
3	36.4	14.1
4	34.6	13.4
5	35.4	13.7
6	35.2	13.6
Average		13.8

3.4.2 Grout

Course grout was used to fill all required cells during wall and prism construction. The grout was mixed on-site to a suitable workability by certified masons. The specified compressive strength of the grout was determined by crushing four 4-in (102-mm) grout cylinders under a concentric axial load as per CSA A179. Each cylinder mold had been filled with grout used directly in the construction of the walls. Results from the tests indicated the specified compressive strength of the grout was 35.9 MPa. Data from the grout cylinder tests are presented in Table 3.4.

Table 3.4 – Grout Cylinder Data

Specimen	Peak Axial Load (kN)	Compressive Strength (MPa)
1	210	26.0
2	320	39.5
3	326	40.2
4	309	38.1
Average		35.9

3.4.3 Masonry Assemblage

Standard 20-cm concrete masonry unit blocks were used to construct a total of 20 masonry prisms. The heights of the prisms varied to reflect the two North American

standards, with 10 prisms being 2 courses (390 mm) in height (representative of the American standard, TMS 402/602-16) and the remaining 10 prisms being 5 courses (990 mm) in height (representative of the Canadian standard, CSA S304-14). For each group, 5 of the 10 prisms were grouted, while the other 5 were hollow. As per testing standards, each of the 5-course prisms was constructed in a running bond pattern, while the 2-course prisms were constructed in stack bond.

The rationale for testing two different prism heights is based on constructability. The current Canadian standard requires prisms to be at least 5-courses high to utilize the full compressive strength of the prisms as the compressive strength of the masonry assemblage. Construction and testing of 5-course prisms, however, are often difficult due to the weight of the prisms and ensuring a uniform loading surface. In consequence, designers often opt to use conservative values for the masonry compressive strength listed within the standard rather than conducting prism tests. In the American standard, designers are permitted to use the compressive strength of a 2-course prism as the compressive strength of the masonry assemblage. If it can be shown that the compressive strength of the 2-course does not vary greatly over the 5-course prism or the compressive strength of the 2-course prism presents a better correlation with numerical models than the 5-course prisms, an argument can be made to allow Canadian designers to test 2-course prisms in means to determine the compressive strength of the masonry assemblage. This would allow simplistic method to more accurately determine the compressive strength of the masonry assemblage resulting in a more economical masonry solution.



Figure 3.8 – 5-Course (Hollow and Grouted) and 2-Course Grouted Masonry Prisms



Figure 3.9 – 2 Course Hollow Masonry Prisms

The masonry prisms were tested under concentric axial load with an MTS-6000 hydraulic jack. Hydrostone was poured on both ends of the grouted prisms (both 2-course and 5-course) to ensure a smooth loading plane. Fibreboard was placed on the top and bottom ends of all specimens during testing. Data collected from the tests include axial load and vertical displacement of the MTS head.

The failure mode for the grouted prisms consisted of diagonal cracking followed by the crushing of the face shell at peak load. Hollow prisms failed with the splitting of the webs. Results from the tests showed the grouted prisms typically had a higher axial load capacity but lower compressive strength than the hollow prisms. The average compressive strength for the 2-course hollow and grouted prisms were 24.6 MPa and 17.6 MPa, respectively. The average compressive strength for the 5-course hollow and grouted prisms were 23.6 MPa and 16.8 MPa, respectively. The average compressive strength of the 20-cm masonry unit was 26.3 MPa. Data from the tests along with the coefficient of variation (CV) are presented in Tables 3.5–3.9, while Table 3.10 provides a summary of the results.

Table 3.5 – 2-Course Hollow Prism Data

Specimen	Peak Axial Load (kN)	Compressive Strength (MPa)
1	1042	26.4
2	815	20.6
3	971	24.6
4	1019	25.8
5	1008	25.5
Average		24.6

Table 3.6 – 2-Course Grouted Prism Data

Specimen	Peak Axial Load (kN)	Compressive Strength (MPa)
1	1389	18.7
2	1026	13.9
3	1343	18.1
4	1372	18.5
5	1391	18.8
Average		17.6

Table 3.7 – 5-Course Hollow Prism Data

Specimen	Peak Axial Load (kN)	Compressive Strength (MPa)
1	654	20.4
2	661	20.7
3	755	23.6
4	806	25.2
5	894	27.9
Average		23.6

Table 3.8 – 5-Course Grouted Prism Data

Specimen	Peak Axial Load (kN)	Compressive Strength (MPa)
1	883	11.9
2	1378	18.6
3	1254	16.9
4	1484	20.0
5	1223	16.5
Average		16.8

Table 3.9 – Single 20-cm Unit Data

Specimen	Peak Axial Load (kN)	Compressive Strength (MPa)
1	1079	27.3
2	984	24.9
3	1053	26.6
4	1103	27.9
5	1084	27.4
Average		26.3

Table 3.10 – Masonry Assemblage Properties Summary

Specimen	Average Compressive Strength (MPa)	Coefficient of Variation
2-Course Hollow Prisms	24.6	0.09
2-Course Grouted Prisms	17.6	0.12
5-Course Hollow Prisms	23.6	0.13
5-Course Grouted Prisms	16.8	0.18
Single 20-cm Masonry Unit	26.3	0.04

3.4.4 Reinforcing Steel

All test specimens were constructed using grade 400 15M steel rebar from the same batch. Three standard tensile tests were conducted to determine the material properties of the rebar. Results from the tests indicated an average yield strength (f_y) of 533 MPa and a modulus of elasticity (E_s) of 198,817 MPa. Data from the rebar tensile tests are presented in Table 3.11.

Table 3.11 – Steel Rebar Properties

Specimen	Yield Strength (MPa)	Elastic Modulus (MPa)	Ultimate Strength (MPa)	Ultimate Strain (mm/mm)
1	530	193,752	690	0.099
2	542	198,171	698	0.108
3	528	204,528	691	0.101
Average	533	198,817	693	0.103

3.4.5 Predicted Ultimate Moment Capacity

The ultimate moment capacity of the wall specimens was predicted using design equations from the Canadian masonry standard (Table 3.12). Material strength reduction factors were set to 1 during the calculations. Values for the compressive strength of the masonry (f'_m) were based on the experimental results of the 2-course and 5-course prism tests. The ultimate moment capacity of the wall specimens using the compressive

strength of the masonry from the 2-course and 5-course masonry prisms was 41.2 kNm and 40.8 kNm respectively.

Table 3.12 – Ultimate Moment Capacity of the Wall Specimens

Type of prism used for Masonry properties	UngROUTED f'_m (MPa)	Grouted f'_m (MPa)	Ultimate Moment Capacity (kNm)
2-course	24.6	17.6	41.2
5-course	23.6	16.8	40.8

3.5 Experimental Setup

The experimental setup used in this program consisted of three major parts: a lateral bracing system, a system for gravity and lateral load application, and the simulation of the rotational stiffness at the base of the wall specimens. Figures 3.10 and 3.11 present the complete experimental setup for walls without and with rotational support stiffness respectively.

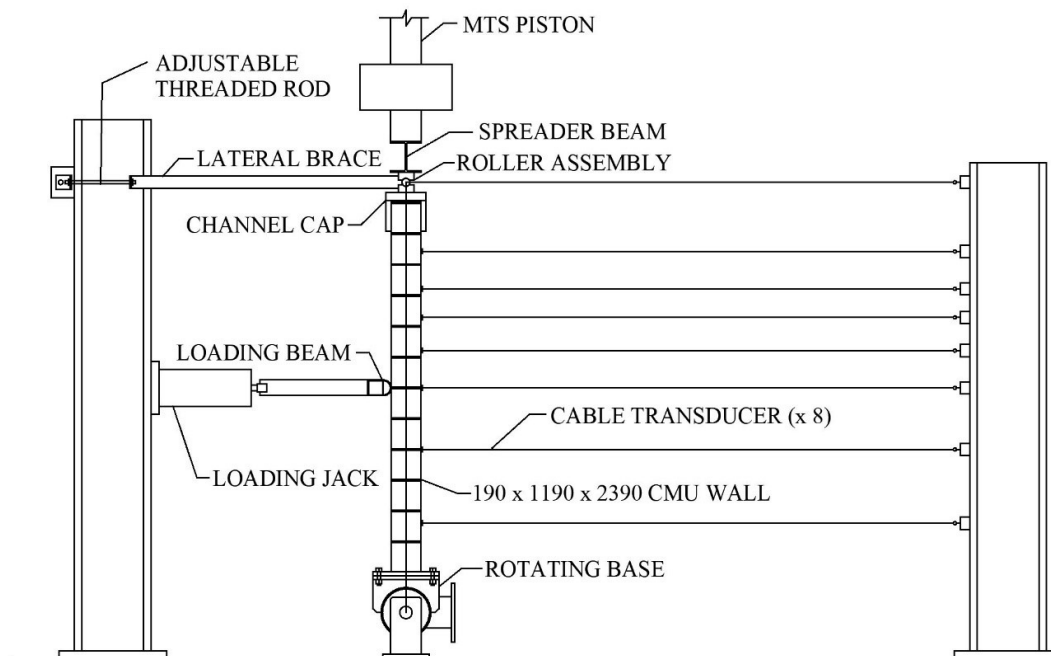


Figure 3.10 – Out-of-Plane Experimental Setup (Without Rotational Stiffness)

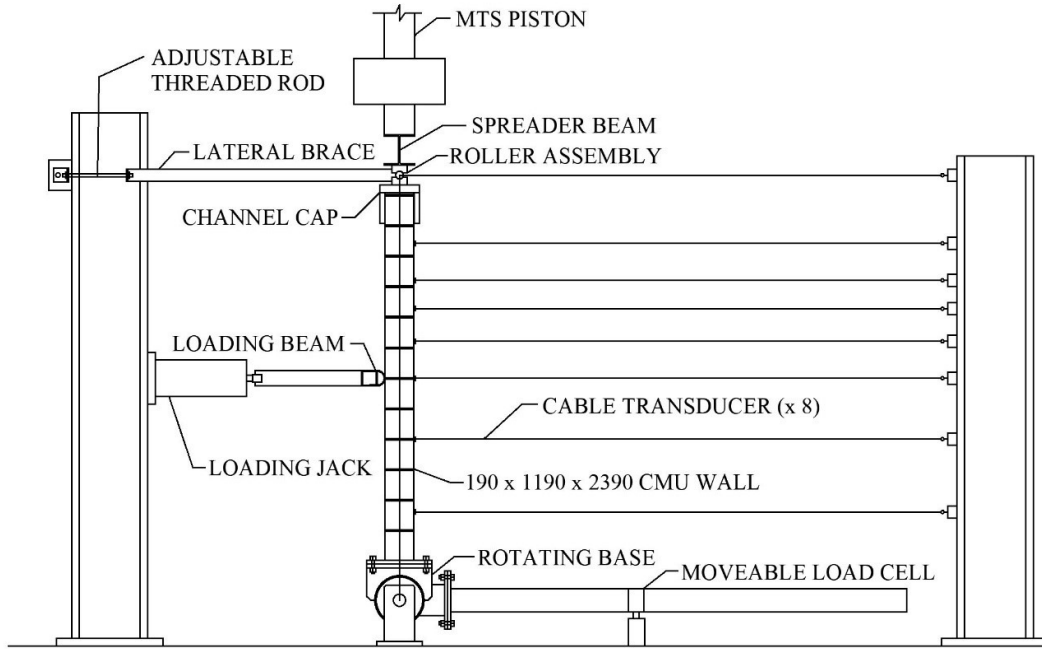


Figure 3.11 – Out-of-Plane Experimental Setup (With Rotational Stiffness)

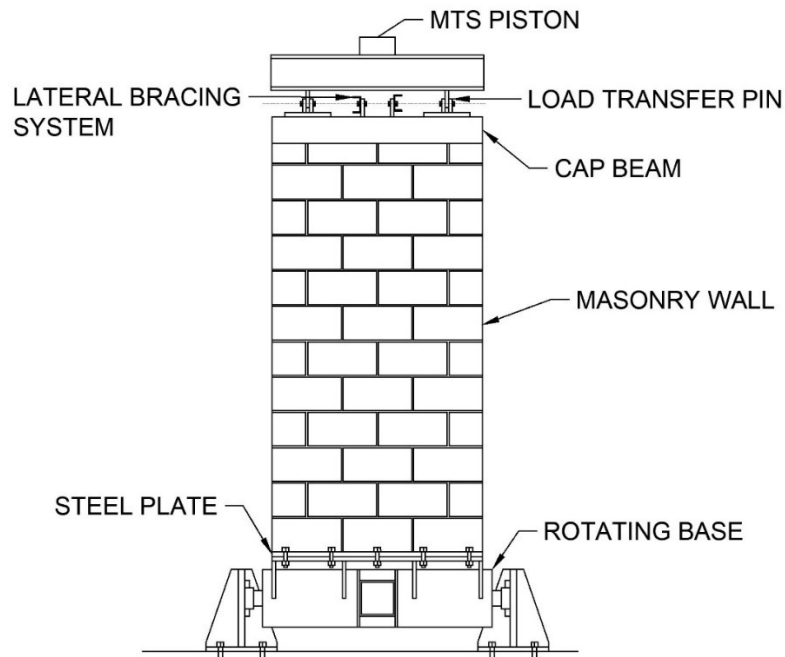


Figure 3.12 – In-Plane Experimental Setup



Figure 3.13 – Experimental Setup

3.5.1 Lateral Bracing System

The testing configuration was designed to simulate simple boundary conditions (i.e., a pinned bottom at the bottom of the wall with a lateral roller at the top). The bottom fixture (Fig. 3.14) consists of a rotating steel cylinder to which the base plate of each wall was bolted to using a total of 10 (5 on each side of the wall) 1-in (25.4-mm) structural bolts. The cylinder itself is hinged between two steel plates that were secured to the strong floor of the lab with 1-in (25.4-mm) floor rods. This system allows for the base of the wall to rotate OOP freely while restricting any horizontal and vertical movement. The top fixture (Fig. 3.15) utilizes a steel channel cap firmly secured to the top of the masonry wall. Two steel channels then have one end bolted to the top channel cap and the other the support column. To ensure no lateral displacement during testing, the channels connected to the channel cap featured an adjustable threaded rod (Fig. 3.16). By tightening the bolts along

the threaded rod, the wall can be pulled back into place during testing if lateral displacement at the top of the wall occurs.



Figure 3.14 – Bottom Lateral Bracing Fixture



Figure 3.15 – Top Lateral Bracing Fixture



Figure 3.16 – Adjustable Threaded Rods

3.5.2 Gravity and Lateral Load Application

The vertical load was applied to the top of the wall using an MTS 6000 hydraulic ram. To transfer the load from the MTS to the top of the wall, a steel loading beam was connected to the MTS crosshead (Fig. 3.17). Contact between the loading beam and channel cap was made through two pins on both ends of the loading beam. These pins allowed for the load to be transferred without restricting any rotation experienced by the top of the wall during testing.

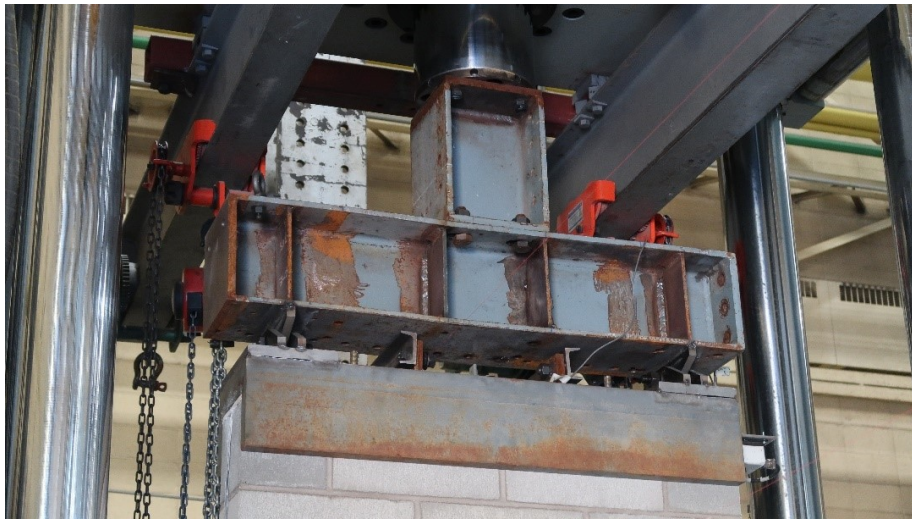


Figure 3.17 – Gravity Load Application

The lateral load was applied to the wall in a three-point bending configuration. A loading jack with a capacity of 539 kN transferred the load through a steel spreader beam constructed of hollow structural steel (HSS) sections (Fig. 3.18) to the wall. A Teflon strip was placed at the point of contact between the spreader beam and masonry wall to ensure a uniform distribution of load along the wall. The spreader beam was levelled before each test.



Figure 3.18 – Lateral Load Application

3.5.3 Simulation of Base Rotational Stiffness

The rotational support stiffness at the base of the wall specimens was simulated by rigidly connecting a steel HSS beam to the bottom fixture of the test setup and simply supporting the other end on the laboratory floor (Fig. 3.19). This allows for the rotational support stiffness at the base of the wall to be approximately proportionate to the flexural stiffness of the steel section. In this study, an HSS 152 x 152 x 6.4-mm steel beam was selected. The rotational support stiffness the beam provided at the base of the wall was varied by modifying the span of the beam. The value of rotational support stiffness provided by the HSS section was determined using a simple numerical model created in the FE program OpenSEES. Within the model, a simple supported HSS section would be subjected to an increasing end moment (Fig. 3.20) until the rotation of the section at the location of the end moment reached a value of 1 radian. The moment required to cause

this rotation was defined as the rotational stiffness of the section. To achieve the desired values of support stiffness listed in section 3.2.2, the unsupported span of the beam was varied, with shorter and longer spans providing larger and smaller values of rotational support stiffness respectively. The material properties of the HSS section were assumed elastic with an elastic modulus of 200,000 MPa. Details of the spans selected, and their respective rotational stiffness can be found in Table 3.13.

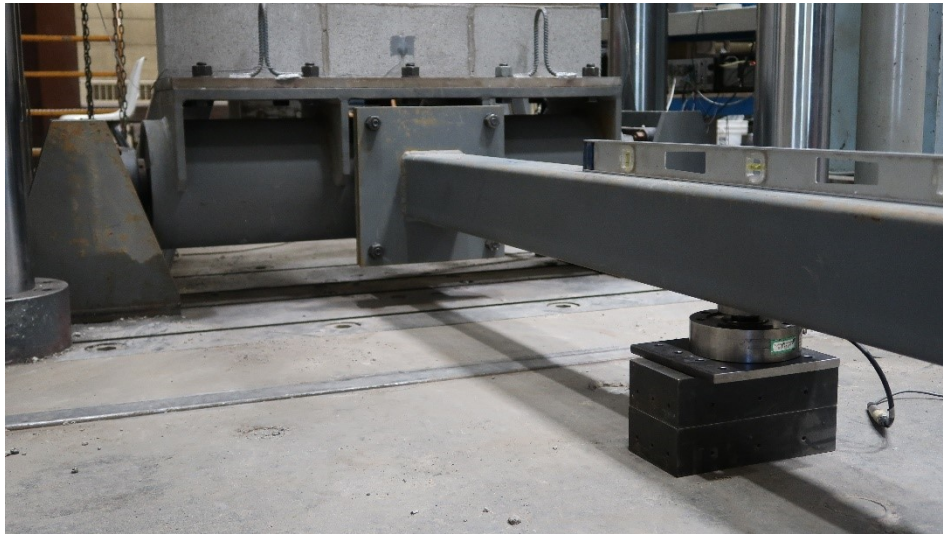


Figure 3.19 – Simulation of Base Rotational Stiffness

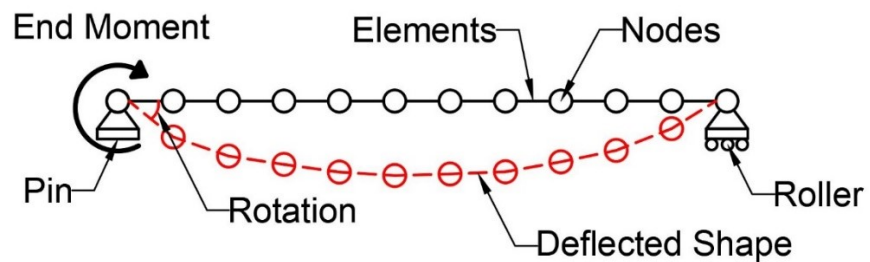


Figure 3.20 – Simulated Support Stiffness FE Model

Table 3.13 – Simulated Rotational Stiffness

Specimen	Rotational Stiffness (kNm/rad)	HSS Section (mm)	HSS Section Span (m)
1	0	-	-
2	2,300	HSS 152 x 152 x 6.4	3.5
3	5,000	HSS 152 x 152 x 6.4	1.5
4	9,500	HSS 152 x 152 x 6.4	0.75

3.6 Instrumentation

Instrumentation consisted of strain gauges, load cells, inclinometers, and linear variable differential transformers (LVDTs), all connected electronically through 31 channels. Each reinforcing bar contained 4 strain gauges: one located at the midpoint, two located 16 in (406 mm) above and below the midpoint, and one located 5 in (127 mm) above the base of the reinforcing bar. Four more strain gauges were also added to the outer compression face of the masonry blocks. Inclinometers were used to determine the rotation at the top and bottom supports for all tests. The lateral deflection was measured through LVDTs placed over the height of the wall (locations presented in Table 3.14). More LVDTs were placed on the upper half of the wall to capture a possible rise in location of maximum deflection. Load cells connected to the MTS and loading jack measured both the vertical and lateral loads during testing. An additional load cell was placed under the simply supported end of the HSS section used to simulate the rotational stiffness at the base of the wall. Details of all instrumentation and strain gauge locations used can be found in Fig. 3.21 and 3.22 respectively.

Table 3.14 – LVDT Locations

LVDT	Location Relative to the Base of the Wall
1	12 in (305 mm)
2	28 in (711 mm)
3 (Midpoint)	44 in (1118 mm)
4	52 in (1321 mm)
5	60 in (1524 mm)
6	68 in (1727 mm)
7	76 in (1930 mm)
8 (Top of the Wall)	94 in (2390 mm)

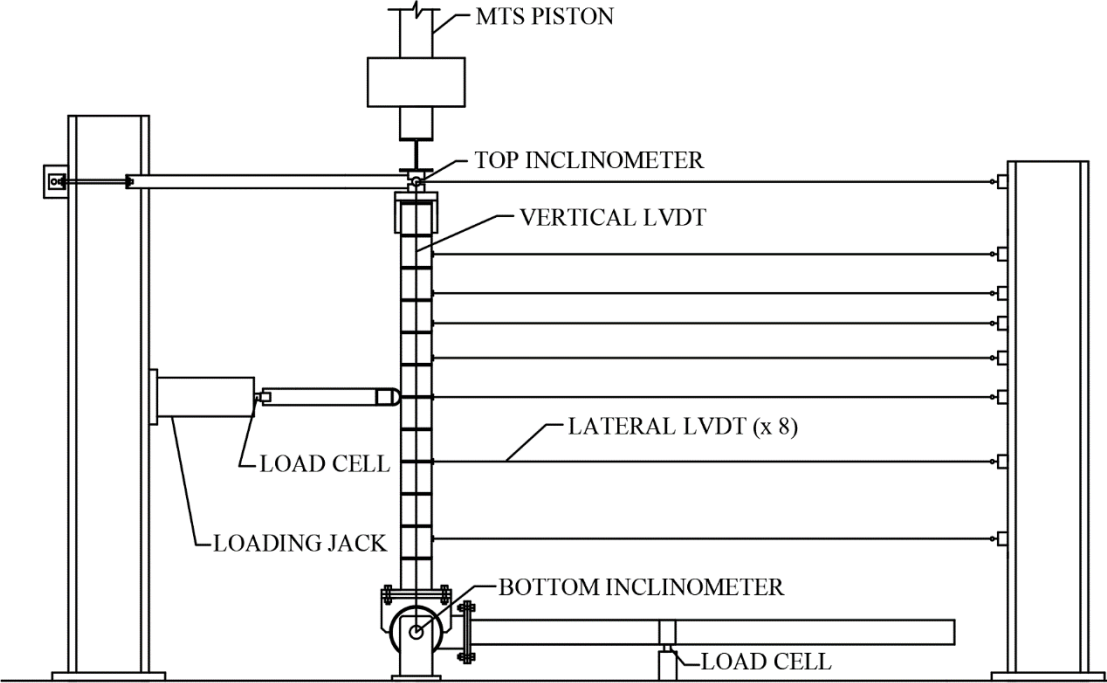


Figure 3.21 – Instrumentation

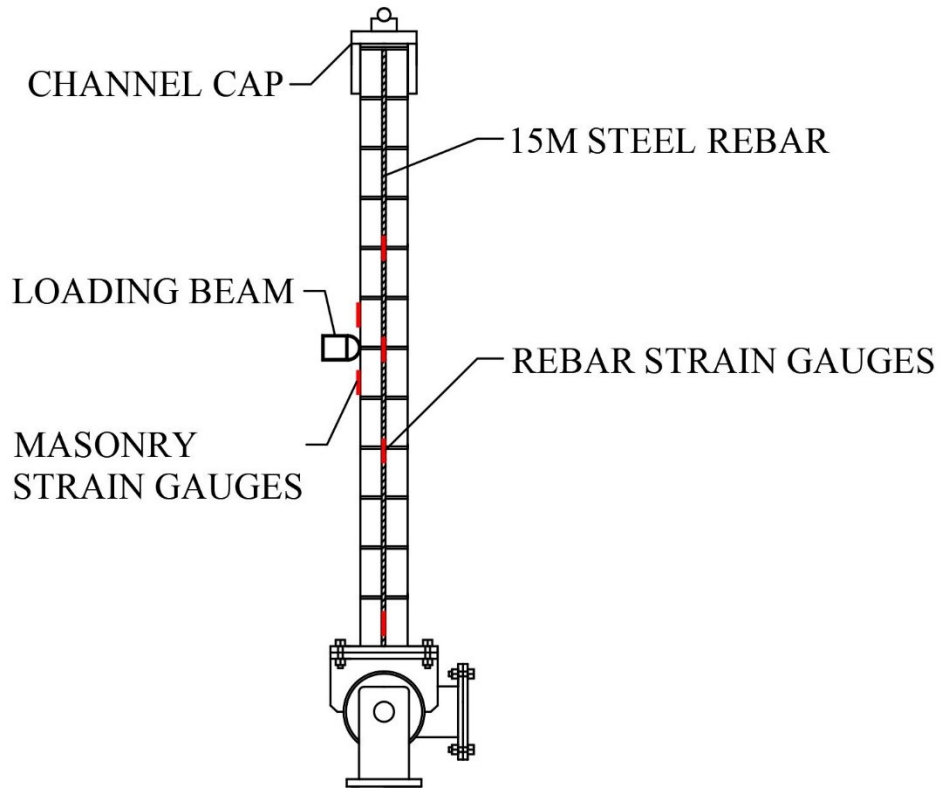


Figure 3.22 – Strain Gauge Locations

3.7 Testing Procedure

The walls were tested in two steps. First, a vertical load was applied to the top of the specimens in load control using the MTS 6000 and held. All test specimens were loaded with an axial load of 250 kN (approximately 10% of the compressive capacity of the specimen; a value commonly used in practice). Then, a hydraulic jack was used to apply a cyclic lateral load to the midpoint of the wall in cycles until failure occurred. A loading rate of 2 mm/min was used for cycles 1 to 4 and was then increased to 4 mm/min for the remainder of the test. The loading protocol of the cycles is shown in Fig. 3.23 and Table 3.15.

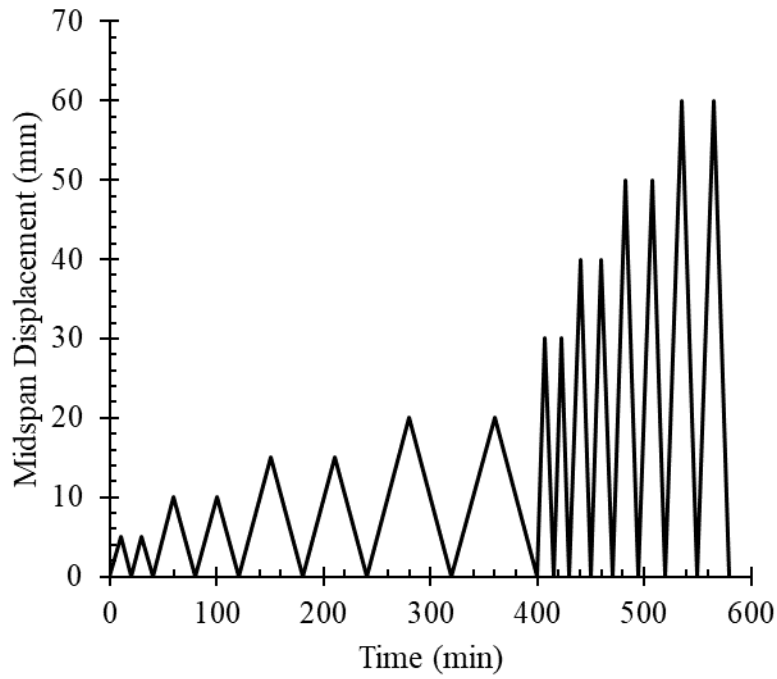


Figure 3.23 – Cyclic Loading Protocol

Table 3.15 – Lateral Loading Protocol

Cycle	Midpoint Displacement (mm)	Number of Runs	Loading Rate (mm/min)
1	5	2	2
2	10	2	2
3	15	2	2
4	20	2	2
5	30	2	4
6	40	2	4
7	50	2	4
8	60	2	4
9	Failure	-	4

3.8 Results and Observations

Results and observations noted during the testing of each wall are discussed below. All displacements and forces were obtained through LVDTs and load cells respectively. Rotations at the top and bottom of the wall were obtained with the clinometers. The load displacement, load rotation, moment profiles, and deflection responses are presented. A summary of all test results is shown in Table 3.16 below.

Table 3.16 – Summary of Test Results

Specimen	Base Stiffness (kNm/rad)	Peak Lateral Load (kN)	Midspan Deflection at Failure (mm)	Midspan Moment at Peak Load (kNm)	Base Moment at Peak Load (kNm)
1	0	52.2	69.1	40.6	0.0
2	2,300	87.4	50.6	40.0	-13.5
3	5,000	101	40.9	45.4	-36.0
4	9,500	95.9	43.2	42.9	-36.0

It is noted that the data presented for the total moment and deflection profiles are between the two points of rotation (i.e., 305 mm below and 75 mm above the masonry wall). As the points of rotation were located above and below the masonry wall, the effective height of the setup is larger than the height of the masonry wall (Fig. 3.24). In the figures that follow, a dashed line is included in the moment and deflection profiles to illustrate where the base of the masonry wall is located with respect to the rotation point.

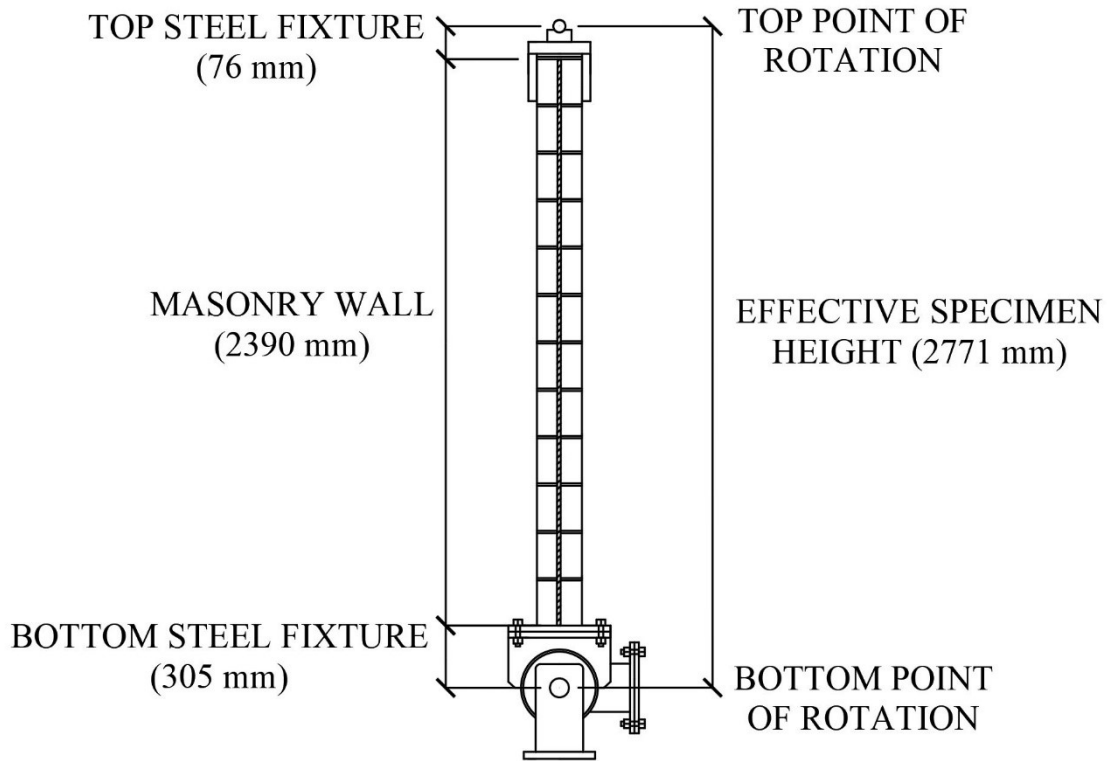


Figure 3.24 – Effective Specimen Height

3.8.1 Test 1 (Rotational Stiffness = 0 kNm/rad)

Specimen 1 was tested with zero rotational stiffness and acted as the reference wall in the experimental program. The cyclic lateral load–midspan displacement history of the specimen is presented in Fig. 3.25. The specimen was able to complete all 8 cycles before failure occurred. The first sign of failure occurred during the 20-mm cycle, when separation between the masonry units and mortar joints near the midspan of the specimen was observed (Fig. 3.29). The peak lateral load for the specimen was 52.2 kN with a corresponding midspan deflection of 29.5 mm. Failure occurred during the last cycle with the crushing of the masonry at the midspan. The midspan deflection at failure was 69.1 mm with a corresponding lateral load of 40.0 kN.

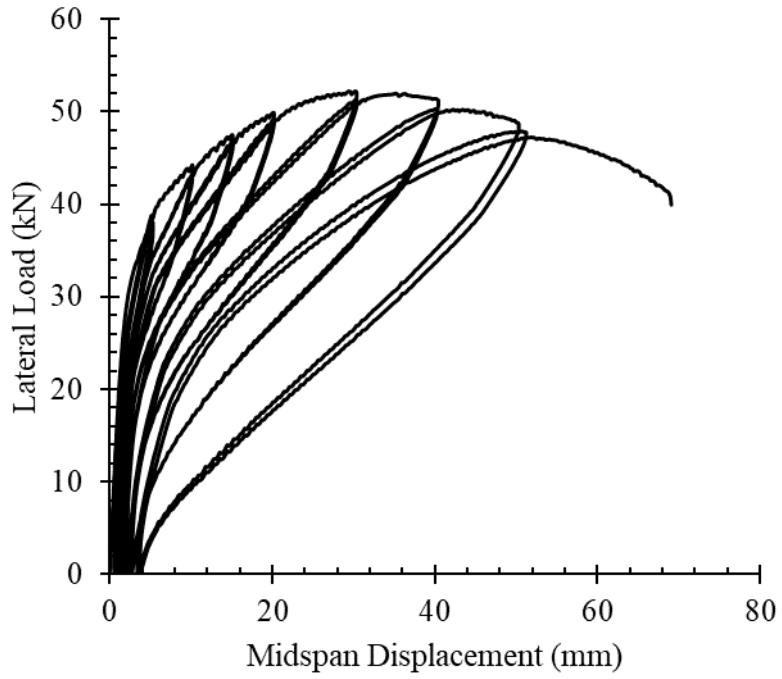


Figure 3.25 – Lateral Load–Midspan Displacement Response (Specimen 1)

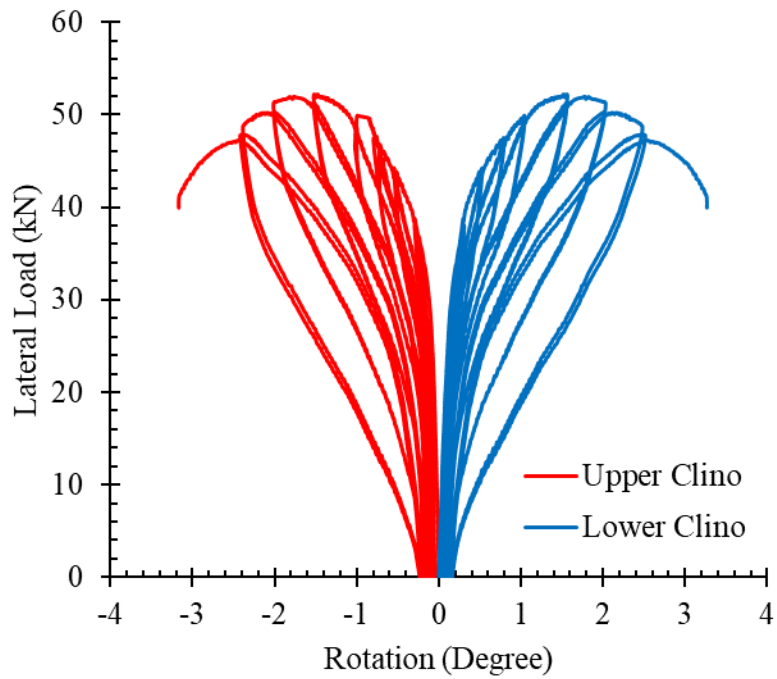


Figure 3.26 – Lateral Load–Base Rotation Response (Specimen 1)

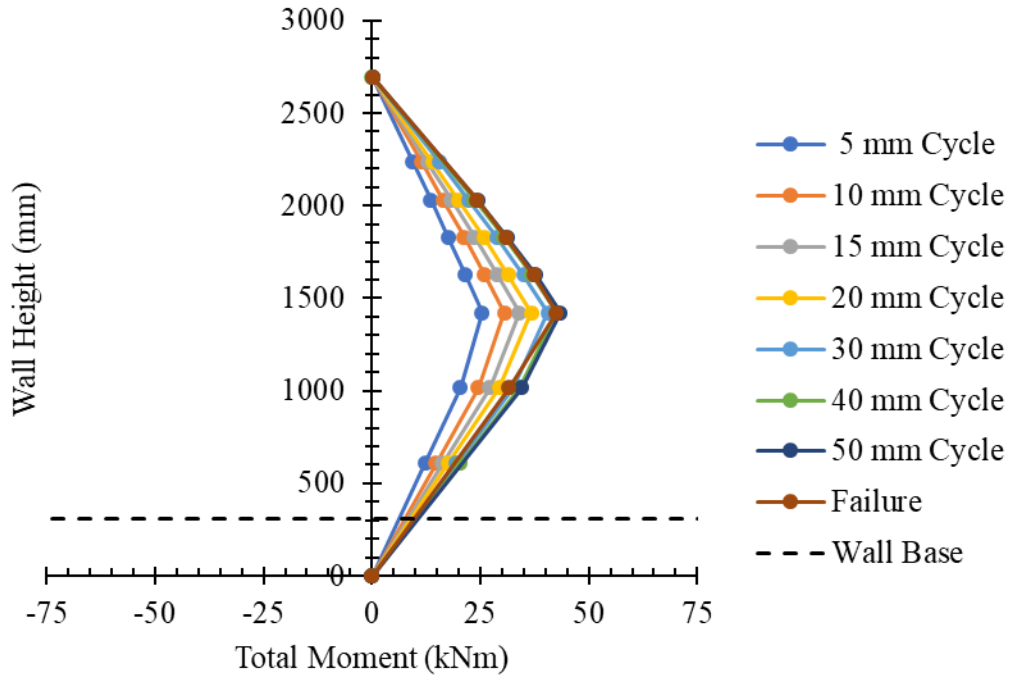


Figure 3.27 – Total Moment Profiles (Specimen 1)

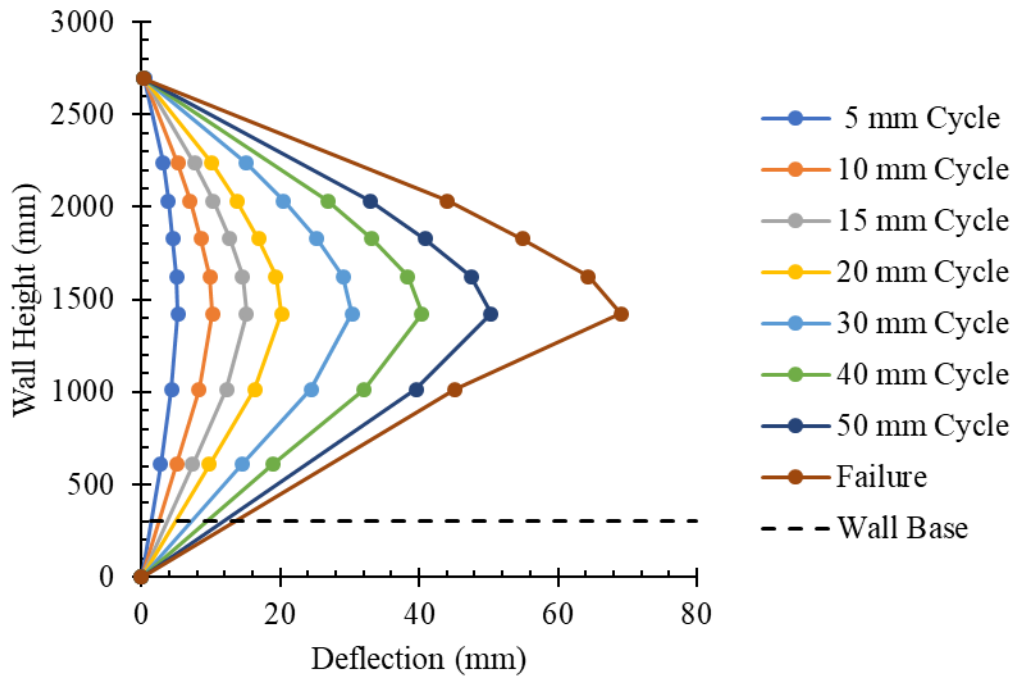


Figure 3.28 – Deflection Profiles (Specimen 1)

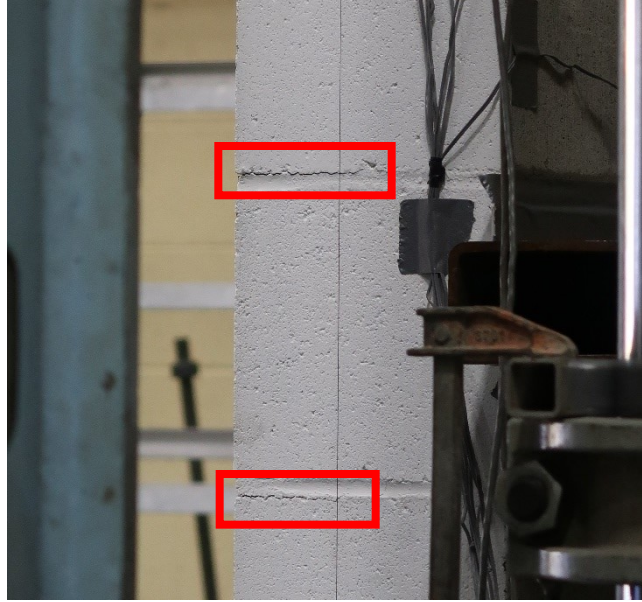


Figure 3.29 – First Signs of Failure (Specimen 1)



Figure 3.30 – Failure (Specimen 1)

3.8.2 Test 2 (Rotational Stiffness = 2,300 kNm/rad)

Specimen 2 was tested with a rotational stiffness of 2,300 kNm/rad at the base of the wall. The cyclic lateral load–midspan displacement history of the specimen is presented in Fig. 3.31. The specimen was not able to complete all 8 cycles before failure occurred. The first sign of failure occurred during the 15-mm cycle when separation between the masonry units and mortar joints near the midspan of the specimen was observed. The peak lateral load for the specimen was 87.4 kN with a corresponding midspan deflection of 38.0 mm. Failure occurred during the first 60-mm cycle, with the simultaneous crushing of the masonry along the bottom half of the wall. The midspan deflection at failure was 50.6 mm with a corresponding lateral load of 76.7 kN.

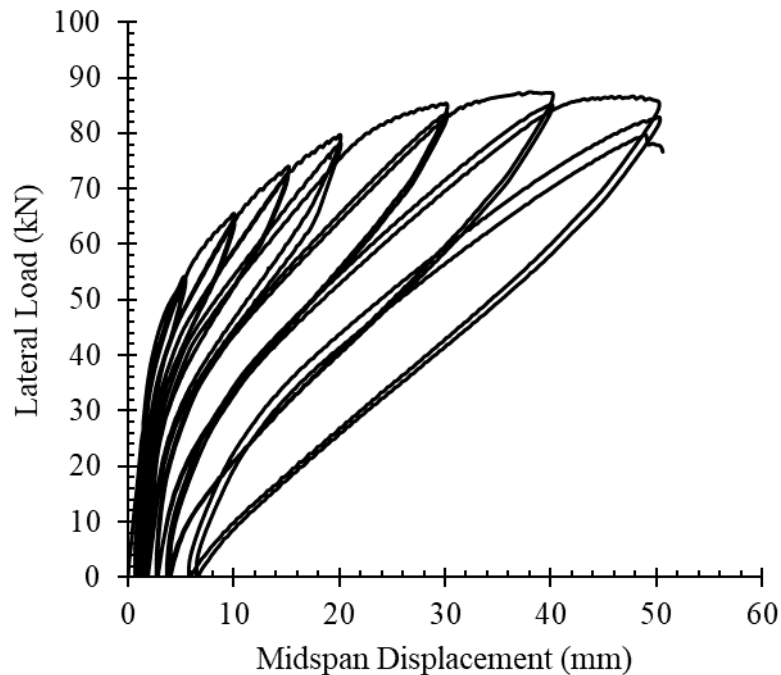


Figure 3.31 – Lateral Load–Midspan Displacement Response (Specimen 2)

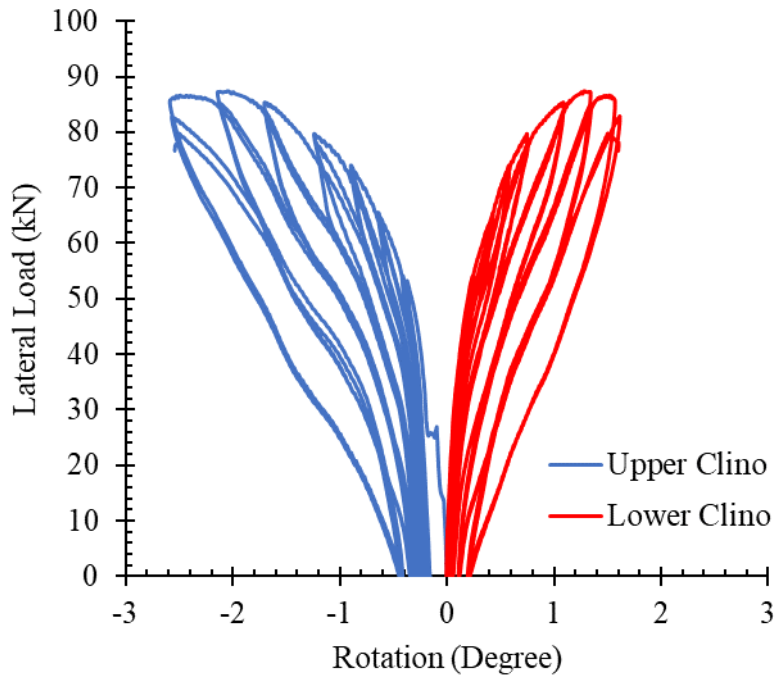


Figure 3.32 – Lateral Load–Base Rotation Response (Specimen 2)

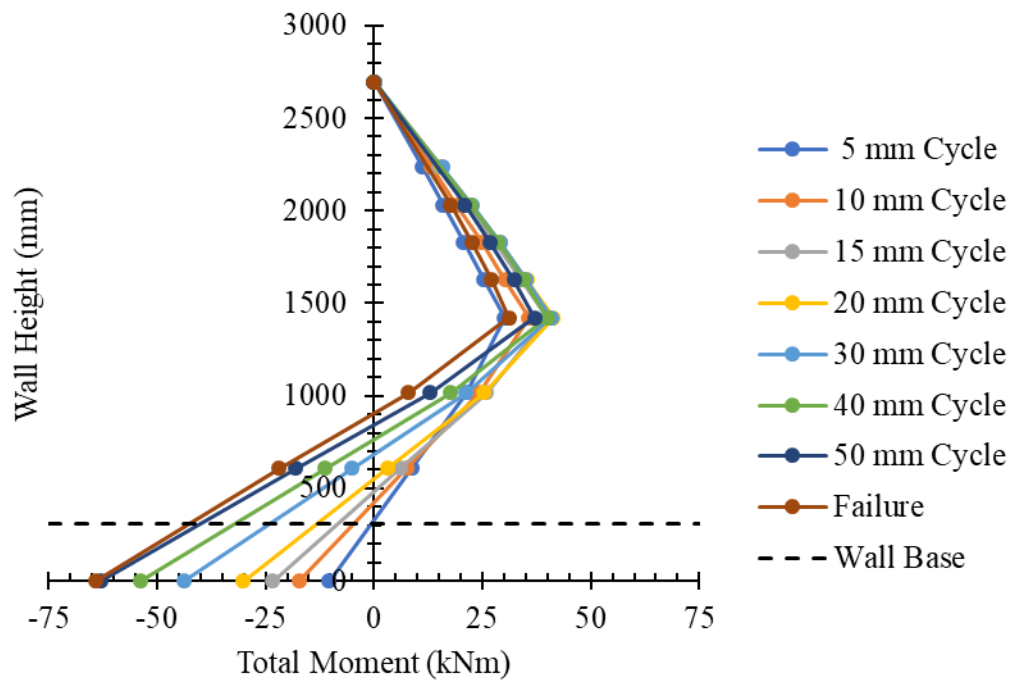


Figure 3.33 – Total Moment Profiles (Specimen 2)

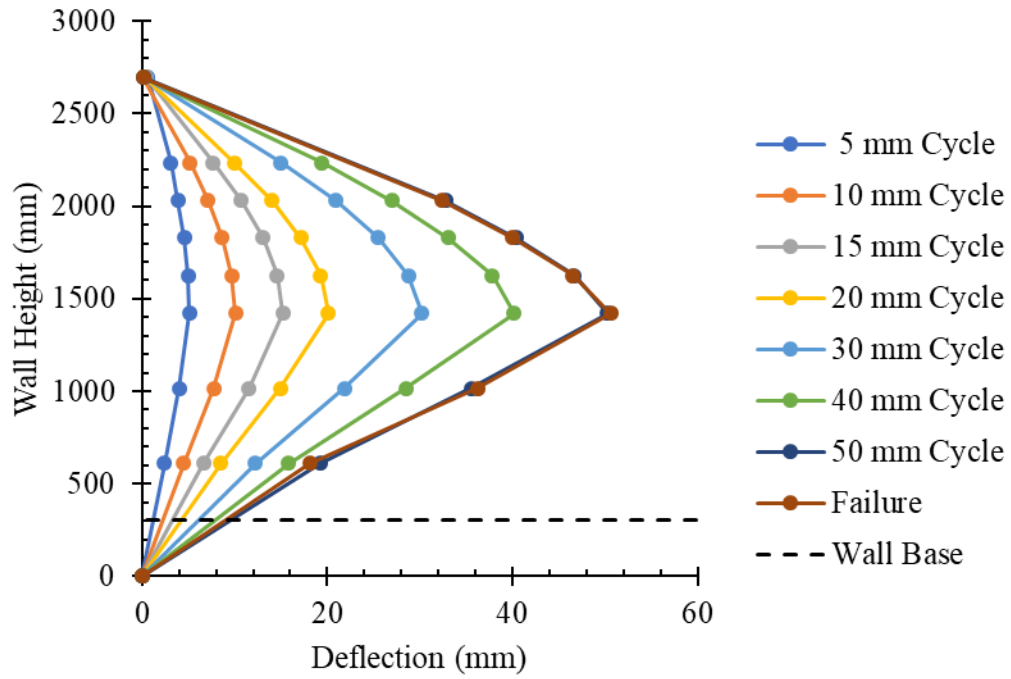


Figure 3.34 – Deflection Profiles (Specimen 2)



Figure 3.35 – Failure (Specimen 2)

3.8.3 Test 3 (Rotational Stiffness = 5,000 kNm/rad)

Specimen 3 was tested with a rotational stiffness of 5,000 kNm/rad at the base of the wall. The cyclic lateral load–midspan displacement history of the specimen is presented in Fig. 3.36. The specimen was not able to complete all 8 cycles before failure occurred. The first sign of failure occurred during the 10-mm cycle when separation between the masonry units and mortar joints near the midspan of the specimen was observed. The peak lateral load for the specimen was 101 kN with a corresponding midspan deflection of 37.0 mm. Failure occurred during the first 50-mm cycle, with the crushing of the masonry at the midspan. The midspan deflection at failure was 40.9 mm with a corresponding lateral load of 94.0 kN. It is worth noting that during the testing of the specimen, the cable for the base inclinometer came loose, resulting in a loss of data for the total moment profile during the 5-mm cycle (Fig. 3.38).

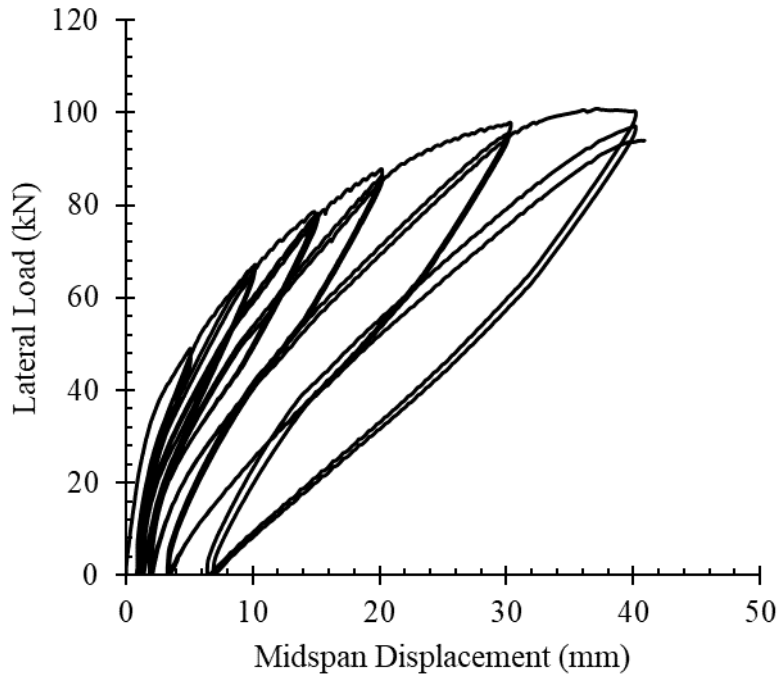


Figure 3.36 – Lateral Load–Midspan Displacement Response (Specimen 3)

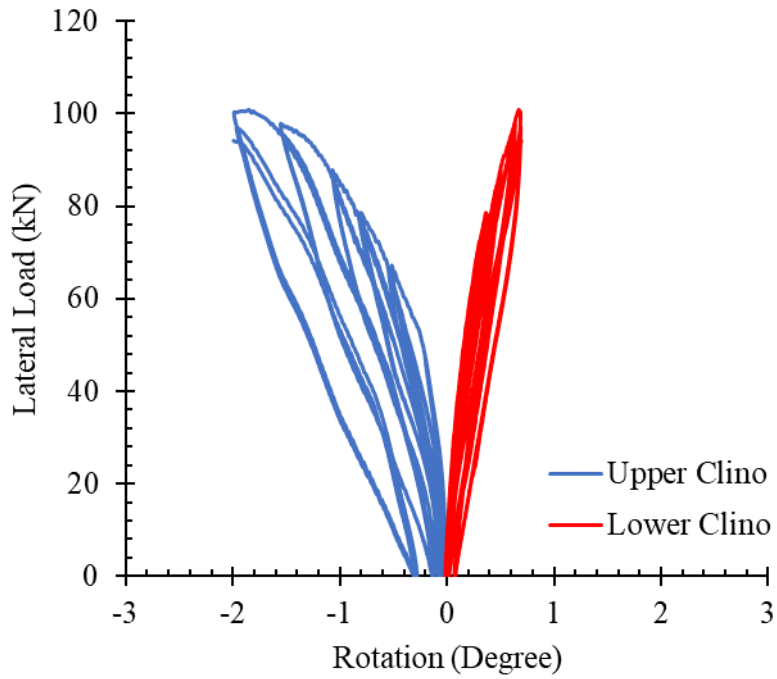


Figure 3.37 – Lateral Load–Base Rotation Response (Specimen 3)

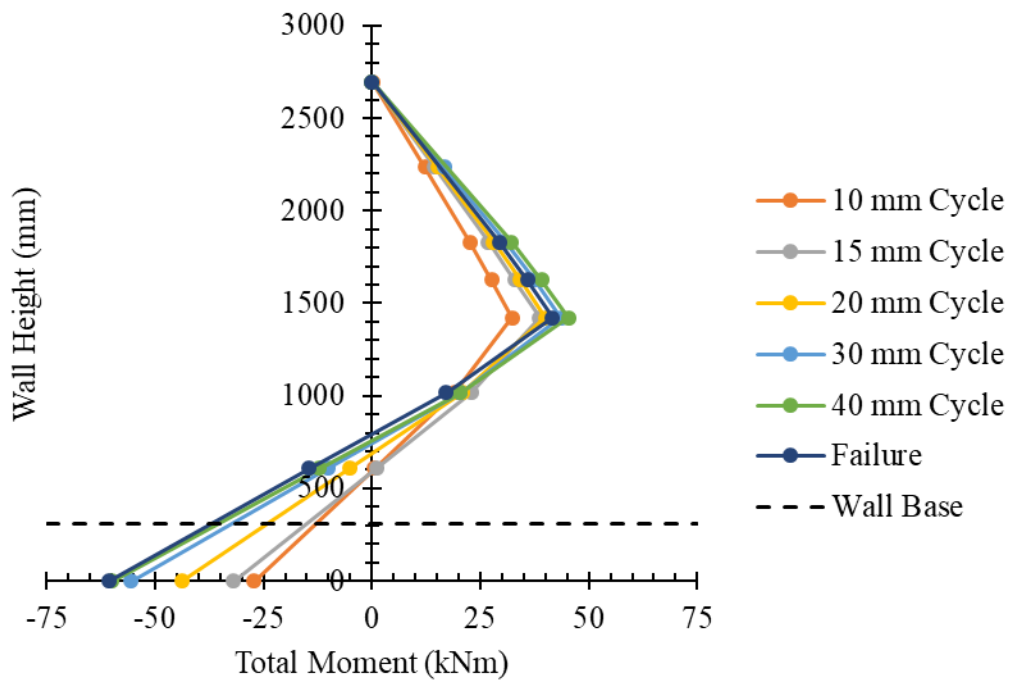


Figure 3.38 – Total Moment Profiles (Specimen 3)

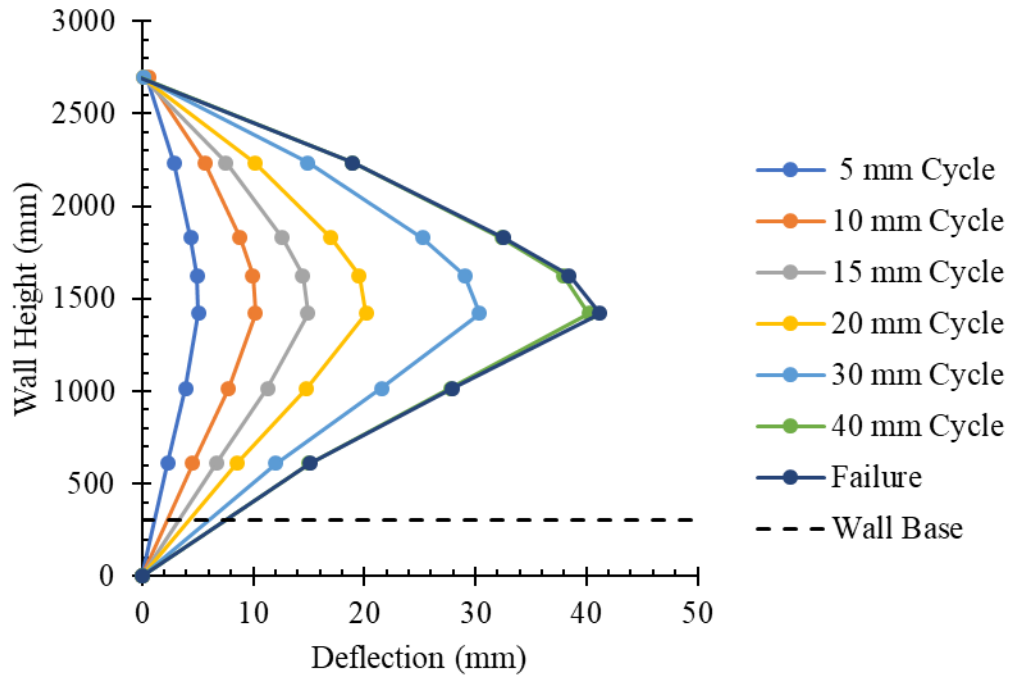


Figure 3.39 – Deflection Profiles (Specimen 3)

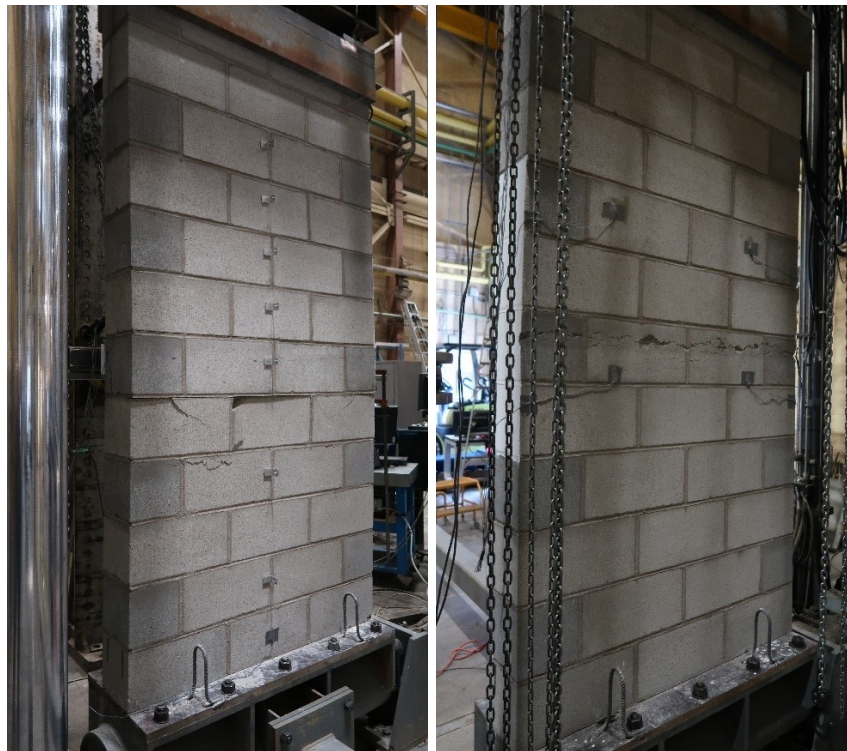


Figure 3.40 – Failure (Specimen 3)

3.8.4 Test 4 (Rotational Stiffness = 9,500 kNm/rad)

Specimen 4 was tested with a rotational stiffness of 9,500 kNm/rad at the base of the wall. The cyclic lateral load–midspan displacement history of the specimen is presented in Fig. 3.41. The specimen was not able to complete all 8 cycles before failure occurred. The first sign of failure occurred during the 10-mm cycle when separation between the masonry units and mortar joints near the midspan of the specimen was observed. The peak lateral load for the specimen was 95.9 kN with a corresponding midspan deflection of 38.8 mm. Failure occurred during the first 50 mm cycle, with the crushing of the masonry at the midspan. The midspan deflection at failure was 43.2 mm with a corresponding lateral load of 90.7 kN.

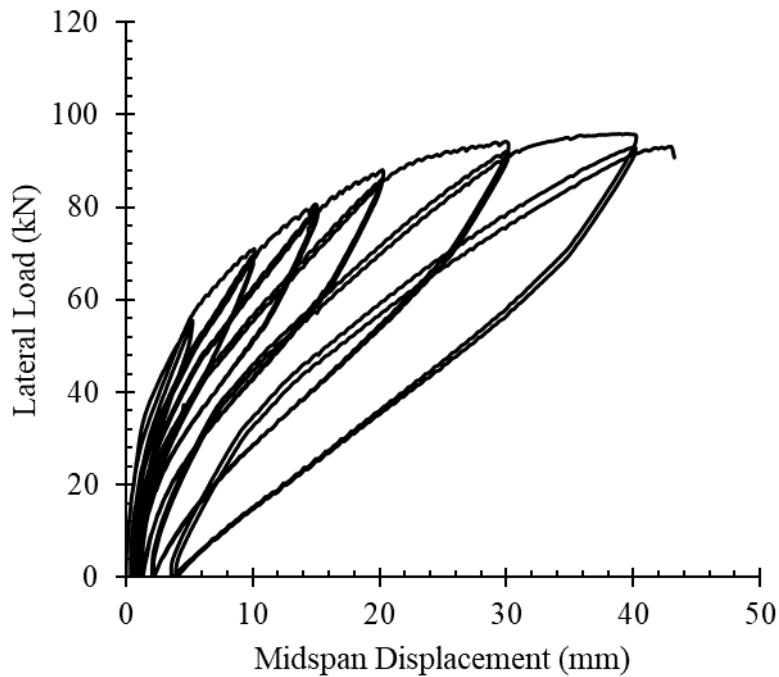


Figure 3.41 – Lateral Load–Midspan Displacement Response (Specimen 4)

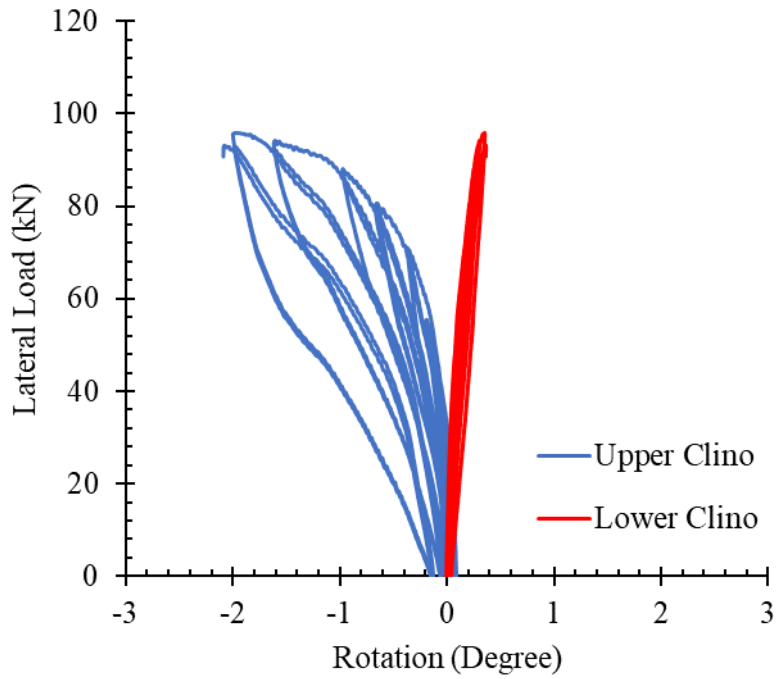


Figure 3.42 – Lateral Load–Base Rotation Response (Specimen 4)

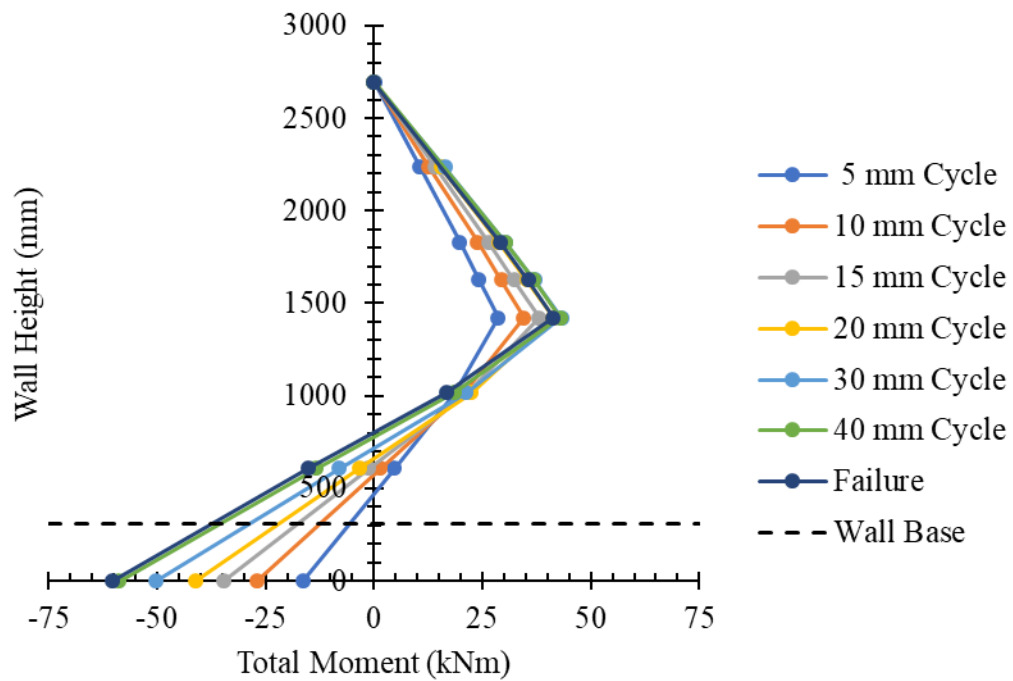


Figure 3.43 – Total Moment Profiles (Specimen 4)

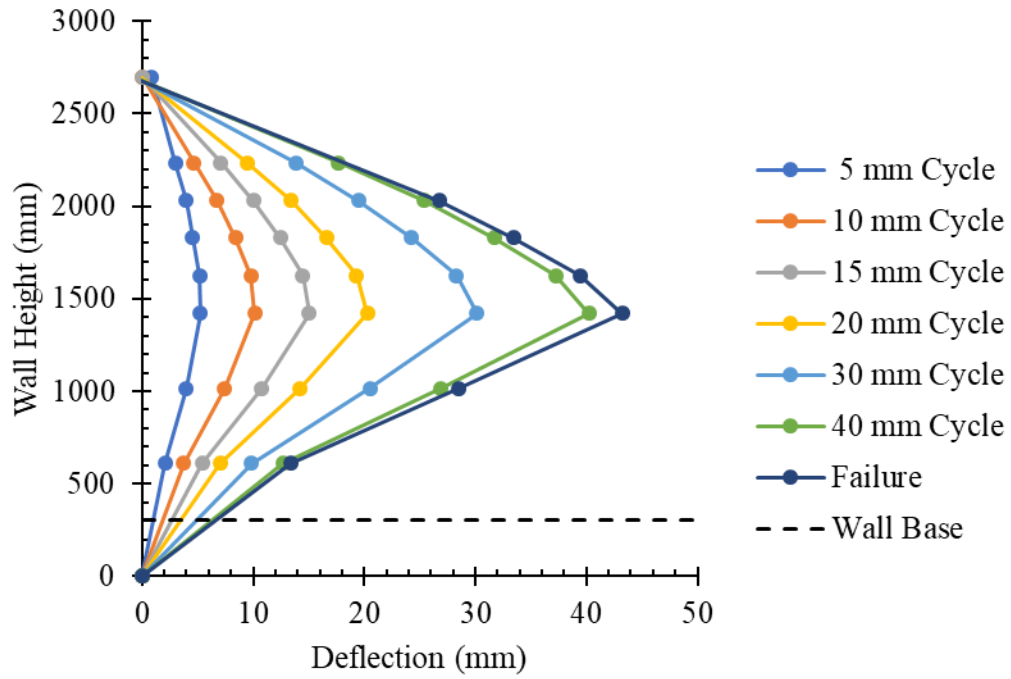


Figure 3.44 – Deflection Profiles (Specimen 4)



Figure 3.45 – Failure (Specimen 4)

3.9 Discussion of Results

3.9.1 Lateral Load–Midspan Displacement

Plotting the backbone curves of the 4 test specimens (Fig. 3.46) shows that, in general, as the level of rotational base stiffness (RBS) is increased, the lateral load-carrying capacity of the wall increase, while the ultimate midspan deflections decrease. This is because the presence of rotational support stiffness at the base of the wall creates a negative moment sub-profile over the height of the wall proportional to the amount of base support stiffness. This negative moment sub-profile redistributes the total moment profile along the height of the wall (Fig. 3.47) resulting in smaller bending moments at the midspan region for walls with a larger base support stiffness, compared to walls with a smaller base support stiffness at the same values of lateral load (Fig. 3.49). Smaller bending moments at any region of the wall translate into smaller deflections, and additional strength if the critical section is located near the same position.

It is important to note that the magnitude of moment redistribution along the height of the wall due to the rotational base stiffness is not constant. As the negative moment sub-profile decreases along the height of the wall, the effect of moment redistribution is much more prevalent as the base of the wall compared to the top of the wall. With the critical moment location of the test specimens at the midspan, the effect of moment redistribution is quite noticeable. However, for walls with the critical moment located near the top of the wall (i.e. walls with large eccentric axial loads) the effects of moment redistribution would be quite small as the negative moment profile would approach zero at the top of the wall (Fig. 3.48).

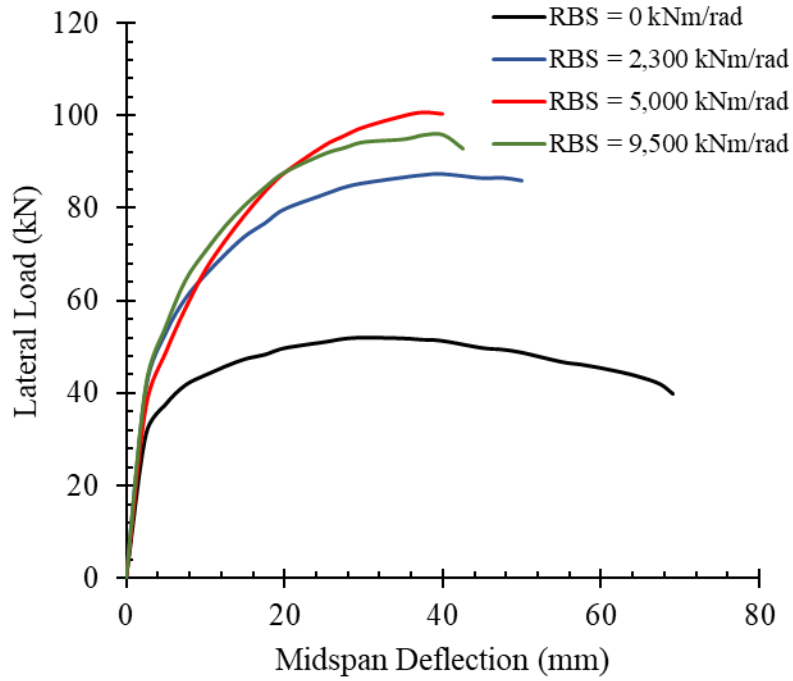


Figure 3.46 – Backbone Lateral Load–Midspan Displacement Comparison

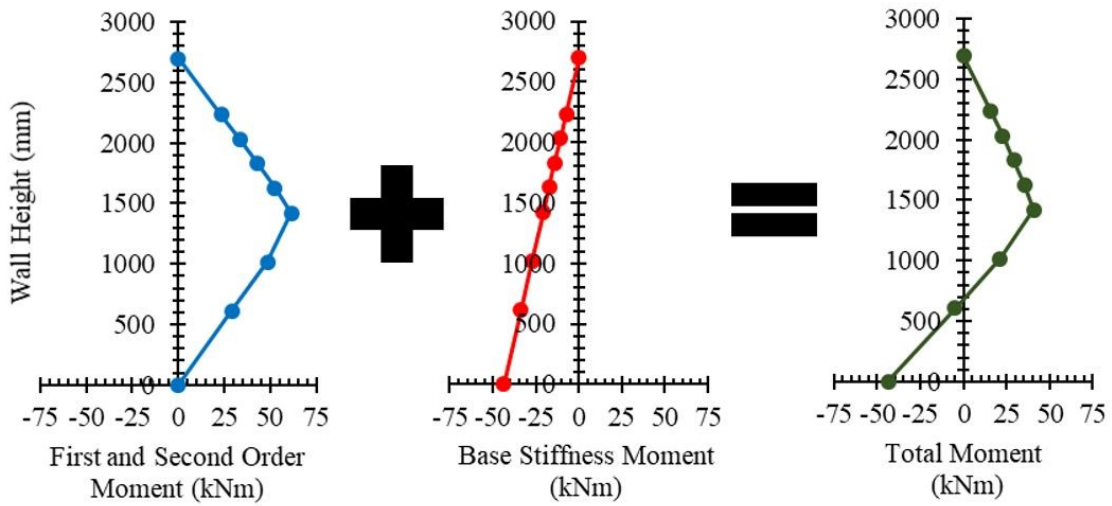


Figure 3.47 – Moment Redistribution of a Point Lateral Load

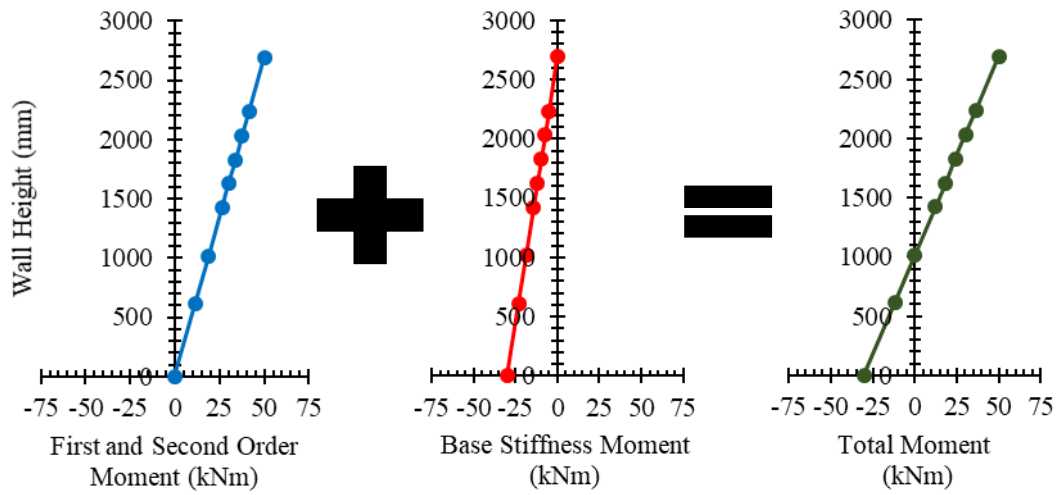


Figure 3.48 – Moment Redistribution of an Eccentric Axial Load

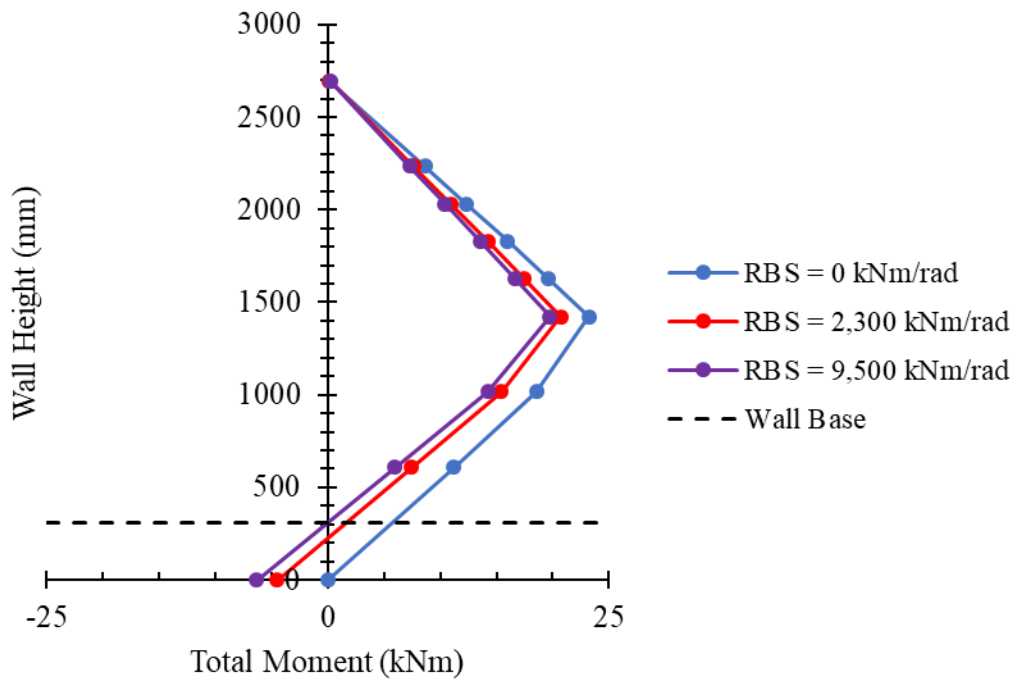


Figure 3.49 – Total Moment Profile of the Wall Specimens at the Same Lateral Load (35 kN)

The lateral load-carrying capacity increase is not linear with the increase in base rotational support stiffness. As the rotational base stiffness is increased, the increase in lateral load capacity begins to plateau. When increasing the base support stiffness from 0 kNm/rad to 2,300 kNm/rad, the lateral load-carrying capacity of the specimens increased from 52.5 kN to 87.4 kN (a relative increase of 66%), while increasing the base stiffness from 2,300 kNm/rad to 9,500 kNm/rad only increased the load-carrying capacity of the specimens from 87.4 kN to 95.9 kN (a relative increase of 10%). This is attributed to the base rotational support stiffness approaching the fixed-pinned boundary condition, which acts as an upper limit on the benefit received from base support stiffness. The relative increase of lateral load capacity with base rotational stiffness is presented in Table 3.18 below.

Table 3.17 – Relative Increase in Lateral Load Capacity

Specimen	Increase in Base Stiffness (kNm/rad)	Increase in Lateral Load Capacity to Wall 1 (pinned)
2	0 to 2,300	66.5%
3	0 to 5,000	92.4%
4	0 to 9,500	82.7%

One anomaly in the experiment was the response of Specimen 3 (base rotational stiffness of 5,000 kNm/rad). The response of Specimen 3 was rather unexpected, as it demonstrated a higher bending moment capacity than the other specimens. In fact, the reported load-carrying capacity of the specimen was higher than that of Specimen 4, even though Specimen 4 featured a higher base rotational support stiffness. Upon further inspection, the reason for this was the misplacement of the reinforcing steel in Specimen 3. Forensic examination showed that the reinforcing steel in Specimen 3 had been placed approximately 2 cm closer to the tension face of the wall compared to other specimens, resulting in a relative increase in bending moment capacity of 10.4%. The reinforcing steel placement in the other 3 specimens was found to be adequate. If the bars in specimen 3 had been placed at the middle of the cell, the predicted increase in lateral capacity, relative to Specimen 1, would have been 83.7%, in line with the results in Table 3.18.

Comparing the response of the specimens to the cyclic loading, all specimens exhibited a similar pattern. As shown in Fig. 3.50 (20-mm cycle for Specimen 1), the initial load path of the specimen exhibited a linear response while the specimen remained elastic. This path became nonlinear as phenomena such as tensile cracking and material nonlinearity reduced the effective flexural rigidity of the specimen. The degradation continued until a midspan deflection of 20 mm was reached. The specimen was then unloaded. After unloading, the midspan deflection did not return to zero. This is because of the permanent strains developed in the wall during the initial loading cycle. When loading the wall in the second run, the load-displacement history closely resembled that of the first run, except that less lateral load was required to displace the wall. This was due to the additional tensile cracking endured during the previous run. The stiffness lost due to this cracking was not recovered, resulting in more displacement under the same lateral load values. When unloading the wall for the second time, it is seen that the second unloading path followed the first unloading path almost identically. This is because the specimen was not displaced further than it had been in the first run, resulting in no additional tensile cracking than what was seen in the first run. Without tensile cracking, the flexural rigidity of the specimen during the second run was comparable to the flexural rigidity of the specimen after the first run.

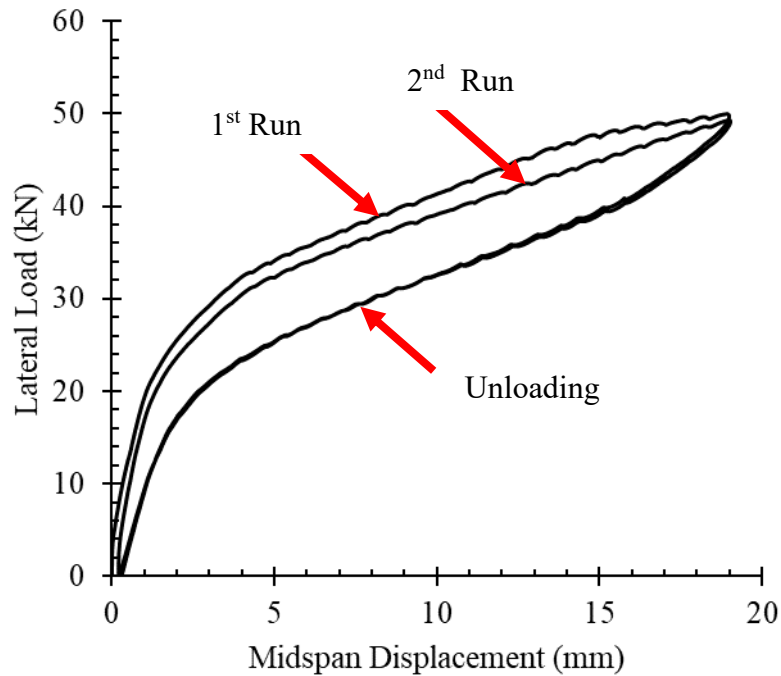


Figure 3.50 – Typical Specimen Response to Cyclic Loading

3.9.2 Lateral Load–Base Rotation

Figure 3.51 shows the base rotation of the specimens as reported by the lower clinometer under applied levels of lateral load. As expected, specimens with higher base rotational support stiffness experienced a lower base rotation compared to those with lower stiffness. Comparing Specimen 1 (RBS = 0 kNm/rad) to Specimen 4 (RBS = 9,500 kNm/rad) at failure, Specimen 4 reported an 89% relative decrease in base rotation as compared to Specimen 1. An interesting phenomenon displayed in the figure is the behaviour of the base rotation. As the level of base support stiffness was increased, the behaviour of the base rotation transitioned from a nonlinear to a more linear behaviour.

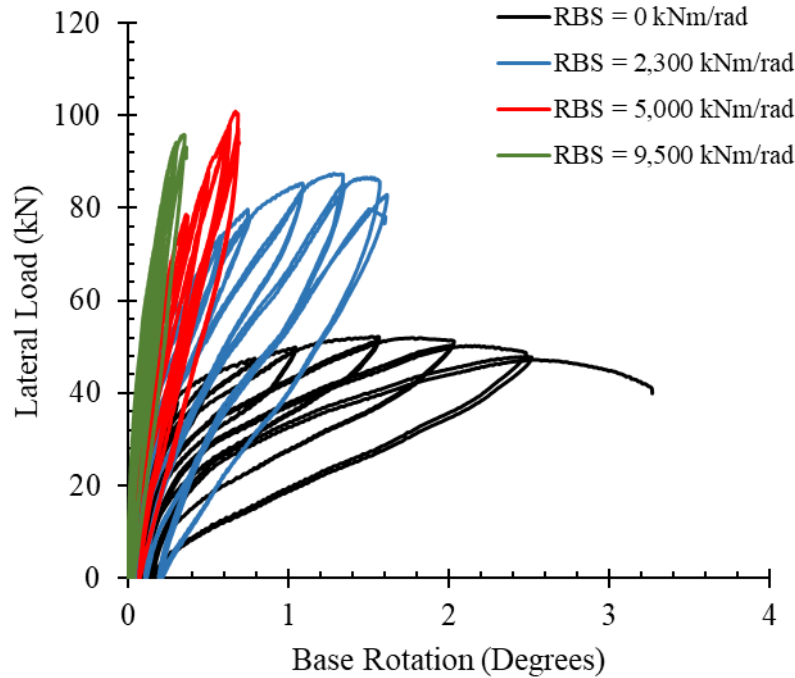


Figure 3.51 – Base Rotation Comparison

3.9.3 Second-Order Effects

Figures 3.52 to 3.55 shows the total moment profile over the height of the specimen along with the sub-profiles used to determine the total moment profile. The total moment profile is comprised of three moment sub-profiles: the first-order moment, second-order moment, and support moment. The first-order moment profile consists of moments caused by the lateral load and was determined by distributing the effects of the lateral load as measured via the load cell, over the height of the specimen using statics. The second-order moment consists of moments caused by the OOP wall deflections creating an eccentricity between the wall and gravity load and was determined by multiplying the gravity load with the OOP deflections recorded by the LVDTs. The support moment consists of moments created from the presence of the base rotational support stiffness and was determined by multiplying the base rotation recorded with the lower clinometer with the level of base rotational support stiffness to get the moment at the base of the wall, then distributing the effects of this moment over the height of the wall using statics. It should be noted that this support moment is technically a second-order moment as it is a

function of base rotation but defined separately in this study to aid in distinguishing it from the traditional second-order moments. To determine the total moment profile over the height of the wall, the three sub-profiles were determined then summed together. Table 3.19 shows the midspan total moment composition at failure for all four specimens.

Table 3.18 – Midspan Moment Composition at Failure

Specimen	First-Order Moment (kNm)	Second-Order Moment (kNm)	Support Moment (kNm)	Total Moment (kNm)
1	25.4	17.1	0.0	42.6
2	48.8	12.6	-30.3	31.1
3	59.9	10.3	-28.6	41.6
4	59.1	10.8	-28.5	41.3

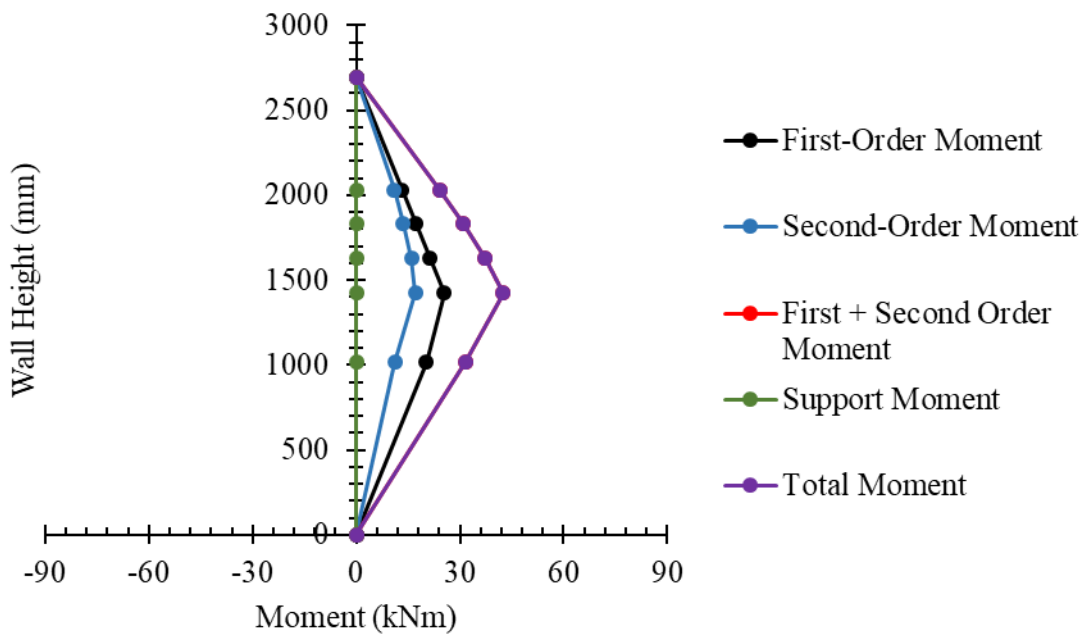


Figure 3.52 – Total Moment Composition at Failure (Specimen 1)

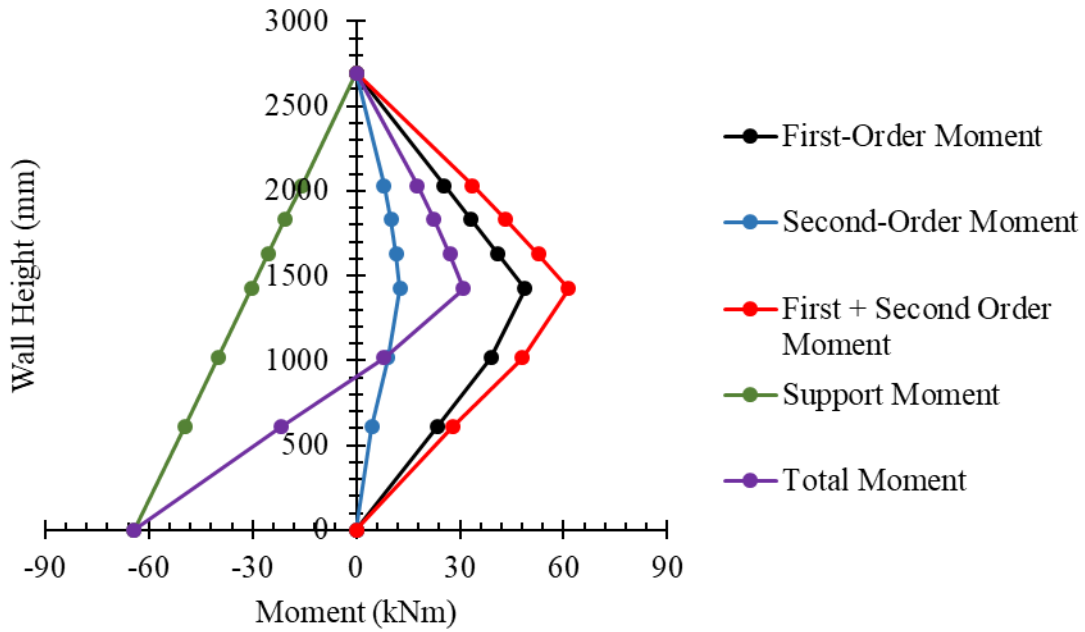


Figure 3.53 – Total Moment Composition at Failure (Specimen 2)

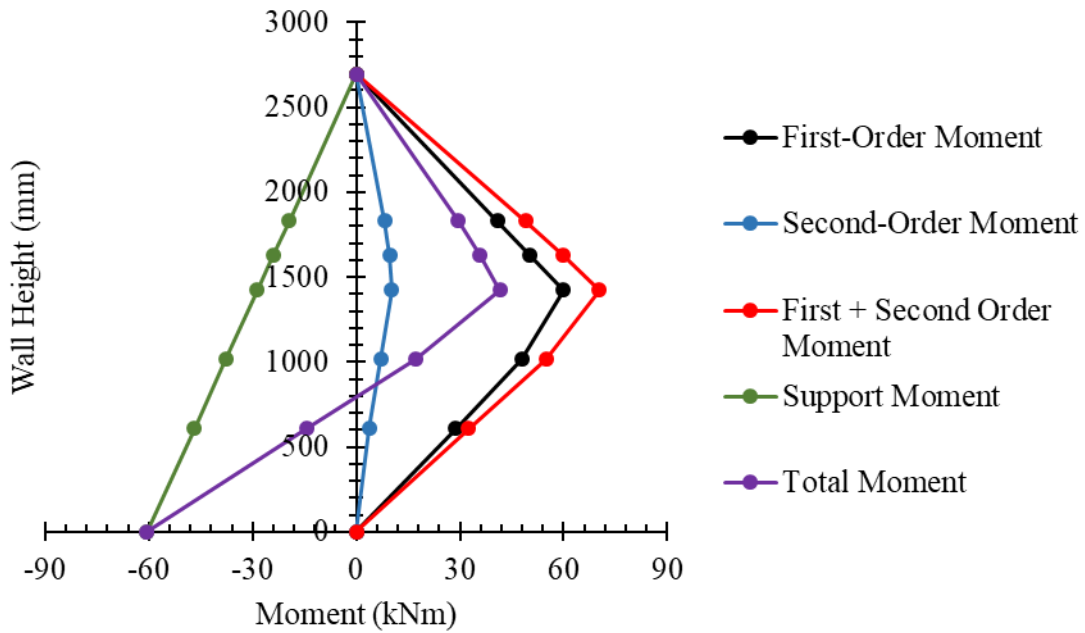


Figure 3.54 – Total Moment Composition at Failure (Specimen 3)

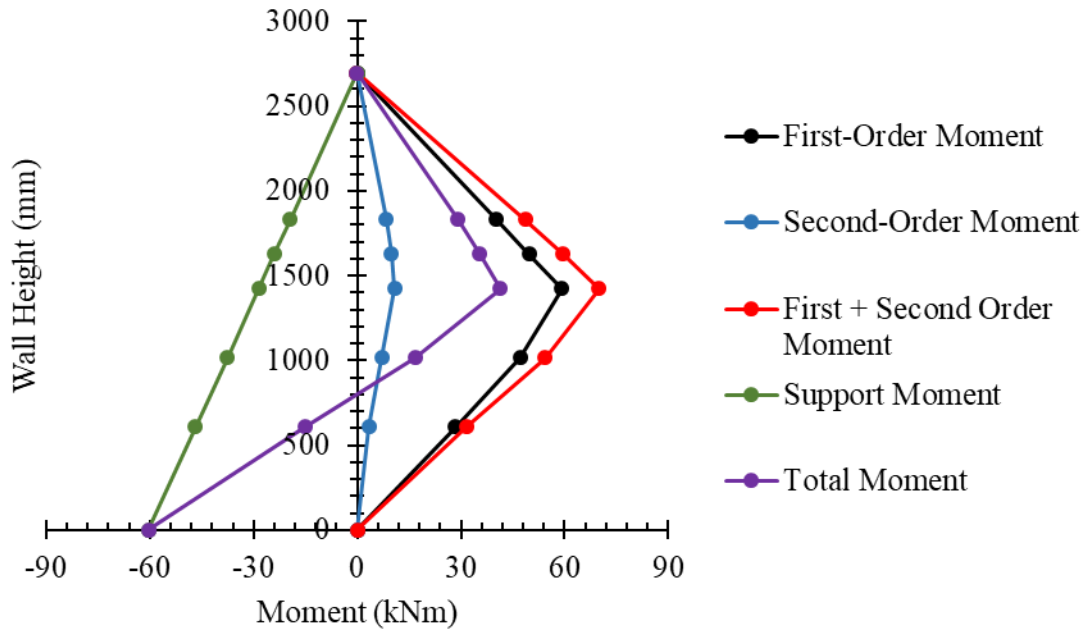


Figure 3.55 – Total Moment Composition at Failure (Specimen 4)

3.9.4 Moment Magnification Factor

Current code provisions provide several methods to determine second-order effects. These consist of the moment magnification method and the $P\delta$ method. The moment magnification method involved the determination of magnification factor which is then used to amplify the first-order moment located at the midspan of the wall to account for second-order effects. As the first-order and total moment at the midspan is known from the experimental data (discussed above), the moment magnification factor was determined for all specimens by dividing the total moment by the first-order moment at failure (Table 3.20).

Comparing the results, it is seen that Specimen 1 was the only specimen with a moment magnification factor greater than 1. This was because of the influence of base rotational support stiffness on Specimens 2 to 4. Without rotational stiffness at the base of Specimen 1, the total moment was composed solely of the first- and second-order moments. However, when base stiffness was introduced in Specimens 2 to 4, the negative support moment sub-profile significantly reduced the total moment profile over the height

of the wall. As seen in the results, this reduction was quite significant, as it was able to counteract the second-order moment sub-profile and even reduce the first-order moment sub-profile (hence the moment magnification factor less than 1).

Table 3.19 – Moment Magnification Factor

Specimen	First-Order Moment (kNm)	Total Moment (kNm)	Moment Magnification Factor
1	25.4	42.6	1.68
2	48.8	43.0	0.88
3	59.9	41.6	0.69
4	59.1	41.3	0.70

3.9.5 Total Moment Profile

Figures 3.56 to 3.63 compare the total moment profiles over the height of the specimens at the end of each cycle.

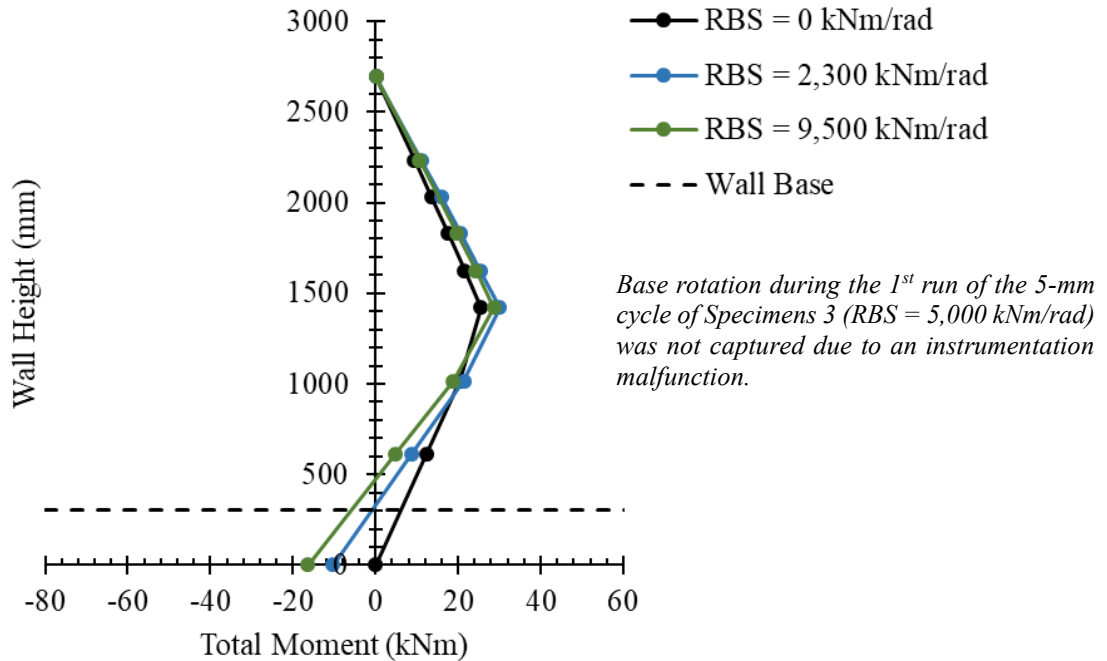


Figure 3.56 – Total Moment Profile (5-mm Cycle)

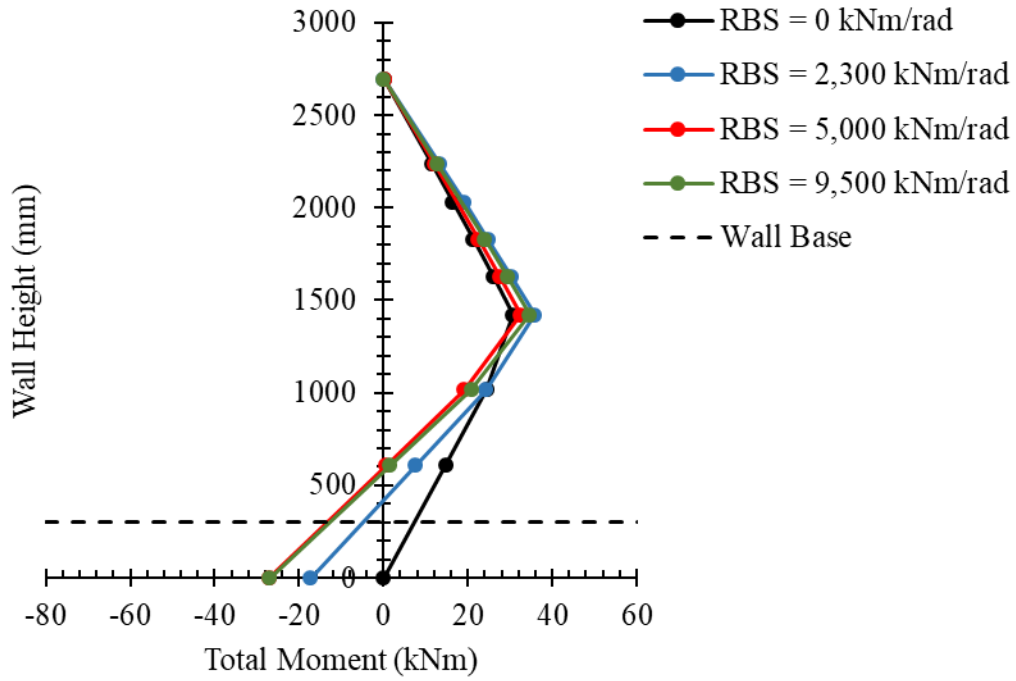


Figure 3.57 – Total Moment Profiles (10-mm Cycle)

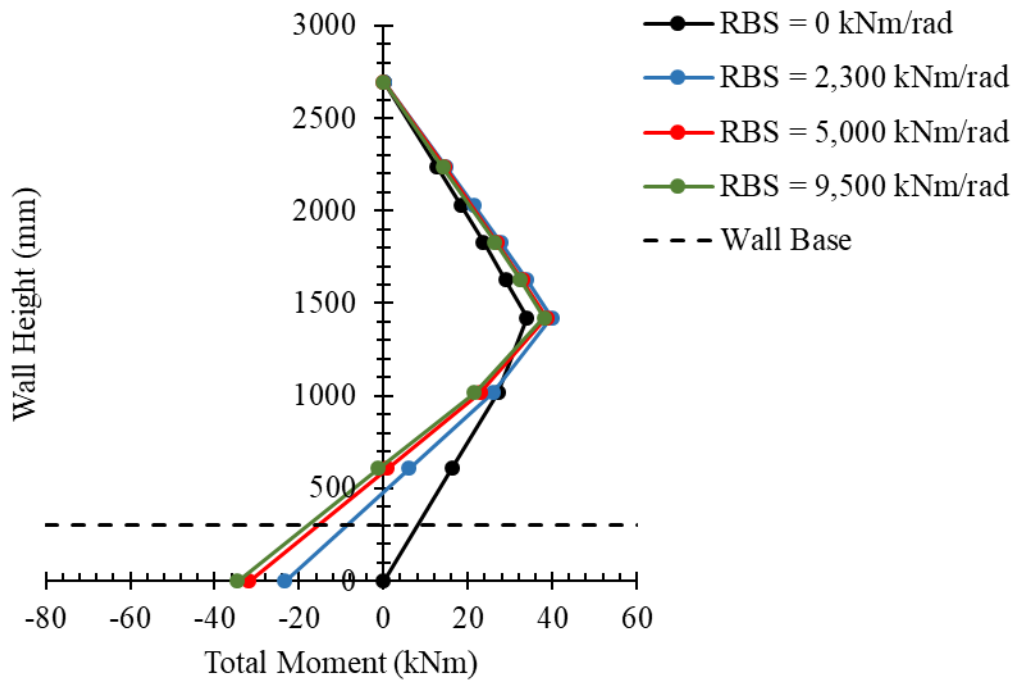


Figure 3.58 – Total Moment Profile (15-mm Cycle)

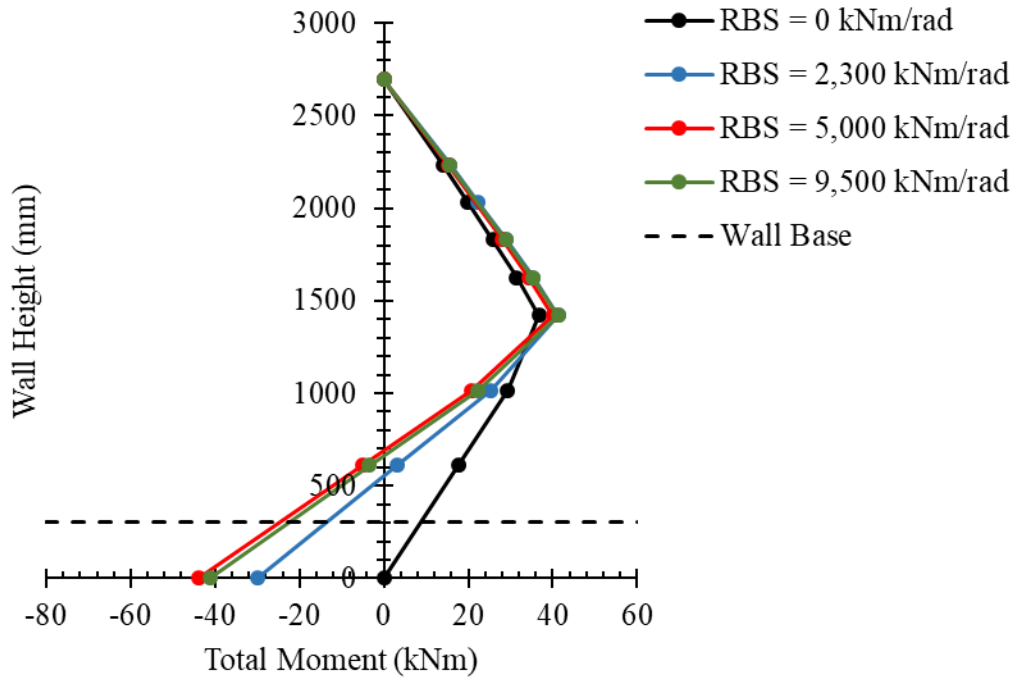


Figure 3.59 – Total Moment Profiles (20-mm Cycle)

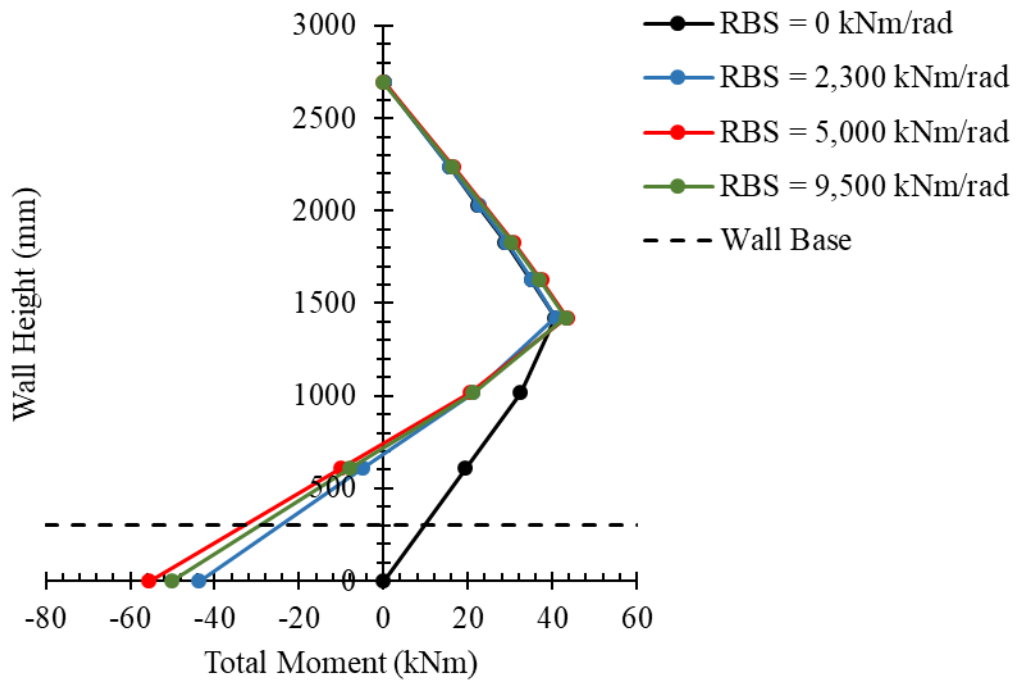


Figure 3.60 – Total Moment Profile (30-mm Cycle)

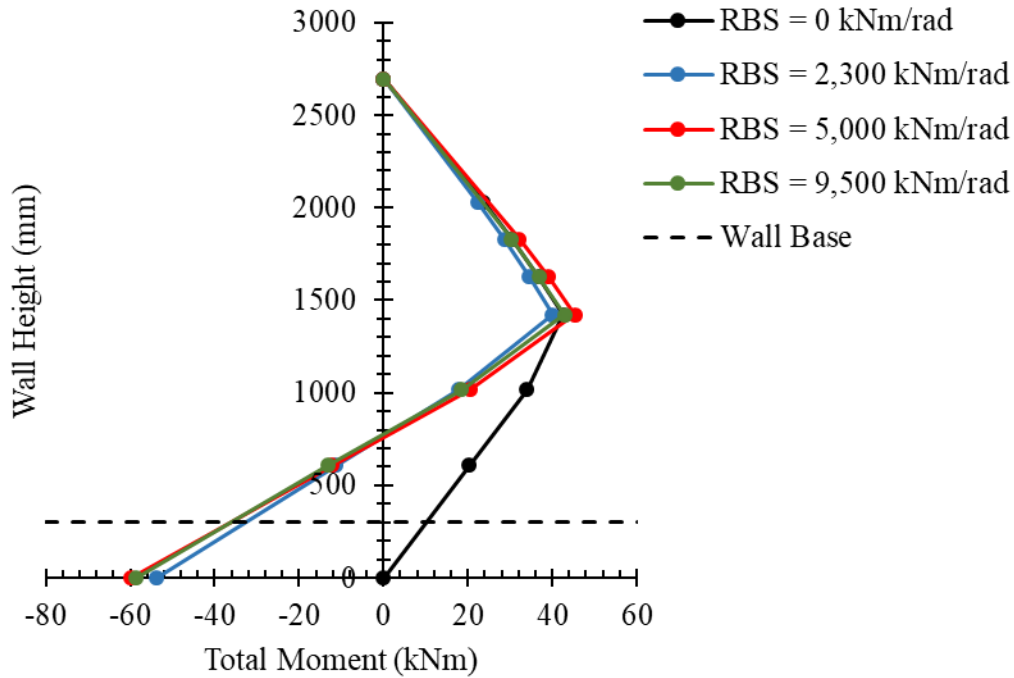


Figure 3.61 – Total Moment Profile (40-mm Cycle)

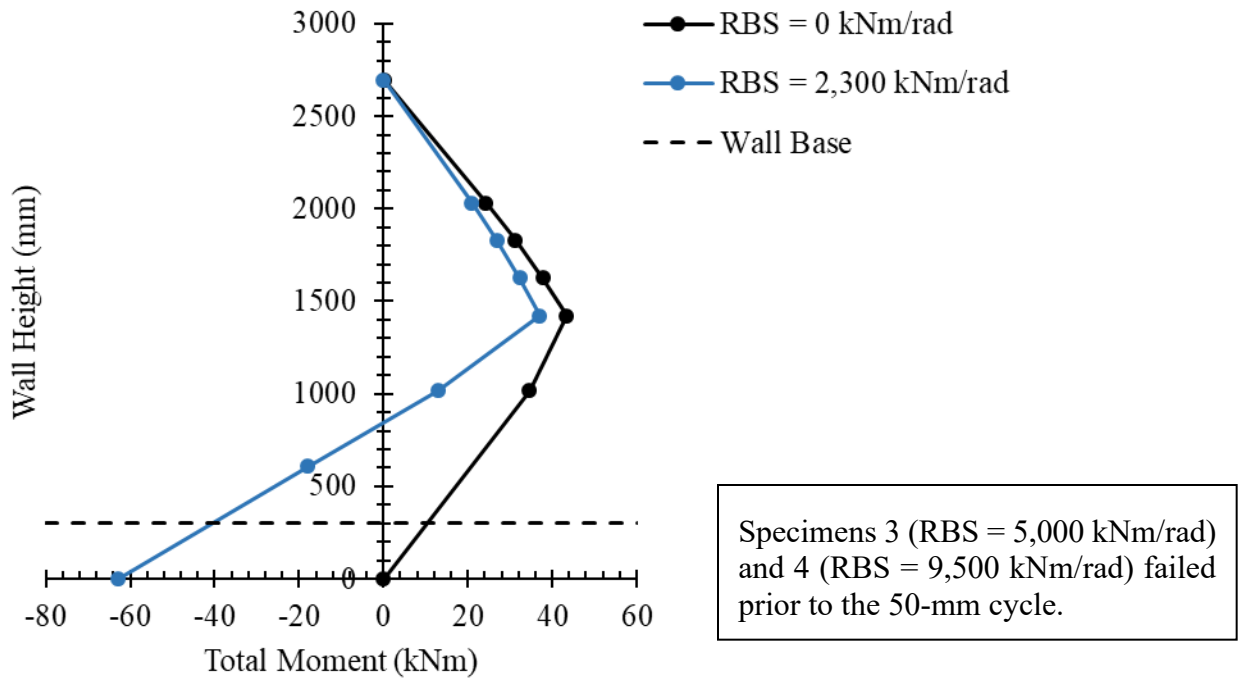


Figure 3.62 – Total Moment Profile (50-mm Cycle)

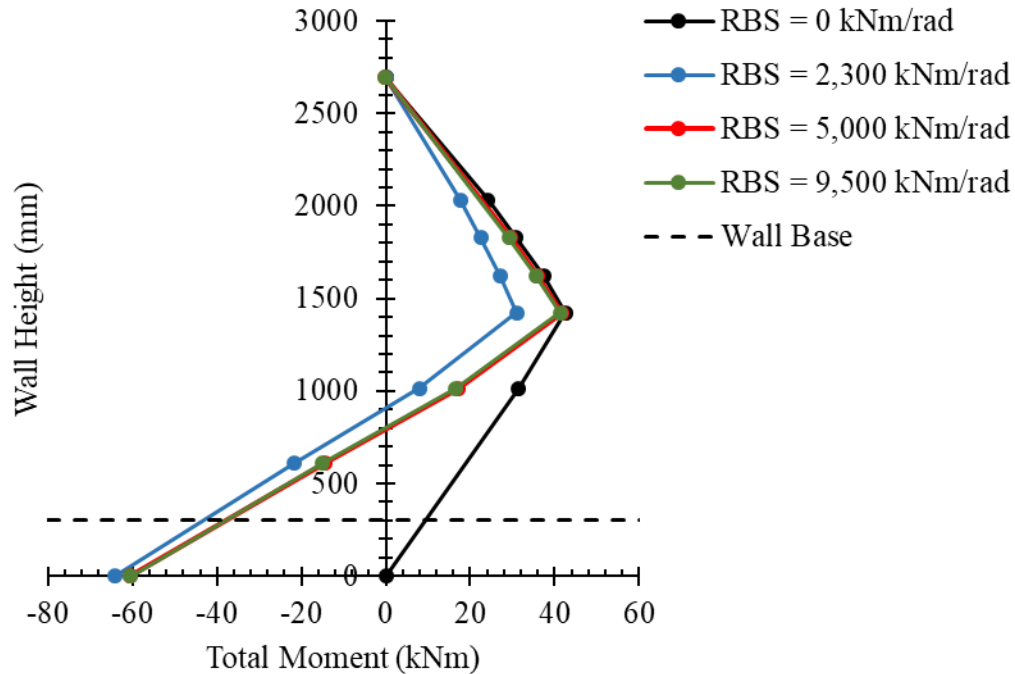


Figure 3.63 – Total Moment Profiles (Failure)

It is seen that the magnitude of the base moment increased with increased support stiffness. Additionally, the presence of a base stiffness created an inflection point indicating the wall acts in double curvature. As the base stiffness increased, the point of inflection moved up the height of the wall. This is expected, as the presence of a larger base rotational stiffness creates a larger base moment, resulting in a larger negative moment profile. Figure 3.64 shows the effect of a larger base stiffness on the total moment profile for a generic wall.

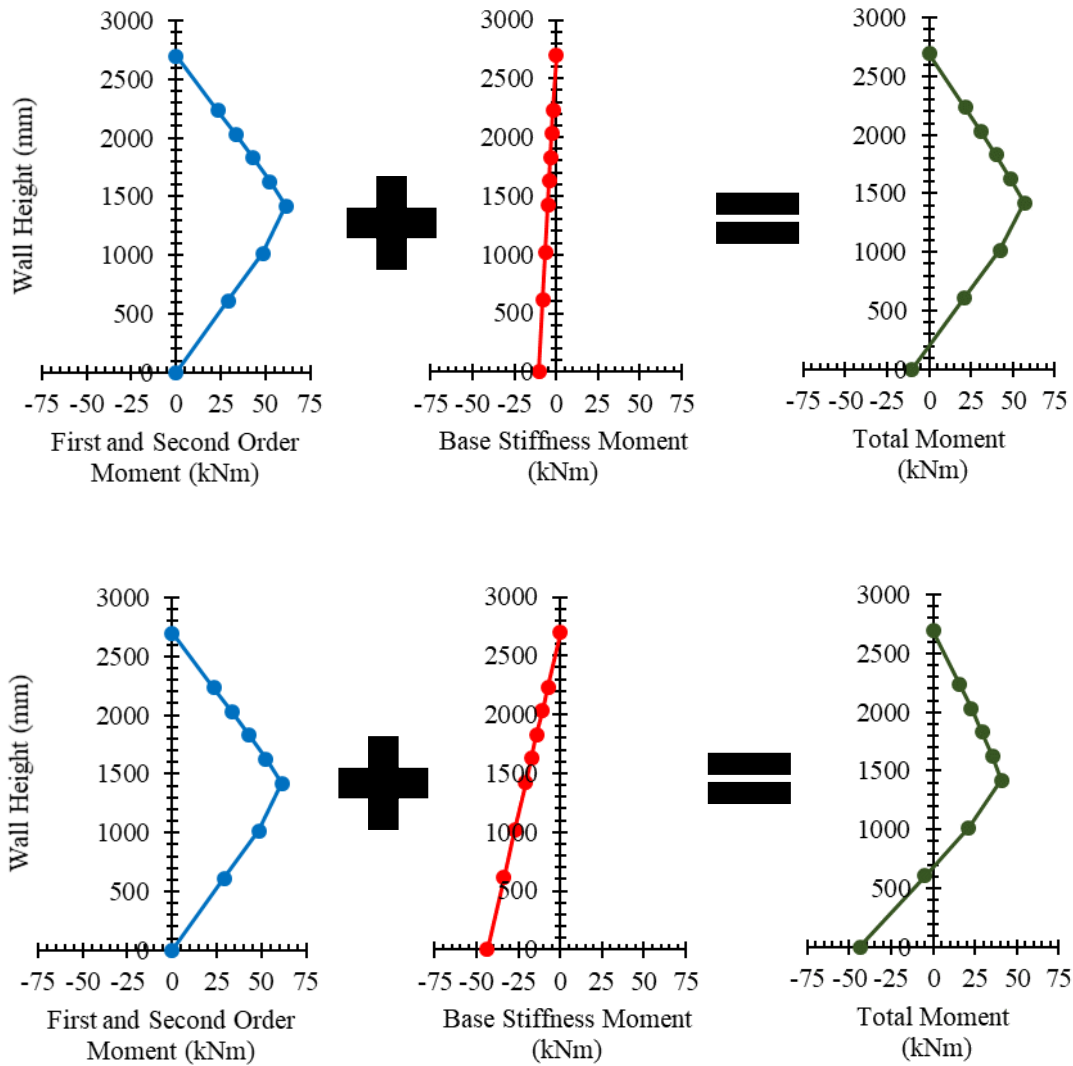


Figure 3.64 – Effect of Base Stiffness on Total Moment Profile

At failure, the largest moment magnitude was a positive moment located at the midspan for Specimens 1, 3 and 4. The largest moment magnitude for Specimen 2 however was a negative moment located at the base of the wall. This was due to the relatively large base rotations (as compared to the other specimens with a rotational base stiffness) sustained by Specimen 2 during testing. After peak load, the lateral load placed on the wall begin to decrease resulting in a decrease in the first-order moment profile. However, the wall deflection and rotation at the base of the specimen continue to increase. As a result, the second-order and support moment profiles continue to grow in magnitude. In

fact, the tests showed that in all cases where the specimen featured a base stiffness, the support moment profile increased at a higher rate than the second-order profile (the first order moment is decreasing). This caused the total moment at the midspan of the walls to decrease during the post peak response.

The post-peak response of the walls depended on the amount of base stiffness. Walls with a smaller base stiffness experienced significantly more base rotation compared to walls with a large base stiffness. This allowed for walls with a smaller base stiffness to develop a larger support moment resulting in more moment redistribution compared to walls with larger base stiffness. As moment redistribution in the post-peak response decreases the total moment profile, as discussed in Section 3.9.1, walls with small values of base stiffness more effectively decrease the total moment profile along the height of the wall and sustain excess deflection before failure as compared to walls with higher values of base stiffness.

Due to the relatively lengthy post-peak response of Specimen 2 as compared to Specimens 3 and 4, the midspan moment of Specimen 2 continuously decreased until the magnitude of midspan moment became less than the moment at the base of the wall. When Specimen 2 failed, the magnitude of the moment at the base of the wall was 27.7% larger than the magnitude of the midspan moment. Specimens 3 and 4 failed prior to the magnitude of the base moment exceeding that of the midspan moment. Figures 3.65 to 3.67 show the development of the total moment profile and base rotation of Specimen 2 to help demonstrate this effect.

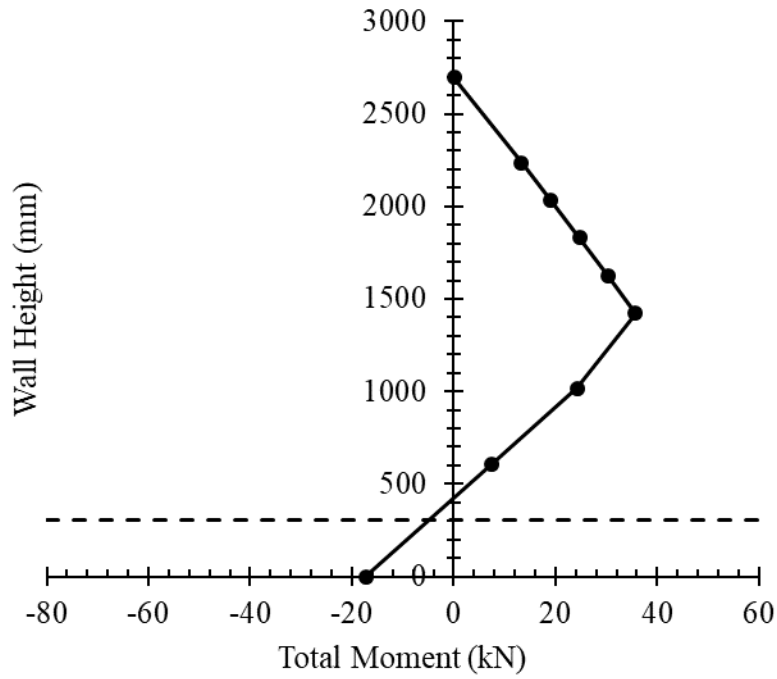


Figure 3.65 – Moment Profile Development of Specimen 2 (Pre-Peak Load)

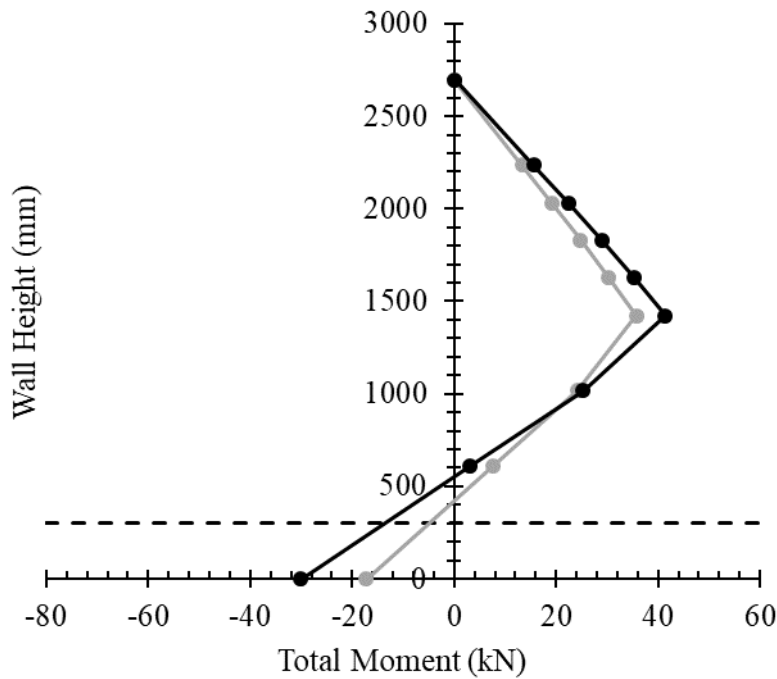


Figure 3.66 – Moment Profile Development of Specimen 2 (Peak Load)

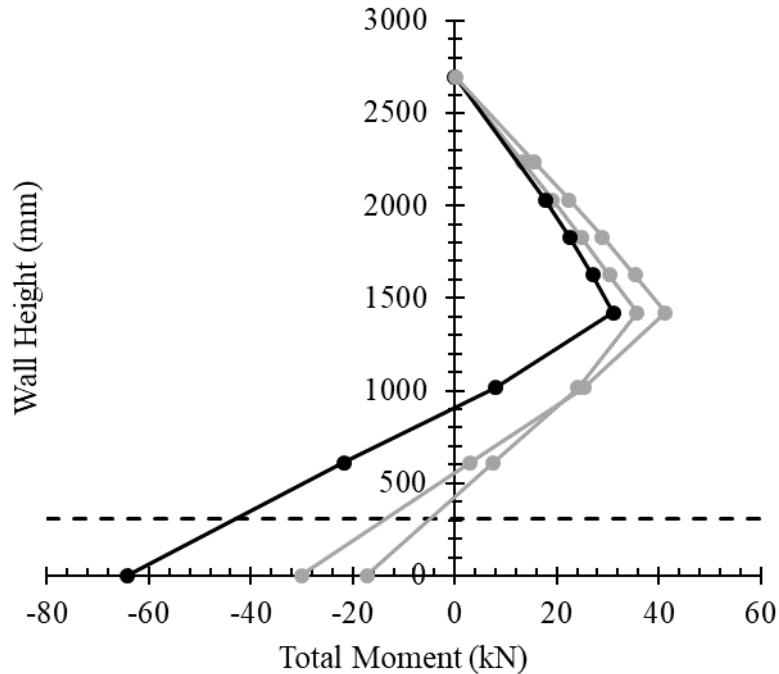


Figure 3.67 – Moment Profile Development of Specimen 2 (Failure)

Comparing the maximum moments sustained by each specimen to the predicted moment capacity, all specimens exceeded the predicted moment capacity. Looking at prism heights, this would conclude that the use of 2-course prisms for the compressive strength of masonry is a viable option as the higher value still resulted in an underestimation of the true moment capacity. As all specimens were able to exceed the predicted moment capacity under a cyclic load, this indicates that the degradation of the walls base due to the rotational support stiffness does not have a significant reduction in the ultimate moment capacity of the wall.

3.9.6 Deflection Profile

It is seen that as the level of base rotational support stiffness was increased, the OOP deflections of the wall decreased. This is because of the larger negative moment found at the base of the wall forcing the wall into double curvature.

At failure, the location of maximum deflection occurred at the midspan of the specimens. This is also expected as the maximum moment of a 3-point bend test is located at the

midspan of the specimen. If the span of the specimens were to be increased, it is expected the location of maximum deflection would shift up the wall. This is due to the larger OOP deflection (accompanied by larger base rotations) creating a larger reactive base moment that would significantly reduce the total moment profile along the bottom half of the wall.

Comparing the four specimens, the ultimate deflection at failure decreases as rotational support stiffness was increased. This is due to the base rotational stiffness creating a negative moment at the base of specimens. This negative moment creates a linear negative moment sub-profile (discussed above), thus reducing the total moment profile (and in turn, OOP deflections) of the wall.

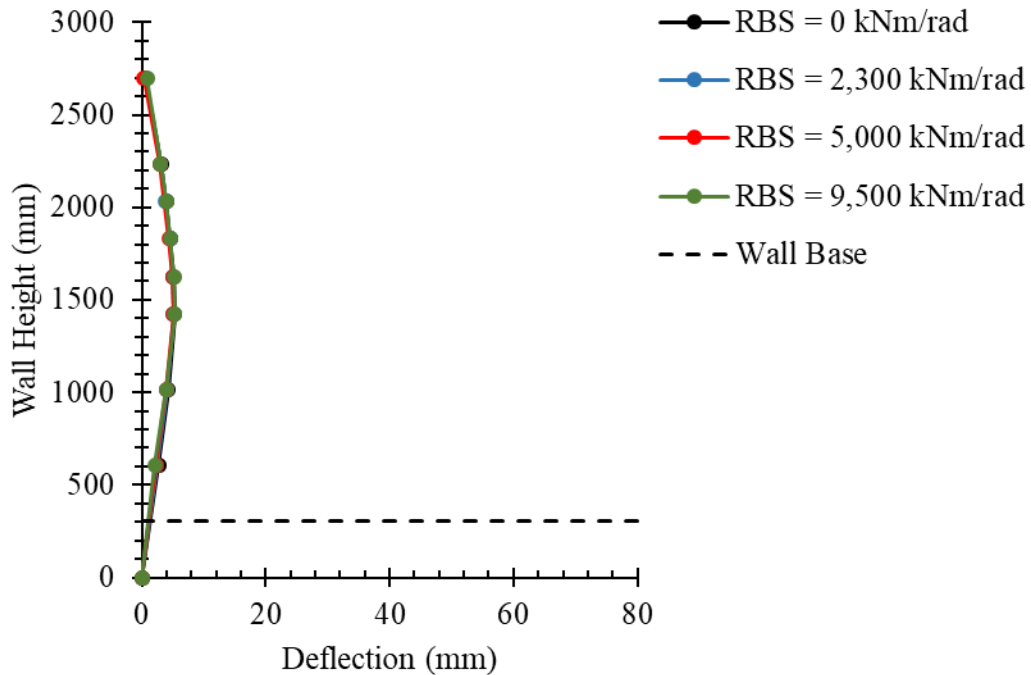


Figure 3.68 – Deflection Profiles (5-mm Cycle)

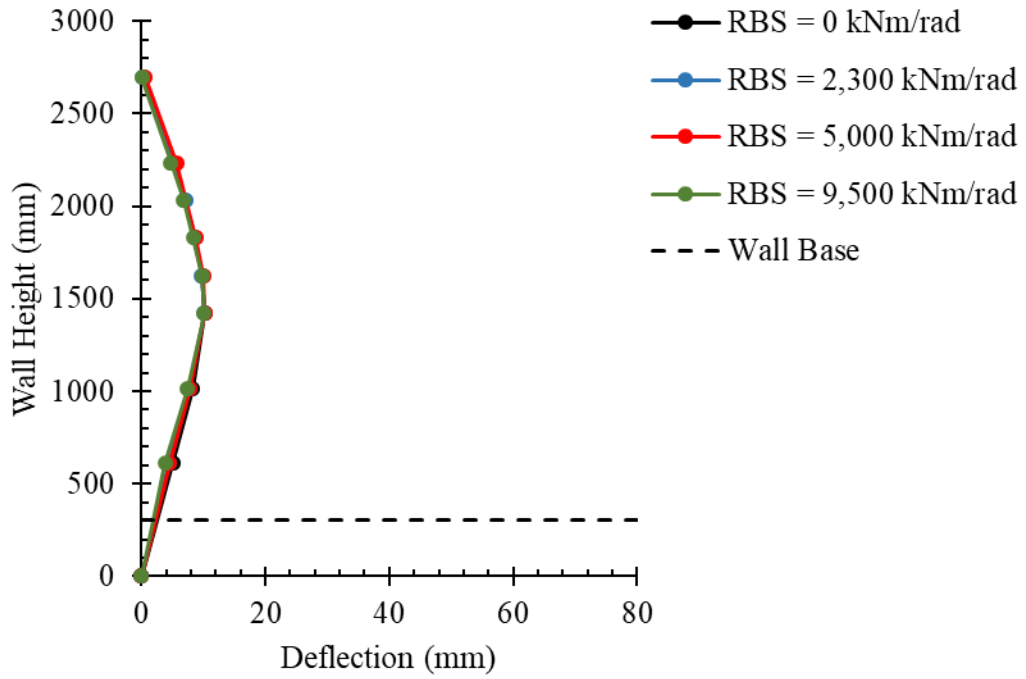


Figure 3.69 – Deflection Profiles (10-mm Cycle)

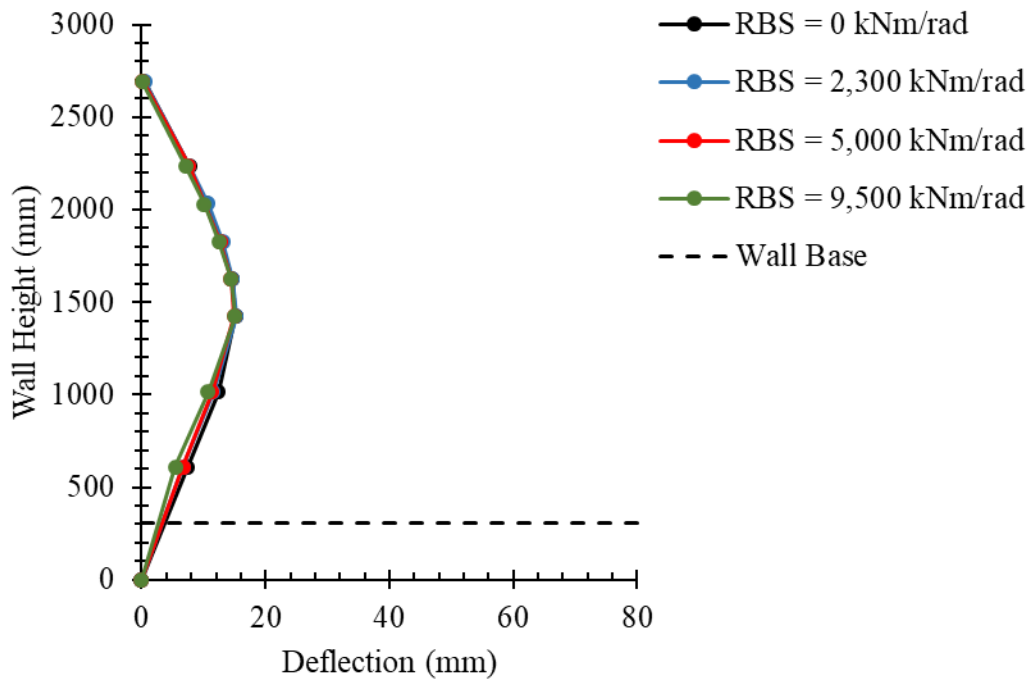


Figure 3.70 – Deflection Profiles (15-mm Cycle)

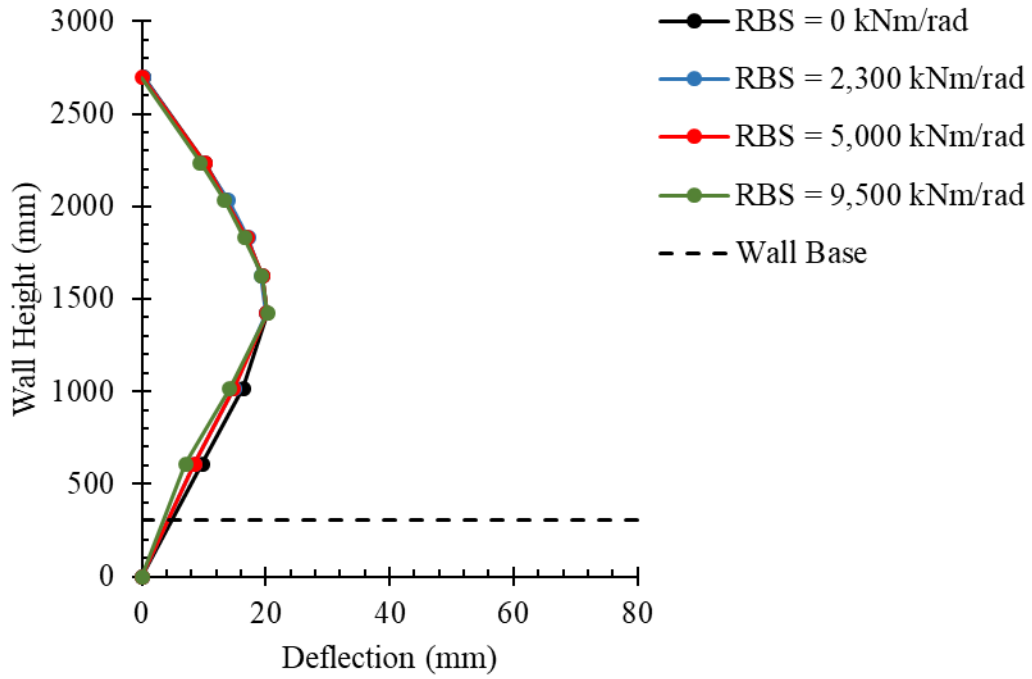


Figure 3.71 – Deflection Profiles (20-mm Cycle)

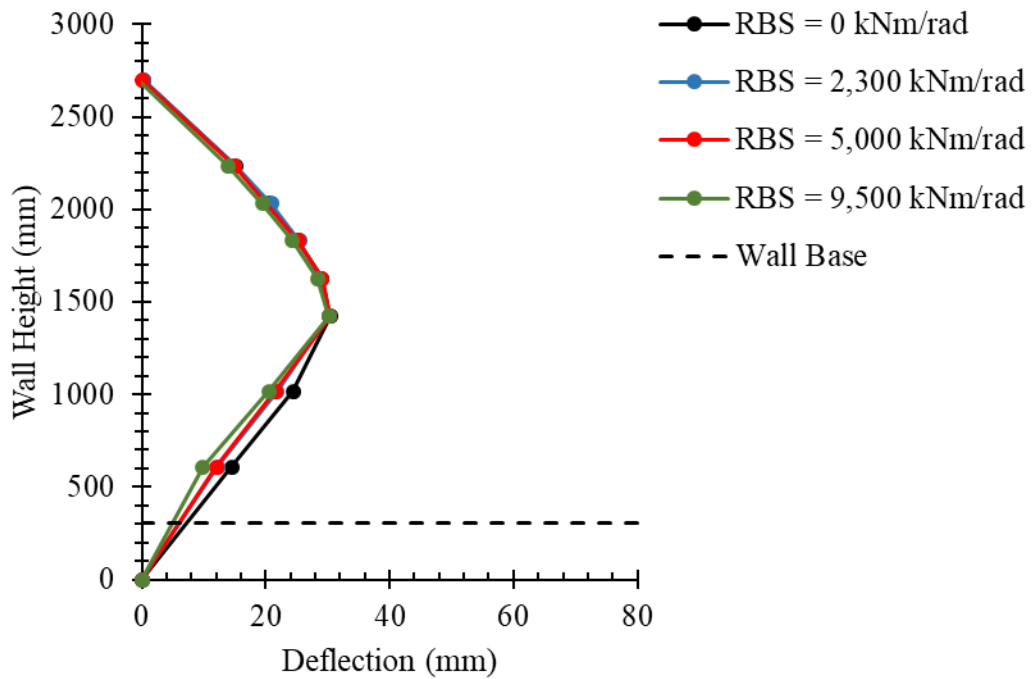


Figure 3.72 – Deflection Profiles (30-mm Cycle)

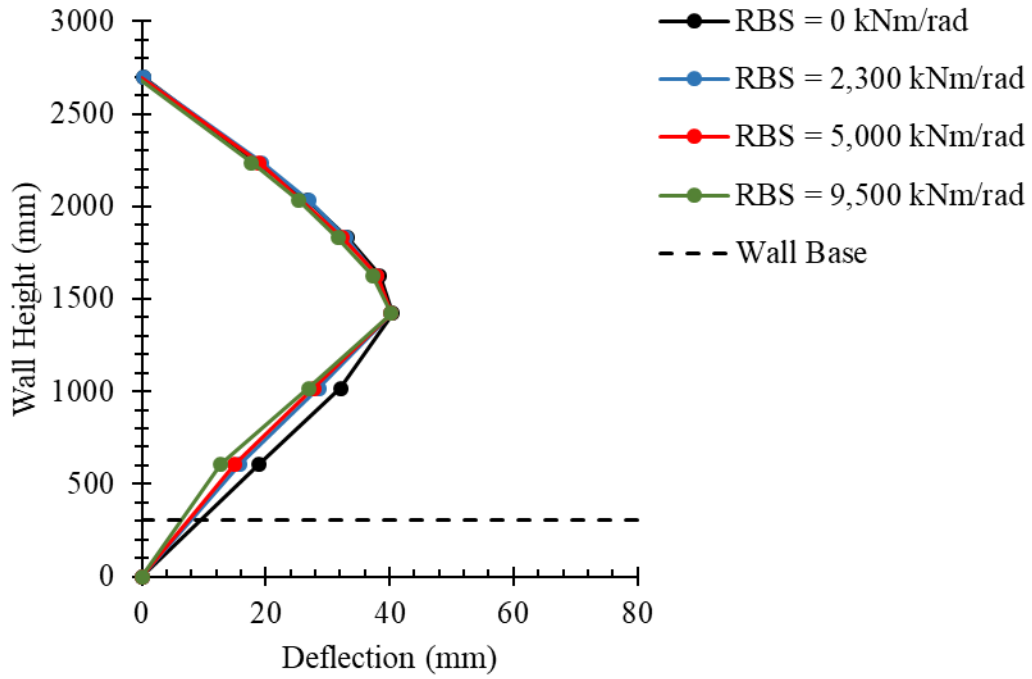


Figure 3.73 – Deflection Profiles (40-mm Cycle)

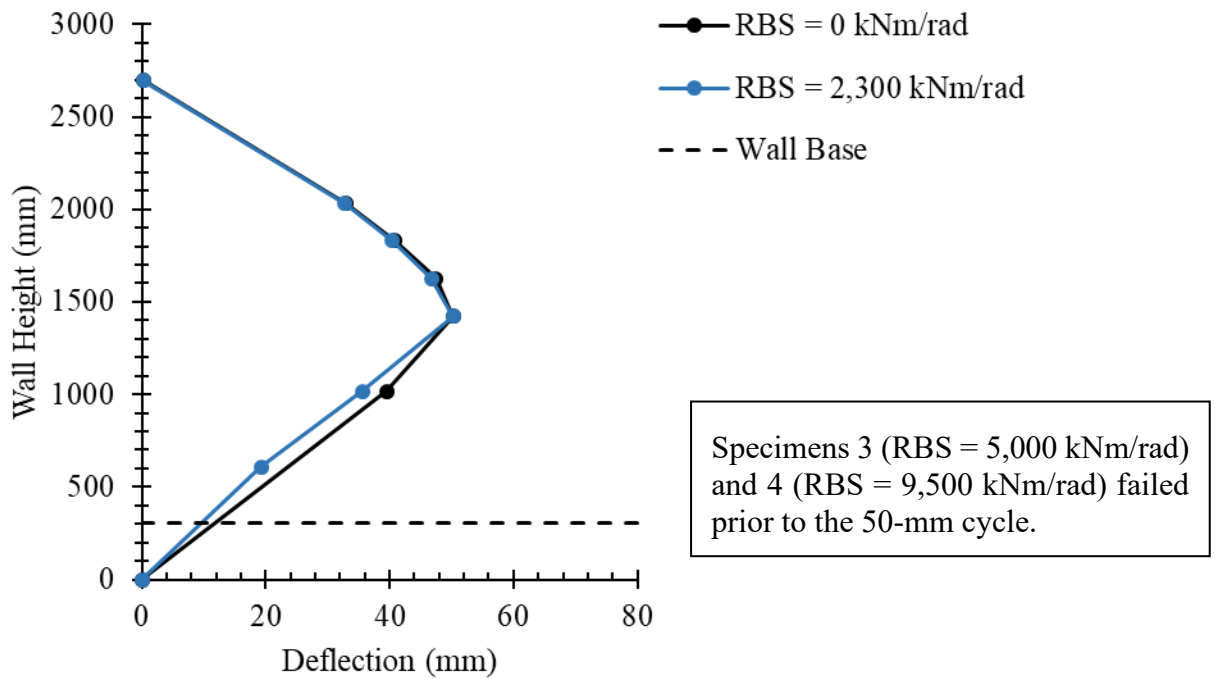


Figure 3.74 – Deflection Profiles (50-mm Cycle)

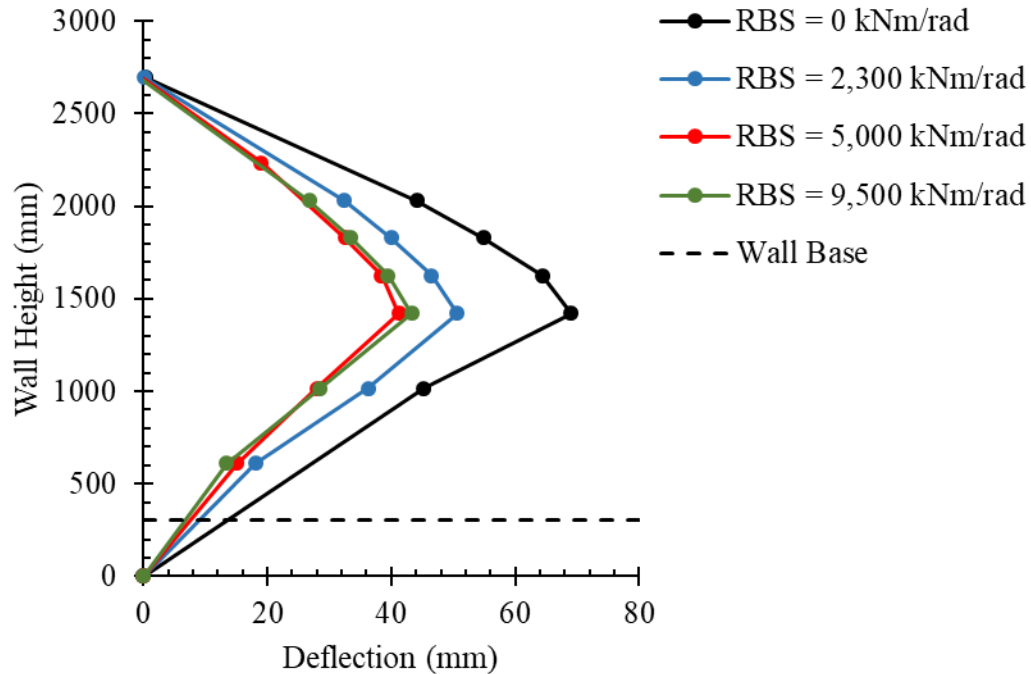


Figure 3.75 – Deflection Profiles (Failure)

3.9.7 Summary

A summary of the test results is presented in Table 3.18. Observations made concerning the effect of base rotational support stiffness on the behaviour and second-order effects experienced by masonry walls are as follows:

- An increase in rotational base support stiffness increases the lateral loadbearing capacity of the wall (up to 92.4%) and decreases OOP deflections.
- The rotation at the base of the wall was greatly reduced as much as 89% as the rotational base stiffness increased.
- The presence of base rotational stiffness creates a linear negative moment profile over the height of the wall resulting in moment redistribution.
- Effects of moment redistribution are more prevalent in the lower half of the wall and significantly reduced the moment at the midspan of the wall.

- Walls featuring a rotational base stiffness contained an inflection point near the base of the wall placing the walls into double curvature. As the magnitude of base stiffness was increased, the inflection point would shift up the wall.
- After peak load, the midspan moment of the walls with a base stiffness would decrease as a result of moment redistribution. The level of midspan moment reduction in Specimen 2 was so significant, the location of maximum moment shifted from the midspan to the base of the specimen before failure occurred resulting in a simultaneous failure along the lower half of the wall. Specimens 3 and 4 failed prior to the magnitude of the moment at the base exceeding that of the midspan moment.
- The moment magnification factor for Specimen 1 (no base rotational support stiffness) was greater than 1 (no negative moment profile to reduce the first- and second-order moments), while the remaining specimens with base rotational support stiffness had a moment magnification factor less than 1.

4 MECHANICS-BASED ANALYSIS MODEL FOR LOADBEARING MASONRY WALLS

4.1 Introduction

An accurate prediction of the behaviour of loadbearing masonry walls is difficult due to the inherent material nonlinearity of masonry, its anisotropic nature, complex tensile cracking mechanisms, and non-homogeneity. Therefore, analytical tools such as the FE method are commonly used to include for the phenomena mentioned above using suitable element and material formulations. However, developing FE models is often quite time consuming and, once complete, can be computationally expensive to run and maintain. As an alternative, this chapter presents the development of a simple mechanics-based model to predict the behaviour of loadbearing masonry walls using beam-column elements. Phenomena such as tensile cracking and material nonlinearity are included within the model through the fibre-section approach. The model development, validation, and application are presented and discussed in this section.

4.2 Formulation

Consider the deflection curves of a pinned-pinned masonry wall as illustrated in Figure 4.1. For the deflection curve seen in Fig. 4.1(a), a function ($u(x)$) can be defined to determine the horizontal deflection at any point (x) along the height of the wall. This function is obtained by solving the differential equation (Timoshenko and Gere 1961) reproduced below for convenience:

$$\frac{\partial^2}{\partial h^2} \left(EI \frac{\partial^2 u(x)}{\partial h^2} \right) + P \frac{\partial^2 u(x)}{\partial h^2} = q(x) \quad (2.4)$$

Due to the cracking of the masonry under tensile loads and the nonlinearity of the constitutive relationships for steel and masonry, the effective stiffness term (EI) in Eq. 2.4 is not constant. Therefore, an exact solution is complex. The solution of Eq. 2.4 can, however, be approximated by a Taylor series expansion as:

$$u(x) = u(a) + \frac{u'(a)}{1!}(x - a) + \frac{u''(a)}{2!}(x - a)^2 + \dots \quad (4.1)$$

where $u(x)$ = deflection function evaluated at point x ,

$u(a)$ = deflection function evaluated at point a ,

$u'(a)$ = first derivative of the deflection function evaluated at point a ,

$u''(a)$ = second derivative of the deflection function evaluated at point a , and

$(x - a)$ = distance between points x and a (element length).

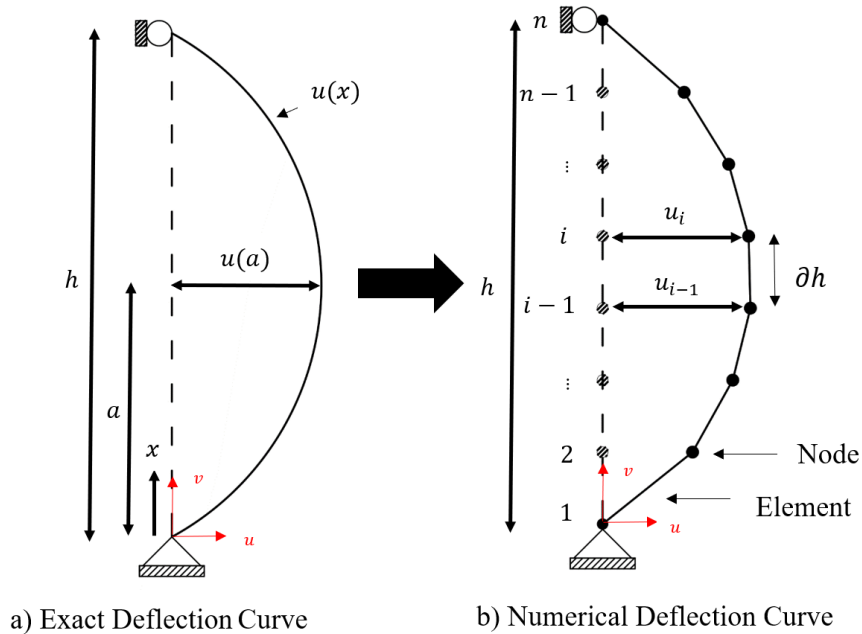


Figure 4.1 – Deflection Curves for Masonry Walls

Equation 4.1 indicates that the horizontal deflection at any point (x) along the masonry wall may be approximated if the parameters at a different point (a) are known. Equation 4.1 can also be further simplified using the relationships between deflection, slope, and curvature shown below:

$$u'(x) = \alpha(x) \quad (4.2)$$

$$u''(x) = \phi(x) \quad (4.3)$$

where $\alpha(x)$ = slope at point x , and

$\phi(x)$ = curvature at point x .

If the wall is discretized into $n - 1$ elements connected by n nodes, a piecewise deflection curve can be used to approximate the exact deflection of the wall, as illustrated in Fig. 4.1(b). Assuming the parameters of node $n - 1$ are known, a Taylor series expansion (Eq. 4.1) truncated after 3 terms can be used to approximate the horizontal deflection at node i :

$$u_i = u_{i-1} + \alpha_{i-1}\delta h + \frac{1}{2}\phi_{i-1}\delta h^2 \quad (4.4)$$

where u_i = deflection at node i ,

u_{i-1} = deflection at node $i - 1$,

α_{i-1} = slope at node $i - 1$,

ϕ_{i-1} = curvature at node $i - 1$, and

δh = distance between nodes i and $i - 1$ (element length).

Thus, to determine the deflection at each node, the deflection, slope, and curvature at the previous node must be known. A relationship for slope between nodes i and $i - 1$ can be determined using a similar methodology:

$$\alpha_i = \alpha_{i-1} + \phi_{i-1}\delta h \quad (4.5)$$

where α_i = slope at node i .

The curvature at each node is determined by a fibre-section approach using strain compatibility, but the internal moment at the section needs to be known. This can be done by equating the external moment to the internal moment (both depicted in Fig. 4.2) as expressed below:

$$M_{ext,i} = M_{int,i} \quad (4.6)$$

where $M_{ext,i}$ = external moment at node i and

$M_{int,i}$ = internal moment at node i .

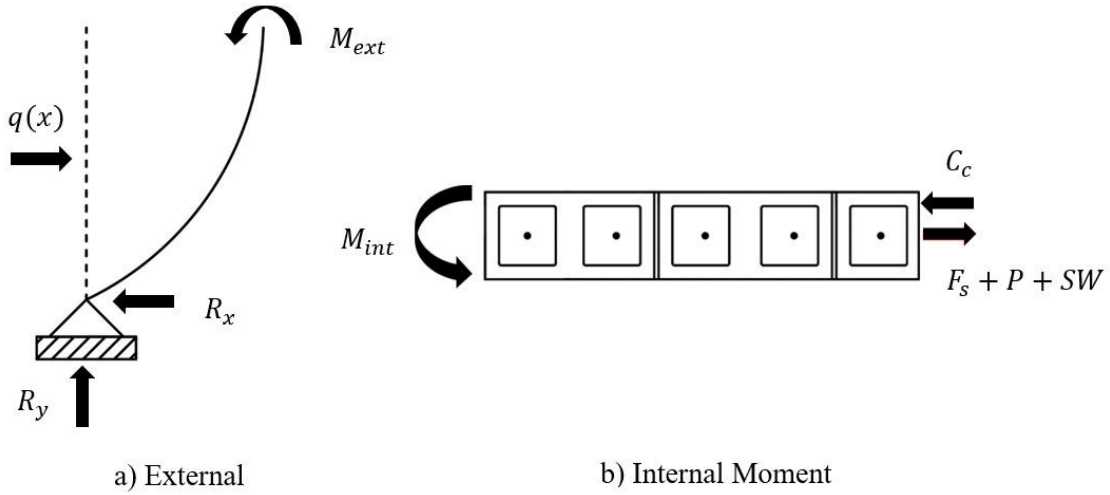


Figure 4.2 – a) External and b) Internal Moments

As shown in Fig. 4.2a, the total external moment at a node can be determined using statics. The external moment consists of the sum of first- and second-order moment. First-order moments are caused by lateral loads and concentrated moments, while second-order moments are caused by the product of the deflection of the wall and the axial load. The total external moment of a node can be determined as

$$M_{ext,i} = M_{o,i} + (P + SW_i) \left(u_{i-1} + \frac{\alpha_{i-1} \delta h}{2} \right) \quad (4.7)$$

where $M_{o,i}$ = first-order moment at node i and

SW_i = self-weight of the masonry above node i .

Once the external moment at a node is known, and thus the internal moment through Eq. 4.6, the associated value of curvature can be obtained through a conventional section compatibility analysis as discussed in the next section.

4.3 Moment–Curvature Relationship

The moment–curvature relationship is developed using strain compatibility. The cross-section is discretized into fibres. Material properties and geometry of the fibres are used to determine the forces present in each fibre for different values of strain using suitable constitutive relationships (discussed Section 4.4). Once equilibrium is satisfied, the resisting moment can be obtained by taking the moment of the forces in the fibres about a reference axis (e.g., the outermost fibre in compression, Eq. 4.8), and the curvature can be obtained by dividing the outermost compressive stresses of the masonry by the depth of the neutral axis (Eq. 4.9), as follows:

$$M_{ext,i} = \sum C_{mi}d_i + \sum T_{mi}d_i + \sum F_{si}d_i + P \left(e + \frac{t}{2} \right) + SW \left(\frac{t}{2} \right) \quad (4.8)$$

$$\phi = \frac{\varepsilon}{N.A.} \quad (4.9)$$

where C_{mi} = compressive force of the masonry in fibre i ,

T_{mi} = tensile force of the masonry in fibre i ,

F_{si} = force in reinforcing steel bar i ,

d_i = distance from fibre i to the reference axis,

ε = strain in the outmost masonry fibre in compression, and

$N.A.$ = neutral axis of the section.

The ultimate moment and curvature correspond either to the point at which the masonry crushes (Fig. 4.3) in compression or the point at which the steel ruptures.

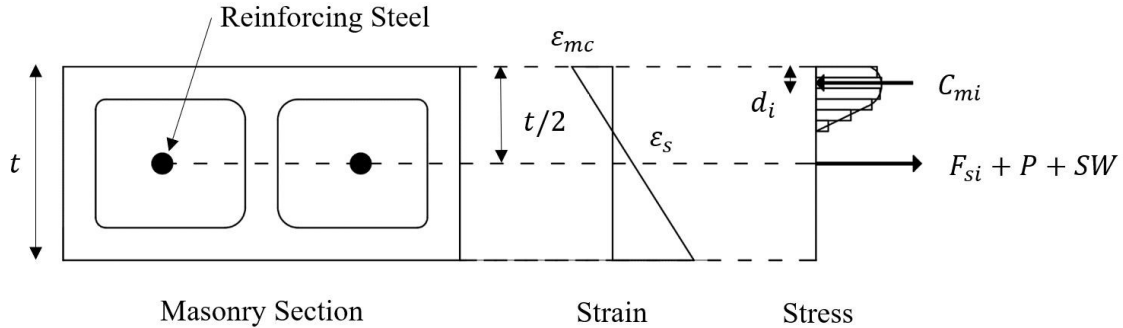


Figure 4.3 – Moment and Curvature at Failure

The location of the neutral axis is determined through an iterative procedure in which equilibrium (Eq. 4.10) is checked in the cross-section.

$$\sum C_{mi} + \sum T_{mi} + \sum F_{si} + P + SW = 0 \quad (4.10)$$

4.4 Material Models

4.4.1 Masonry

To simulate the response of masonry under compression, a modified version of the model proposed by Priestley and Elder (1983) was selected. The model assumes the maximum stress of the masonry to occur at a strain of 0.002 (Drysdale and Hamid 2005). For tension, the masonry is assumed to be elastic until its cracking stress is reached. Following the cracking stress, a tension softening model proposed by Wahalathantri et al. (2011) is implemented. The model consists of three linear branches which, as the tensile strain in the masonry increases, reduce the tensile capacity of the masonry. Figures 4.4 and 4.5 present the response of the masonry material in compression and tension respectively.

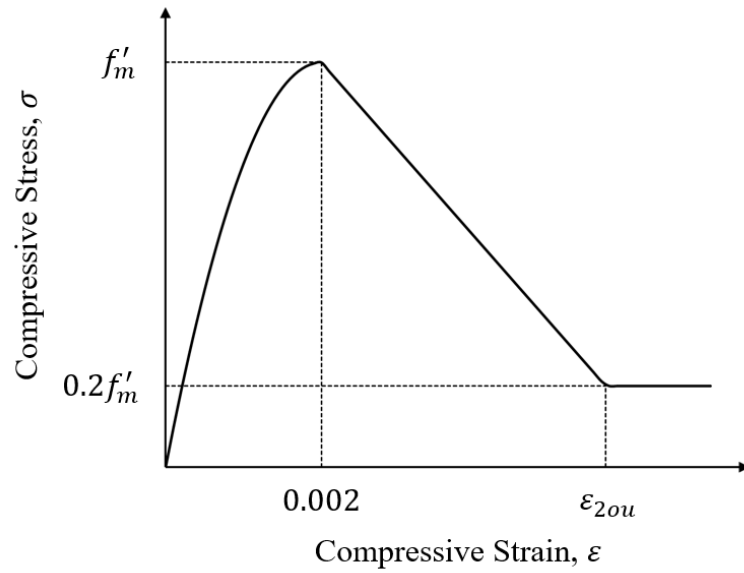


Figure 4.4 – Behaviour of Masonry under Compression

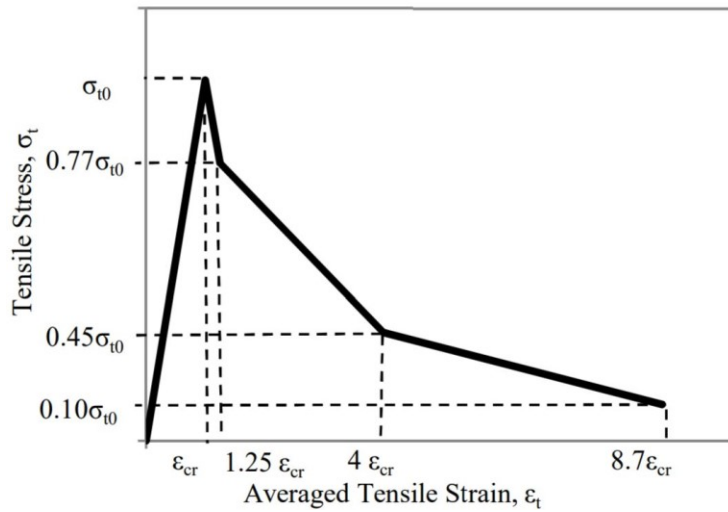


Figure 4.5 – Behaviour of Masonry under Tension (Wahalathantri et al. 2011)

4.4.2 Reinforcing Steel

The behaviour of the steel is assumed to be elastic until yield, followed by a linear strain hardening profile. The response is considered identical for both compression and tension. This behaviour is presented in Fig. 4.6 below.

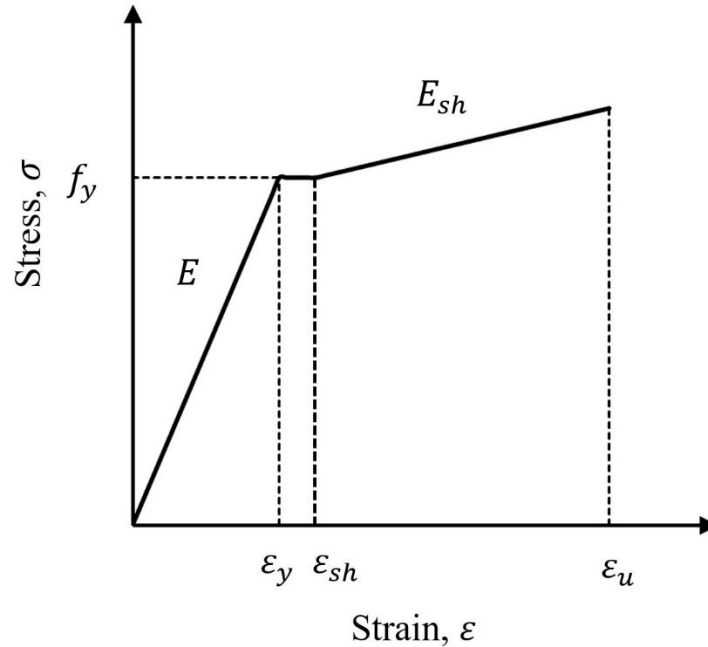


Figure 4.6 – Behaviour of Reinforcing Steel

4.5 Failure Modes

Three failure modes are defined in the model:

1. Crushing of the masonry: triggered when the strain in the masonry in compression exceeds the specified crushing strain.
2. Reinforcing bar rupture: triggered when then tensile strain in the reinforcing bars exceeds the specified rupture strain.
3. Wall instability: triggered when the axial load placed on the wall exceeds the critical bucking load.

4.6 Model Implementation

To begin the analysis, the deflection, slope, and curvature at the first node are required. These can be determined from the boundary conditions of the wall. For example, if the base of the wall features a pinned condition, it is known that the deflection at the base (i.e., the first node) is zero along with the curvature. The only unknown is the slope at the first node. This is determined through a trial and error process. To begin, an initial

slope is assumed, and the deflection equations are solved for all the nodes. Once the analysis is completed, the deflection at the final node (i.e., the top of the wall) is compared to the actual boundary condition at the top of the wall. For example, if the boundary condition at the top of the wall is restrained against deflection, the deflection at the final node must be zero. If the deflection is non-zero, a new guess of initial slope must be assumed, and analysis repeated until the top boundary condition is satisfied. This process is illustrated in Figure 4.7 below.

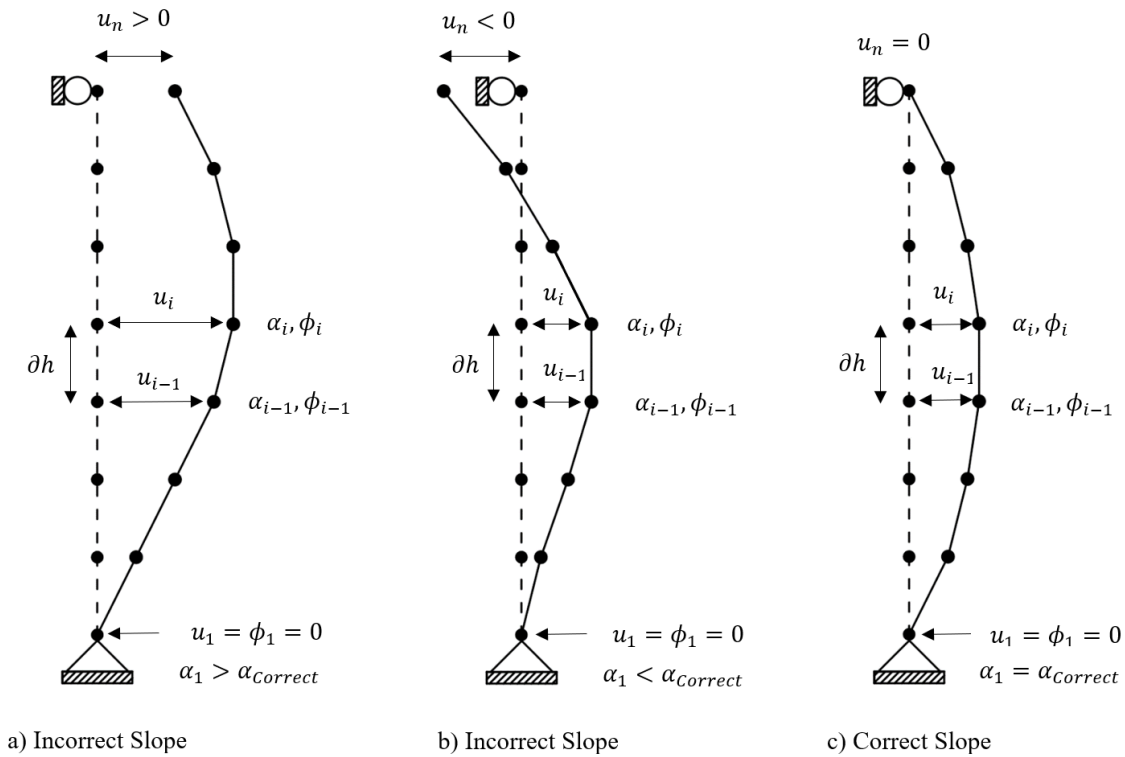


Figure 4.7 – Iteration of Initial Slope

Figure 4.8 outlines the process of the analysis model below. The analysis model described above was implemented in a script using MATLAB (MATLAB 2016). The script can be found in Appendix B.

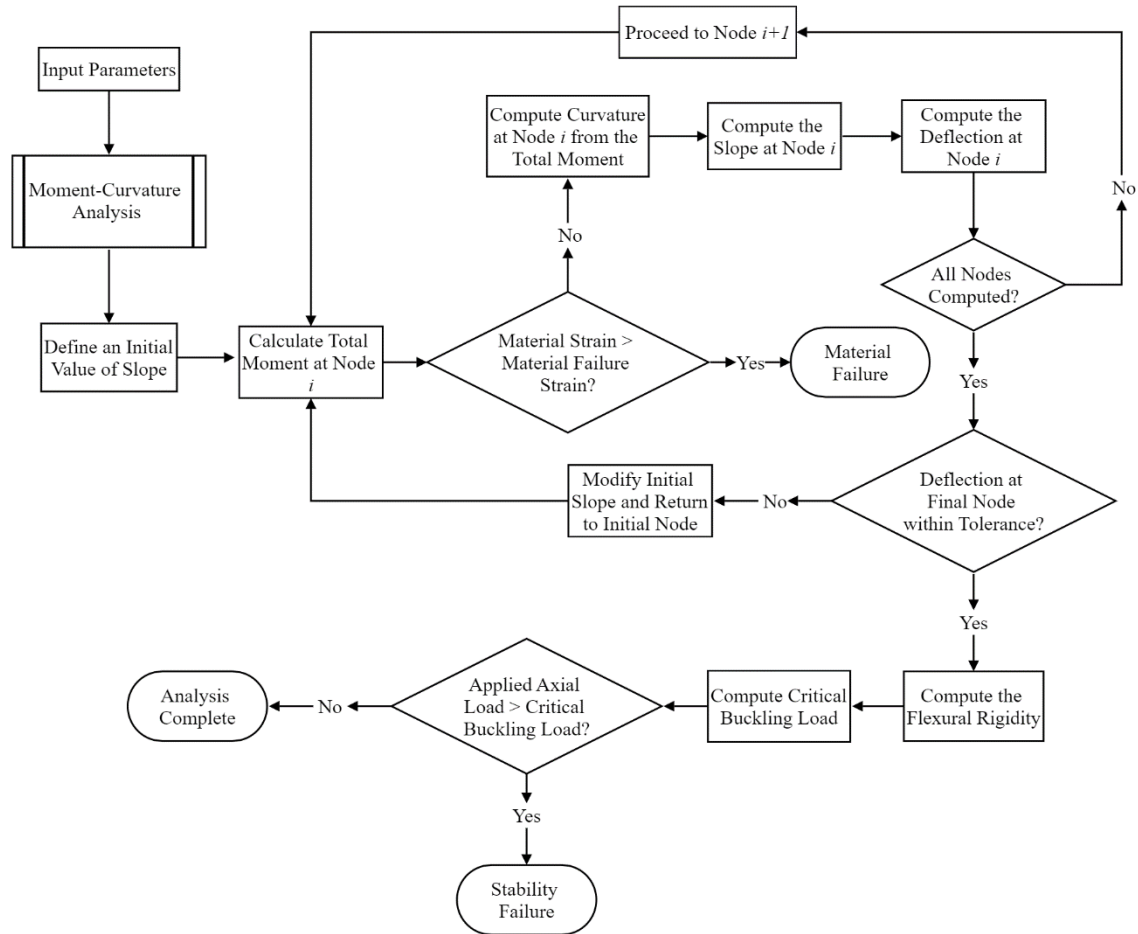


Figure 4.8 – Analysis Model Process

4.7 Model Limitations

The model is only valid for masonry walls with statically determinant boundary conditions loaded monotonically. In its current state, only load-control analysis is implemented in the analysis model. This prevents the model from predicting any post-peak response. However, the model is capable post-peak prediction if displacement-control is added. This can be accomplished by continuously increasing values of initial slope and iterating values of load until the top boundary condition is satisfied.

4.8 Validation

To determine the validity of the model, several walls from experimental campaigns, including those tested during this study, were modelled and the results compared with the measured data.

4.8.1 Study 1: Slender walls without a base stiffness subjected to a monotonic lateral load (SEASC 1982)

4.8.1.1 Experimental Setup

The experimental program was designed to test pinned-pinned slender masonry walls. Each wall specimen was subjected to a combination of axial and lateral loads. During the test, the axial load was held constant while the lateral load was increased until the specimen was judged to be close to failure. The lateral load consisted of a uniform pressure along the wall created with an airbag. The axial loads placed on the specimens were created through a pulley system in which a drum of water pulled downward. This axial load was applied eccentrically. The mid-wall displacements and lateral pressure were recorded at intervals during the experiment. Figure 4.10 below illustrates the test setup and specimen details.

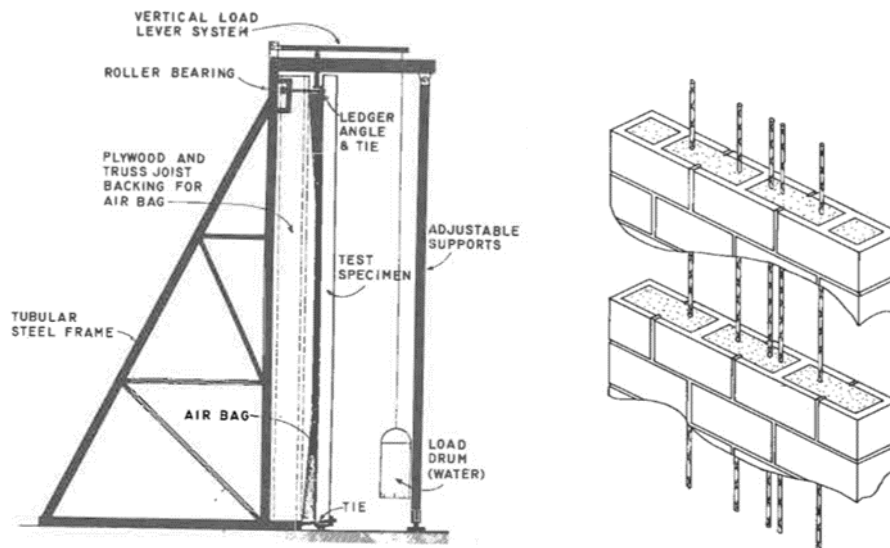


Figure 4.9 – ACI-SEASC Experimental Setup (ACI-SEASC 1982)

4.8.1.2 Masonry properties

Different thicknesses of concrete masonry units were used: 6 in (143 mm), 8 in (194 mm), and 10 in (246 mm). Material properties of the units were determined on-site through prism testing. The geometric and material properties of the walls are shown in Tables 4.1 and 4.2, respectively.

Table 4.1 – Masonry Wall Panel Summary (SEASC 1982)

Panel	Panel Thickness (mm)	Axial Load (kN)	Slenderness Ratio	Failure Mode
1	246	5.7	30.6	Stopped Test
2	246	15.3	30.6	Stopped Test
3	246	15.3	30.6	Stopped Test
4	194	15.3	38.8	Stopped Test
5	194	15.3	38.8	Stopped Test
6	194	5.7	38.8	Stopped Test
7	143	5.7	52.6	Masonry Crushing
8	143	5.7	52.6	Masonry Crushing
9	143	5.7	52.6	Stopped Test

Table 4.2 – Masonry Material Properties (SEASC 1982)

Masonry Unit	Compressive Strength (MPa)	Modulus of Elasticity (MPa)
10 in (246 mm)	17.0	14,962
8 in (194 mm)	17.9	11,859
6 in (143 mm)	22.0	10,963

Each panel was reinforced with five #4 bars of Grade 60 (420 MPa) steel (Fig. 4.10). The material properties of the steel rebar are shown in Table 4.3.

Table 4.3 – Reinforcing Steel Properties (SEASC 1982)

Grade	Yield Strength (MPa)	Ultimate Strength (MPa)	Yield Strain	Elastic Modulus (MPa)
60	483	758	0.0025	197,190

4.8.1.3 Results

For the initial elastic response prior to tensile cracking, the analytical model predicts an accurate load-displacement response in the elastic region for each panel. Graphs presenting the lateral pressure as a function of midpoint deflection for all panels can be found in Figures 4.15 to 4.23 below.

After cracking, but before yielding, the model predicts slightly greater deflections for given lateral loads than those obtained during the experiment for all panels. This is a result of a dip phenomena in the moment-curvature response after cracking occurs.

The dip in the moment-curvature response is a result of the tensile force in the masonry exceeding that of the axial load on the cross-section. This will either occur when a large axial load is present on the cross-section or the cross-section is relatively thick (i.e. large masonry units). If the tensile force in the masonry exceeds the axial load on the cross-section, force equilibrium within the cross-section will be controlled by the tensile force of the masonry. From this, when the masonry begins to crack and the tensile forces in the cross-section decrease, the compressive force in the masonry will also decrease. This decrease will continue until enough tensile strain is developed in the reinforcing bars to compensate for the lacking tensile capacity of the masonry (Fig. 4.10). With both the tensile and compressive forces in the masonry decreasing, the moment capacity of the section will also decrease resulting in the dip in the moment-curvature response (Fig. 4.11).

The opposite is true when the axial load on the cross-section exceeds that of the tensile force produced by the masonry. In this case, force equilibrium is controlled by the axial load, which will force the compressive force in the masonry to continuously increase

throughout the moment-curvature analysis (Fig. 4.12). This continuous increase allows for the moment capacity of the section to always increase with curvature (Fig. 4.13).

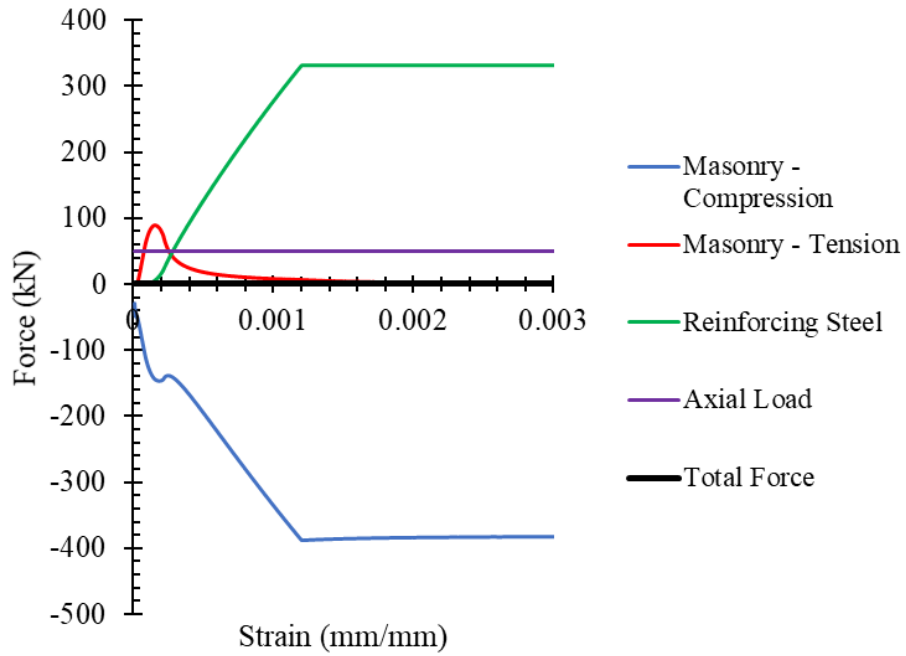


Figure 4.10 – Analysis Model Force Equilibrium (Axial Load < Masonry Tensile Force)

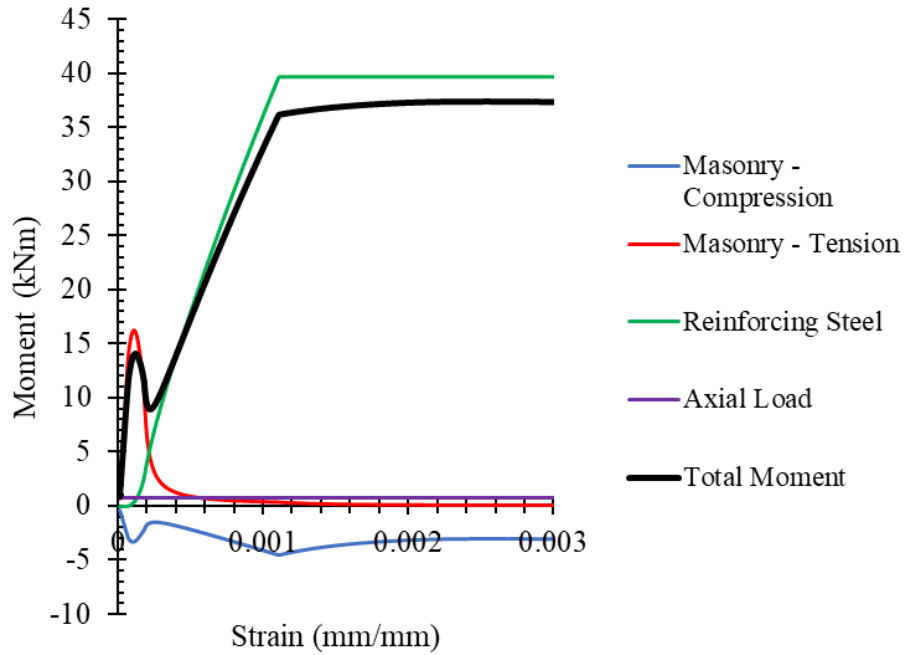


Figure 4.11 – Analysis Model Moment Composition (Axial Load < Masonry Tensile Force)

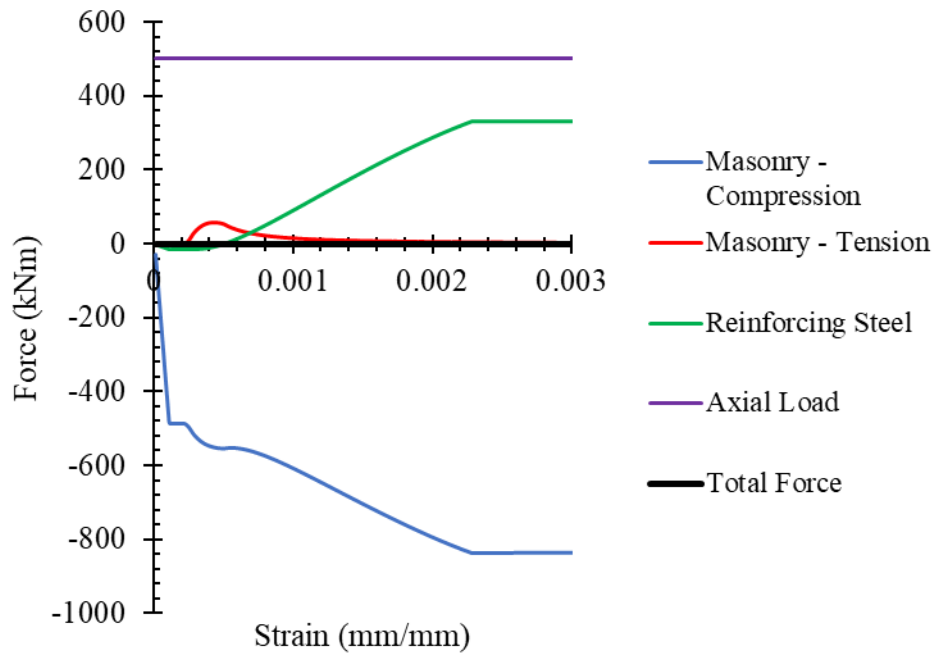


Figure 4.12 – Analysis Model Force Equilibrium (Axial Load > Masonry Tensile Force)

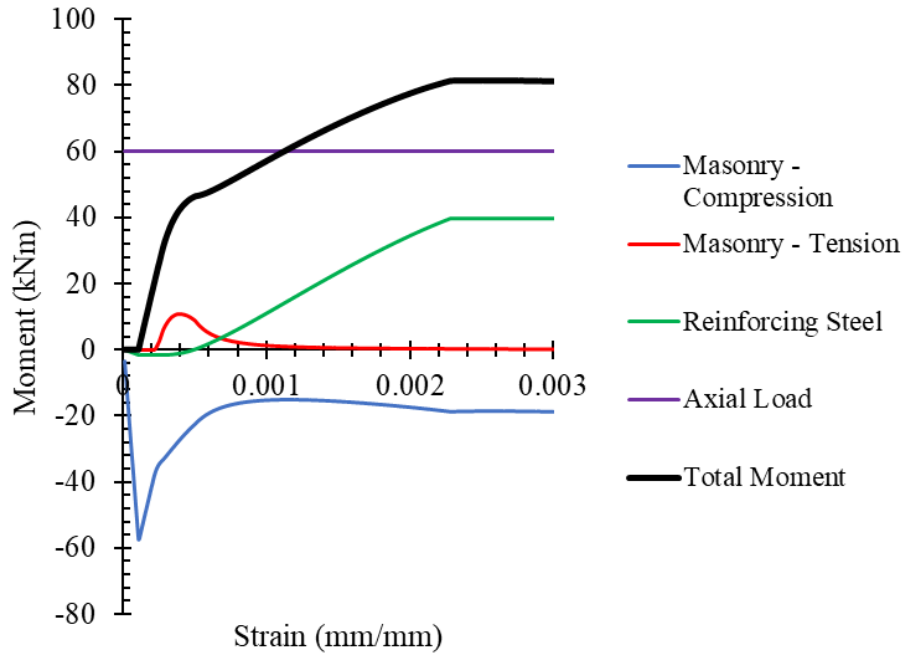


Figure 4.13 – Analysis Model Moment Composition (Axial Load > Masonry Tensile Force)

The dip is problematic as it produces multiple values of curvature for the same value of moment. To avoid computation errors, the dip is removed from the response and replaced with a linear line (Fig. 4.14). As a result, there is a noticeable jump in curvature in the moment-curvature response after yielding with magnitude of the jump increasing with block size. This jump would result in the analysis model predicting excess deflections after yielding which is exactly what was experienced during the simulation of the panels. The analytical predictions for panels 1, 4, and 8 closely resemble the behaviour of the experimental tests, with only minor variations.

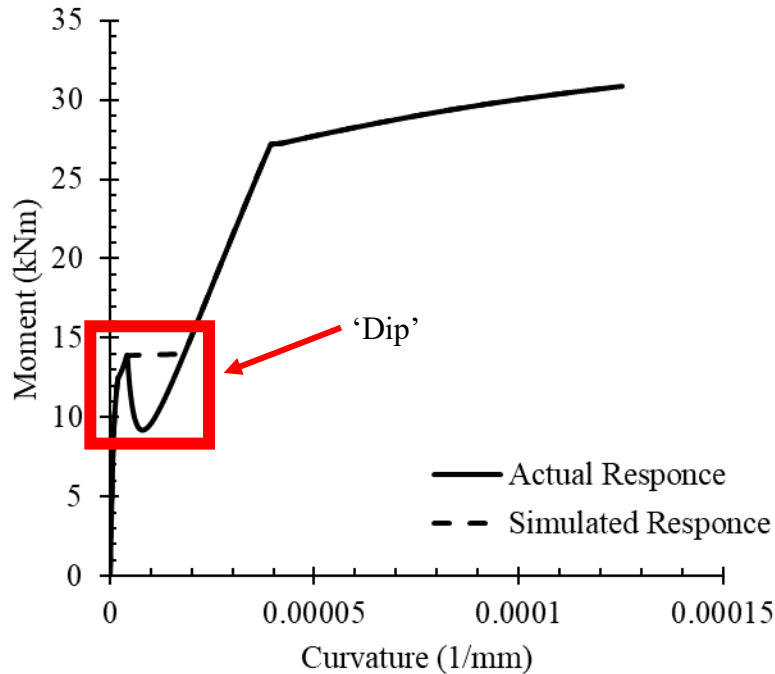


Figure 4.14 – Moment-Curvature Response

Analytical predictions for panels 2, 3, 5, 6, 7, and 9, overestimate the stiffness of the panels by an average of 30.2%, as the slope of their load-displacement curves are higher than those from experimental results.

When approaching the ultimate moment of the panels, many of the analytical result curves for the panels predict a greater failure displacement than seen with the experimental results, with the exceptions being panels 3, 7, and 8. This behaviour is expected for Panels 7 and 8, as experimental testing of the panels (except for panels 7 and 8) was stopped before failure occurred. Although Panel 3 was stopped prior to failure, the amount of deflection reported when the test was stopped greatly exceeds those of Panels 1 and 2, indicating failure was near. This would explain why the experimental results show a greater deflection at failure as compared to the analytical results. For panels 7 and 8, the failure points predicted by the analytical model match well those of the experimental results. The failure lateral pressure predicted by the analytical model also approximates that of the experimental testing for the remaining panels, suggesting the analytical model retains a reasonable level of accuracy.

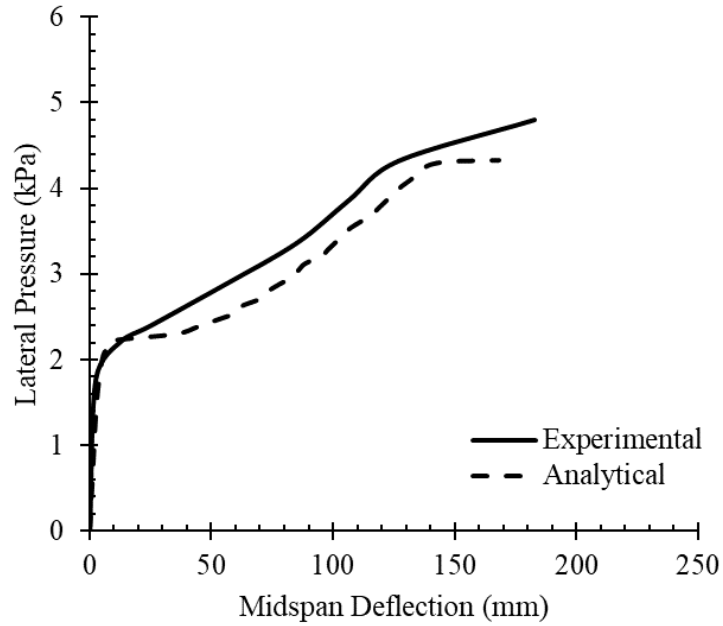


Figure 4.15 – Comparison of Analytical Model Prediction to Results of SEASC Experiment (Panel 1, $h/t = 31$, Base Stiffness = 0 kNm/rad)

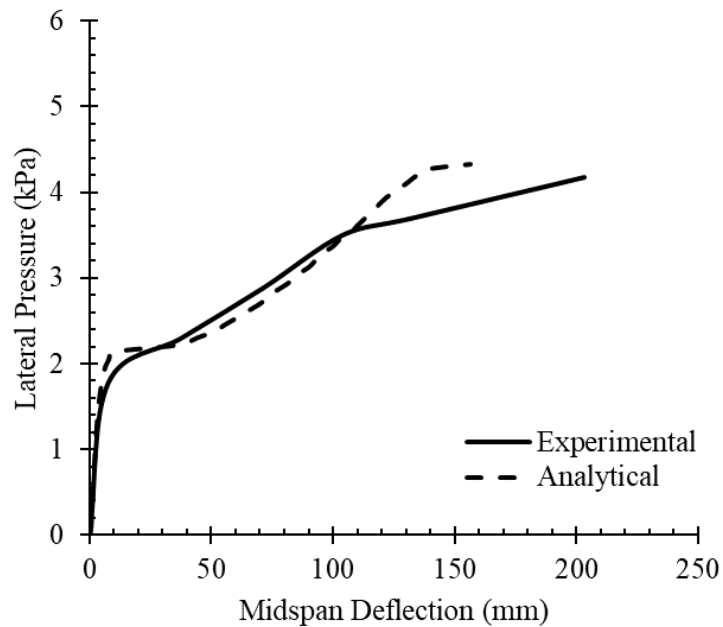


Figure 4.16 – Comparison of Analytical Model Prediction to Results of SEASC Experiment (Panel 2, $h/t = 31$, Base Stiffness = 0 kNm/rad)

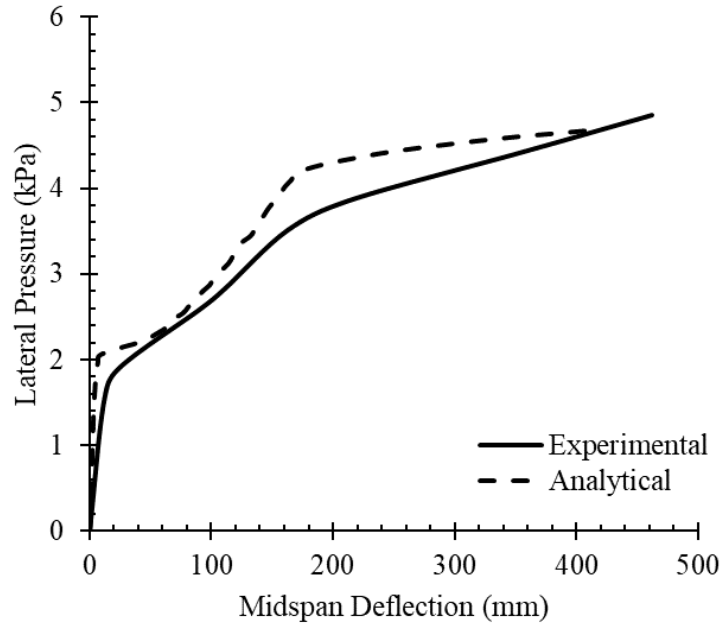


Figure 4.17 – Comparison of Analytical Model Prediction to Results of SEASC Experiment (Panel 3, $h/t = 31$, Base Stiffness = 0 kNm/rad)

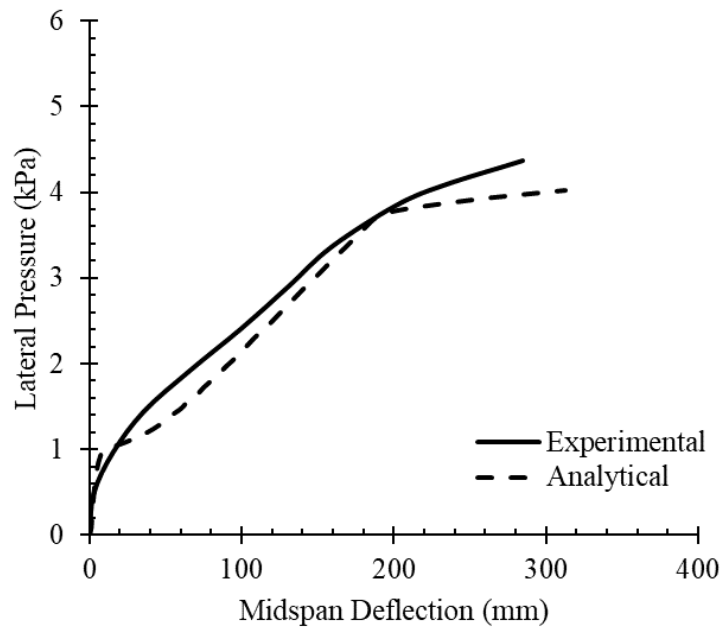


Figure 4.18 – Comparison of Analytical Model Prediction to Results of SEASC Experiment (Panel 4, $h/t = 39$, Base Stiffness = 0 kNm/rad)

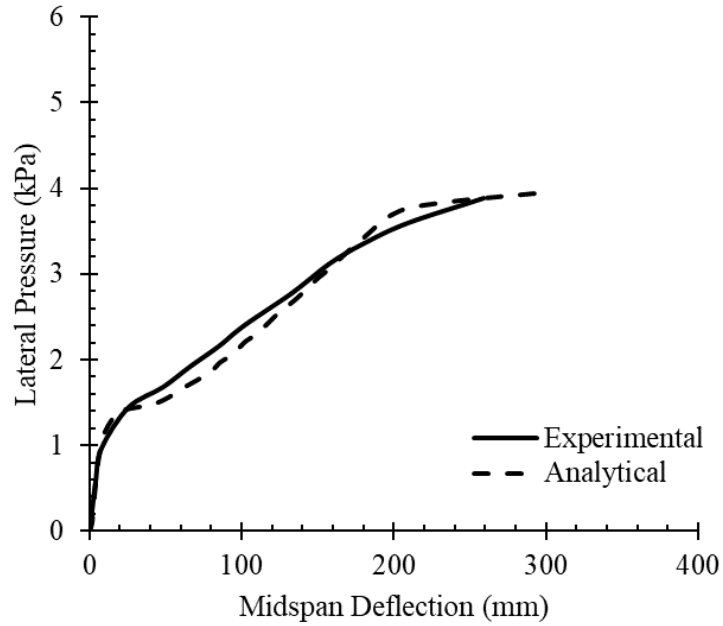


Figure 4.19 – Comparison of Analytical Model Prediction to Results of SEASC Experiment (Panel 5, $h/t = 39$, Base Stiffness = 0 kNm/rad)

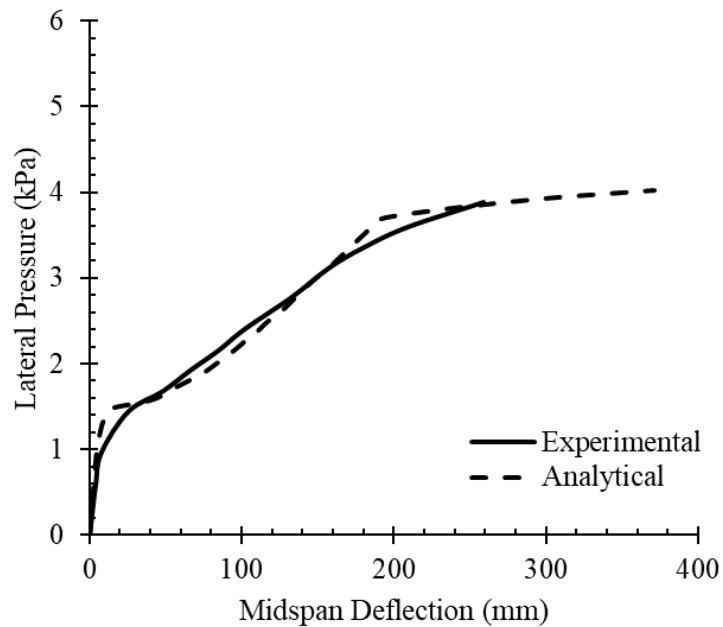


Figure 4.20 – Comparison of Analytical Model Prediction to Results of SEASC Experiment (Panel 6, $h/t = 39$, Base Stiffness = 0 kNm/rad)

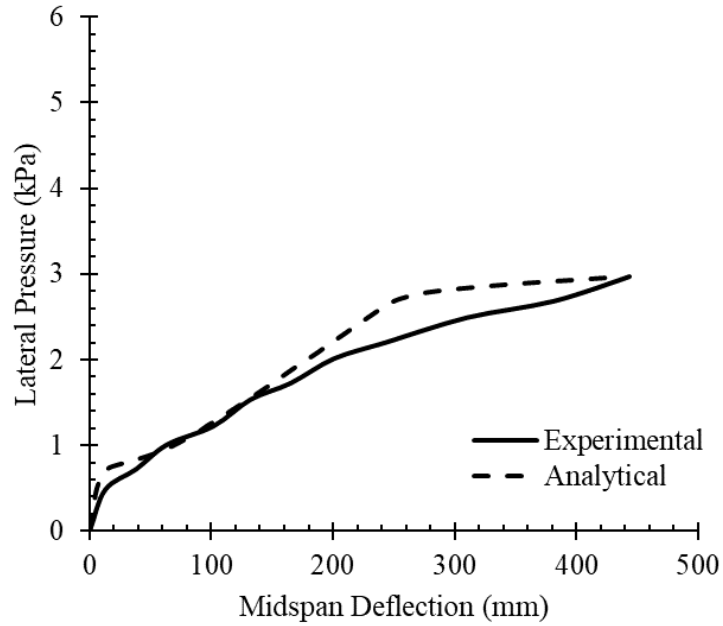


Figure 4.21 – Comparison of Analytical Model Prediction to Results of SEASC Experiment (Panel 7, $h/t = 51$, Base Stiffness = 0 kNm/rad)

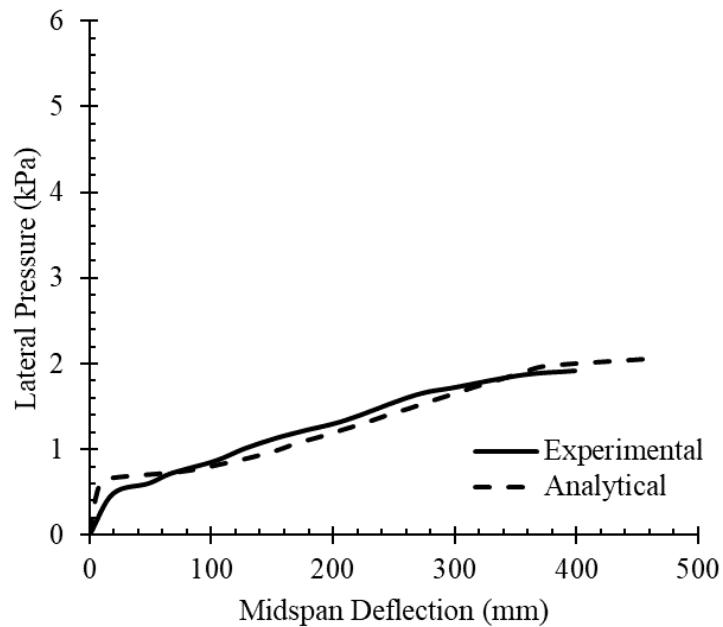


Figure 4.22 – Comparison of Analytical Model Prediction to Results of SEASC Experiment (Panel 8, $h/t = 51$, Base Stiffness = 0 kNm/rad)

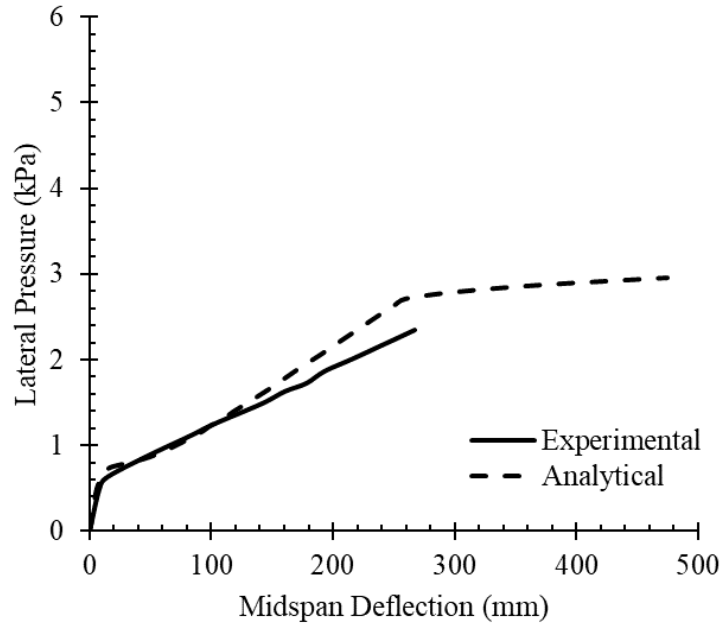


Figure 4.23 – Comparison of Analytical Model Prediction to Results of SEASC Experiment (Panel 9, $h/t = 51$, Base Stiffness = 0 kNm/rad)

4.8.2 Study 2: Slender walls with a base stiffness subjected to a monotonic gravity load (Mohsin 2003)

4.8.2.1 Experimental Setup

Eight slender concrete masonry walls were tested under an eccentric axial load with reactive support conditions. The testing was conducted in two groups. The first group consisted of 4 walls with a slenderness ratio (h/t) of 28.6, while the second group consisted of 4 walls with $h/t = 33.9$. Within each group, the amount of support stiffness provided at the base of each wall was varied during testing, including pinned base conditions. Figure 4.24 depicts the testing setup used.

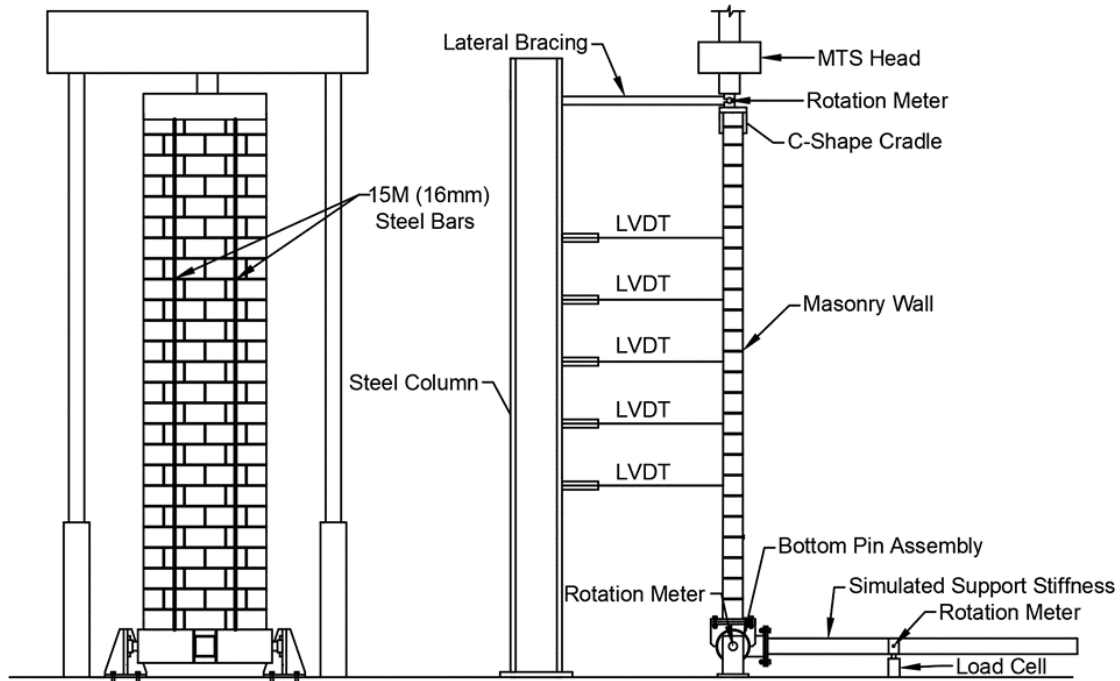


Figure 4.24 – Mohsin Experimental Setup (Mohsin 2003)

4.8.2.2 Masonry Assemblage

Results for 8 masonry walls panels are available. All panels had an identical cross-section (Fig. 4.25) and contained two 15M reinforcing steel bars. The material properties of the units were determined through prism testing. The geometric and material properties of the walls are shown in Tables 4.4 and 4.5, respectively.

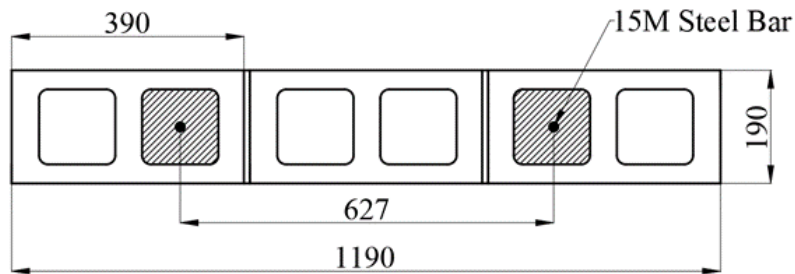


Figure 4.25 – Specimen Cross-Section (Mohsin 2003)

Table 4.4 – Test Specimen Summary (Mohsin 2003)

Specimen	Height (mm)	Slenderness Ratio	Base Rotational Stiffness (kNm/rad)
W1	5,437	28.6	0
W2	5,437	28.6	1,000
W3	5,437	28.6	5,000
W4	5,437	28.6	10,000
W5	6,437	33.9	0
W6	6,437	33.9	1,000
W7	6,437	33.9	5,000
W8	6,437	33.9	10,000

Table 4.5 – Masonry Material Properties (Mohsin 2003)

Prism Type	Compressive Strength (MPa)	Modulus of Elasticity (MPa)
Hollow	14.6	14,335
Grouted	10.2	7,379

Each panel was reinforced with two 15M steel rebars of Grade 400. The material properties of the steel rebar are shown in Table 4.6.

Table 4.6 – Reinforcing Steel Properties (Mohsin 2003)

Grade	Yield Strength (MPa)	Ultimate Strength (MPa)	Yield Strain	Elastic Modulus (MPa)
400	423	568	0.00197	215,000

4.8.2.3 Results

Comparing the results produced by the analysis model with those obtained from the experimental testing, it is seen that the model can predict the behaviour of the walls with reasonable accuracy. The experimental elastic response of the wall is very similar to that produced by the analysis model, with only minor discrepancies present in specimens W3 and W8. This minor error can be attributed to some variation in material properties or

some possible slack in the experimental setup (any slack would neglect the influence of base rotational stiffness for the initial stage of the test).

The largest discrepancy present in all cases of the comparison is the underprediction of both the peak eccentric axial load and the corresponding midspan deflection. This may also be due to a possible discrepancy in material properties, as the underprediction is within 10% for all cases except for Specimen W3. This is expected as Specimen W3 failed locally at the top of the wall due to inadequate anchorage. Graphs presenting the eccentric axial load as a function of midpoint deflection for all panels can be found in Figures 4.26 to 4.33 below.

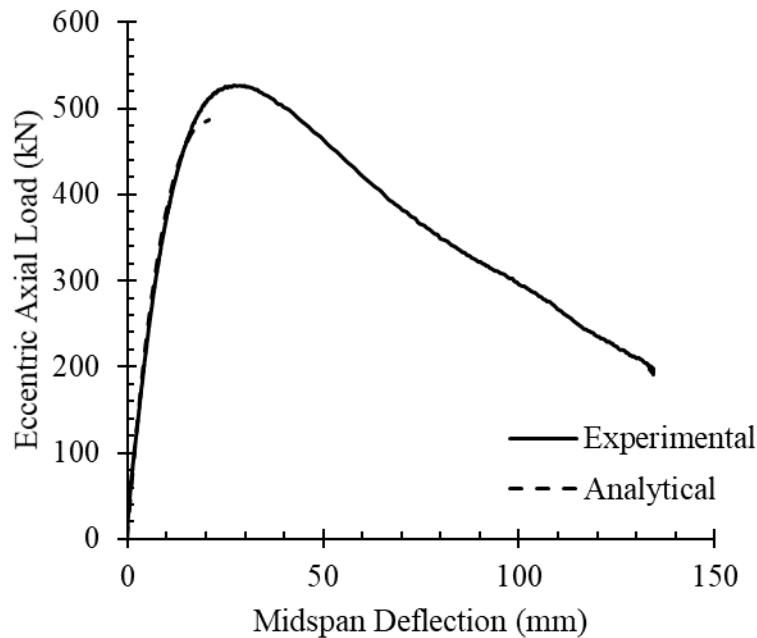


Figure 4.26 – Comparison of Analytical Model Prediction to Results of Mohsin Experiment (W1, $h/t = 29$, Base Stiffness = 0 kNm/rad)

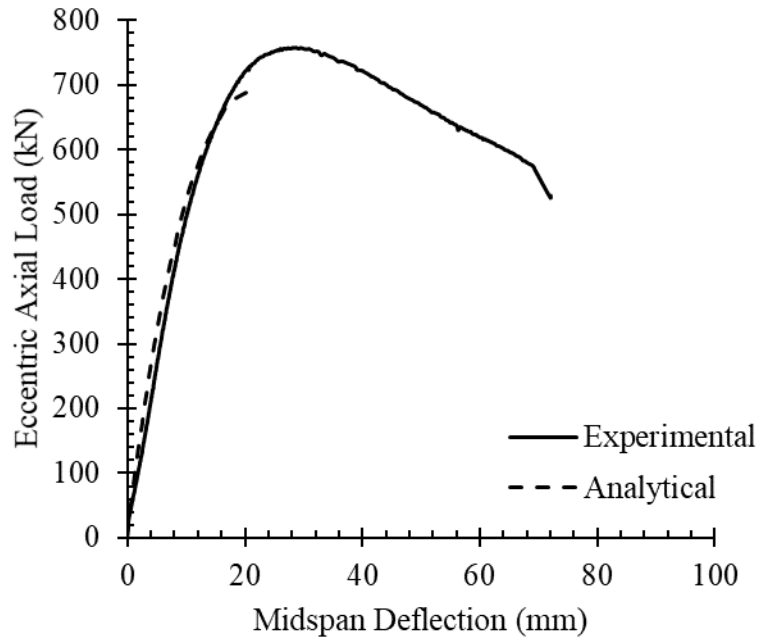


Figure 4.27 – Comparison of Analytical Model Prediction to Results of Mohsin Experiment (W2, $h/t = 29$, Base Stiffness = 1,000 kNm/rad)

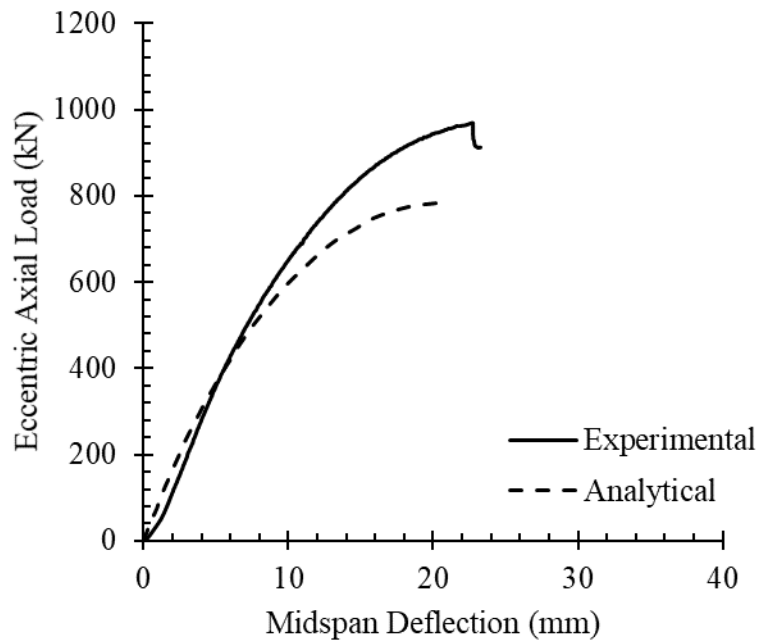


Figure 4.28 – Comparison of Analytical Model Prediction to Results of Mohsin Experiment (W3, $h/t = 29$, Base Stiffness = 5,000 kNm/rad)

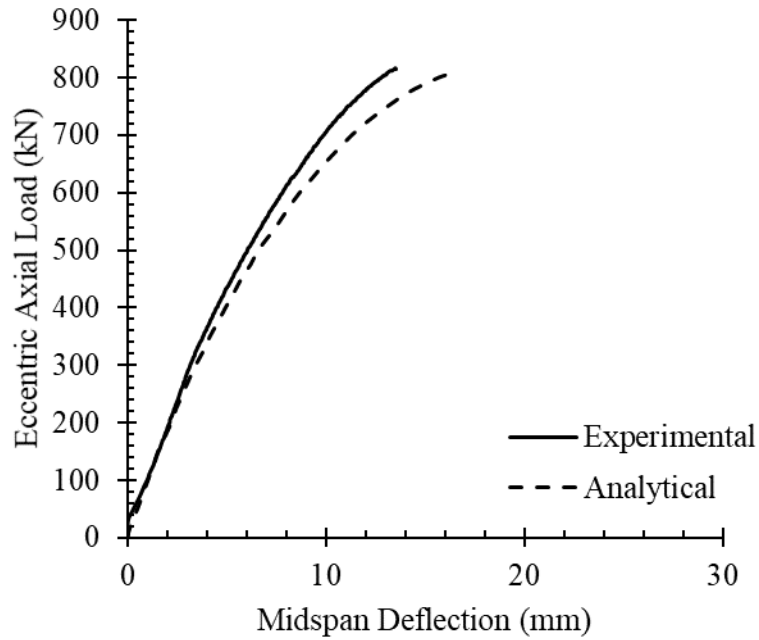


Figure 4.29 – Comparison of Analytical Model Prediction to Results of Mohsin Experiment (W4, $h/t = 29$, Base Stiffness = 10,000 kNm/rad)

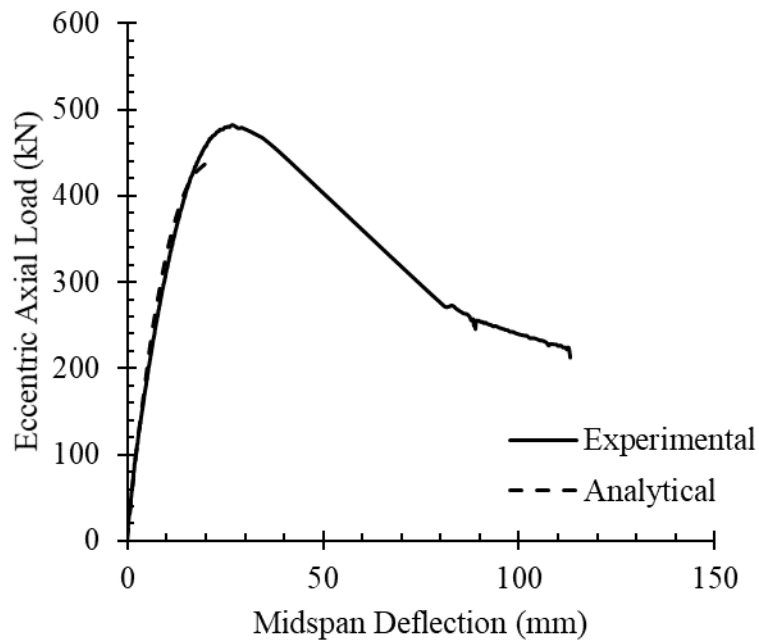


Figure 4.30 – Comparison of Analytical Model Prediction to Results of Mohsin Experiment (W5, $h/t = 34$, Base Stiffness = 0 kNm/rad)

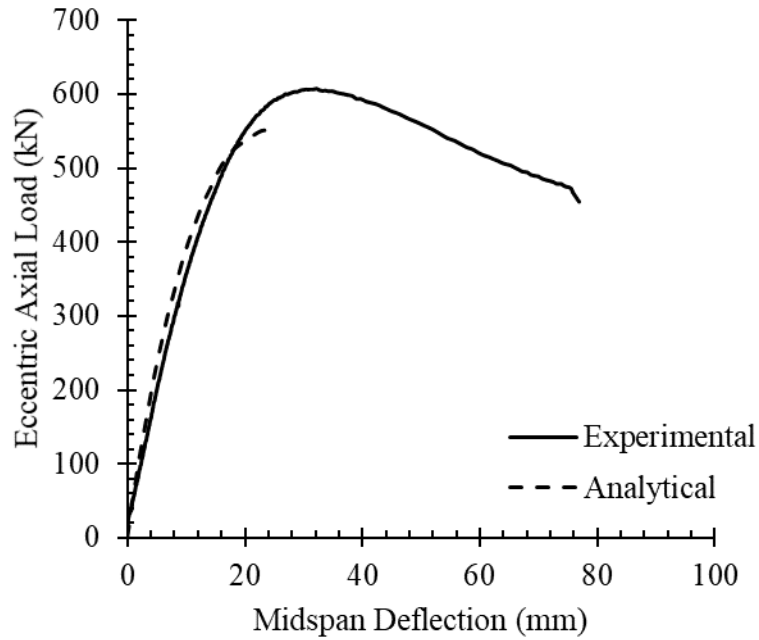


Figure 4.31 – Comparison of Analytical Model Prediction to Results of Mohsin Experiment (W6, $h/t = 34$, Base Stiffness = 1,000 kNm/rad)

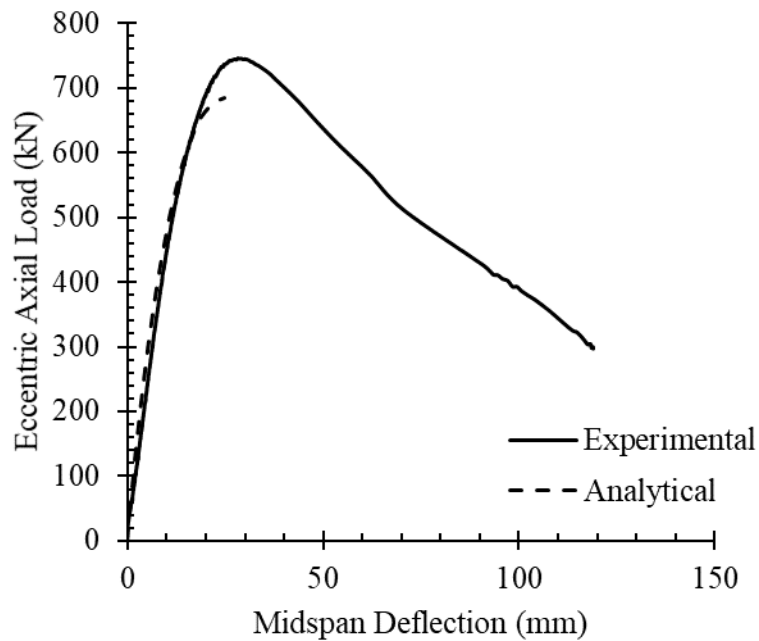


Figure 4.32 – Comparison of Analytical Model Prediction to Results of Mohsin Experiment (W7, $h/t = 34$, Base Stiffness = 5,000 kNm/rad)

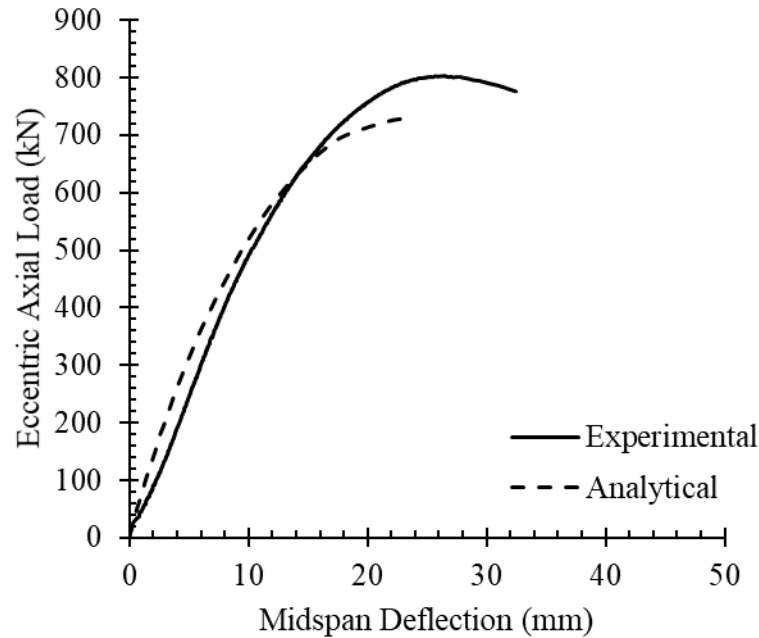


Figure 4.33 – Comparison of Analytical Model Prediction to Results of Mohsin Experiment (W8, $h/t = 34$, Base Stiffness = 10,000 kNm/rad)

4.8.3 Study 3: Non-slender walls with a base stiffness subjected to a cyclic lateral load

In this section, the walls tested in this study will be analyzed with the model. Details of the experimental setup and material properties were discussed in Chapter 3. Comparing the analytical results from the analysis model to the experimentally obtained results reveals that the analysis model can predict the elastic region with reasonable accuracy. However, as the moment begins to exceed the cracking moment, the stiffness of the walls reported by the analysis model is slightly less than the experimental results. This is because of the dip in the moment-curvature response discussed above.

Looking at the peak lateral load, the model is able to successfully account for the increase in lateral load capacity when the base rotational stiffness is increased, with the average difference between predicted and actual peak lateral load being 5.69%. Table 4.7 compares the peak lateral loads obtained from the analysis model and experimental testing.

Table 4.7 – Peak Lateral Load Comparison

Specimen	Base Rotational Stiffness (kNm/rad)	Peak Lateral Load (kN)		Relative Difference
		Analysis Model	Experimental Test	
1	0	50.2	52.5	4.38%
2	2,300	84.3	87.4	3.55%
3	5,000	93.1	101	7.62%
4	9,500	89.0	95.9	7.19%

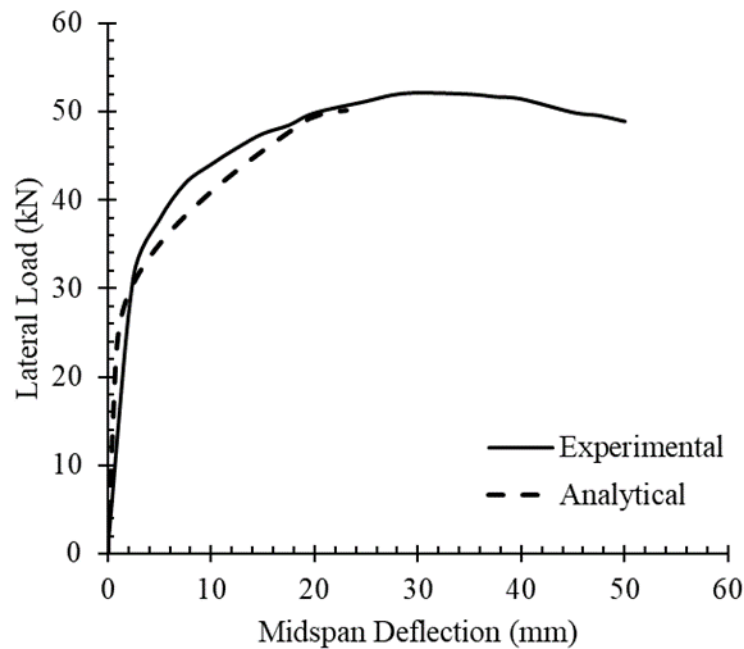


Figure 4.34 – Comparison of Analytical Model Prediction to Results of Chapter 3 Experiment (Specimen 1, $h/t = 12$, Base Support Stiffness = 0 kNm/rad)

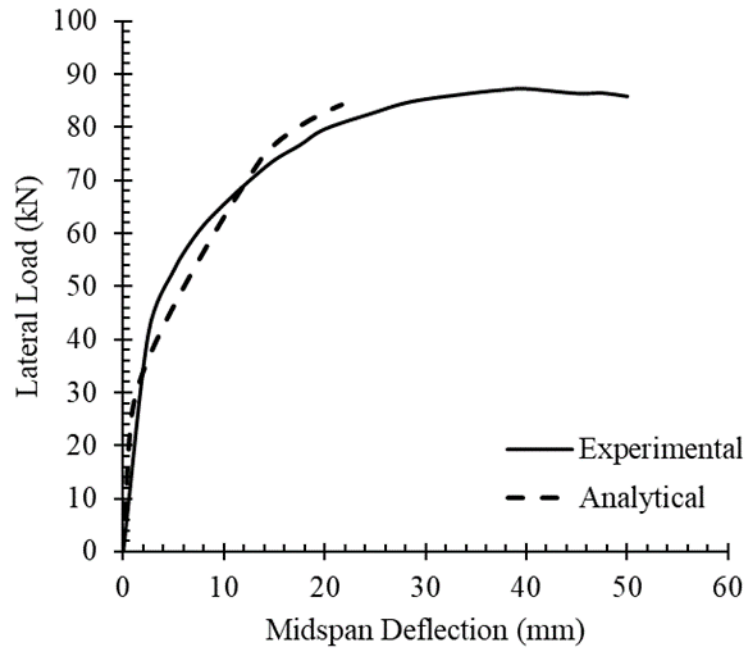


Figure 4.35 – Comparison of Analytical Model Prediction to Results of Chapter 3 Experiment (Specimen 2, $h/t = 12$, Base Stiffness = 2,300 kNm/rad)

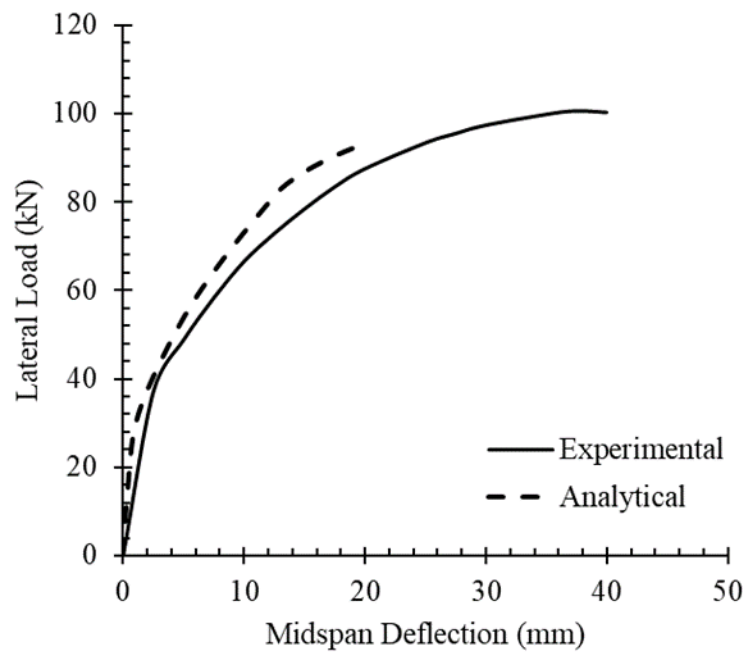


Figure 4.36 – Comparison of Analytical Model Prediction to Results of Chapter 3 Experiment (Specimen 3, $h/t = 12$, Base Stiffness = 5,000 kNm/rad)

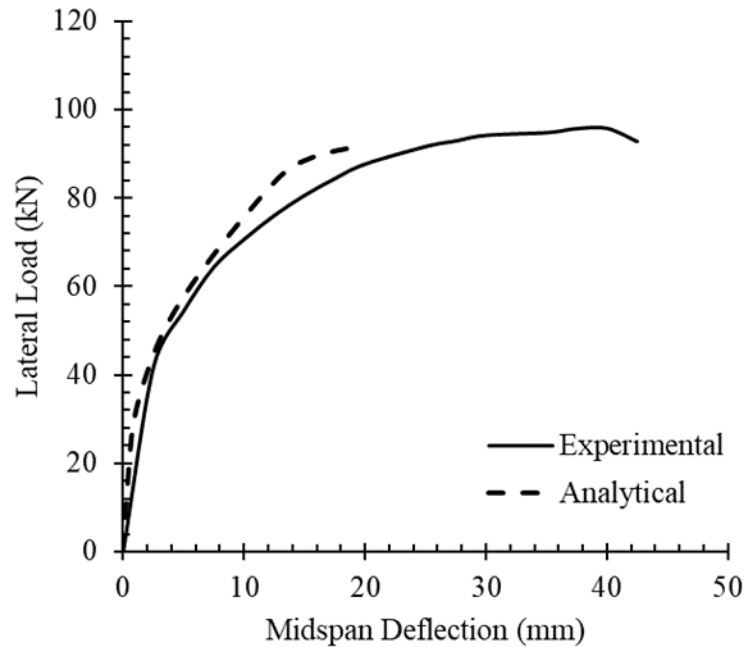


Figure 4.37 – Comparison of Analytical Model Prediction to Results of Chapter 3 Experiment (Specimen 4, $h/t = 12$, Base Stiffness = 9,500 kNm/rad)

4.9 Discussion

Based on the comparisons between the analysis model and experimental tests, it can be concluded the model provides a viable option to analyze the behaviour of slender loadbearing masonry walls with and without a base rotational support stiffness. As seen when comparing the model predictions with results from the studies above, the model shows a reasonable agreement with the experimental results for the pre-cracked behaviour of the wall while slightly overpredicting the deflection after cracking has occurred. This is due to the dip phenomenon in the moment-curvature analysis mentioned above. Walls subjected to low axial loads (Study 1) are much more susceptible to this effect compared to walls compared to with higher levels of axial load (Study 2). Comparing the peak axial or lateral load predicted by the analysis model to experimental results, the model was able to predict the ultimate load within 10% for the majority of the cases.

Comparing results from the analytical model to slender wall experiments (SEASC and Mohsin), the model was able to accurately predict the large deformations and second-

order effects present in slender masonry walls. When base rotational support stiffness was introduced, the model was effectively able to determine the influence of the rotational stiffness and predict the rise in either eccentric axial load capacity or lateral load capacity.

4.10 Application – Slenderness Interaction Diagrams

With the goal of the model to aid designers in determining the second-order effects of loadbearing masonry walls, it is important to develop a method to present designers with the maximum first order moment a wall can sustain before failure. This comes in the form of slenderness interaction diagrams. When designing a masonry wall, designers typically magnify the first-order moment using either the moment magnifier or the $P\Delta$ method to determine the total moment on the wall. As previously mentioned, this process is rather tedious and often overly conservative, due to the severe underestimation of the effective flexural rigidity by the Canadian code for masonry structures (CSA S304-14).

As an alternative, the current analysis model can produce allowable applied moment tables with the effects of slenderness and base stiffness already considered. This is done by analyzing the desired wall at various levels of axial load. For each level of axial load, the magnitude of distributed lateral load is iteratively increased until failure is reported. The maximum applied moment is then reported as the primary moment at the midspan of the wall during the last successful iteration of lateral load before failure occurred. With this method, complex phenomena such as tensile cracking and material nonlinearity are effectively captured. Table 4.9 shows the maximum allowable applied moment of a standard wall (Table 4.8) at various levels of slenderness, axial load and base fixity.

Table 4.8 – Example Wall Section Properties

Parameter	Value
Block Thickness (t)	290 mm
Grouted Masonry Strength ($f'_{m,g}$)	7.5 MPa
Ungouted Masonry Strength ($f'_{m,ug}$)	10 MPa
Rebar Spacing (s)	800 mm o.c.
Rebar Size	20M
Steel Yield Strength (f_y)	400 MPa

Table 4.9 – Maximum Applied Moment for a Standard Wall

Slenderness Ratio (h/t)	Base Stiffness (kNm/rad)	Axial Load (kN)	Maximum Allowable Applied Moment (kNm)
20	0	50	24.4
20	0	250	29.4
20	0	350	33.6
20	2,500	50	39.5
20	2,500	250	53.8
20	2,500	350	54.2
20	5,000	50	35.3
20	5,000	250	55.4
20	5,000	350	60.9
30	0	50	18.0
30	0	250	20.8
30	0	350	24.6
30	2,500	50	35.0
30	2,500	250	36.9
30	2,500	350	38.8
30	5,000	50	32.1
30	5,000	250	41.6
30	5,000	350	45.4
40	0	50	11.8
40	0	250	15.1
40	0	350	16.8
40	2,500	50	28.6
40	2,500	250	26.9
40	2,500	350	28.6
40	5,000	50	28.6
40	5,000	250	30.2
40	5,000	350	35.3

Table 4.10 compares the moment magnification factors obtained by the Canadian code (CSA S304-14) to those from the analysis model (for the model without a base stiffness) for specific axial load values. The moment capacity of the wall refers to the total moment

capacity of the section, while the max applied moment is the maximum moment that may be applied considering slenderness. The moment magnification factor is the factor the maximum applied moment must be multiplied by to equal the moment capacity of the wall.

Table 4.10 – Comparison of Moment Magnification Factors

h/t Ratio	Axial Load (kN)	Moment Capacity (kNm)	Max Applied Moment (kNm)		Moment Magnification Factor		Relative Difference in Moment Magnification Factor
			CSA S304-14	Analysis Model	CSA S304-14	Analysis Model	
20	50	26.7	20.2	24.8	1.32	1.08	18.2%
20	150	38.4	10.6	28.1	3.62	1.37	62.2%
20	250	49.0	11.7	34.9	4.19	1.40	66.6%
30	50	26.7	10.9	17.0	2.45	1.57	35.9%
30	150	38.4	-	24.6	-	1.56	-
30	250	49.0	-	28.4	-	1.73	-

Comparing moment magnification factors obtained using the Canadian code (CSA S304-14) to those obtained from the analysis model reveals significant differences. In all cases, the factors produced by the analysis model are much lower than those calculated using the code. When setting the slenderness ratio of the wall to 20, the moment magnification factors calculated using the code are up to 3.5 times higher than those produced by the analysis model. Increasing the slenderness ratio to 30 resulted in moment magnifiers calculated by CSA S304-14 to be so large, it would force designers to use heavier, stronger masonry units resulting in an uneconomical design.

The differences in moment magnification factors calculated using the analysis model and CSA S304-14 arise from differences in both the effective flexural rigidity and effective length parameters. The model accounts for the gradual deration of flexural rigidity by directly determining the level of tensile cracking and material nonlinearity in the section while CSA S304-14 relies on conservative approximations. The shift in inflection point in the wall due to the presence of a base rotational support stiffness is accounted for as the model determines the deflection profile of the wall under loading. CSA S304-14

attempts to account for this by allowing designers to use an effective length coefficient (k) for non-slender walls, but this is restricted for slender walls, forcing designers to neglect any shift in inflection point.

4.11 Summary

Comments on the accuracy of the analysis model to predict the behaviour of loadbearing masonry walls and determine the second-order effects a wall experiences are as follows:

- Comparing the analysis model prediction to experimental programs dealing with loadbearing masonry walls produced a good agreement.
- The accuracy of the model in the elastic region showed a good agreement with the experimental data while the analysis model tends to slightly overestimate the deflection post cracking. This is because of a phenomenon in the moment-curvature analysis where a dip would appear post cracking.
- The prediction of the ultimate load for the wall specimen by the analysis model was within 10% of the experimental results for the majority of the cases.
- The analysis model was effectively able to predict the influence of a rotational base support stiffness. This includes the model's ability to predict the increase in lateral or eccentric axial load capacity, decrease in midspan deflections, and decrease in second-order effects.
- Using the model, slenderness interaction diagrams are easily created. These diagrams provide designers with a powerful tool to allow for the quick determine of the maximum applied moment a wall can sustain before failure.
- Moment magnification factors produced by the analysis model were compared to those produced by CSA S304-14. In all cases examined, the moment magnification factor calculated with CSA S304-14 was much greater (up to a factor of 3) than the analysis model indicating possible conservatism in the code.
- The effect of moment redistribution caused by a stiffness at the base of the wall has a significant impact on the interaction diagram of non-slender walls. Moments that were greater than the cross-section capacity of the wall were reported as safe as moment redistribution would lower them to a suitable level.

5 CONCLUSIONS AND RECOMMENDATIONS

This chapter provides a summary, conclusion, and recommendations from the study of the effects of base stiffness on loadbearing masonry walls.

5.1 Summary

The objective of determining the effect of rotational base stiffness on the behaviour of loadbearing masonry walls was achieved by the following:

1. Experimental testing of 4 moderately slender masonry wall specimens with a base rotational support stiffness:
 - 4 wall specimens were constructed 3 courses wide and 12 courses high with standard 20-cm, 15 MPa masonry units. Each wall was constructed in running bond pattern by certified masons.
 - Each specimen contained two 15M steel reinforcing bars for vertical reinforcement and a combination of bond beams and bed joint reinforcement for vertical reinforcement. The location of reinforcement was identical for all specimens.
 - Experimental setup was designed to test the specimens under simply boundary conditions in a 3-point bend configuration.
 - Specimens were tested under a combination of lateral and gravity loads. The gravity load was held constant at 250 kN while the lateral load was applied cyclically in displacement control.
 - Specimen 1 was a control wall and did not feature any base rotational support stiffness while Specimens 2-4 featured unique levels of base rotational support stiffness.
 - Parameters recorded during the test included: deflections at 8 points along the height of the wall including the midspan, rotation at the top and bottom of the wall, loads applied to the wall and, strain in both the reinforcing bars and masonry.
2. Develop a mechanics-based analysis model to predict the behaviour of loadbearing masonry walls with and without a base rotational support stiffness:

- A mechanics-based analysis model was developed using the theory of beam-columns and mechanics of materials to analyze the behaviour of loadbearing masonry walls.
- Phenomena such as tensile cracking and material nonlinearity were accounted for within the model through a fibre-section analysis.
- Verification of the model was conducted through a comparison of the model's prediction to experimental programs conducted both in this thesis by other researchers (SEASC (1982), Mohsin (2005)). This allowed for verification of the model with both slender and moderately slender walls, along with walls featuring a base rotational support stiffness.
- The model was used to create slenderness interaction diagrams; a tool used to aid designers in determining the maximum applied moment a wall can sustain before failure without having to calculate manually calculate second-order effects.

5.2 Conclusions

Conclusions drawn from the experimental and analytical modelling of loadbearing masonry walls with a base rotational support stiffness are as follows. It is noted that these conclusions are valid for walls in which the first order moment is caused by lateral loads.

- The effect of base stiffness on loadbearing masonry walls is quite significant. Walls with a base stiffness demonstrate much higher loadbearing capacity and smaller midspan OOP deflections compared to pinned-pinned walls.
- As the rotational base stiffness is increased, the rotation at the base of the wall is significantly decreased.
- As the magnitude of rotational base stiffness is increased, the ductility of the wall is decreased. This is because decrease in rotation at the base of the wall for large values of rotational base stiffness.
- The negative moment created at the base of the wall by the rotational base stiffness redistributes the moments along the height of the wall. Total moments along the bottom half of the wall and including the midspan are significantly decreased as a result.

- Moment redistribution created by the rotational stiffness shifts the location of the maximum moment. The presence of a rotational base stiffness creates an inflection point near the base of the wall placing the wall into double curvature. The height of the inflection point is a function of base stiffness. The larger the rotational stiffness at the base of the wall, the further from the base the inflection point will be.
- The cyclic testing showed that the degradation at the base did not cause a significant reduction in strength.
- The mechanics-based analysis model developed to analyze walls with a rotational base stiffness produced a reasonable correlation with experimental results from a variety of experimental programs for the pre-peak strength, stiffness, and displacement response.
- The analysis model was able to predict the peak load of all examined specimens within 10% of the experimentally determined value.
- The analysis model can be used to create slenderness interaction diagrams. These diagrams automatically determine the second-order effects to provide designers with the maximum applied moment a wall can sustain before failure.
- Comparison of second-order effects predicted by the analysis model to those from the Canadian code showed the current Canadian code for masonry structures is quite conservative.

5.3 Recommendations and Future Research

This study aimed to determine the effect of base stiffness on loadbearing masonry walls and to develop a simple tool to predict the effects of rotational base support stiffness on the behaviour of loadbearing masonry walls. As this was the initial work with more studies to come, there are several recommendations for future work based on the outcomes of this thesis.

- Future experimental programs should explore the testing of slender masonry walls with a rotational base support stiffness subjected to OOP loads. Currently there is only a single experimental study dealing with slender masonry walls featuring

a base rotational support stiffness, and in this study the walls were loaded with an eccentric axial load. As the governing forces in slender masonry walls are typically OOP wind loads, more studies should be conducted to determine the true behaviour of these walls.

- Future research should consider changing the lateral loading type of the specimens from a concentrated force to a distributed load. This study was conducted as a trial to future studies, thus a simple lateral loading procedure (3-point bend) was proposed. However, a distributed load would be considered more realistic and reflect the wind loads that are typically seen on these types of walls.
- Future experiments should explore the use of digital image correlation (DIC) to capture the strain distributions through the cross-section of the wall. This would allow for the calculation of curvature and in turn, the effective flexural rigidity of the wall during loading. As the moment magnification method present in CSA S304-14 is heavily dependant on this value, a more accurate prediction is desired.
- Perform a parametric study using the analysis model to determine key parameters in the behaviour of loadbearing masonry walls. These include compressive strength, slenderness ratio, loading type, base stiffness, and reinforcement ratio.
- Use the previously mentioned parametric study to determine expressions to estimate the effective flexural rigidity of loadbearing masonry walls. The expression must be kept simple and suitable for design offices.

REFERENCES

- ACI-SEASC Task Committee on Slender Walls, “Test Report on Slender Walls”, American Concrete Institute and the Structural Engineers Association of Southern California, February 1980 - September 1982, Los Angeles.
- Ali, S., Page, A. ., and Kleeman, P. W. (1986). “Non-Linear Finite Element Model for Concrete Masonry with Particular Reference to Concentrated Loads.” *4th Canadian Masonry Symposium*, New Brunswick, CA, 137–148.
- Bean Popehn, J. R., Schultz, A. E., and Tanner, J. E. (2009). “Influence of Second Order Effects on Slender, Unreinforced Masonry Walls.” *Proceedings of the 11th Canadian Masonry Symposium*, Toronto, ON, Canada.
- Cranston, W. B., and Roberts, J. J. (1976). “Structural Behaviour of Concrete Masonry - Reinforced and Unreinforced.” *Structural Engineer*, 54(11), 423–436.
- Creazza, G., Matteazzi, R., Saetta, A., and Vitaliani, R. (2002). “Analyses of masonry vaults: A macro approach based on three-dimensional damage model.” *Journal of Structural Engineering*, 128(5), 646–654.
- Entz, J., Cruz-Noguez, C., Guzman Sanchez, O., and Banting, B. (2017). “Tall Masonry Walls with In-Line Boundary Elements.” *Effect of boundary elements confinement level on the behaviour of reinforced masonry structural walls with boundary elements*, 4–14.
- Hatzinikolas, M., Longworth, J., and Warwaruk, J. (1978a). *Concrete Masonry Walls. University of Alberta - Structural Engineering Report No. 70.*
- Hatzinikolas, M., Longworth, J., and Warwaruk, J. (1978b). *Experimental Data for Concrete Masonry Walls. University of Alberta - Structural Engineering Report No. 71.*
- Isfeld, A. C., Müller, A. L., Hagel, M., and Shrive, N. G. (2019). “Analysis of safety of slender concrete masonry walls in relation to CSA S304-14.” *Canadian Journal of*

Civil Engineering, 46(5), 424–438.

Kent, D.C., and Park, R. (1971) "Flexural members with confined concrete", *Journal of the Structural Division*, ASCE, 97(7), pp. 1969-1990.

Karsan, I.D., and Jirsa, J.O. (1969), "Behavior of concrete under compressive loadings", *Journal of the Structural Division*, ASCE, 95(ST12), pp. 2543-2563.

Liu, Y., and Dawe, J. L. (2001). "Experimental determination of masonry beam-column behaviour." *Canadian Journal of Civil Engineering*, 28(5), 794–803.

Liu, Y., and Dawe, J. L. (2003). "Analytical modeling of masonry loadbearing walls." *Canadian Journal of Civil Engineering*, 30(5), 795–806.

Liu, Y., and Hu, K. (2007). "Experimental study of reinforced masonry walls subjected to combined axial load and out-of-plane bending." *Canadian Journal of Civil Engineering*, 34(11), 1486–1494.

Lopez, J., Oller, S., Oñate, E., and Lubliner, J. (1999). "A homogeneous constitutive model for masonry." *International Journal for Numerical Methods in Engineering*, 46(10), 1651–1671.

Lotfi, H. R., and Shing, P. B. (1994). "Interface Model Applied to Fracture of Masonry Structures." *Journal of Structural Engineering*, ASCE, 120(1), 63–80.

Ma, G., Hao, H., and Lu, Y. (2001). "Homogenization of Masonry Using Numerical Simulations." *Journal of Engineering Mechanics*, 9399(July), 646–652.

MacGregor, J. G., Breen, J., and Pfrang, E. (1970). "Design of Slender Concrete Columns." *ACI Structural Journal*, 67(1), 6–28.

Mohsin, E. (2005). "Support Stiffness Effect on Tall Load Bearing Masonry Walls." University of Alberta.

Muqtadir, M. A. (1991). "Slenderness Effects in Eccentrically Loaded Masonry Walls." University of Alberta.

- Page, A. (1978). "Finite Element Model for Masonry." *Journal of the Structural Division*, 104(8), 1267–1285.
- Sayed-Ahmed, E. Y., and Shrive, N. G. (1994). "Numerical Modelling of Face-Shell Bedded Hollow Masonry." *10th International Brick and Block Masonry Conference*, Calgary, AB, 117–126.
- Sayed-Ahmed, E. Y., and Shrive, N. G. (1996). "Nonlinear finite-element model of hollow masonry." *Journal of Structural Engineering*, 122(6), 683–690.
- Simpson, W., Adham, S., Amrhein, J., Coil, J., Dobrowolski, J., Foth, U., Johnson, J., Lai, J., Lee, D., McLean, R., Selna, L., and Tobin, R. (1982). *Test Report on Slender Walls*. Los Angeles.
- Wang, R., Elwi, A. E., Hatzinikolas, M. A., and Warwaruk, J. (1997). "Tests of Tall Cavity Walls Subjected to Eccentric Loading." *Journal of Structural Engineering, ASCE*, 123(7), 912–919.
- Yokel, F., Mathey, R., and Dikkers, R. (1970). "Compressive Strength of Slender Concrete Masonry Walls." *National Bureau of Standards*, (Building Science Series 33).
- Yokel, F., Mathey, R., and Dikkers, R. (1971). "Strength of Masonry Walls Under Compressive and Transverse Loads." *National Bureau of Standards*, (Building Science Series 34).

APPENDIX A: ROTATIONAL SUPPORT STIFFNESS PROVIDED BY A VARIETY OF FOUNDATIONS

The base rotational support stiffness for a variety of foundations and soil types can be found in the table below.

ID	Applied Axial Load (kN)	Applied Moment (kNm)	Soil Type	Modulus of Subgrade (kN/m³)	Foundation Height (m)	Foundation Length (m)	Foundation Width (m)	Rotational Base Support Stiffness (kNm/rad)
1	25	2.5	Loose Sand	5,600	1.5	1.0	0.2	4
2	25	5.0	Loose Sand	5,600	1.5	1.0	0.2	4
3	25	7.5	Loose Sand	5,600	1.5	1.0	0.3	13
4	25	10.0	Loose Sand	5,600	1.5	1.0	0.4	31
5	25	12.5	Loose Sand	5,600	1.5	1.0	0.5	60
6	25	15.0	Loose Sand	5,600	1.5	1.0	0.6	104
7	25	17.5	Loose Sand	5,600	1.5	1.0	0.7	165
8	25	20.0	Loose Sand	5,600	1.5	1.0	0.7	165
9	25	22.5	Loose Sand	5,600	1.5	1.0	0.8	247
10	25	25.0	Loose Sand	5,600	1.5	1.0	0.9	351
11	25	27.5	Loose Sand	5,600	1.5	1.0	1.0	482
12	25	30.0	Loose Sand	5,600	1.5	1.0	1.1	641
13	25	32.5	Loose Sand	5,600	1.5	1.0	1.2	833
14	25	35.0	Loose Sand	5,600	1.5	1.0	1.3	1,059
15	25	37.5	Loose Sand	5,600	1.5	1.0	1.3	1,059
16	25	40.0	Loose Sand	5,600	1.5	1.0	1.4	1,322
17	50	2.5	Loose Sand	5,600	1.5	1.0	0.3	13
18	50	5.0	Loose Sand	5,600	1.5	1.0	0.3	13
19	50	7.5	Loose Sand	5,600	1.5	1.0	0.3	13
20	50	10.0	Loose Sand	5,600	1.5	1.0	0.4	31
21	50	12.5	Loose Sand	5,600	1.5	1.0	0.4	31
22	50	15.0	Loose Sand	5,600	1.5	1.0	0.5	60
23	50	17.5	Loose Sand	5,600	1.5	1.0	0.6	104
24	50	20.0	Loose Sand	5,600	1.5	1.0	0.7	165
25	50	22.5	Loose Sand	5,600	1.5	1.0	0.7	165
26	50	25.0	Loose Sand	5,600	1.5	1.0	0.8	247
27	50	27.5	Loose Sand	5,600	1.5	1.0	0.9	351
28	50	30.0	Loose Sand	5,600	1.5	1.0	0.9	351
29	50	32.5	Loose Sand	5,600	1.5	1.0	1.0	482
30	50	35.0	Loose Sand	5,600	1.5	1.0	1.1	641
31	50	37.5	Loose Sand	5,600	1.5	1.0	1.2	833
32	50	40.0	Loose Sand	5,600	1.5	1.0	1.3	1,059
33	75	2.5	Loose Sand	5,600	1.5	1.0	0.4	31
34	75	5.0	Loose Sand	5,600	1.5	1.0	0.4	31
35	75	7.5	Loose Sand	5,600	1.5	1.0	0.4	31
36	75	10.0	Loose Sand	5,600	1.5	1.0	0.4	31
37	75	12.5	Loose Sand	5,600	1.5	1.0	0.4	31
38	75	15.0	Loose Sand	5,600	1.5	1.0	0.4	31
39	75	17.5	Loose Sand	5,600	1.5	1.0	0.5	60
40	75	20.0	Loose Sand	5,600	1.5	1.0	0.6	104
41	75	22.5	Loose Sand	5,600	1.5	1.0	0.7	165

ID	Applied Axial Load (kN)	Applied Moment (kNm)	Soil Type	Modulus of Subgrade (kN/m ³)	Foundation Height (m)	Foundation Length (m)	Foundation Width (m)	Rotational Base Support Stiffness (kNm/rad)
42	75	25.0	Loose Sand	5,600	1.5	1.0	0.7	165
43	75	27.5	Loose Sand	5,600	1.5	1.0	0.8	247
44	75	30.0	Loose Sand	5,600	1.5	1.0	0.8	247
45	75	32.5	Loose Sand	5,600	1.5	1.0	0.9	351
46	75	35.0	Loose Sand	5,600	1.5	1.0	1.0	482
47	75	37.5	Loose Sand	5,600	1.5	1.0	1.0	482
48	75	40.0	Loose Sand	5,600	1.5	1.0	1.1	641
49	100	2.5	Loose Sand	5,600	1.5	1.0	0.5	60
50	100	5.0	Loose Sand	5,600	1.5	1.0	0.5	60
51	100	7.5	Loose Sand	5,600	1.5	1.0	0.5	60
52	100	10.0	Loose Sand	5,600	1.5	1.0	0.5	60
53	100	12.5	Loose Sand	5,600	1.5	1.0	0.5	60
54	100	15.0	Loose Sand	5,600	1.5	1.0	0.5	60
55	100	17.5	Loose Sand	5,600	1.5	1.0	0.5	60
56	100	20.0	Loose Sand	5,600	1.5	1.0	0.5	60
57	100	22.5	Loose Sand	5,600	1.5	1.0	0.6	104
58	100	25.0	Loose Sand	5,600	1.5	1.0	0.7	165
59	100	27.5	Loose Sand	5,600	1.5	1.0	0.7	165
60	100	30.0	Loose Sand	5,600	1.5	1.0	0.8	247
61	100	32.5	Loose Sand	5,600	1.5	1.0	0.8	247
62	100	35.0	Loose Sand	5,600	1.5	1.0	0.9	351
63	100	37.5	Loose Sand	5,600	1.5	1.0	0.9	351
64	100	40.0	Loose Sand	5,600	1.5	1.0	1.0	482
65	125	2.5	Loose Sand	5,600	1.5	1.0	0.6	104
66	125	5.0	Loose Sand	5,600	1.5	1.0	0.6	104
67	125	7.5	Loose Sand	5,600	1.5	1.0	0.6	104
68	125	10.0	Loose Sand	5,600	1.5	1.0	0.6	104
69	125	12.5	Loose Sand	5,600	1.5	1.0	0.6	104
70	125	15.0	Loose Sand	5,600	1.5	1.0	0.6	104
71	125	17.5	Loose Sand	5,600	1.5	1.0	0.6	104
72	125	20.0	Loose Sand	5,600	1.5	1.0	0.6	104
73	125	22.5	Loose Sand	5,600	1.5	1.0	0.6	104
74	125	25.0	Loose Sand	5,600	1.5	1.0	0.6	104
75	125	27.5	Loose Sand	5,600	1.5	1.0	0.7	165
76	125	30.0	Loose Sand	5,600	1.5	1.0	0.7	165
77	125	32.5	Loose Sand	5,600	1.5	1.0	0.8	247
78	125	35.0	Loose Sand	5,600	1.5	1.0	0.8	247
79	125	37.5	Loose Sand	5,600	1.5	1.0	0.9	351
80	125	40.0	Loose Sand	5,600	1.5	1.0	0.9	351
81	150	2.5	Loose Sand	5,600	1.5	1.0	0.8	247
82	150	5.0	Loose Sand	5,600	1.5	1.0	0.8	247
83	150	7.5	Loose Sand	5,600	1.5	1.0	0.8	247
84	150	10.0	Loose Sand	5,600	1.5	1.0	0.8	247
85	150	12.5	Loose Sand	5,600	1.5	1.0	0.8	247
86	150	15.0	Loose Sand	5,600	1.5	1.0	0.8	247
87	150	17.5	Loose Sand	5,600	1.5	1.0	0.8	247
88	150	20.0	Loose Sand	5,600	1.5	1.0	0.8	247
89	150	22.5	Loose Sand	5,600	1.5	1.0	0.8	247
90	150	25.0	Loose Sand	5,600	1.5	1.0	0.8	247
91	150	27.5	Loose Sand	5,600	1.5	1.0	0.8	247

ID	Applied Axial Load (kN)	Applied Moment (kNm)	Soil Type	Modulus of Subgrade (kN/m ³)	Foundation Height (m)	Foundation Length (m)	Foundation Width (m)	Rotational Base Support Stiffness (kNm/rad)
92	150	30.0	Loose Sand	5,600	1.5	1.0	0.8	247
93	150	32.5	Loose Sand	5,600	1.5	1.0	0.8	247
94	150	35.0	Loose Sand	5,600	1.5	1.0	0.8	247
95	150	37.5	Loose Sand	5,600	1.5	1.0	0.8	247
96	150	40.0	Loose Sand	5,600	1.5	1.0	0.8	247
97	175	2.5	Loose Sand	5,600	1.5	1.0	0.9	351
98	175	5.0	Loose Sand	5,600	1.5	1.0	0.9	351
99	175	7.5	Loose Sand	5,600	1.5	1.0	0.9	351
100	175	10.0	Loose Sand	5,600	1.5	1.0	0.9	351
101	175	12.5	Loose Sand	5,600	1.5	1.0	0.9	351
102	175	15.0	Loose Sand	5,600	1.5	1.0	0.9	351
103	175	17.5	Loose Sand	5,600	1.5	1.0	0.9	351
104	175	20.0	Loose Sand	5,600	1.5	1.0	0.9	351
105	175	22.5	Loose Sand	5,600	1.5	1.0	0.9	351
106	175	25.0	Loose Sand	5,600	1.5	1.0	0.9	351
107	175	27.5	Loose Sand	5,600	1.5	1.0	0.9	351
108	175	30.0	Loose Sand	5,600	1.5	1.0	0.9	351
109	175	32.5	Loose Sand	5,600	1.5	1.0	0.9	351
110	175	35.0	Loose Sand	5,600	1.5	1.0	0.9	351
111	175	37.5	Loose Sand	5,600	1.5	1.0	0.9	351
112	175	40.0	Loose Sand	5,600	1.5	1.0	0.9	351
113	200	2.5	Loose Sand	5,600	1.5	1.0	1.0	482
114	200	5.0	Loose Sand	5,600	1.5	1.0	1.0	482
115	200	7.5	Loose Sand	5,600	1.5	1.0	1.0	482
116	200	10.0	Loose Sand	5,600	1.5	1.0	1.0	482
117	200	12.5	Loose Sand	5,600	1.5	1.0	1.0	482
118	200	15.0	Loose Sand	5,600	1.5	1.0	1.0	482
119	200	17.5	Loose Sand	5,600	1.5	1.0	1.0	482
120	200	20.0	Loose Sand	5,600	1.5	1.0	1.0	482
121	200	22.5	Loose Sand	5,600	1.5	1.0	1.0	482
122	200	25.0	Loose Sand	5,600	1.5	1.0	1.0	482
123	200	27.5	Loose Sand	5,600	1.5	1.0	1.0	482
124	200	30.0	Loose Sand	5,600	1.5	1.0	1.0	482
125	200	32.5	Loose Sand	5,600	1.5	1.0	1.0	482
126	200	35.0	Loose Sand	5,600	1.5	1.0	1.0	482
127	200	37.5	Loose Sand	5,600	1.5	1.0	1.0	482
128	200	40.0	Loose Sand	5,600	1.5	1.0	1.0	482
129	225	2.5	Loose Sand	5,600	1.5	1.0	1.1	641
130	225	5.0	Loose Sand	5,600	1.5	1.0	1.1	641
131	225	7.5	Loose Sand	5,600	1.5	1.0	1.1	641
132	225	10.0	Loose Sand	5,600	1.5	1.0	1.1	641
133	225	12.5	Loose Sand	5,600	1.5	1.0	1.1	641
134	225	15.0	Loose Sand	5,600	1.5	1.0	1.1	641
135	225	17.5	Loose Sand	5,600	1.5	1.0	1.1	641
136	225	20.0	Loose Sand	5,600	1.5	1.0	1.1	641
137	225	22.5	Loose Sand	5,600	1.5	1.0	1.1	641
138	225	25.0	Loose Sand	5,600	1.5	1.0	1.1	641
139	225	27.5	Loose Sand	5,600	1.5	1.0	1.1	641
140	225	30.0	Loose Sand	5,600	1.5	1.0	1.1	641
141	225	32.5	Loose Sand	5,600	1.5	1.0	1.1	641

ID	Applied Axial Load (kN)	Applied Moment (kNm)	Soil Type	Modulus of Subgrade (kN/m ³)	Foundation Height (m)	Foundation Length (m)	Foundation Width (m)	Rotational Base Support Stiffness (kNm/rad)
142	225	35.0	Loose Sand	5,600	1.5	1.0	1.1	641
143	225	37.5	Loose Sand	5,600	1.5	1.0	1.1	641
144	225	40.0	Loose Sand	5,600	1.5	1.0	1.1	641
145	250	2.5	Loose Sand	5,600	1.5	1.0	1.2	833
146	250	5.0	Loose Sand	5,600	1.5	1.0	1.2	833
147	250	7.5	Loose Sand	5,600	1.5	1.0	1.2	833
148	250	10.0	Loose Sand	5,600	1.5	1.0	1.2	833
149	250	12.5	Loose Sand	5,600	1.5	1.0	1.2	833
150	250	15.0	Loose Sand	5,600	1.5	1.0	1.2	833
151	250	17.5	Loose Sand	5,600	1.5	1.0	1.2	833
152	250	20.0	Loose Sand	5,600	1.5	1.0	1.2	833
153	250	22.5	Loose Sand	5,600	1.5	1.0	1.2	833
154	250	25.0	Loose Sand	5,600	1.5	1.0	1.2	833
155	250	27.5	Loose Sand	5,600	1.5	1.0	1.2	833
156	250	30.0	Loose Sand	5,600	1.5	1.0	1.2	833
157	250	32.5	Loose Sand	5,600	1.5	1.0	1.2	833
158	250	35.0	Loose Sand	5,600	1.5	1.0	1.2	833
159	250	37.5	Loose Sand	5,600	1.5	1.0	1.2	833
160	250	40.0	Loose Sand	5,600	1.5	1.0	1.2	833
161	275	2.5	Loose Sand	5,600	1.5	1.0	1.4	1,322
162	275	5.0	Loose Sand	5,600	1.5	1.0	1.4	1,322
163	275	7.5	Loose Sand	5,600	1.5	1.0	1.4	1,322
164	275	10.0	Loose Sand	5,600	1.5	1.0	1.4	1,322
165	275	12.5	Loose Sand	5,600	1.5	1.0	1.4	1,322
166	275	15.0	Loose Sand	5,600	1.5	1.0	1.4	1,322
167	275	17.5	Loose Sand	5,600	1.5	1.0	1.4	1,322
168	275	20.0	Loose Sand	5,600	1.5	1.0	1.4	1,322
169	275	22.5	Loose Sand	5,600	1.5	1.0	1.4	1,322
170	275	25.0	Loose Sand	5,600	1.5	1.0	1.4	1,322
171	275	27.5	Loose Sand	5,600	1.5	1.0	1.4	1,322
172	275	30.0	Loose Sand	5,600	1.5	1.0	1.4	1,322
173	275	32.5	Loose Sand	5,600	1.5	1.0	1.4	1,322
174	275	35.0	Loose Sand	5,600	1.5	1.0	1.4	1,322
175	275	37.5	Loose Sand	5,600	1.5	1.0	1.4	1,322
176	275	40.0	Loose Sand	5,600	1.5	1.0	1.4	1,322
177	300	2.5	Loose Sand	5,600	1.5	1.0	1.5	1,627
178	300	5.0	Loose Sand	5,600	1.5	1.0	1.5	1,627
179	300	7.5	Loose Sand	5,600	1.5	1.0	1.5	1,627
180	300	10.0	Loose Sand	5,600	1.5	1.0	1.5	1,627
181	300	12.5	Loose Sand	5,600	1.5	1.0	1.5	1,627
182	300	15.0	Loose Sand	5,600	1.5	1.0	1.5	1,627
183	300	17.5	Loose Sand	5,600	1.5	1.0	1.5	1,627
184	300	20.0	Loose Sand	5,600	1.5	1.0	1.5	1,627
185	300	22.5	Loose Sand	5,600	1.5	1.0	1.5	1,627
186	300	25.0	Loose Sand	5,600	1.5	1.0	1.5	1,627
187	300	27.5	Loose Sand	5,600	1.5	1.0	1.5	1,627
188	300	30.0	Loose Sand	5,600	1.5	1.0	1.5	1,627
189	300	32.5	Loose Sand	5,600	1.5	1.0	1.5	1,627
190	300	35.0	Loose Sand	5,600	1.5	1.0	1.5	1,627
191	300	37.5	Loose Sand	5,600	1.5	1.0	1.5	1,627

ID	Applied Axial Load (kN)	Applied Moment (kNm)	Soil Type	Modulus of Subgrade (kN/m ³)	Foundation Height (m)	Foundation Length (m)	Foundation Width (m)	Rotational Base Support Stiffness (kNm/rad)
192	300	40.0	Loose Sand	5,600	1.5	1.0	1.5	1,627
193	325	2.5	Loose Sand	5,600	1.5	1.0	1.6	1,974
194	325	5.0	Loose Sand	5,600	1.5	1.0	1.6	1,974
195	325	7.5	Loose Sand	5,600	1.5	1.0	1.6	1,974
196	325	10.0	Loose Sand	5,600	1.5	1.0	1.6	1,974
197	325	12.5	Loose Sand	5,600	1.5	1.0	1.6	1,974
198	325	15.0	Loose Sand	5,600	1.5	1.0	1.6	1,974
199	325	17.5	Loose Sand	5,600	1.5	1.0	1.6	1,974
200	325	20.0	Loose Sand	5,600	1.5	1.0	1.6	1,974
201	325	22.5	Loose Sand	5,600	1.5	1.0	1.6	1,974
202	325	25.0	Loose Sand	5,600	1.5	1.0	1.6	1,974
203	325	27.5	Loose Sand	5,600	1.5	1.0	1.6	1,974
204	325	30.0	Loose Sand	5,600	1.5	1.0	1.6	1,974
205	325	32.5	Loose Sand	5,600	1.5	1.0	1.6	1,974
206	325	35.0	Loose Sand	5,600	1.5	1.0	1.6	1,974
207	325	37.5	Loose Sand	5,600	1.5	1.0	1.6	1,974
208	325	40.0	Loose Sand	5,600	1.5	1.0	1.6	1,974
209	350	2.5	Loose Sand	5,600	1.5	1.0	1.7	2,368
210	350	5.0	Loose Sand	5,600	1.5	1.0	1.7	2,368
211	350	7.5	Loose Sand	5,600	1.5	1.0	1.7	2,368
212	350	10.0	Loose Sand	5,600	1.5	1.0	1.7	2,368
213	350	12.5	Loose Sand	5,600	1.5	1.0	1.7	2,368
214	350	15.0	Loose Sand	5,600	1.5	1.0	1.7	2,368
215	350	17.5	Loose Sand	5,600	1.5	1.0	1.7	2,368
216	350	20.0	Loose Sand	5,600	1.5	1.0	1.7	2,368
217	350	22.5	Loose Sand	5,600	1.5	1.0	1.7	2,368
218	350	25.0	Loose Sand	5,600	1.5	1.0	1.7	2,368
219	350	27.5	Loose Sand	5,600	1.5	1.0	1.7	2,368
220	350	30.0	Loose Sand	5,600	1.5	1.0	1.7	2,368
221	350	32.5	Loose Sand	5,600	1.5	1.0	1.7	2,368
222	350	35.0	Loose Sand	5,600	1.5	1.0	1.7	2,368
223	350	37.5	Loose Sand	5,600	1.5	1.0	1.7	2,368
224	350	40.0	Loose Sand	5,600	1.5	1.0	1.7	2,368
225	25	2.5	Medium Dense Sand	35,200	1.5	1.0	0.2	24
226	25	5.0	Medium Dense Sand	35,200	1.5	1.0	0.2	24
227	25	7.5	Medium Dense Sand	35,200	1.5	1.0	0.3	82
228	25	10.0	Medium Dense Sand	35,200	1.5	1.0	0.4	194
229	25	12.5	Medium Dense Sand	35,200	1.5	1.0	0.5	379
230	25	15.0	Medium Dense Sand	35,200	1.5	1.0	0.6	654
231	25	17.5	Medium Dense Sand	35,200	1.5	1.0	0.7	1,039
232	25	20.0	Medium Dense Sand	35,200	1.5	1.0	0.7	1,039
233	25	22.5	Medium	35,200	1.5	1.0	0.8	1,551

ID	Applied Axial Load (kN)	Applied Moment (kNm)	Soil Type	Modulus of Subgrade (kN/m ³)	Foundation Height (m)	Foundation Length (m)	Foundation Width (m)	Rotational Base Support Stiffness (kNm/rad)
234	25	25.0	Dense Sand Medium Dense Sand	35,200	1.5	1.0	0.9	2,208
235	25	27.5	Medium Dense Sand	35,200	1.5	1.0	1.0	3,029
236	25	30.0	Medium Dense Sand	35,200	1.5	1.0	1.1	4,032
237	25	32.5	Medium Dense Sand	35,200	1.5	1.0	1.2	5,235
238	25	35.0	Medium Dense Sand	35,200	1.5	1.0	1.3	6,656
239	25	37.5	Medium Dense Sand	35,200	1.5	1.0	1.3	6,656
240	25	40.0	Medium Dense Sand	35,200	1.5	1.0	1.4	8,313
241	50	2.5	Medium Dense Sand	35,200	1.5	1.0	0.3	82
242	50	5.0	Medium Dense Sand	35,200	1.5	1.0	0.3	82
243	50	7.5	Medium Dense Sand	35,200	1.5	1.0	0.3	82
244	50	10.0	Medium Dense Sand	35,200	1.5	1.0	0.4	194
245	50	12.5	Medium Dense Sand	35,200	1.5	1.0	0.4	194
246	50	15.0	Medium Dense Sand	35,200	1.5	1.0	0.5	379
247	50	17.5	Medium Dense Sand	35,200	1.5	1.0	0.6	654
248	50	20.0	Medium Dense Sand	35,200	1.5	1.0	0.7	1,039
249	50	22.5	Medium Dense Sand	35,200	1.5	1.0	0.7	1,039
250	50	25.0	Medium Dense Sand	35,200	1.5	1.0	0.8	1,551
251	50	27.5	Medium Dense Sand	35,200	1.5	1.0	0.9	2,208
252	50	30.0	Medium Dense Sand	35,200	1.5	1.0	0.9	2,208
253	50	32.5	Medium Dense Sand	35,200	1.5	1.0	1.0	3,029
254	50	35.0	Medium Dense Sand	35,200	1.5	1.0	1.1	4,032
255	50	37.5	Medium Dense Sand	35,200	1.5	1.0	1.2	5,235
256	50	40.0	Medium Dense Sand	35,200	1.5	1.0	1.3	6,656
257	75	2.5	Medium Dense Sand	35,200	1.5	1.0	0.4	194
258	75	5.0	Medium	35,200	1.5	1.0	0.4	194

ID	Applied Axial Load (kN)	Applied Moment (kNm)	Soil Type	Modulus of Subgrade (kN/m ³)	Foundation Height (m)	Foundation Length (m)	Foundation Width (m)	Rotational Base Support Stiffness (kNm/rad)
259	75	7.5	Dense Sand Medium Dense Sand	35,200	1.5	1.0	0.4	194
260	75	10.0	Medium Dense Sand	35,200	1.5	1.0	0.4	194
261	75	12.5	Medium Dense Sand	35,200	1.5	1.0	0.4	194
262	75	15.0	Medium Dense Sand	35,200	1.5	1.0	0.4	194
263	75	17.5	Medium Dense Sand	35,200	1.5	1.0	0.5	379
264	75	20.0	Medium Dense Sand	35,200	1.5	1.0	0.6	654
265	75	22.5	Medium Dense Sand	35,200	1.5	1.0	0.7	1,039
266	75	25.0	Medium Dense Sand	35,200	1.5	1.0	0.7	1,039
267	75	27.5	Medium Dense Sand	35,200	1.5	1.0	0.8	1,551
268	75	30.0	Medium Dense Sand	35,200	1.5	1.0	0.8	1,551
269	75	32.5	Medium Dense Sand	35,200	1.5	1.0	0.9	2,208
270	75	35.0	Medium Dense Sand	35,200	1.5	1.0	1.0	3,029
271	75	37.5	Medium Dense Sand	35,200	1.5	1.0	1.0	3,029
272	75	40.0	Medium Dense Sand	35,200	1.5	1.0	1.1	4,032
273	100	2.5	Medium Dense Sand	35,200	1.5	1.0	0.5	379
274	100	5.0	Medium Dense Sand	35,200	1.5	1.0	0.5	379
275	100	7.5	Medium Dense Sand	35,200	1.5	1.0	0.5	379
276	100	10.0	Medium Dense Sand	35,200	1.5	1.0	0.5	379
277	100	12.5	Medium Dense Sand	35,200	1.5	1.0	0.5	379
278	100	15.0	Medium Dense Sand	35,200	1.5	1.0	0.5	379
279	100	17.5	Medium Dense Sand	35,200	1.5	1.0	0.5	379
280	100	20.0	Medium Dense Sand	35,200	1.5	1.0	0.5	379
281	100	22.5	Medium Dense Sand	35,200	1.5	1.0	0.6	654
282	100	25.0	Medium Dense Sand	35,200	1.5	1.0	0.7	1,039
283	100	27.5	Medium	35,200	1.5	1.0	0.7	1,039

ID	Applied Axial Load (kN)	Applied Moment (kNm)	Soil Type	Modulus of Subgrade (kN/m ³)	Foundation Height (m)	Foundation Length (m)	Foundation Width (m)	Rotational Base Support Stiffness (kNm/rad)
284	100	30.0	Dense Sand Medium Dense Sand	35,200	1.5	1.0	0.8	1,551
285	100	32.5	Medium Dense Sand	35,200	1.5	1.0	0.8	1,551
286	100	35.0	Medium Dense Sand	35,200	1.5	1.0	0.9	2,208
287	100	37.5	Medium Dense Sand	35,200	1.5	1.0	0.9	2,208
288	100	40.0	Medium Dense Sand	35,200	1.5	1.0	1.0	3,029
289	125	2.5	Medium Dense Sand	35,200	1.5	1.0	0.6	654
290	125	5.0	Medium Dense Sand	35,200	1.5	1.0	0.6	654
291	125	7.5	Medium Dense Sand	35,200	1.5	1.0	0.6	654
292	125	10.0	Medium Dense Sand	35,200	1.5	1.0	0.6	654
293	125	12.5	Medium Dense Sand	35,200	1.5	1.0	0.6	654
294	125	15.0	Medium Dense Sand	35,200	1.5	1.0	0.6	654
295	125	17.5	Medium Dense Sand	35,200	1.5	1.0	0.6	654
296	125	20.0	Medium Dense Sand	35,200	1.5	1.0	0.6	654
297	125	22.5	Medium Dense Sand	35,200	1.5	1.0	0.6	654
298	125	25.0	Medium Dense Sand	35,200	1.5	1.0	0.6	654
299	125	27.5	Medium Dense Sand	35,200	1.5	1.0	0.7	1,039
300	125	30.0	Medium Dense Sand	35,200	1.5	1.0	0.7	1,039
301	125	32.5	Medium Dense Sand	35,200	1.5	1.0	0.8	1,551
302	125	35.0	Medium Dense Sand	35,200	1.5	1.0	0.8	1,551
303	125	37.5	Medium Dense Sand	35,200	1.5	1.0	0.9	2,208
304	125	40.0	Medium Dense Sand	35,200	1.5	1.0	0.9	2,208
305	150	2.5	Medium Dense Sand	35,200	1.5	1.0	0.8	1,551
306	150	5.0	Medium Dense Sand	35,200	1.5	1.0	0.8	1,551
307	150	7.5	Medium Dense Sand	35,200	1.5	1.0	0.8	1,551
308	150	10.0	Medium	35,200	1.5	1.0	0.8	1,551

ID	Applied Axial Load (kN)	Applied Moment (kNm)	Soil Type	Modulus of Subgrade (kN/m ³)	Foundation Height (m)	Foundation Length (m)	Foundation Width (m)	Rotational Base Support Stiffness (kNm/rad)
309	150	12.5	Dense Sand Medium Dense Sand	35,200	1.5	1.0	0.8	1,551
310	150	15.0	Medium Dense Sand	35,200	1.5	1.0	0.8	1,551
311	150	17.5	Medium Dense Sand	35,200	1.5	1.0	0.8	1,551
312	150	20.0	Medium Dense Sand	35,200	1.5	1.0	0.8	1,551
313	150	22.5	Medium Dense Sand	35,200	1.5	1.0	0.8	1,551
314	150	25.0	Medium Dense Sand	35,200	1.5	1.0	0.8	1,551
315	150	27.5	Medium Dense Sand	35,200	1.5	1.0	0.8	1,551
316	150	30.0	Medium Dense Sand	35,200	1.5	1.0	0.8	1,551
317	150	32.5	Medium Dense Sand	35,200	1.5	1.0	0.8	1,551
318	150	35.0	Medium Dense Sand	35,200	1.5	1.0	0.8	1,551
319	150	37.5	Medium Dense Sand	35,200	1.5	1.0	0.8	1,551
320	150	40.0	Medium Dense Sand	35,200	1.5	1.0	0.8	1,551
321	175	2.5	Medium Dense Sand	35,200	1.5	1.0	0.9	2,208
322	175	5.0	Medium Dense Sand	35,200	1.5	1.0	0.9	2,208
323	175	7.5	Medium Dense Sand	35,200	1.5	1.0	0.9	2,208
324	175	10.0	Medium Dense Sand	35,200	1.5	1.0	0.9	2,208
325	175	12.5	Medium Dense Sand	35,200	1.5	1.0	0.9	2,208
326	175	15.0	Medium Dense Sand	35,200	1.5	1.0	0.9	2,208
327	175	17.5	Medium Dense Sand	35,200	1.5	1.0	0.9	2,208
328	175	20.0	Medium Dense Sand	35,200	1.5	1.0	0.9	2,208
329	175	22.5	Medium Dense Sand	35,200	1.5	1.0	0.9	2,208
330	175	25.0	Medium Dense Sand	35,200	1.5	1.0	0.9	2,208
331	175	27.5	Medium Dense Sand	35,200	1.5	1.0	0.9	2,208
332	175	30.0	Medium Dense Sand	35,200	1.5	1.0	0.9	2,208
333	175	32.5	Medium	35,200	1.5	1.0	0.9	2,208

ID	Applied Axial Load (kN)	Applied Moment (kNm)	Soil Type	Modulus of Subgrade (kN/m ³)	Foundation Height (m)	Foundation Length (m)	Foundation Width (m)	Rotational Base Support Stiffness (kNm/rad)
334	175	35.0	Dense Sand Medium Dense Sand	35,200	1.5	1.0	0.9	2,208
335	175	37.5	Medium Dense Sand	35,200	1.5	1.0	0.9	2,208
336	175	40.0	Medium Dense Sand	35,200	1.5	1.0	0.9	2,208
337	200	2.5	Medium Dense Sand	35,200	1.5	1.0	1.0	3,029
338	200	5.0	Medium Dense Sand	35,200	1.5	1.0	1.0	3,029
339	200	7.5	Medium Dense Sand	35,200	1.5	1.0	1.0	3,029
340	200	10.0	Medium Dense Sand	35,200	1.5	1.0	1.0	3,029
341	200	12.5	Medium Dense Sand	35,200	1.5	1.0	1.0	3,029
342	200	15.0	Medium Dense Sand	35,200	1.5	1.0	1.0	3,029
343	200	17.5	Medium Dense Sand	35,200	1.5	1.0	1.0	3,029
344	200	20.0	Medium Dense Sand	35,200	1.5	1.0	1.0	3,029
345	200	22.5	Medium Dense Sand	35,200	1.5	1.0	1.0	3,029
346	200	25.0	Medium Dense Sand	35,200	1.5	1.0	1.0	3,029
347	200	27.5	Medium Dense Sand	35,200	1.5	1.0	1.0	3,029
348	200	30.0	Medium Dense Sand	35,200	1.5	1.0	1.0	3,029
349	200	32.5	Medium Dense Sand	35,200	1.5	1.0	1.0	3,029
350	200	35.0	Medium Dense Sand	35,200	1.5	1.0	1.0	3,029
351	200	37.5	Medium Dense Sand	35,200	1.5	1.0	1.0	3,029
352	200	40.0	Medium Dense Sand	35,200	1.5	1.0	1.0	3,029
353	225	2.5	Medium Dense Sand	35,200	1.5	1.0	1.1	4,032
354	225	5.0	Medium Dense Sand	35,200	1.5	1.0	1.1	4,032
355	225	7.5	Medium Dense Sand	35,200	1.5	1.0	1.1	4,032
356	225	10.0	Medium Dense Sand	35,200	1.5	1.0	1.1	4,032
357	225	12.5	Medium Dense Sand	35,200	1.5	1.0	1.1	4,032
358	225	15.0	Medium	35,200	1.5	1.0	1.1	4,032

ID	Applied Axial Load (kN)	Applied Moment (kNm)	Soil Type	Modulus of Subgrade (kN/m ³)	Foundation Height (m)	Foundation Length (m)	Foundation Width (m)	Rotational Base Support Stiffness (kNm/rad)
359	225	17.5	Dense Sand Medium Dense Sand	35,200	1.5	1.0	1.1	4,032
360	225	20.0	Medium Dense Sand	35,200	1.5	1.0	1.1	4,032
361	225	22.5	Medium Dense Sand	35,200	1.5	1.0	1.1	4,032
362	225	25.0	Medium Dense Sand	35,200	1.5	1.0	1.1	4,032
363	225	27.5	Medium Dense Sand	35,200	1.5	1.0	1.1	4,032
364	225	30.0	Medium Dense Sand	35,200	1.5	1.0	1.1	4,032
365	225	32.5	Medium Dense Sand	35,200	1.5	1.0	1.1	4,032
366	225	35.0	Medium Dense Sand	35,200	1.5	1.0	1.1	4,032
367	225	37.5	Medium Dense Sand	35,200	1.5	1.0	1.1	4,032
368	225	40.0	Medium Dense Sand	35,200	1.5	1.0	1.1	4,032
369	250	2.5	Medium Dense Sand	35,200	1.5	1.0	1.2	5,235
370	250	5.0	Medium Dense Sand	35,200	1.5	1.0	1.2	5,235
371	250	7.5	Medium Dense Sand	35,200	1.5	1.0	1.2	5,235
372	250	10.0	Medium Dense Sand	35,200	1.5	1.0	1.2	5,235
373	250	12.5	Medium Dense Sand	35,200	1.5	1.0	1.2	5,235
374	250	15.0	Medium Dense Sand	35,200	1.5	1.0	1.2	5,235
375	250	17.5	Medium Dense Sand	35,200	1.5	1.0	1.2	5,235
376	250	20.0	Medium Dense Sand	35,200	1.5	1.0	1.2	5,235
377	250	22.5	Medium Dense Sand	35,200	1.5	1.0	1.2	5,235
378	250	25.0	Medium Dense Sand	35,200	1.5	1.0	1.2	5,235
379	250	27.5	Medium Dense Sand	35,200	1.5	1.0	1.2	5,235
380	250	30.0	Medium Dense Sand	35,200	1.5	1.0	1.2	5,235
381	250	32.5	Medium Dense Sand	35,200	1.5	1.0	1.2	5,235
382	250	35.0	Medium Dense Sand	35,200	1.5	1.0	1.2	5,235
383	250	37.5	Medium	35,200	1.5	1.0	1.2	5,235

ID	Applied Axial Load (kN)	Applied Moment (kNm)	Soil Type	Modulus of Subgrade (kN/m ³)	Foundation Height (m)	Foundation Length (m)	Foundation Width (m)	Rotational Base Support Stiffness (kNm/rad)
384	250	40.0	Dense Sand Medium Dense Sand	35,200	1.5	1.0	1.2	5,235
385	275	2.5	Medium Dense Sand	35,200	1.5	1.0	1.4	8,313
386	275	5.0	Medium Dense Sand	35,200	1.5	1.0	1.4	8,313
387	275	7.5	Medium Dense Sand	35,200	1.5	1.0	1.4	8,313
388	275	10.0	Medium Dense Sand	35,200	1.5	1.0	1.4	8,313
389	275	12.5	Medium Dense Sand	35,200	1.5	1.0	1.4	8,313
390	275	15.0	Medium Dense Sand	35,200	1.5	1.0	1.4	8,313
391	275	17.5	Medium Dense Sand	35,200	1.5	1.0	1.4	8,313
392	275	20.0	Medium Dense Sand	35,200	1.5	1.0	1.4	8,313
393	275	22.5	Medium Dense Sand	35,200	1.5	1.0	1.4	8,313
394	275	25.0	Medium Dense Sand	35,200	1.5	1.0	1.4	8,313
395	275	27.5	Medium Dense Sand	35,200	1.5	1.0	1.4	8,313
396	275	30.0	Medium Dense Sand	35,200	1.5	1.0	1.4	8,313
397	275	32.5	Medium Dense Sand	35,200	1.5	1.0	1.4	8,313
398	275	35.0	Medium Dense Sand	35,200	1.5	1.0	1.4	8,313
399	275	37.5	Medium Dense Sand	35,200	1.5	1.0	1.4	8,313
400	275	40.0	Medium Dense Sand	35,200	1.5	1.0	1.4	8,313
401	300	2.5	Medium Dense Sand	35,200	1.5	1.0	1.5	10,224
402	300	5.0	Medium Dense Sand	35,200	1.5	1.0	1.5	10,224
403	300	7.5	Medium Dense Sand	35,200	1.5	1.0	1.5	10,224
404	300	10.0	Medium Dense Sand	35,200	1.5	1.0	1.5	10,224
405	300	12.5	Medium Dense Sand	35,200	1.5	1.0	1.5	10,224
406	300	15.0	Medium Dense Sand	35,200	1.5	1.0	1.5	10,224
407	300	17.5	Medium Dense Sand	35,200	1.5	1.0	1.5	10,224
408	300	20.0	Medium Dense Sand	35,200	1.5	1.0	1.5	10,224

ID	Applied Axial Load (kN)	Applied Moment (kNm)	Soil Type	Modulus of Subgrade (kN/m ³)	Foundation Height (m)	Foundation Length (m)	Foundation Width (m)	Rotational Base Support Stiffness (kNm/rad)
409	300	22.5	Dense Sand Medium Dense Sand	35,200	1.5	1.0	1.5	10,224
410	300	25.0	Medium Dense Sand	35,200	1.5	1.0	1.5	10,224
411	300	27.5	Medium Dense Sand	35,200	1.5	1.0	1.5	10,224
412	300	30.0	Medium Dense Sand	35,200	1.5	1.0	1.5	10,224
413	300	32.5	Medium Dense Sand	35,200	1.5	1.0	1.5	10,224
414	300	35.0	Medium Dense Sand	35,200	1.5	1.0	1.5	10,224
415	300	37.5	Medium Dense Sand	35,200	1.5	1.0	1.5	10,224
416	300	40.0	Medium Dense Sand	35,200	1.5	1.0	1.5	10,224
417	325	2.5	Medium Dense Sand	35,200	1.5	1.0	1.6	12,408
418	325	5.0	Medium Dense Sand	35,200	1.5	1.0	1.6	12,408
419	325	7.5	Medium Dense Sand	35,200	1.5	1.0	1.6	12,408
420	325	10.0	Medium Dense Sand	35,200	1.5	1.0	1.6	12,408
421	325	12.5	Medium Dense Sand	35,200	1.5	1.0	1.6	12,408
422	325	15.0	Medium Dense Sand	35,200	1.5	1.0	1.6	12,408
423	325	17.5	Medium Dense Sand	35,200	1.5	1.0	1.6	12,408
424	325	20.0	Medium Dense Sand	35,200	1.5	1.0	1.6	12,408
425	325	22.5	Medium Dense Sand	35,200	1.5	1.0	1.6	12,408
426	325	25.0	Medium Dense Sand	35,200	1.5	1.0	1.6	12,408
427	325	27.5	Medium Dense Sand	35,200	1.5	1.0	1.6	12,408
428	325	30.0	Medium Dense Sand	35,200	1.5	1.0	1.6	12,408
429	325	32.5	Medium Dense Sand	35,200	1.5	1.0	1.6	12,408
430	325	35.0	Medium Dense Sand	35,200	1.5	1.0	1.6	12,408
431	325	37.5	Medium Dense Sand	35,200	1.5	1.0	1.6	12,408
432	325	40.0	Medium Dense Sand	35,200	1.5	1.0	1.6	12,408
433	350	2.5	Medium	35,200	1.5	1.0	1.7	14,883

ID	Applied Axial Load (kN)	Applied Moment (kNm)	Soil Type	Modulus of Subgrade (kN/m ³)	Foundation Height (m)	Foundation Length (m)	Foundation Width (m)	Rotational Base Support Stiffness (kNm/rad)
434	350	5.0	Dense Sand Medium Dense Sand	35,200	1.5	1.0	1.7	14,883
435	350	7.5	Medium Dense Sand	35,200	1.5	1.0	1.7	14,883
436	350	10.0	Medium Dense Sand	35,200	1.5	1.0	1.7	14,883
437	350	12.5	Medium Dense Sand	35,200	1.5	1.0	1.7	14,883
438	350	15.0	Medium Dense Sand	35,200	1.5	1.0	1.7	14,883
439	350	17.5	Medium Dense Sand	35,200	1.5	1.0	1.7	14,883
440	350	20.0	Medium Dense Sand	35,200	1.5	1.0	1.7	14,883
441	350	22.5	Medium Dense Sand	35,200	1.5	1.0	1.7	14,883
442	350	25.0	Medium Dense Sand	35,200	1.5	1.0	1.7	14,883
443	350	27.5	Medium Dense Sand	35,200	1.5	1.0	1.7	14,883
444	350	30.0	Medium Dense Sand	35,200	1.5	1.0	1.7	14,883
445	350	32.5	Medium Dense Sand	35,200	1.5	1.0	1.7	14,883
446	350	35.0	Medium Dense Sand	35,200	1.5	1.0	1.7	14,883
447	350	37.5	Medium Dense Sand	35,200	1.5	1.0	1.7	14,883
448	350	40.0	Medium Dense Sand	35,200	1.5	1.0	1.7	14,883
449	25	2.5	Dense Sand	96,000	1.5	1.0	0.2	70
450	25	5.0	Dense Sand	96,000	1.5	1.0	0.2	70
451	25	7.5	Dense Sand	96,000	1.5	1.0	0.3	235
452	25	10.0	Dense Sand	96,000	1.5	1.0	0.4	556
453	25	12.5	Dense Sand	96,000	1.5	1.0	0.5	1,087
454	25	15.0	Dense Sand	96,000	1.5	1.0	0.6	1,878
455	25	17.5	Dense Sand	96,000	1.5	1.0	0.7	2,981
456	25	20.0	Dense Sand	96,000	1.5	1.0	0.7	2,981
457	25	22.5	Dense Sand	96,000	1.5	1.0	0.8	4,450
458	25	25.0	Dense Sand	96,000	1.5	1.0	0.9	6,337
459	25	27.5	Dense Sand	96,000	1.5	1.0	1.0	8,692
460	25	30.0	Dense Sand	96,000	1.5	1.0	1.1	11,569
461	25	32.5	Dense Sand	96,000	1.5	1.0	1.2	15,020
462	25	35.0	Dense Sand	96,000	1.5	1.0	1.3	19,097
463	25	37.5	Dense Sand	96,000	1.5	1.0	1.3	19,097
464	25	40.0	Dense Sand	96,000	1.5	1.0	1.4	23,851
465	50	2.5	Dense Sand	96,000	1.5	1.0	0.3	235
466	50	5.0	Dense Sand	96,000	1.5	1.0	0.3	235
467	50	7.5	Dense Sand	96,000	1.5	1.0	0.3	235

ID	Applied Axial Load (kN)	Applied Moment (kNm)	Soil Type	Modulus of Subgrade (kN/m ³)	Foundation Height (m)	Foundation Length (m)	Foundation Width (m)	Rotational Base Support Stiffness (kNm/rad)
468	50	10.0	Dense Sand	96,000	1.5	1.0	0.4	556
469	50	12.5	Dense Sand	96,000	1.5	1.0	0.4	556
470	50	15.0	Dense Sand	96,000	1.5	1.0	0.5	1,087
471	50	17.5	Dense Sand	96,000	1.5	1.0	0.6	1,878
472	50	20.0	Dense Sand	96,000	1.5	1.0	0.7	2,981
473	50	22.5	Dense Sand	96,000	1.5	1.0	0.7	2,981
474	50	25.0	Dense Sand	96,000	1.5	1.0	0.8	4,450
475	50	27.5	Dense Sand	96,000	1.5	1.0	0.9	6,337
476	50	30.0	Dense Sand	96,000	1.5	1.0	0.9	6,337
477	50	32.5	Dense Sand	96,000	1.5	1.0	1.0	8,692
478	50	35.0	Dense Sand	96,000	1.5	1.0	1.1	11,569
479	50	37.5	Dense Sand	96,000	1.5	1.0	1.2	15,020
480	50	40.0	Dense Sand	96,000	1.5	1.0	1.3	19,097
481	75	2.5	Dense Sand	96,000	1.5	1.0	0.4	556
482	75	5.0	Dense Sand	96,000	1.5	1.0	0.4	556
483	75	7.5	Dense Sand	96,000	1.5	1.0	0.4	556
484	75	10.0	Dense Sand	96,000	1.5	1.0	0.4	556
485	75	12.5	Dense Sand	96,000	1.5	1.0	0.4	556
486	75	15.0	Dense Sand	96,000	1.5	1.0	0.4	556
487	75	17.5	Dense Sand	96,000	1.5	1.0	0.5	1,087
488	75	20.0	Dense Sand	96,000	1.5	1.0	0.6	1,878
489	75	22.5	Dense Sand	96,000	1.5	1.0	0.7	2,981
490	75	25.0	Dense Sand	96,000	1.5	1.0	0.7	2,981
491	75	27.5	Dense Sand	96,000	1.5	1.0	0.8	4,450
492	75	30.0	Dense Sand	96,000	1.5	1.0	0.8	4,450
493	75	32.5	Dense Sand	96,000	1.5	1.0	0.9	6,337
494	75	35.0	Dense Sand	96,000	1.5	1.0	1.0	8,692
495	75	37.5	Dense Sand	96,000	1.5	1.0	1.0	8,692
496	75	40.0	Dense Sand	96,000	1.5	1.0	1.1	11,569
497	100	2.5	Dense Sand	96,000	1.5	1.0	0.5	1,087
498	100	5.0	Dense Sand	96,000	1.5	1.0	0.5	1,087
499	100	7.5	Dense Sand	96,000	1.5	1.0	0.5	1,087
500	100	10.0	Dense Sand	96,000	1.5	1.0	0.5	1,087
501	100	12.5	Dense Sand	96,000	1.5	1.0	0.5	1,087
502	100	15.0	Dense Sand	96,000	1.5	1.0	0.5	1,087
503	100	17.5	Dense Sand	96,000	1.5	1.0	0.5	1,087
504	100	20.0	Dense Sand	96,000	1.5	1.0	0.5	1,087
505	100	22.5	Dense Sand	96,000	1.5	1.0	0.6	1,878
506	100	25.0	Dense Sand	96,000	1.5	1.0	0.7	2,981
507	100	27.5	Dense Sand	96,000	1.5	1.0	0.7	2,981
508	100	30.0	Dense Sand	96,000	1.5	1.0	0.8	4,450
509	100	32.5	Dense Sand	96,000	1.5	1.0	0.8	4,450
510	100	35.0	Dense Sand	96,000	1.5	1.0	0.9	6,337
511	100	37.5	Dense Sand	96,000	1.5	1.0	0.9	6,337
512	100	40.0	Dense Sand	96,000	1.5	1.0	1.0	8,692
513	125	2.5	Dense Sand	96,000	1.5	1.0	0.6	1,878
514	125	5.0	Dense Sand	96,000	1.5	1.0	0.6	1,878
515	125	7.5	Dense Sand	96,000	1.5	1.0	0.6	1,878
516	125	10.0	Dense Sand	96,000	1.5	1.0	0.6	1,878
517	125	12.5	Dense Sand	96,000	1.5	1.0	0.6	1,878

ID	Applied Axial Load (kN)	Applied Moment (kNm)	Soil Type	Modulus of Subgrade (kN/m ³)	Foundation Height (m)	Foundation Length (m)	Foundation Width (m)	Rotational Base Support Stiffness (kNm/rad)
518	125	15.0	Dense Sand	96,000	1.5	1.0	0.6	1,878
519	125	17.5	Dense Sand	96,000	1.5	1.0	0.6	1,878
520	125	20.0	Dense Sand	96,000	1.5	1.0	0.6	1,878
521	125	22.5	Dense Sand	96,000	1.5	1.0	0.6	1,878
522	125	25.0	Dense Sand	96,000	1.5	1.0	0.6	1,878
523	125	27.5	Dense Sand	96,000	1.5	1.0	0.7	2,981
524	125	30.0	Dense Sand	96,000	1.5	1.0	0.7	2,981
525	125	32.5	Dense Sand	96,000	1.5	1.0	0.8	4,450
526	125	35.0	Dense Sand	96,000	1.5	1.0	0.8	4,450
527	125	37.5	Dense Sand	96,000	1.5	1.0	0.9	6,337
528	125	40.0	Dense Sand	96,000	1.5	1.0	0.9	6,337
529	150	2.5	Dense Sand	96,000	1.5	1.0	0.8	4,450
530	150	5.0	Dense Sand	96,000	1.5	1.0	0.8	4,450
531	150	7.5	Dense Sand	96,000	1.5	1.0	0.8	4,450
532	150	10.0	Dense Sand	96,000	1.5	1.0	0.8	4,450
533	150	12.5	Dense Sand	96,000	1.5	1.0	0.8	4,450
534	150	15.0	Dense Sand	96,000	1.5	1.0	0.8	4,450
535	150	17.5	Dense Sand	96,000	1.5	1.0	0.8	4,450
536	150	20.0	Dense Sand	96,000	1.5	1.0	0.8	4,450
537	150	22.5	Dense Sand	96,000	1.5	1.0	0.8	4,450
538	150	25.0	Dense Sand	96,000	1.5	1.0	0.8	4,450
539	150	27.5	Dense Sand	96,000	1.5	1.0	0.8	4,450
540	150	30.0	Dense Sand	96,000	1.5	1.0	0.8	4,450
541	150	32.5	Dense Sand	96,000	1.5	1.0	0.8	4,450
542	150	35.0	Dense Sand	96,000	1.5	1.0	0.8	4,450
543	150	37.5	Dense Sand	96,000	1.5	1.0	0.8	4,450
544	150	40.0	Dense Sand	96,000	1.5	1.0	0.8	4,450
545	175	2.5	Dense Sand	96,000	1.5	1.0	0.9	6,337
546	175	5.0	Dense Sand	96,000	1.5	1.0	0.9	6,337
547	175	7.5	Dense Sand	96,000	1.5	1.0	0.9	6,337
548	175	10.0	Dense Sand	96,000	1.5	1.0	0.9	6,337
549	175	12.5	Dense Sand	96,000	1.5	1.0	0.9	6,337
550	175	15.0	Dense Sand	96,000	1.5	1.0	0.9	6,337
551	175	17.5	Dense Sand	96,000	1.5	1.0	0.9	6,337
552	175	20.0	Dense Sand	96,000	1.5	1.0	0.9	6,337
553	175	22.5	Dense Sand	96,000	1.5	1.0	0.9	6,337
554	175	25.0	Dense Sand	96,000	1.5	1.0	0.9	6,337
555	175	27.5	Dense Sand	96,000	1.5	1.0	0.9	6,337
556	175	30.0	Dense Sand	96,000	1.5	1.0	0.9	6,337
557	175	32.5	Dense Sand	96,000	1.5	1.0	0.9	6,337
558	175	35.0	Dense Sand	96,000	1.5	1.0	0.9	6,337
559	175	37.5	Dense Sand	96,000	1.5	1.0	0.9	6,337
560	175	40.0	Dense Sand	96,000	1.5	1.0	0.9	6,337
561	200	2.5	Dense Sand	96,000	1.5	1.0	1.0	8,692
562	200	5.0	Dense Sand	96,000	1.5	1.0	1.0	8,692
563	200	7.5	Dense Sand	96,000	1.5	1.0	1.0	8,692
564	200	10.0	Dense Sand	96,000	1.5	1.0	1.0	8,692
565	200	12.5	Dense Sand	96,000	1.5	1.0	1.0	8,692
566	200	15.0	Dense Sand	96,000	1.5	1.0	1.0	8,692
567	200	17.5	Dense Sand	96,000	1.5	1.0	1.0	8,692

ID	Applied Axial Load (kN)	Applied Moment (kNm)	Soil Type	Modulus of Subgrade (kN/m ³)	Foundation Height (m)	Foundation Length (m)	Foundation Width (m)	Rotational Base Support Stiffness (kNm/rad)
568	200	20.0	Dense Sand	96,000	1.5	1.0	1.0	8,692
569	200	22.5	Dense Sand	96,000	1.5	1.0	1.0	8,692
570	200	25.0	Dense Sand	96,000	1.5	1.0	1.0	8,692
571	200	27.5	Dense Sand	96,000	1.5	1.0	1.0	8,692
572	200	30.0	Dense Sand	96,000	1.5	1.0	1.0	8,692
573	200	32.5	Dense Sand	96,000	1.5	1.0	1.0	8,692
574	200	35.0	Dense Sand	96,000	1.5	1.0	1.0	8,692
575	200	37.5	Dense Sand	96,000	1.5	1.0	1.0	8,692
576	200	40.0	Dense Sand	96,000	1.5	1.0	1.0	8,692
577	225	2.5	Dense Sand	96,000	1.5	1.0	1.1	11,569
578	225	5.0	Dense Sand	96,000	1.5	1.0	1.1	11,569
579	225	7.5	Dense Sand	96,000	1.5	1.0	1.1	11,569
580	225	10.0	Dense Sand	96,000	1.5	1.0	1.1	11,569
581	225	12.5	Dense Sand	96,000	1.5	1.0	1.1	11,569
582	225	15.0	Dense Sand	96,000	1.5	1.0	1.1	11,569
583	225	17.5	Dense Sand	96,000	1.5	1.0	1.1	11,569
584	225	20.0	Dense Sand	96,000	1.5	1.0	1.1	11,569
585	225	22.5	Dense Sand	96,000	1.5	1.0	1.1	11,569
586	225	25.0	Dense Sand	96,000	1.5	1.0	1.1	11,569
587	225	27.5	Dense Sand	96,000	1.5	1.0	1.1	11,569
588	225	30.0	Dense Sand	96,000	1.5	1.0	1.1	11,569
589	225	32.5	Dense Sand	96,000	1.5	1.0	1.1	11,569
590	225	35.0	Dense Sand	96,000	1.5	1.0	1.1	11,569
591	225	37.5	Dense Sand	96,000	1.5	1.0	1.1	11,569
592	225	40.0	Dense Sand	96,000	1.5	1.0	1.1	11,569
593	250	2.5	Dense Sand	96,000	1.5	1.0	1.2	15,020
594	250	5.0	Dense Sand	96,000	1.5	1.0	1.2	15,020
595	250	7.5	Dense Sand	96,000	1.5	1.0	1.2	15,020
596	250	10.0	Dense Sand	96,000	1.5	1.0	1.2	15,020
597	250	12.5	Dense Sand	96,000	1.5	1.0	1.2	15,020
598	250	15.0	Dense Sand	96,000	1.5	1.0	1.2	15,020
599	250	17.5	Dense Sand	96,000	1.5	1.0	1.2	15,020
600	250	20.0	Dense Sand	96,000	1.5	1.0	1.2	15,020
601	250	22.5	Dense Sand	96,000	1.5	1.0	1.2	15,020
602	250	25.0	Dense Sand	96,000	1.5	1.0	1.2	15,020
603	250	27.5	Dense Sand	96,000	1.5	1.0	1.2	15,020
604	250	30.0	Dense Sand	96,000	1.5	1.0	1.2	15,020
605	250	32.5	Dense Sand	96,000	1.5	1.0	1.2	15,020
606	250	35.0	Dense Sand	96,000	1.5	1.0	1.2	15,020
607	250	37.5	Dense Sand	96,000	1.5	1.0	1.2	15,020
608	250	40.0	Dense Sand	96,000	1.5	1.0	1.2	15,020
609	275	2.5	Dense Sand	96,000	1.5	1.0	1.4	23,851
610	275	5.0	Dense Sand	96,000	1.5	1.0	1.4	23,851
611	275	7.5	Dense Sand	96,000	1.5	1.0	1.4	23,851
612	275	10.0	Dense Sand	96,000	1.5	1.0	1.4	23,851
613	275	12.5	Dense Sand	96,000	1.5	1.0	1.4	23,851
614	275	15.0	Dense Sand	96,000	1.5	1.0	1.4	23,851
615	275	17.5	Dense Sand	96,000	1.5	1.0	1.4	23,851
616	275	20.0	Dense Sand	96,000	1.5	1.0	1.4	23,851
617	275	22.5	Dense Sand	96,000	1.5	1.0	1.4	23,851

ID	Applied Axial Load (kN)	Applied Moment (kNm)	Soil Type	Modulus of Subgrade (kN/m ³)	Foundation Height (m)	Foundation Length (m)	Foundation Width (m)	Rotational Base Support Stiffness (kNm/rad)
618	275	25.0	Dense Sand	96,000	1.5	1.0	1.4	23,851
619	275	27.5	Dense Sand	96,000	1.5	1.0	1.4	23,851
620	275	30.0	Dense Sand	96,000	1.5	1.0	1.4	23,851
621	275	32.5	Dense Sand	96,000	1.5	1.0	1.4	23,851
622	275	35.0	Dense Sand	96,000	1.5	1.0	1.4	23,851
623	275	37.5	Dense Sand	96,000	1.5	1.0	1.4	23,851
624	275	40.0	Dense Sand	96,000	1.5	1.0	1.4	23,851
625	300	2.5	Dense Sand	96,000	1.5	1.0	1.5	29,336
626	300	5.0	Dense Sand	96,000	1.5	1.0	1.5	29,336
627	300	7.5	Dense Sand	96,000	1.5	1.0	1.5	29,336
628	300	10.0	Dense Sand	96,000	1.5	1.0	1.5	29,336
629	300	12.5	Dense Sand	96,000	1.5	1.0	1.5	29,336
630	300	15.0	Dense Sand	96,000	1.5	1.0	1.5	29,336
631	300	17.5	Dense Sand	96,000	1.5	1.0	1.5	29,336
632	300	20.0	Dense Sand	96,000	1.5	1.0	1.5	29,336
633	300	22.5	Dense Sand	96,000	1.5	1.0	1.5	29,336
634	300	25.0	Dense Sand	96,000	1.5	1.0	1.5	29,336
635	300	27.5	Dense Sand	96,000	1.5	1.0	1.5	29,336
636	300	30.0	Dense Sand	96,000	1.5	1.0	1.5	29,336
637	300	32.5	Dense Sand	96,000	1.5	1.0	1.5	29,336
638	300	35.0	Dense Sand	96,000	1.5	1.0	1.5	29,336
639	300	37.5	Dense Sand	96,000	1.5	1.0	1.5	29,336
640	300	40.0	Dense Sand	96,000	1.5	1.0	1.5	29,336
641	325	2.5	Dense Sand	96,000	1.5	1.0	1.6	35,603
642	325	5.0	Dense Sand	96,000	1.5	1.0	1.6	35,603
643	325	7.5	Dense Sand	96,000	1.5	1.0	1.6	35,603
644	325	10.0	Dense Sand	96,000	1.5	1.0	1.6	35,603
645	325	12.5	Dense Sand	96,000	1.5	1.0	1.6	35,603
646	325	15.0	Dense Sand	96,000	1.5	1.0	1.6	35,603
647	325	17.5	Dense Sand	96,000	1.5	1.0	1.6	35,603
648	325	20.0	Dense Sand	96,000	1.5	1.0	1.6	35,603
649	325	22.5	Dense Sand	96,000	1.5	1.0	1.6	35,603
650	325	25.0	Dense Sand	96,000	1.5	1.0	1.6	35,603
651	325	27.5	Dense Sand	96,000	1.5	1.0	1.6	35,603
652	325	30.0	Dense Sand	96,000	1.5	1.0	1.6	35,603
653	325	32.5	Dense Sand	96,000	1.5	1.0	1.6	35,603
654	325	35.0	Dense Sand	96,000	1.5	1.0	1.6	35,603
655	325	37.5	Dense Sand	96,000	1.5	1.0	1.6	35,603
656	325	40.0	Dense Sand	96,000	1.5	1.0	1.6	35,603
657	350	2.5	Dense Sand	96,000	1.5	1.0	1.7	42,705
658	350	5.0	Dense Sand	96,000	1.5	1.0	1.7	42,705
659	350	7.5	Dense Sand	96,000	1.5	1.0	1.7	42,705
660	350	10.0	Dense Sand	96,000	1.5	1.0	1.7	42,705
661	350	12.5	Dense Sand	96,000	1.5	1.0	1.7	42,705
662	350	15.0	Dense Sand	96,000	1.5	1.0	1.7	42,705
663	350	17.5	Dense Sand	96,000	1.5	1.0	1.7	42,705
664	350	20.0	Dense Sand	96,000	1.5	1.0	1.7	42,705
665	350	22.5	Dense Sand	96,000	1.5	1.0	1.7	42,705
666	350	25.0	Dense Sand	96,000	1.5	1.0	1.7	42,705
667	350	27.5	Dense Sand	96,000	1.5	1.0	1.7	42,705

ID	Applied Axial Load (kN)	Applied Moment (kNm)	Soil Type	Modulus of Subgrade (kN/m ³)	Foundation Height (m)	Foundation Length (m)	Foundation Width (m)	Rotational Base Support Stiffness (kNm/rad)
668	350	30.0	Dense Sand	96,000	1.5	1.0	1.7	42,705
669	350	32.5	Dense Sand	96,000	1.5	1.0	1.7	42,705
670	350	35.0	Dense Sand	96,000	1.5	1.0	1.7	42,705
671	350	37.5	Dense Sand	96,000	1.5	1.0	1.7	42,705
672	350	40.0	Dense Sand	96,000	1.5	1.0	1.7	42,705
673	25	2.5	Clayey Medium Dense Sand	56,000	1.5	1.0	0.2	39
674	25	5.0	Clayey Medium Dense Sand	56,000	1.5	1.0	0.2	39
675	25	7.5	Clayey Medium Dense Sand	56,000	1.5	1.0	0.3	130
676	25	10.0	Clayey Medium Dense Sand	56,000	1.5	1.0	0.4	308
677	25	12.5	Clayey Medium Dense Sand	56,000	1.5	1.0	0.5	602
678	25	15.0	Clayey Medium Dense Sand	56,000	1.5	1.0	0.6	1,041
679	25	17.5	Clayey Medium Dense Sand	56,000	1.5	1.0	0.7	1,653
680	25	20.0	Clayey Medium Dense Sand	56,000	1.5	1.0	0.7	1,653
681	25	22.5	Clayey Medium Dense Sand	56,000	1.5	1.0	0.8	2,468
682	25	25.0	Clayey Medium Dense Sand	56,000	1.5	1.0	0.9	3,513
683	25	27.5	Clayey Medium Dense Sand	56,000	1.5	1.0	1.0	4,819
684	25	30.0	Clayey Medium Dense Sand	56,000	1.5	1.0	1.1	6,415
685	25	32.5	Clayey Medium Dense Sand	56,000	1.5	1.0	1.2	8,328
686	25	35.0	Clayey Medium Dense Sand	56,000	1.5	1.0	1.3	10,588
687	25	37.5	Clayey Medium Dense Sand	56,000	1.5	1.0	1.3	10,588

ID	Applied Axial Load (kN)	Applied Moment (kNm)	Soil Type	Modulus of Subgrade (kN/m ³)	Foundation Height (m)	Foundation Length (m)	Foundation Width (m)	Rotational Base Support Stiffness (kNm/rad)
688	25	40.0	Clayey Medium Dense Sand	56,000	1.5	1.0	1.4	13,225
689	50	2.5	Clayey Medium Dense Sand	56,000	1.5	1.0	0.3	130
690	50	5.0	Clayey Medium Dense Sand	56,000	1.5	1.0	0.3	130
691	50	7.5	Clayey Medium Dense Sand	56,000	1.5	1.0	0.3	130
692	50	10.0	Clayey Medium Dense Sand	56,000	1.5	1.0	0.4	308
693	50	12.5	Clayey Medium Dense Sand	56,000	1.5	1.0	0.4	308
694	50	15.0	Clayey Medium Dense Sand	56,000	1.5	1.0	0.5	602
695	50	17.5	Clayey Medium Dense Sand	56,000	1.5	1.0	0.6	1,041
696	50	20.0	Clayey Medium Dense Sand	56,000	1.5	1.0	0.7	1,653
697	50	22.5	Clayey Medium Dense Sand	56,000	1.5	1.0	0.7	1,653
698	50	25.0	Clayey Medium Dense Sand	56,000	1.5	1.0	0.8	2,468
699	50	27.5	Clayey Medium Dense Sand	56,000	1.5	1.0	0.9	3,513
700	50	30.0	Clayey Medium Dense Sand	56,000	1.5	1.0	0.9	3,513
701	50	32.5	Clayey Medium Dense Sand	56,000	1.5	1.0	1.0	4,819
702	50	35.0	Clayey Medium Dense Sand	56,000	1.5	1.0	1.1	6,415
703	50	37.5	Clayey Medium Dense Sand	56,000	1.5	1.0	1.2	8,328
704	50	40.0	Clayey Medium	56,000	1.5	1.0	1.3	10,588

ID	Applied Axial Load (kN)	Applied Moment (kNm)	Soil Type	Modulus of Subgrade (kN/m ³)	Foundation Height (m)	Foundation Length (m)	Foundation Width (m)	Rotational Base Support Stiffness (kNm/rad)
705	75	2.5	Dense Sand Clayey Medium	56,000	1.5	1.0	0.4	308
706	75	5.0	Dense Sand Clayey Medium	56,000	1.5	1.0	0.4	308
707	75	7.5	Dense Sand Clayey Medium	56,000	1.5	1.0	0.4	308
708	75	10.0	Dense Sand Clayey Medium	56,000	1.5	1.0	0.4	308
709	75	12.5	Dense Sand Clayey Medium	56,000	1.5	1.0	0.4	308
710	75	15.0	Dense Sand Clayey Medium	56,000	1.5	1.0	0.4	308
711	75	17.5	Dense Sand Clayey Medium	56,000	1.5	1.0	0.5	602
712	75	20.0	Dense Sand Clayey Medium	56,000	1.5	1.0	0.6	1,041
713	75	22.5	Dense Sand Clayey Medium	56,000	1.5	1.0	0.7	1,653
714	75	25.0	Dense Sand Clayey Medium	56,000	1.5	1.0	0.7	1,653
715	75	27.5	Dense Sand Clayey Medium	56,000	1.5	1.0	0.8	2,468
716	75	30.0	Dense Sand Clayey Medium	56,000	1.5	1.0	0.8	2,468
717	75	32.5	Dense Sand Clayey Medium	56,000	1.5	1.0	0.9	3,513
718	75	35.0	Dense Sand Clayey Medium	56,000	1.5	1.0	1.0	4,819
719	75	37.5	Dense Sand Clayey Medium	56,000	1.5	1.0	1.0	4,819
720	75	40.0	Dense Sand Clayey Medium	56,000	1.5	1.0	1.1	6,415
721	100	2.5	Dense Sand Clayey	56,000	1.5	1.0	0.5	602

ID	Applied Axial Load (kN)	Applied Moment (kNm)	Soil Type	Modulus of Subgrade (kN/m ³)	Foundation Height (m)	Foundation Length (m)	Foundation Width (m)	Rotational Base Support Stiffness (kNm/rad)
722	100	5.0	Medium Dense Sand Clayey	56,000	1.5	1.0	0.5	602
723	100	7.5	Medium Dense Sand Clayey	56,000	1.5	1.0	0.5	602
724	100	10.0	Medium Dense Sand Clayey	56,000	1.5	1.0	0.5	602
725	100	12.5	Medium Dense Sand Clayey	56,000	1.5	1.0	0.5	602
726	100	15.0	Medium Dense Sand Clayey	56,000	1.5	1.0	0.5	602
727	100	17.5	Medium Dense Sand Clayey	56,000	1.5	1.0	0.5	602
728	100	20.0	Medium Dense Sand Clayey	56,000	1.5	1.0	0.5	602
729	100	22.5	Medium Dense Sand Clayey	56,000	1.5	1.0	0.6	1,041
730	100	25.0	Medium Dense Sand Clayey	56,000	1.5	1.0	0.7	1,653
731	100	27.5	Medium Dense Sand Clayey	56,000	1.5	1.0	0.7	1,653
732	100	30.0	Medium Dense Sand Clayey	56,000	1.5	1.0	0.8	2,468
733	100	32.5	Medium Dense Sand Clayey	56,000	1.5	1.0	0.8	2,468
734	100	35.0	Medium Dense Sand Clayey	56,000	1.5	1.0	0.9	3,513
735	100	37.5	Medium Dense Sand Clayey	56,000	1.5	1.0	0.9	3,513
736	100	40.0	Medium Dense Sand Clayey	56,000	1.5	1.0	1.0	4,819
737	125	2.5	Medium Dense Sand Clayey	56,000	1.5	1.0	0.6	1,041

ID	Applied Axial Load (kN)	Applied Moment (kNm)	Soil Type	Modulus of Subgrade (kN/m ³)	Foundation Height (m)	Foundation Length (m)	Foundation Width (m)	Rotational Base Support Stiffness (kNm/rad)
738	125	5.0	Clayey Medium Dense Sand	56,000	1.5	1.0	0.6	1,041
739	125	7.5	Clayey Medium Dense Sand	56,000	1.5	1.0	0.6	1,041
740	125	10.0	Clayey Medium Dense Sand	56,000	1.5	1.0	0.6	1,041
741	125	12.5	Clayey Medium Dense Sand	56,000	1.5	1.0	0.6	1,041
742	125	15.0	Clayey Medium Dense Sand	56,000	1.5	1.0	0.6	1,041
743	125	17.5	Clayey Medium Dense Sand	56,000	1.5	1.0	0.6	1,041
744	125	20.0	Clayey Medium Dense Sand	56,000	1.5	1.0	0.6	1,041
745	125	22.5	Clayey Medium Dense Sand	56,000	1.5	1.0	0.6	1,041
746	125	25.0	Clayey Medium Dense Sand	56,000	1.5	1.0	0.6	1,041
747	125	27.5	Clayey Medium Dense Sand	56,000	1.5	1.0	0.7	1,653
748	125	30.0	Clayey Medium Dense Sand	56,000	1.5	1.0	0.7	1,653
749	125	32.5	Clayey Medium Dense Sand	56,000	1.5	1.0	0.8	2,468
750	125	35.0	Clayey Medium Dense Sand	56,000	1.5	1.0	0.8	2,468
751	125	37.5	Clayey Medium Dense Sand	56,000	1.5	1.0	0.9	3,513
752	125	40.0	Clayey Medium Dense Sand	56,000	1.5	1.0	0.9	3,513
753	150	2.5	Clayey Medium Dense Sand	56,000	1.5	1.0	0.8	2,468
754	150	5.0	Clayey Medium	56,000	1.5	1.0	0.8	2,468

ID	Applied Axial Load (kN)	Applied Moment (kNm)	Soil Type	Modulus of Subgrade (kN/m ³)	Foundation Height (m)	Foundation Length (m)	Foundation Width (m)	Rotational Base Support Stiffness (kNm/rad)
755	150	7.5	Dense Sand Clayey Medium	56,000	1.5	1.0	0.8	2,468
756	150	10.0	Dense Sand Clayey Medium	56,000	1.5	1.0	0.8	2,468
757	150	12.5	Dense Sand Clayey Medium	56,000	1.5	1.0	0.8	2,468
758	150	15.0	Dense Sand Clayey Medium	56,000	1.5	1.0	0.8	2,468
759	150	17.5	Dense Sand Clayey Medium	56,000	1.5	1.0	0.8	2,468
760	150	20.0	Dense Sand Clayey Medium	56,000	1.5	1.0	0.8	2,468
761	150	22.5	Dense Sand Clayey Medium	56,000	1.5	1.0	0.8	2,468
762	150	25.0	Dense Sand Clayey Medium	56,000	1.5	1.0	0.8	2,468
763	150	27.5	Dense Sand Clayey Medium	56,000	1.5	1.0	0.8	2,468
764	150	30.0	Dense Sand Clayey Medium	56,000	1.5	1.0	0.8	2,468
765	150	32.5	Dense Sand Clayey Medium	56,000	1.5	1.0	0.8	2,468
766	150	35.0	Dense Sand Clayey Medium	56,000	1.5	1.0	0.8	2,468
767	150	37.5	Dense Sand Clayey Medium	56,000	1.5	1.0	0.8	2,468
768	150	40.0	Dense Sand Clayey Medium	56,000	1.5	1.0	0.8	2,468
769	175	2.5	Dense Sand Clayey Medium	56,000	1.5	1.0	0.9	3,513
770	175	5.0	Dense Sand Clayey Medium	56,000	1.5	1.0	0.9	3,513
771	175	7.5	Dense Sand Clayey	56,000	1.5	1.0	0.9	3,513

ID	Applied Axial Load (kN)	Applied Moment (kNm)	Soil Type	Modulus of Subgrade (kN/m ³)	Foundation Height (m)	Foundation Length (m)	Foundation Width (m)	Rotational Base Support Stiffness (kNm/rad)
772	175	10.0	Medium Dense Sand Clayey	56,000	1.5	1.0	0.9	3,513
773	175	12.5	Medium Dense Sand Clayey	56,000	1.5	1.0	0.9	3,513
774	175	15.0	Medium Dense Sand Clayey	56,000	1.5	1.0	0.9	3,513
775	175	17.5	Medium Dense Sand Clayey	56,000	1.5	1.0	0.9	3,513
776	175	20.0	Medium Dense Sand Clayey	56,000	1.5	1.0	0.9	3,513
777	175	22.5	Medium Dense Sand Clayey	56,000	1.5	1.0	0.9	3,513
778	175	25.0	Medium Dense Sand Clayey	56,000	1.5	1.0	0.9	3,513
779	175	27.5	Medium Dense Sand Clayey	56,000	1.5	1.0	0.9	3,513
780	175	30.0	Medium Dense Sand Clayey	56,000	1.5	1.0	0.9	3,513
781	175	32.5	Medium Dense Sand Clayey	56,000	1.5	1.0	0.9	3,513
782	175	35.0	Medium Dense Sand Clayey	56,000	1.5	1.0	0.9	3,513
783	175	37.5	Medium Dense Sand Clayey	56,000	1.5	1.0	0.9	3,513
784	175	40.0	Medium Dense Sand Clayey	56,000	1.5	1.0	0.9	3,513
785	200	2.5	Medium Dense Sand Clayey	56,000	1.5	1.0	1.0	4,819
786	200	5.0	Medium Dense Sand Clayey	56,000	1.5	1.0	1.0	4,819
787	200	7.5	Medium Dense Sand Clayey	56,000	1.5	1.0	1.0	4,819

ID	Applied Axial Load (kN)	Applied Moment (kNm)	Soil Type	Modulus of Subgrade (kN/m ³)	Foundation Height (m)	Foundation Length (m)	Foundation Width (m)	Rotational Base Support Stiffness (kNm/rad)
788	200	10.0	Clayey Medium Dense Sand	56,000	1.5	1.0	1.0	4,819
789	200	12.5	Clayey Medium Dense Sand	56,000	1.5	1.0	1.0	4,819
790	200	15.0	Clayey Medium Dense Sand	56,000	1.5	1.0	1.0	4,819
791	200	17.5	Clayey Medium Dense Sand	56,000	1.5	1.0	1.0	4,819
792	200	20.0	Clayey Medium Dense Sand	56,000	1.5	1.0	1.0	4,819
793	200	22.5	Clayey Medium Dense Sand	56,000	1.5	1.0	1.0	4,819
794	200	25.0	Clayey Medium Dense Sand	56,000	1.5	1.0	1.0	4,819
795	200	27.5	Clayey Medium Dense Sand	56,000	1.5	1.0	1.0	4,819
796	200	30.0	Clayey Medium Dense Sand	56,000	1.5	1.0	1.0	4,819
797	200	32.5	Clayey Medium Dense Sand	56,000	1.5	1.0	1.0	4,819
798	200	35.0	Clayey Medium Dense Sand	56,000	1.5	1.0	1.0	4,819
799	200	37.5	Clayey Medium Dense Sand	56,000	1.5	1.0	1.0	4,819
800	200	40.0	Clayey Medium Dense Sand	56,000	1.5	1.0	1.0	4,819
801	225	2.5	Clayey Medium Dense Sand	56,000	1.5	1.0	1.1	6,415
802	225	5.0	Clayey Medium Dense Sand	56,000	1.5	1.0	1.1	6,415
803	225	7.5	Clayey Medium Dense Sand	56,000	1.5	1.0	1.1	6,415
804	225	10.0	Clayey Medium	56,000	1.5	1.0	1.1	6,415

ID	Applied Axial Load (kN)	Applied Moment (kNm)	Soil Type	Modulus of Subgrade (kN/m ³)	Foundation Height (m)	Foundation Length (m)	Foundation Width (m)	Rotational Base Support Stiffness (kNm/rad)
805	225	12.5	Dense Sand Clayey Medium	56,000	1.5	1.0	1.1	6,415
806	225	15.0	Dense Sand Clayey Medium	56,000	1.5	1.0	1.1	6,415
807	225	17.5	Dense Sand Clayey Medium	56,000	1.5	1.0	1.1	6,415
808	225	20.0	Dense Sand Clayey Medium	56,000	1.5	1.0	1.1	6,415
809	225	22.5	Dense Sand Clayey Medium	56,000	1.5	1.0	1.1	6,415
810	225	25.0	Dense Sand Clayey Medium	56,000	1.5	1.0	1.1	6,415
811	225	27.5	Dense Sand Clayey Medium	56,000	1.5	1.0	1.1	6,415
812	225	30.0	Dense Sand Clayey Medium	56,000	1.5	1.0	1.1	6,415
813	225	32.5	Dense Sand Clayey Medium	56,000	1.5	1.0	1.1	6,415
814	225	35.0	Dense Sand Clayey Medium	56,000	1.5	1.0	1.1	6,415
815	225	37.5	Dense Sand Clayey Medium	56,000	1.5	1.0	1.1	6,415
816	225	40.0	Dense Sand Clayey Medium	56,000	1.5	1.0	1.1	6,415
817	250	2.5	Dense Sand Clayey Medium	56,000	1.5	1.0	1.2	8,328
818	250	5.0	Dense Sand Clayey Medium	56,000	1.5	1.0	1.2	8,328
819	250	7.5	Dense Sand Clayey Medium	56,000	1.5	1.0	1.2	8,328
820	250	10.0	Dense Sand Clayey Medium	56,000	1.5	1.0	1.2	8,328
821	250	12.5	Dense Sand Clayey	56,000	1.5	1.0	1.2	8,328

ID	Applied Axial Load (kN)	Applied Moment (kNm)	Soil Type	Modulus of Subgrade (kN/m ³)	Foundation Height (m)	Foundation Length (m)	Foundation Width (m)	Rotational Base Support Stiffness (kNm/rad)
822	250	15.0	Medium Dense Sand Clayey	56,000	1.5	1.0	1.2	8,328
823	250	17.5	Medium Dense Sand Clayey	56,000	1.5	1.0	1.2	8,328
824	250	20.0	Medium Dense Sand Clayey	56,000	1.5	1.0	1.2	8,328
825	250	22.5	Medium Dense Sand Clayey	56,000	1.5	1.0	1.2	8,328
826	250	25.0	Medium Dense Sand Clayey	56,000	1.5	1.0	1.2	8,328
827	250	27.5	Medium Dense Sand Clayey	56,000	1.5	1.0	1.2	8,328
828	250	30.0	Medium Dense Sand Clayey	56,000	1.5	1.0	1.2	8,328
829	250	32.5	Medium Dense Sand Clayey	56,000	1.5	1.0	1.2	8,328
830	250	35.0	Medium Dense Sand Clayey	56,000	1.5	1.0	1.2	8,328
831	250	37.5	Medium Dense Sand Clayey	56,000	1.5	1.0	1.2	8,328
832	250	40.0	Medium Dense Sand Clayey	56,000	1.5	1.0	1.2	8,328
833	275	2.5	Medium Dense Sand Clayey	56,000	1.5	1.0	1.4	13,225
834	275	5.0	Medium Dense Sand Clayey	56,000	1.5	1.0	1.4	13,225
835	275	7.5	Medium Dense Sand Clayey	56,000	1.5	1.0	1.4	13,225
836	275	10.0	Medium Dense Sand Clayey	56,000	1.5	1.0	1.4	13,225
837	275	12.5	Medium Dense Sand Clayey	56,000	1.5	1.0	1.4	13,225

ID	Applied Axial Load (kN)	Applied Moment (kNm)	Soil Type	Modulus of Subgrade (kN/m ³)	Foundation Height (m)	Foundation Length (m)	Foundation Width (m)	Rotational Base Support Stiffness (kNm/rad)
838	275	15.0	Clayey Medium Dense Sand	56,000	1.5	1.0	1.4	13,225
839	275	17.5	Clayey Medium Dense Sand	56,000	1.5	1.0	1.4	13,225
840	275	20.0	Clayey Medium Dense Sand	56,000	1.5	1.0	1.4	13,225
841	275	22.5	Clayey Medium Dense Sand	56,000	1.5	1.0	1.4	13,225
842	275	25.0	Clayey Medium Dense Sand	56,000	1.5	1.0	1.4	13,225
843	275	27.5	Clayey Medium Dense Sand	56,000	1.5	1.0	1.4	13,225
844	275	30.0	Clayey Medium Dense Sand	56,000	1.5	1.0	1.4	13,225
845	275	32.5	Clayey Medium Dense Sand	56,000	1.5	1.0	1.4	13,225
846	275	35.0	Clayey Medium Dense Sand	56,000	1.5	1.0	1.4	13,225
847	275	37.5	Clayey Medium Dense Sand	56,000	1.5	1.0	1.4	13,225
848	275	40.0	Clayey Medium Dense Sand	56,000	1.5	1.0	1.4	13,225
849	300	2.5	Clayey Medium Dense Sand	56,000	1.5	1.0	1.5	16,266
850	300	5.0	Clayey Medium Dense Sand	56,000	1.5	1.0	1.5	16,266
851	300	7.5	Clayey Medium Dense Sand	56,000	1.5	1.0	1.5	16,266
852	300	10.0	Clayey Medium Dense Sand	56,000	1.5	1.0	1.5	16,266
853	300	12.5	Clayey Medium Dense Sand	56,000	1.5	1.0	1.5	16,266
854	300	15.0	Clayey Medium	56,000	1.5	1.0	1.5	16,266

ID	Applied Axial Load (kN)	Applied Moment (kNm)	Soil Type	Modulus of Subgrade (kN/m ³)	Foundation Height (m)	Foundation Length (m)	Foundation Width (m)	Rotational Base Support Stiffness (kNm/rad)
855	300	17.5	Dense Sand Clayey Medium	56,000	1.5	1.0	1.5	16,266
856	300	20.0	Dense Sand Clayey Medium	56,000	1.5	1.0	1.5	16,266
857	300	22.5	Dense Sand Clayey Medium	56,000	1.5	1.0	1.5	16,266
858	300	25.0	Dense Sand Clayey Medium	56,000	1.5	1.0	1.5	16,266
859	300	27.5	Dense Sand Clayey Medium	56,000	1.5	1.0	1.5	16,266
860	300	30.0	Dense Sand Clayey Medium	56,000	1.5	1.0	1.5	16,266
861	300	32.5	Dense Sand Clayey Medium	56,000	1.5	1.0	1.5	16,266
862	300	35.0	Dense Sand Clayey Medium	56,000	1.5	1.0	1.5	16,266
863	300	37.5	Dense Sand Clayey Medium	56,000	1.5	1.0	1.5	16,266
864	300	40.0	Dense Sand Clayey Medium	56,000	1.5	1.0	1.5	16,266
865	325	2.5	Dense Sand Clayey Medium	56,000	1.5	1.0	1.6	19,741
866	325	5.0	Dense Sand Clayey Medium	56,000	1.5	1.0	1.6	19,741
867	325	7.5	Dense Sand Clayey Medium	56,000	1.5	1.0	1.6	19,741
868	325	10.0	Dense Sand Clayey Medium	56,000	1.5	1.0	1.6	19,741
869	325	12.5	Dense Sand Clayey Medium	56,000	1.5	1.0	1.6	19,741
870	325	15.0	Dense Sand Clayey Medium	56,000	1.5	1.0	1.6	19,741
871	325	17.5	Dense Sand Clayey	56,000	1.5	1.0	1.6	19,741

ID	Applied Axial Load (kN)	Applied Moment (kNm)	Soil Type	Modulus of Subgrade (kN/m ³)	Foundation Height (m)	Foundation Length (m)	Foundation Width (m)	Rotational Base Support Stiffness (kNm/rad)
872	325	20.0	Medium Dense Sand Clayey	56,000	1.5	1.0	1.6	19,741
873	325	22.5	Medium Dense Sand Clayey	56,000	1.5	1.0	1.6	19,741
874	325	25.0	Medium Dense Sand Clayey	56,000	1.5	1.0	1.6	19,741
875	325	27.5	Medium Dense Sand Clayey	56,000	1.5	1.0	1.6	19,741
876	325	30.0	Medium Dense Sand Clayey	56,000	1.5	1.0	1.6	19,741
877	325	32.5	Medium Dense Sand Clayey	56,000	1.5	1.0	1.6	19,741
878	325	35.0	Medium Dense Sand Clayey	56,000	1.5	1.0	1.6	19,741
879	325	37.5	Medium Dense Sand Clayey	56,000	1.5	1.0	1.6	19,741
880	325	40.0	Medium Dense Sand Clayey	56,000	1.5	1.0	1.6	19,741
881	350	2.5	Medium Dense Sand Clayey	56,000	1.5	1.0	1.7	23,678
882	350	5.0	Medium Dense Sand Clayey	56,000	1.5	1.0	1.7	23,678
883	350	7.5	Medium Dense Sand Clayey	56,000	1.5	1.0	1.7	23,678
884	350	10.0	Medium Dense Sand Clayey	56,000	1.5	1.0	1.7	23,678
885	350	12.5	Medium Dense Sand Clayey	56,000	1.5	1.0	1.7	23,678
886	350	15.0	Medium Dense Sand Clayey	56,000	1.5	1.0	1.7	23,678
887	350	17.5	Medium Dense Sand Clayey	56,000	1.5	1.0	1.7	23,678

ID	Applied Axial Load (kN)	Applied Moment (kNm)	Soil Type	Modulus of Subgrade (kN/m ³)	Foundation Height (m)	Foundation Length (m)	Foundation Width (m)	Rotational Base Support Stiffness (kNm/rad)
888	350	20.0	Clayey Medium Dense Sand	56,000	1.5	1.0	1.7	23,678
889	350	22.5	Clayey Medium Dense Sand	56,000	1.5	1.0	1.7	23,678
890	350	25.0	Clayey Medium Dense Sand	56,000	1.5	1.0	1.7	23,678
891	350	27.5	Clayey Medium Dense Sand	56,000	1.5	1.0	1.7	23,678
892	350	30.0	Clayey Medium Dense Sand	56,000	1.5	1.0	1.7	23,678
893	350	32.5	Clayey Medium Dense Sand	56,000	1.5	1.0	1.7	23,678
894	350	35.0	Clayey Medium Dense Sand	56,000	1.5	1.0	1.7	23,678
895	350	37.5	Clayey Medium Dense Sand	56,000	1.5	1.0	1.7	23,678
896	350	40.0	Clayey Medium Dense Sand	56,000	1.5	1.0	1.7	23,678
897	25	2.5	Silty Dense Sand	36,000	1.5	1.0	0.2	25
898	25	5.0	Silty Dense Sand	36,000	1.5	1.0	0.2	25
899	25	7.5	Silty Dense Sand	36,000	1.5	1.0	0.3	84
900	25	10.0	Silty Dense Sand	36,000	1.5	1.0	0.4	198
901	25	12.5	Silty Dense Sand	36,000	1.5	1.0	0.5	387
902	25	15.0	Silty Dense Sand	36,000	1.5	1.0	0.6	669
903	25	17.5	Silty Dense Sand	36,000	1.5	1.0	0.7	1,063
904	25	20.0	Silty Dense Sand	36,000	1.5	1.0	0.7	1,063
905	25	22.5	Silty Dense Sand	36,000	1.5	1.0	0.8	1,586
906	25	25.0	Silty Dense Sand	36,000	1.5	1.0	0.9	2,259
907	25	27.5	Silty Dense Sand	36,000	1.5	1.0	1.0	3,098
908	25	30.0	Silty Dense	36,000	1.5	1.0	1.1	4,124

ID	Applied Axial Load (kN)	Applied Moment (kNm)	Soil Type	Modulus of Subgrade (kN/m ³)	Foundation Height (m)	Foundation Length (m)	Foundation Width (m)	Rotational Base Support Stiffness (kNm/rad)
909	25	32.5	Sand Silty Dense Sand	36,000	1.5	1.0	1.2	5,354
910	25	35.0	Silty Dense Sand	36,000	1.5	1.0	1.3	6,807
911	25	37.5	Silty Dense Sand	36,000	1.5	1.0	1.3	6,807
912	25	40.0	Silty Dense Sand	36,000	1.5	1.0	1.4	8,502
913	50	2.5	Silty Dense Sand	36,000	1.5	1.0	0.3	84
914	50	5.0	Silty Dense Sand	36,000	1.5	1.0	0.3	84
915	50	7.5	Silty Dense Sand	36,000	1.5	1.0	0.3	84
916	50	10.0	Silty Dense Sand	36,000	1.5	1.0	0.4	198
917	50	12.5	Silty Dense Sand	36,000	1.5	1.0	0.4	198
918	50	15.0	Silty Dense Sand	36,000	1.5	1.0	0.5	387
919	50	17.5	Silty Dense Sand	36,000	1.5	1.0	0.6	669
920	50	20.0	Silty Dense Sand	36,000	1.5	1.0	0.7	1,063
921	50	22.5	Silty Dense Sand	36,000	1.5	1.0	0.7	1,063
922	50	25.0	Silty Dense Sand	36,000	1.5	1.0	0.8	1,586
923	50	27.5	Silty Dense Sand	36,000	1.5	1.0	0.9	2,259
924	50	30.0	Silty Dense Sand	36,000	1.5	1.0	0.9	2,259
925	50	32.5	Silty Dense Sand	36,000	1.5	1.0	1.0	3,098
926	50	35.0	Silty Dense Sand	36,000	1.5	1.0	1.1	4,124
927	50	37.5	Silty Dense Sand	36,000	1.5	1.0	1.2	5,354
928	50	40.0	Silty Dense Sand	36,000	1.5	1.0	1.3	6,807
929	75	2.5	Silty Dense Sand	36,000	1.5	1.0	0.4	198
930	75	5.0	Silty Dense Sand	36,000	1.5	1.0	0.4	198
931	75	7.5	Silty Dense Sand	36,000	1.5	1.0	0.4	198
932	75	10.0	Silty Dense Sand	36,000	1.5	1.0	0.4	198
933	75	12.5	Silty Dense Sand	36,000	1.5	1.0	0.4	198

ID	Applied Axial Load (kN)	Applied Moment (kNm)	Soil Type	Modulus of Subgrade (kN/m ³)	Foundation Height (m)	Foundation Length (m)	Foundation Width (m)	Rotational Base Support Stiffness (kNm/rad)
			Sand					
934	75	15.0	Silty Dense Sand	36,000	1.5	1.0	0.4	198
935	75	17.5	Silty Dense Sand	36,000	1.5	1.0	0.5	387
936	75	20.0	Silty Dense Sand	36,000	1.5	1.0	0.6	669
937	75	22.5	Silty Dense Sand	36,000	1.5	1.0	0.7	1,063
938	75	25.0	Silty Dense Sand	36,000	1.5	1.0	0.7	1,063
939	75	27.5	Silty Dense Sand	36,000	1.5	1.0	0.8	1,586
940	75	30.0	Silty Dense Sand	36,000	1.5	1.0	0.8	1,586
941	75	32.5	Silty Dense Sand	36,000	1.5	1.0	0.9	2,259
942	75	35.0	Silty Dense Sand	36,000	1.5	1.0	1.0	3,098
943	75	37.5	Silty Dense Sand	36,000	1.5	1.0	1.0	3,098
944	75	40.0	Silty Dense Sand	36,000	1.5	1.0	1.1	4,124
945	100	2.5	Silty Dense Sand	36,000	1.5	1.0	0.5	387
946	100	5.0	Silty Dense Sand	36,000	1.5	1.0	0.5	387
947	100	7.5	Silty Dense Sand	36,000	1.5	1.0	0.5	387
948	100	10.0	Silty Dense Sand	36,000	1.5	1.0	0.5	387
949	100	12.5	Silty Dense Sand	36,000	1.5	1.0	0.5	387
950	100	15.0	Silty Dense Sand	36,000	1.5	1.0	0.5	387
951	100	17.5	Silty Dense Sand	36,000	1.5	1.0	0.5	387
952	100	20.0	Silty Dense Sand	36,000	1.5	1.0	0.5	387
953	100	22.5	Silty Dense Sand	36,000	1.5	1.0	0.6	669
954	100	25.0	Silty Dense Sand	36,000	1.5	1.0	0.7	1,063
955	100	27.5	Silty Dense Sand	36,000	1.5	1.0	0.7	1,063
956	100	30.0	Silty Dense Sand	36,000	1.5	1.0	0.8	1,586
957	100	32.5	Silty Dense Sand	36,000	1.5	1.0	0.8	1,586
958	100	35.0	Silty Dense Sand	36,000	1.5	1.0	0.9	2,259

ID	Applied Axial Load (kN)	Applied Moment (kNm)	Soil Type	Modulus of Subgrade (kN/m ³)	Foundation Height (m)	Foundation Length (m)	Foundation Width (m)	Rotational Base Support Stiffness (kNm/rad)
			Sand					
959	100	37.5	Silty Dense Sand	36,000	1.5	1.0	0.9	2,259
960	100	40.0	Silty Dense Sand	36,000	1.5	1.0	1.0	3,098
961	125	2.5	Silty Dense Sand	36,000	1.5	1.0	0.6	669
962	125	5.0	Silty Dense Sand	36,000	1.5	1.0	0.6	669
963	125	7.5	Silty Dense Sand	36,000	1.5	1.0	0.6	669
964	125	10.0	Silty Dense Sand	36,000	1.5	1.0	0.6	669
965	125	12.5	Silty Dense Sand	36,000	1.5	1.0	0.6	669
966	125	15.0	Silty Dense Sand	36,000	1.5	1.0	0.6	669
967	125	17.5	Silty Dense Sand	36,000	1.5	1.0	0.6	669
968	125	20.0	Silty Dense Sand	36,000	1.5	1.0	0.6	669
969	125	22.5	Silty Dense Sand	36,000	1.5	1.0	0.6	669
970	125	25.0	Silty Dense Sand	36,000	1.5	1.0	0.6	669
971	125	27.5	Silty Dense Sand	36,000	1.5	1.0	0.7	1,063
972	125	30.0	Silty Dense Sand	36,000	1.5	1.0	0.7	1,063
973	125	32.5	Silty Dense Sand	36,000	1.5	1.0	0.8	1,586
974	125	35.0	Silty Dense Sand	36,000	1.5	1.0	0.8	1,586
975	125	37.5	Silty Dense Sand	36,000	1.5	1.0	0.9	2,259
976	125	40.0	Silty Dense Sand	36,000	1.5	1.0	0.9	2,259
977	150	2.5	Silty Dense Sand	36,000	1.5	1.0	0.8	1,586
978	150	5.0	Silty Dense Sand	36,000	1.5	1.0	0.8	1,586
979	150	7.5	Silty Dense Sand	36,000	1.5	1.0	0.8	1,586
980	150	10.0	Silty Dense Sand	36,000	1.5	1.0	0.8	1,586
981	150	12.5	Silty Dense Sand	36,000	1.5	1.0	0.8	1,586
982	150	15.0	Silty Dense Sand	36,000	1.5	1.0	0.8	1,586
983	150	17.5	Silty Dense	36,000	1.5	1.0	0.8	1,586

ID	Applied Axial Load (kN)	Applied Moment (kNm)	Soil Type	Modulus of Subgrade (kN/m ³)	Foundation Height (m)	Foundation Length (m)	Foundation Width (m)	Rotational Base Support Stiffness (kNm/rad)
			Sand					
984	150	20.0	Silty Dense Sand	36,000	1.5	1.0	0.8	1,586
985	150	22.5	Silty Dense Sand	36,000	1.5	1.0	0.8	1,586
986	150	25.0	Silty Dense Sand	36,000	1.5	1.0	0.8	1,586
987	150	27.5	Silty Dense Sand	36,000	1.5	1.0	0.8	1,586
988	150	30.0	Silty Dense Sand	36,000	1.5	1.0	0.8	1,586
989	150	32.5	Silty Dense Sand	36,000	1.5	1.0	0.8	1,586
990	150	35.0	Silty Dense Sand	36,000	1.5	1.0	0.8	1,586
991	150	37.5	Silty Dense Sand	36,000	1.5	1.0	0.8	1,586
992	150	40.0	Silty Dense Sand	36,000	1.5	1.0	0.8	1,586
993	175	2.5	Silty Dense Sand	36,000	1.5	1.0	0.9	2,259
994	175	5.0	Silty Dense Sand	36,000	1.5	1.0	0.9	2,259
995	175	7.5	Silty Dense Sand	36,000	1.5	1.0	0.9	2,259
996	175	10.0	Silty Dense Sand	36,000	1.5	1.0	0.9	2,259
997	175	12.5	Silty Dense Sand	36,000	1.5	1.0	0.9	2,259
998	175	15.0	Silty Dense Sand	36,000	1.5	1.0	0.9	2,259
999	175	17.5	Silty Dense Sand	36,000	1.5	1.0	0.9	2,259
1000	175	20.0	Silty Dense Sand	36,000	1.5	1.0	0.9	2,259
1001	175	22.5	Silty Dense Sand	36,000	1.5	1.0	0.9	2,259
1002	175	25.0	Silty Dense Sand	36,000	1.5	1.0	0.9	2,259
1003	175	27.5	Silty Dense Sand	36,000	1.5	1.0	0.9	2,259
1004	175	30.0	Silty Dense Sand	36,000	1.5	1.0	0.9	2,259
1005	175	32.5	Silty Dense Sand	36,000	1.5	1.0	0.9	2,259
1006	175	35.0	Silty Dense Sand	36,000	1.5	1.0	0.9	2,259
1007	175	37.5	Silty Dense Sand	36,000	1.5	1.0	0.9	2,259
1008	175	40.0	Silty Dense Sand	36,000	1.5	1.0	0.9	2,259

ID	Applied Axial Load (kN)	Applied Moment (kNm)	Soil Type	Modulus of Subgrade (kN/m ³)	Foundation Height (m)	Foundation Length (m)	Foundation Width (m)	Rotational Base Support Stiffness (kNm/rad)
1009	200	2.5	Sand Silty Dense Sand	36,000	1.5	1.0	1.0	3,098
1010	200	5.0	Silty Dense Sand	36,000	1.5	1.0	1.0	3,098
1011	200	7.5	Silty Dense Sand	36,000	1.5	1.0	1.0	3,098
1012	200	10.0	Silty Dense Sand	36,000	1.5	1.0	1.0	3,098
1013	200	12.5	Silty Dense Sand	36,000	1.5	1.0	1.0	3,098
1014	200	15.0	Silty Dense Sand	36,000	1.5	1.0	1.0	3,098
1015	200	17.5	Silty Dense Sand	36,000	1.5	1.0	1.0	3,098
1016	200	20.0	Silty Dense Sand	36,000	1.5	1.0	1.0	3,098
1017	200	22.5	Silty Dense Sand	36,000	1.5	1.0	1.0	3,098
1018	200	25.0	Silty Dense Sand	36,000	1.5	1.0	1.0	3,098
1019	200	27.5	Silty Dense Sand	36,000	1.5	1.0	1.0	3,098
1020	200	30.0	Silty Dense Sand	36,000	1.5	1.0	1.0	3,098
1021	200	32.5	Silty Dense Sand	36,000	1.5	1.0	1.0	3,098
1022	200	35.0	Silty Dense Sand	36,000	1.5	1.0	1.0	3,098
1023	200	37.5	Silty Dense Sand	36,000	1.5	1.0	1.0	3,098
1024	200	40.0	Silty Dense Sand	36,000	1.5	1.0	1.0	3,098
1025	225	2.5	Silty Dense Sand	36,000	1.5	1.0	1.1	4,124
1026	225	5.0	Silty Dense Sand	36,000	1.5	1.0	1.1	4,124
1027	225	7.5	Silty Dense Sand	36,000	1.5	1.0	1.1	4,124
1028	225	10.0	Silty Dense Sand	36,000	1.5	1.0	1.1	4,124
1029	225	12.5	Silty Dense Sand	36,000	1.5	1.0	1.1	4,124
1030	225	15.0	Silty Dense Sand	36,000	1.5	1.0	1.1	4,124
1031	225	17.5	Silty Dense Sand	36,000	1.5	1.0	1.1	4,124
1032	225	20.0	Silty Dense Sand	36,000	1.5	1.0	1.1	4,124
1033	225	22.5	Silty Dense Sand	36,000	1.5	1.0	1.1	4,124

ID	Applied Axial Load (kN)	Applied Moment (kNm)	Soil Type	Modulus of Subgrade (kN/m ³)	Foundation Height (m)	Foundation Length (m)	Foundation Width (m)	Rotational Base Support Stiffness (kNm/rad)
1034	225	25.0	Sand Silty Dense Sand	36,000	1.5	1.0	1.1	4,124
1035	225	27.5	Silty Dense Sand	36,000	1.5	1.0	1.1	4,124
1036	225	30.0	Silty Dense Sand	36,000	1.5	1.0	1.1	4,124
1037	225	32.5	Silty Dense Sand	36,000	1.5	1.0	1.1	4,124
1038	225	35.0	Silty Dense Sand	36,000	1.5	1.0	1.1	4,124
1039	225	37.5	Silty Dense Sand	36,000	1.5	1.0	1.1	4,124
1040	225	40.0	Silty Dense Sand	36,000	1.5	1.0	1.1	4,124
1041	250	2.5	Silty Dense Sand	36,000	1.5	1.0	1.2	5,354
1042	250	5.0	Silty Dense Sand	36,000	1.5	1.0	1.2	5,354
1043	250	7.5	Silty Dense Sand	36,000	1.5	1.0	1.2	5,354
1044	250	10.0	Silty Dense Sand	36,000	1.5	1.0	1.2	5,354
1045	250	12.5	Silty Dense Sand	36,000	1.5	1.0	1.2	5,354
1046	250	15.0	Silty Dense Sand	36,000	1.5	1.0	1.2	5,354
1047	250	17.5	Silty Dense Sand	36,000	1.5	1.0	1.2	5,354
1048	250	20.0	Silty Dense Sand	36,000	1.5	1.0	1.2	5,354
1049	250	22.5	Silty Dense Sand	36,000	1.5	1.0	1.2	5,354
1050	250	25.0	Silty Dense Sand	36,000	1.5	1.0	1.2	5,354
1051	250	27.5	Silty Dense Sand	36,000	1.5	1.0	1.2	5,354
1052	250	30.0	Silty Dense Sand	36,000	1.5	1.0	1.2	5,354
1053	250	32.5	Silty Dense Sand	36,000	1.5	1.0	1.2	5,354
1054	250	35.0	Silty Dense Sand	36,000	1.5	1.0	1.2	5,354
1055	250	37.5	Silty Dense Sand	36,000	1.5	1.0	1.2	5,354
1056	250	40.0	Silty Dense Sand	36,000	1.5	1.0	1.2	5,354
1057	275	2.5	Silty Dense Sand	36,000	1.5	1.0	1.4	8,502
1058	275	5.0	Silty Dense Sand	36,000	1.5	1.0	1.4	8,502

ID	Applied Axial Load (kN)	Applied Moment (kNm)	Soil Type	Modulus of Subgrade (kN/m ³)	Foundation Height (m)	Foundation Length (m)	Foundation Width (m)	Rotational Base Support Stiffness (kNm/rad)
			Sand					
1059	275	7.5	Silty Dense Sand	36,000	1.5	1.0	1.4	8,502
1060	275	10.0	Silty Dense Sand	36,000	1.5	1.0	1.4	8,502
1061	275	12.5	Silty Dense Sand	36,000	1.5	1.0	1.4	8,502
1062	275	15.0	Silty Dense Sand	36,000	1.5	1.0	1.4	8,502
1063	275	17.5	Silty Dense Sand	36,000	1.5	1.0	1.4	8,502
1064	275	20.0	Silty Dense Sand	36,000	1.5	1.0	1.4	8,502
1065	275	22.5	Silty Dense Sand	36,000	1.5	1.0	1.4	8,502
1066	275	25.0	Silty Dense Sand	36,000	1.5	1.0	1.4	8,502
1067	275	27.5	Silty Dense Sand	36,000	1.5	1.0	1.4	8,502
1068	275	30.0	Silty Dense Sand	36,000	1.5	1.0	1.4	8,502
1069	275	32.5	Silty Dense Sand	36,000	1.5	1.0	1.4	8,502
1070	275	35.0	Silty Dense Sand	36,000	1.5	1.0	1.4	8,502
1071	275	37.5	Silty Dense Sand	36,000	1.5	1.0	1.4	8,502
1072	275	40.0	Silty Dense Sand	36,000	1.5	1.0	1.4	8,502
1073	300	2.5	Silty Dense Sand	36,000	1.5	1.0	1.5	10,457
1074	300	5.0	Silty Dense Sand	36,000	1.5	1.0	1.5	10,457
1075	300	7.5	Silty Dense Sand	36,000	1.5	1.0	1.5	10,457
1076	300	10.0	Silty Dense Sand	36,000	1.5	1.0	1.5	10,457
1077	300	12.5	Silty Dense Sand	36,000	1.5	1.0	1.5	10,457
1078	300	15.0	Silty Dense Sand	36,000	1.5	1.0	1.5	10,457
1079	300	17.5	Silty Dense Sand	36,000	1.5	1.0	1.5	10,457
1080	300	20.0	Silty Dense Sand	36,000	1.5	1.0	1.5	10,457
1081	300	22.5	Silty Dense Sand	36,000	1.5	1.0	1.5	10,457
1082	300	25.0	Silty Dense Sand	36,000	1.5	1.0	1.5	10,457
1083	300	27.5	Silty Dense Sand	36,000	1.5	1.0	1.5	10,457

ID	Applied Axial Load (kN)	Applied Moment (kNm)	Soil Type	Modulus of Subgrade (kN/m ³)	Foundation Height (m)	Foundation Length (m)	Foundation Width (m)	Rotational Base Support Stiffness (kNm/rad)
1084	300	30.0	Sand Silty Dense Sand	36,000	1.5	1.0	1.5	10,457
1085	300	32.5	Silty Dense Sand	36,000	1.5	1.0	1.5	10,457
1086	300	35.0	Silty Dense Sand	36,000	1.5	1.0	1.5	10,457
1087	300	37.5	Silty Dense Sand	36,000	1.5	1.0	1.5	10,457
1088	300	40.0	Silty Dense Sand	36,000	1.5	1.0	1.5	10,457
1089	325	2.5	Silty Dense Sand	36,000	1.5	1.0	1.6	12,690
1090	325	5.0	Silty Dense Sand	36,000	1.5	1.0	1.6	12,690
1091	325	7.5	Silty Dense Sand	36,000	1.5	1.0	1.6	12,690
1092	325	10.0	Silty Dense Sand	36,000	1.5	1.0	1.6	12,690
1093	325	12.5	Silty Dense Sand	36,000	1.5	1.0	1.6	12,690
1094	325	15.0	Silty Dense Sand	36,000	1.5	1.0	1.6	12,690
1095	325	17.5	Silty Dense Sand	36,000	1.5	1.0	1.6	12,690
1096	325	20.0	Silty Dense Sand	36,000	1.5	1.0	1.6	12,690
1097	325	22.5	Silty Dense Sand	36,000	1.5	1.0	1.6	12,690
1098	325	25.0	Silty Dense Sand	36,000	1.5	1.0	1.6	12,690
1099	325	27.5	Silty Dense Sand	36,000	1.5	1.0	1.6	12,690
1100	325	30.0	Silty Dense Sand	36,000	1.5	1.0	1.6	12,690
1101	325	32.5	Silty Dense Sand	36,000	1.5	1.0	1.6	12,690
1102	325	35.0	Silty Dense Sand	36,000	1.5	1.0	1.6	12,690
1103	325	37.5	Silty Dense Sand	36,000	1.5	1.0	1.6	12,690
1104	325	40.0	Silty Dense Sand	36,000	1.5	1.0	1.6	12,690
1105	350	2.5	Silty Dense Sand	36,000	1.5	1.0	1.7	15,222
1106	350	5.0	Silty Dense Sand	36,000	1.5	1.0	1.7	15,222
1107	350	7.5	Silty Dense Sand	36,000	1.5	1.0	1.7	15,222
1108	350	10.0	Silty Dense Sand	36,000	1.5	1.0	1.7	15,222

ID	Applied Axial Load (kN)	Applied Moment (kNm)	Soil Type	Modulus of Subgrade (kN/m ³)	Foundation Height (m)	Foundation Length (m)	Foundation Width (m)	Rotational Base Support Stiffness (kNm/rad)
1109	350	12.5	Silty Dense Sand	36,000	1.5	1.0	1.7	15,222
1110	350	15.0	Silty Dense Sand	36,000	1.5	1.0	1.7	15,222
1111	350	17.5	Silty Dense Sand	36,000	1.5	1.0	1.7	15,222
1112	350	20.0	Silty Dense Sand	36,000	1.5	1.0	1.7	15,222
1113	350	22.5	Silty Dense Sand	36,000	1.5	1.0	1.7	15,222
1114	350	25.0	Silty Dense Sand	36,000	1.5	1.0	1.7	15,222
1115	350	27.5	Silty Dense Sand	36,000	1.5	1.0	1.7	15,222
1116	350	30.0	Silty Dense Sand	36,000	1.5	1.0	1.7	15,222
1117	350	32.5	Silty Dense Sand	36,000	1.5	1.0	1.7	15,222
1118	350	35.0	Silty Dense Sand	36,000	1.5	1.0	1.7	15,222
1119	350	37.5	Silty Dense Sand	36,000	1.5	1.0	1.7	15,222
1120	350	40.0	Silty Dense Sand	36,000	1.5	1.0	1.7	15,222
1121	25	2.5	Clay Soil	30,000	1.5	1.0	0.2	21
1122	25	5.0	Clay Soil	30,000	1.5	1.0	0.2	21
1123	25	7.5	Clay Soil	30,000	1.5	1.0	0.3	70
1124	25	10.0	Clay Soil	30,000	1.5	1.0	0.4	165
1125	25	12.5	Clay Soil	30,000	1.5	1.0	0.5	323
1126	25	15.0	Clay Soil	30,000	1.5	1.0	0.6	558
1127	25	17.5	Clay Soil	30,000	1.5	1.0	0.7	886
1128	25	20.0	Clay Soil	30,000	1.5	1.0	0.7	886
1129	25	22.5	Clay Soil	30,000	1.5	1.0	0.8	1,322
1130	25	25.0	Clay Soil	30,000	1.5	1.0	0.9	1,882
1131	25	27.5	Clay Soil	30,000	1.5	1.0	1.0	2,582
1132	25	30.0	Clay Soil	30,000	1.5	1.0	1.1	3,436
1133	25	32.5	Clay Soil	30,000	1.5	1.0	1.2	4,461
1134	25	35.0	Clay Soil	30,000	1.5	1.0	1.3	5,672
1135	25	37.5	Clay Soil	30,000	1.5	1.0	1.3	5,672
1136	25	40.0	Clay Soil	30,000	1.5	1.0	1.4	7,085
1137	50	2.5	Clay Soil	30,000	1.5	1.0	0.3	70
1138	50	5.0	Clay Soil	30,000	1.5	1.0	0.3	70
1139	50	7.5	Clay Soil	30,000	1.5	1.0	0.3	70
1140	50	10.0	Clay Soil	30,000	1.5	1.0	0.4	165
1141	50	12.5	Clay Soil	30,000	1.5	1.0	0.4	165
1142	50	15.0	Clay Soil	30,000	1.5	1.0	0.5	323
1143	50	17.5	Clay Soil	30,000	1.5	1.0	0.6	558
1144	50	20.0	Clay Soil	30,000	1.5	1.0	0.7	886
1145	50	22.5	Clay Soil	30,000	1.5	1.0	0.7	886

ID	Applied Axial Load (kN)	Applied Moment (kNm)	Soil Type	Modulus of Subgrade (kN/m ³)	Foundation Height (m)	Foundation Length (m)	Foundation Width (m)	Rotational Base Support Stiffness (kNm/rad)
1146	50	25.0	Clay Soil	30,000	1.5	1.0	0.8	1,322
1147	50	27.5	Clay Soil	30,000	1.5	1.0	0.9	1,882
1148	50	30.0	Clay Soil	30,000	1.5	1.0	0.9	1,882
1149	50	32.5	Clay Soil	30,000	1.5	1.0	1.0	2,582
1150	50	35.0	Clay Soil	30,000	1.5	1.0	1.1	3,436
1151	50	37.5	Clay Soil	30,000	1.5	1.0	1.2	4,461
1152	50	40.0	Clay Soil	30,000	1.5	1.0	1.3	5,672
1153	75	2.5	Clay Soil	30,000	1.5	1.0	0.4	165
1154	75	5.0	Clay Soil	30,000	1.5	1.0	0.4	165
1155	75	7.5	Clay Soil	30,000	1.5	1.0	0.4	165
1156	75	10.0	Clay Soil	30,000	1.5	1.0	0.4	165
1157	75	12.5	Clay Soil	30,000	1.5	1.0	0.4	165
1158	75	15.0	Clay Soil	30,000	1.5	1.0	0.4	165
1159	75	17.5	Clay Soil	30,000	1.5	1.0	0.5	323
1160	75	20.0	Clay Soil	30,000	1.5	1.0	0.6	558
1161	75	22.5	Clay Soil	30,000	1.5	1.0	0.7	886
1162	75	25.0	Clay Soil	30,000	1.5	1.0	0.7	886
1163	75	27.5	Clay Soil	30,000	1.5	1.0	0.8	1,322
1164	75	30.0	Clay Soil	30,000	1.5	1.0	0.8	1,322
1165	75	32.5	Clay Soil	30,000	1.5	1.0	0.9	1,882
1166	75	35.0	Clay Soil	30,000	1.5	1.0	1.0	2,582
1167	75	37.5	Clay Soil	30,000	1.5	1.0	1.0	2,582
1168	75	40.0	Clay Soil	30,000	1.5	1.0	1.1	3,436
1169	100	2.5	Clay Soil	30,000	1.5	1.0	0.5	323
1170	100	5.0	Clay Soil	30,000	1.5	1.0	0.5	323
1171	100	7.5	Clay Soil	30,000	1.5	1.0	0.5	323
1172	100	10.0	Clay Soil	30,000	1.5	1.0	0.5	323
1173	100	12.5	Clay Soil	30,000	1.5	1.0	0.5	323
1174	100	15.0	Clay Soil	30,000	1.5	1.0	0.5	323
1175	100	17.5	Clay Soil	30,000	1.5	1.0	0.5	323
1176	100	20.0	Clay Soil	30,000	1.5	1.0	0.5	323
1177	100	22.5	Clay Soil	30,000	1.5	1.0	0.6	558
1178	100	25.0	Clay Soil	30,000	1.5	1.0	0.7	886
1179	100	27.5	Clay Soil	30,000	1.5	1.0	0.7	886
1180	100	30.0	Clay Soil	30,000	1.5	1.0	0.8	1,322
1181	100	32.5	Clay Soil	30,000	1.5	1.0	0.8	1,322
1182	100	35.0	Clay Soil	30,000	1.5	1.0	0.9	1,882
1183	100	37.5	Clay Soil	30,000	1.5	1.0	0.9	1,882
1184	100	40.0	Clay Soil	30,000	1.5	1.0	1.0	2,582
1185	125	2.5	Clay Soil	30,000	1.5	1.0	0.6	558
1186	125	5.0	Clay Soil	30,000	1.5	1.0	0.6	558
1187	125	7.5	Clay Soil	30,000	1.5	1.0	0.6	558
1188	125	10.0	Clay Soil	30,000	1.5	1.0	0.6	558
1189	125	12.5	Clay Soil	30,000	1.5	1.0	0.6	558
1190	125	15.0	Clay Soil	30,000	1.5	1.0	0.6	558
1191	125	17.5	Clay Soil	30,000	1.5	1.0	0.6	558
1192	125	20.0	Clay Soil	30,000	1.5	1.0	0.6	558
1193	125	22.5	Clay Soil	30,000	1.5	1.0	0.6	558
1194	125	25.0	Clay Soil	30,000	1.5	1.0	0.6	558
1195	125	27.5	Clay Soil	30,000	1.5	1.0	0.7	886

ID	Applied Axial Load (kN)	Applied Moment (kNm)	Soil Type	Modulus of Subgrade (kN/m ³)	Foundation Height (m)	Foundation Length (m)	Foundation Width (m)	Rotational Base Support Stiffness (kNm/rad)
1196	125	30.0	Clay Soil	30,000	1.5	1.0	0.7	886
1197	125	32.5	Clay Soil	30,000	1.5	1.0	0.8	1,322
1198	125	35.0	Clay Soil	30,000	1.5	1.0	0.8	1,322
1199	125	37.5	Clay Soil	30,000	1.5	1.0	0.9	1,882
1200	125	40.0	Clay Soil	30,000	1.5	1.0	0.9	1,882
1201	150	2.5	Clay Soil	30,000	1.5	1.0	0.8	1,322
1202	150	5.0	Clay Soil	30,000	1.5	1.0	0.8	1,322
1203	150	7.5	Clay Soil	30,000	1.5	1.0	0.8	1,322
1204	150	10.0	Clay Soil	30,000	1.5	1.0	0.8	1,322
1205	150	12.5	Clay Soil	30,000	1.5	1.0	0.8	1,322
1206	150	15.0	Clay Soil	30,000	1.5	1.0	0.8	1,322
1207	150	17.5	Clay Soil	30,000	1.5	1.0	0.8	1,322
1208	150	20.0	Clay Soil	30,000	1.5	1.0	0.8	1,322
1209	150	22.5	Clay Soil	30,000	1.5	1.0	0.8	1,322
1210	150	25.0	Clay Soil	30,000	1.5	1.0	0.8	1,322
1211	150	27.5	Clay Soil	30,000	1.5	1.0	0.8	1,322
1212	150	30.0	Clay Soil	30,000	1.5	1.0	0.8	1,322
1213	150	32.5	Clay Soil	30,000	1.5	1.0	0.8	1,322
1214	150	35.0	Clay Soil	30,000	1.5	1.0	0.8	1,322
1215	150	37.5	Clay Soil	30,000	1.5	1.0	0.8	1,322
1216	150	40.0	Clay Soil	30,000	1.5	1.0	0.8	1,322
1217	175	2.5	Clay Soil	30,000	1.5	1.0	0.9	1,882
1218	175	5.0	Clay Soil	30,000	1.5	1.0	0.9	1,882
1219	175	7.5	Clay Soil	30,000	1.5	1.0	0.9	1,882
1220	175	10.0	Clay Soil	30,000	1.5	1.0	0.9	1,882
1221	175	12.5	Clay Soil	30,000	1.5	1.0	0.9	1,882
1222	175	15.0	Clay Soil	30,000	1.5	1.0	0.9	1,882
1223	175	17.5	Clay Soil	30,000	1.5	1.0	0.9	1,882
1224	175	20.0	Clay Soil	30,000	1.5	1.0	0.9	1,882
1225	175	22.5	Clay Soil	30,000	1.5	1.0	0.9	1,882
1226	175	25.0	Clay Soil	30,000	1.5	1.0	0.9	1,882
1227	175	27.5	Clay Soil	30,000	1.5	1.0	0.9	1,882
1228	175	30.0	Clay Soil	30,000	1.5	1.0	0.9	1,882
1229	175	32.5	Clay Soil	30,000	1.5	1.0	0.9	1,882
1230	175	35.0	Clay Soil	30,000	1.5	1.0	0.9	1,882
1231	175	37.5	Clay Soil	30,000	1.5	1.0	0.9	1,882
1232	175	40.0	Clay Soil	30,000	1.5	1.0	0.9	1,882
1233	200	2.5	Clay Soil	30,000	1.5	1.0	1.0	2,582
1234	200	5.0	Clay Soil	30,000	1.5	1.0	1.0	2,582
1235	200	7.5	Clay Soil	30,000	1.5	1.0	1.0	2,582
1236	200	10.0	Clay Soil	30,000	1.5	1.0	1.0	2,582
1237	200	12.5	Clay Soil	30,000	1.5	1.0	1.0	2,582
1238	200	15.0	Clay Soil	30,000	1.5	1.0	1.0	2,582
1239	200	17.5	Clay Soil	30,000	1.5	1.0	1.0	2,582
1240	200	20.0	Clay Soil	30,000	1.5	1.0	1.0	2,582
1241	200	22.5	Clay Soil	30,000	1.5	1.0	1.0	2,582
1242	200	25.0	Clay Soil	30,000	1.5	1.0	1.0	2,582
1243	200	27.5	Clay Soil	30,000	1.5	1.0	1.0	2,582
1244	200	30.0	Clay Soil	30,000	1.5	1.0	1.0	2,582
1245	200	32.5	Clay Soil	30,000	1.5	1.0	1.0	2,582

ID	Applied Axial Load (kN)	Applied Moment (kNm)	Soil Type	Modulus of Subgrade (kN/m ³)	Foundation Height (m)	Foundation Length (m)	Foundation Width (m)	Rotational Base Support Stiffness (kNm/rad)
1246	200	35.0	Clay Soil	30,000	1.5	1.0	1.0	2,582
1247	200	37.5	Clay Soil	30,000	1.5	1.0	1.0	2,582
1248	200	40.0	Clay Soil	30,000	1.5	1.0	1.0	2,582
1249	225	2.5	Clay Soil	30,000	1.5	1.0	1.1	3,436
1250	225	5.0	Clay Soil	30,000	1.5	1.0	1.1	3,436
1251	225	7.5	Clay Soil	30,000	1.5	1.0	1.1	3,436
1252	225	10.0	Clay Soil	30,000	1.5	1.0	1.1	3,436
1253	225	12.5	Clay Soil	30,000	1.5	1.0	1.1	3,436
1254	225	15.0	Clay Soil	30,000	1.5	1.0	1.1	3,436
1255	225	17.5	Clay Soil	30,000	1.5	1.0	1.1	3,436
1256	225	20.0	Clay Soil	30,000	1.5	1.0	1.1	3,436
1257	225	22.5	Clay Soil	30,000	1.5	1.0	1.1	3,436
1258	225	25.0	Clay Soil	30,000	1.5	1.0	1.1	3,436
1259	225	27.5	Clay Soil	30,000	1.5	1.0	1.1	3,436
1260	225	30.0	Clay Soil	30,000	1.5	1.0	1.1	3,436
1261	225	32.5	Clay Soil	30,000	1.5	1.0	1.1	3,436
1262	225	35.0	Clay Soil	30,000	1.5	1.0	1.1	3,436
1263	225	37.5	Clay Soil	30,000	1.5	1.0	1.1	3,436
1264	225	40.0	Clay Soil	30,000	1.5	1.0	1.1	3,436
1265	250	2.5	Clay Soil	30,000	1.5	1.0	1.2	4,461
1266	250	5.0	Clay Soil	30,000	1.5	1.0	1.2	4,461
1267	250	7.5	Clay Soil	30,000	1.5	1.0	1.2	4,461
1268	250	10.0	Clay Soil	30,000	1.5	1.0	1.2	4,461
1269	250	12.5	Clay Soil	30,000	1.5	1.0	1.2	4,461
1270	250	15.0	Clay Soil	30,000	1.5	1.0	1.2	4,461
1271	250	17.5	Clay Soil	30,000	1.5	1.0	1.2	4,461
1272	250	20.0	Clay Soil	30,000	1.5	1.0	1.2	4,461
1273	250	22.5	Clay Soil	30,000	1.5	1.0	1.2	4,461
1274	250	25.0	Clay Soil	30,000	1.5	1.0	1.2	4,461
1275	250	27.5	Clay Soil	30,000	1.5	1.0	1.2	4,461
1276	250	30.0	Clay Soil	30,000	1.5	1.0	1.2	4,461
1277	250	32.5	Clay Soil	30,000	1.5	1.0	1.2	4,461
1278	250	35.0	Clay Soil	30,000	1.5	1.0	1.2	4,461
1279	250	37.5	Clay Soil	30,000	1.5	1.0	1.2	4,461
1280	250	40.0	Clay Soil	30,000	1.5	1.0	1.2	4,461
1281	275	2.5	Clay Soil	30,000	1.5	1.0	1.4	7,085
1282	275	5.0	Clay Soil	30,000	1.5	1.0	1.4	7,085
1283	275	7.5	Clay Soil	30,000	1.5	1.0	1.4	7,085
1284	275	10.0	Clay Soil	30,000	1.5	1.0	1.4	7,085
1285	275	12.5	Clay Soil	30,000	1.5	1.0	1.4	7,085
1286	275	15.0	Clay Soil	30,000	1.5	1.0	1.4	7,085
1287	275	17.5	Clay Soil	30,000	1.5	1.0	1.4	7,085
1288	275	20.0	Clay Soil	30,000	1.5	1.0	1.4	7,085
1289	275	22.5	Clay Soil	30,000	1.5	1.0	1.4	7,085
1290	275	25.0	Clay Soil	30,000	1.5	1.0	1.4	7,085
1291	275	27.5	Clay Soil	30,000	1.5	1.0	1.4	7,085
1292	275	30.0	Clay Soil	30,000	1.5	1.0	1.4	7,085
1293	275	32.5	Clay Soil	30,000	1.5	1.0	1.4	7,085
1294	275	35.0	Clay Soil	30,000	1.5	1.0	1.4	7,085
1295	275	37.5	Clay Soil	30,000	1.5	1.0	1.4	7,085

ID	Applied Axial Load (kN)	Applied Moment (kNm)	Soil Type	Modulus of Subgrade (kN/m ³)	Foundation Height (m)	Foundation Length (m)	Foundation Width (m)	Rotational Base Support Stiffness (kNm/rad)
1296	275	40.0	Clay Soil	30,000	1.5	1.0	1.4	7,085
1297	300	2.5	Clay Soil	30,000	1.5	1.0	1.5	8,714
1298	300	5.0	Clay Soil	30,000	1.5	1.0	1.5	8,714
1299	300	7.5	Clay Soil	30,000	1.5	1.0	1.5	8,714
1300	300	10.0	Clay Soil	30,000	1.5	1.0	1.5	8,714
1301	300	12.5	Clay Soil	30,000	1.5	1.0	1.5	8,714
1302	300	15.0	Clay Soil	30,000	1.5	1.0	1.5	8,714
1303	300	17.5	Clay Soil	30,000	1.5	1.0	1.5	8,714
1304	300	20.0	Clay Soil	30,000	1.5	1.0	1.5	8,714
1305	300	22.5	Clay Soil	30,000	1.5	1.0	1.5	8,714
1306	300	25.0	Clay Soil	30,000	1.5	1.0	1.5	8,714
1307	300	27.5	Clay Soil	30,000	1.5	1.0	1.5	8,714
1308	300	30.0	Clay Soil	30,000	1.5	1.0	1.5	8,714
1309	300	32.5	Clay Soil	30,000	1.5	1.0	1.5	8,714
1310	300	35.0	Clay Soil	30,000	1.5	1.0	1.5	8,714
1311	300	37.5	Clay Soil	30,000	1.5	1.0	1.5	8,714
1312	300	40.0	Clay Soil	30,000	1.5	1.0	1.5	8,714
1313	325	2.5	Clay Soil	30,000	1.5	1.0	1.6	10,575
1314	325	5.0	Clay Soil	30,000	1.5	1.0	1.6	10,575
1315	325	7.5	Clay Soil	30,000	1.5	1.0	1.6	10,575
1316	325	10.0	Clay Soil	30,000	1.5	1.0	1.6	10,575
1317	325	12.5	Clay Soil	30,000	1.5	1.0	1.6	10,575
1318	325	15.0	Clay Soil	30,000	1.5	1.0	1.6	10,575
1319	325	17.5	Clay Soil	30,000	1.5	1.0	1.6	10,575
1320	325	20.0	Clay Soil	30,000	1.5	1.0	1.6	10,575
1321	325	22.5	Clay Soil	30,000	1.5	1.0	1.6	10,575
1322	325	25.0	Clay Soil	30,000	1.5	1.0	1.6	10,575
1323	325	27.5	Clay Soil	30,000	1.5	1.0	1.6	10,575
1324	325	30.0	Clay Soil	30,000	1.5	1.0	1.6	10,575
1325	325	32.5	Clay Soil	30,000	1.5	1.0	1.6	10,575
1326	325	35.0	Clay Soil	30,000	1.5	1.0	1.6	10,575
1327	325	37.5	Clay Soil	30,000	1.5	1.0	1.6	10,575
1328	325	40.0	Clay Soil	30,000	1.5	1.0	1.6	10,575
1329	350	2.5	Clay Soil	30,000	1.5	1.0	1.7	12,685
1330	350	5.0	Clay Soil	30,000	1.5	1.0	1.7	12,685
1331	350	7.5	Clay Soil	30,000	1.5	1.0	1.7	12,685
1332	350	10.0	Clay Soil	30,000	1.5	1.0	1.7	12,685
1333	350	12.5	Clay Soil	30,000	1.5	1.0	1.7	12,685
1334	350	15.0	Clay Soil	30,000	1.5	1.0	1.7	12,685
1335	350	17.5	Clay Soil	30,000	1.5	1.0	1.7	12,685
1336	350	20.0	Clay Soil	30,000	1.5	1.0	1.7	12,685
1337	350	22.5	Clay Soil	30,000	1.5	1.0	1.7	12,685
1338	350	25.0	Clay Soil	30,000	1.5	1.0	1.7	12,685
1339	350	27.5	Clay Soil	30,000	1.5	1.0	1.7	12,685
1340	350	30.0	Clay Soil	30,000	1.5	1.0	1.7	12,685
1341	350	32.5	Clay Soil	30,000	1.5	1.0	1.7	12,685
1342	350	35.0	Clay Soil	30,000	1.5	1.0	1.7	12,685
1343	350	37.5	Clay Soil	30,000	1.5	1.0	1.7	12,685
1344	350	40.0	Clay Soil	30,000	1.5	1.0	1.7	12,685

APPENDIX B: MECHANICS-BASED MODEL MATLAB CODE

Below is the MATLAB script for the analysis model described in Chapter 4. The model contains 6 analysis features: moment–curvature analysis, interaction diagrams, slenderness interaction diagram, wall behaviour from an increasing eccentric axial load, wall behaviour from an increasing distributed load, and wall behaviour from an increasing point load located at the midspan (3-point bend).

```
% ANALYSIS MODEL FOR LAOD-BEARING MASONRY WALLS BY CLAYTON PETTIT
clear;clc;

%% MASONRY PARAMETERS %

% THICKNESS OF THE WALL (mm)
TotalThickness = 0;
% TOTAL LENGTH OF THE WALL (mm)
TotalWallLength = 0;
% GROUTED LENGTH OF THE WALL (mm)
GroutedLength = 0;
% HEIGHT OF THE WALL (mm)
WallHeight = 0;
% FACE SHELL THICKNESS (mm)
FaceShell = 0;

% COMPRESSIVE STRENGTH OF THE MASONRY (MPa)
GroutedMasonryStrength = 0;
% STRAIN AT WHICH THE MASONRY REACHES ITS MAXIMUM VALUE OF STRENGTH
PeakStrainGrouted = -0.002;

% COMPRESSIVE STRENGTH OF THE MASONRY (MPa)
UngoutedMasonryStrength = 0;
% STRAIN AT WHICH THE MASONRY REACHES ITS MAXIMUM VALUE OF STRENGTH
PeakStrainUngouted = -0.002;

% ELASTIC MODULUS OF THE MASONRY (MPa)
MasonryModulusGrouted = 0;
MasonryModulusUngouted = 0;

% STRAIN AT WHICH THE MASONRY WILL CRUSH (FAILURE)
MasonryFailureStrain = -0.0030;
% MASONRY RUPTURE STRESS (MPa)
MasonryStrengthTension = 0;
% WEIGHT OF THE MASONRY (kg/m^3)
MasonryDeadLoad = (0*9.81)*(1/(1000^3));
```

```

%% REINFORCEMENT MATERIAL PARAMETERS %

% TOTAL NUMBER OF REBAR
NumberOfRebar = 0;

% YIELD STRENGTH (MPa)
SteelStrength = 0;
% YOUNDS MODULUS OF ELASTICITY (MPa)
SteelModulus = 0;
% STRAIN AT PEAK STRENGTH
StrainHardeningStrain = 0;
% STRAIN HARDENING MODULUS (MPa)
StrainHardeningModulus = 0;
% STRAIN AT WHICH STEEL RUPTURES
SteelRuptureStrain = 0;

% AREA OF THE STEEL REBAR USED (mm^2)
AreaOfSteel{1} = 0;
AreaOfSteel{2} = 0;
AreaOfSteel{3} = 0;
AreaOfSteel{4} = 0;
AreaOfSteel{5} = 0;
% DISTANCE FROM THE EDGE OF THE WALL TO THE CENTER OF THE STEEL (mm)
SteelDistance{1} = 0;
SteelDistance{2} = 0;
SteelDistance{3} = 0;
SteelDistance{4} = 0;
SteelDistance{5} = 0;

%% ANALYSIS TYPE %

% ANALYSIS TYPE 1 = MOMENT CURVATURE ANALYSIS
% ANALYSIS TYPE 2 = INTERACTION DIAGRAM
% ANALYSIS TYPE 3 = SLENDERNESS INTERACTION DIAGRAM
% ANALYSIS TYPE 4 = ECCENTRIC AXIAL LOAD*
% ANALYSIS TYPE 5 = ECCENTRIC AXIAL LOAD + DISTRIBUTED LATERAL LOAD*
% ANALYSIS TYPE 6 = ECCENTRIC AXIAL LOAD + 3 POINT BEND*
% * = THE PARAMETER THAT INCREASES
AnalysisType = 1;

% AXIAL LOAD (N) (FOR ANALYSIS TYPES 1,2,4,5)
AxialLoad = 0*1000;

% ECCENTRICITY OF THE AXIAL LOAD ON THE WALL (mm)
Eccentricity = 0;

% SECOND-ORDER EFFECTS ( 1 = YES , 2 = NO)
SecondOrderEffects = 1;

% SUPPORT STIFFNESS ( 1 = YES (FOUNDATION) , 2 = YES (SPECIFIED) , 3 =
NO)
SupportStiffness = 3;
SpecifiedSupportStiffness = 0;

```

```

% TOP BOUNDARY CONDITION TOLERANCE
Tolerance = 0.1;

% METHOD TO CALCULATE EI (1 = DIFFERENTIAL EQUATION, 2 - CURVATURE)
EI_Method = 2;

% LOAD INCREMENT (N FOR AXIAL , kN/m FOR LATERAL)
AxialLoadFactor = 25*1000;
AxialLoadFactor2 = 1*1000;
LateralLoadFactor = 0.1;
PointLateralLoadFactor = 0.1*1000;

% SLNEDERNESS RATIO (ANALYSIS TYPE 3)
SlendernessRatio = 30;

% SEASC WALL? ( 1 = YES , 2 = NO)
SEASC = 2;

% DEBUGGING
Debugging = 0;
TestSlope = -0.008;

%% ELEMENT DEFINITION %

% NUMBER OF FIBER SECTIONS DESIRED FOR THE MOMENT-CURVATURE ANALYSIS
NumberOfSlices = 500;
% NUMBER OF STRAINS TO BE ANALYZED DURING THE MOMENT-CURVATURE
ANALYSIS
NumberOfStrains = 500;
% NUMBER OF ELEMENTS TO BE ANALYZED OVER THE HEIGHT OF THE WALL
NumberOfElements = 101;

%% FOUNDATION PROPERTIES %
FoundationHeight = 1.2;
FoundationWidth = 0.7;      % 0.6      0.9      1.0
FoundationThickness = 1.0;

ModulusOfSubgrade = 108000;  % 56000      76000      108000

%% SAFETY FACTORS %

% MASONRY
PhiM = 1;
% STEEL REINFORCEMENT
PhiS = 1;

fprintf('Parameters Sucessfully Defined! \n')
fprintf('\n')

%% FOUNDATION STIFFNESS (IF APPLICABLE) %
if SupportStiffness == 1

% NUMBER OF SPRINGS
if ModulusOfSubgrade <= 60000;

```

```

        NumberOfSprings = 9;
else
        NumberOfSprings = 7;
end

% PRELIMINARY CALCULATIONS
EffectiveWidth = FoundationWidth/(NumberOfSprings-1);
InteriorSpring = ModulusOfSubgrade*EffectiveWidth*FoundationThickness;
ExteriorSpring =
ModulusOfSubgrade*(EffectiveWidth/2)*FoundationThickness;
AnalysisSprings = (NumberOfSprings-1)/2;
RotationalStiffness = 0;
Spring = 1;

% CALCULATE FORCES IN EACH INTERIOR SPRING
for i = 1:(AnalysisSprings-1)

        EffectiveDistance(Spring) = (Spring)*EffectiveWidth;
        VerticalDeformation(Spring) = sin(1)*EffectiveDistance(Spring);
        HorizontalDeformation(Spring) = cos(1)*EffectiveDistance(Spring);

        VerticalSpringForce(Spring) =
InteriorSpring*VerticalDeformation(Spring);
        HorizontalSpringForce(Spring) =
InteriorSpring*HorizontalDeformation(Spring);

        SpringMoment(Spring) =
VerticalSpringForce(Spring)*HorizontalDeformation(Spring) +
HorizontalSpringForce(Spring)*VerticalDeformation(Spring);

        RotationalStiffness = RotationalStiffness + SpringMoment(Spring);

        Spring = Spring + 1;
end

% CALCULATE FORCES IN THE EXTERIOR SPRING
EndEffectiveDistance = FoundationWidth/2;
EndVerticalDeformation = sin(1)*EndEffectiveDistance;
EndHorizontalDeformation = cos(1)*EndEffectiveDistance;

EndVerticalSpringForce = ExteriorSpring*EndVerticalDeformation;
EndHorizontalSpringForce = ExteriorSpring*EndVerticalDeformation;

EndSpringMoment = EndVerticalSpringForce*EndHorizontalDeformation +
EndHorizontalSpringForce*EndVerticalDeformation;
RotationalStiffness = RotationalStiffness + EndSpringMoment;

RotationalStiffness = 2*RotationalStiffness;

% PRINT THE VALUE OF SUPPORT STIFFNESS PROVIDED
fprintf('The Rotational Stiffness of the Foundation is %0.0f
kNm/radian. \n',RotationalStiffness)
fprintf('\n')
fprintf('Support Stiffness Successfully Defined \n')

```

```

fprintf('\n')
end

%% ANALYSIS TYPE 1 - MOMENT CURVATURE ANALYSIS

if AnalysisType == 1
fprintf('Analysis Started! \n')
fprintf('\n')

% PRELIMINARY CALCULATIONS
StrainIncrement = abs(MasonryFailureStrain)/NumberOfStrains;
ThicknessIncrement = TotalThickness/NumberOfSlices;
YieldStrain = SteelStrength/SteelModulus;
StrainHardeningIntercept = SteelStrength -
(StrainHardeningModulus*StrainHardeningStrain);
UngroudedZ =
0.5/(((3+0.29*UngroudedMasonryStrength)/(145*UngroudedMasonryStrength-
1000))-0.002);
GroudedZ =
0.5/(((3+0.29*GroudedMasonryStrength)/(145*GroudedMasonryStrength-
1000))-0.002);
UltimateStrainGrouded = MasonryFailureStrain-0.001;
UltimateStrainUngrouded = MasonryFailureStrain-0.001;
UngroudedLength = TotalWallLength - GroudedLength;

MasonryTensionStrainUngrouded1 =
MasonryStrengthTension/MasonryModulusUngrouded;
MasonryTensionStrainGrouded1 =
MasonryStrengthTension/MasonryModulusGrouded;
MasonryTensionStrainUngrouded2 = 4*MasonryTensionStrainUngrouded1;
MasonryTensionStrainGrouded2 = 4*MasonryTensionStrainGrouded1;
MasonryTensionStrainUngrouded3 = 10*MasonryTensionStrainUngrouded1;
MasonryTensionStrainGrouded3 = 10*MasonryTensionStrainGrouded1;
TensionSlope1 = (-0.35*MasonryStrengthTension)/3;
TensionSlope2 = (-0.45*MasonryStrengthTension)/6;
TensionIntercept1 = (0.8*MasonryStrengthTension)-(TensionSlope1);
TensionIntercept2 = (0.45*MasonryStrengthTension)-(TensionSlope2*4);

% NO DEAD LOAD
if MasonryDeadLoad == 0

Strain = 0;
NeutralAxis = TotalThickness/2;

for j = 1:(NumberOfStrains+1)

    DeviationChange = 100;
    ErrorChange = 100;

for k = 1:10000000

    GroudedSlice = (ThicknessIncrement/2);
    TotalGroudedForce = 0;
    TotalGroudedMoment = 0;

```

```

for f = 1:NumberOfSlices

    SliceStrain = Strain*((GroutedSlice-NeutralAxis)/NeutralAxis);

    if PeakStrainGrouted <= SliceStrain && SliceStrain <= 0
        SliceStressGrouted = (-
1)*GroutedMasonryStrength*((2*abs(SliceStrain)/0.002)-
((abs(SliceStrain))/0.002)^2));
        elseif UltimateStrainGrouted <= SliceStrain && SliceStrain <
PeakStrainGrouted
            SliceStressGrouted = (-1)*GroutedMasonryStrength*(1-
GroutedZ*(abs(SliceStrain)-abs(PeakStrainGrouted)));
            elseif 0 < SliceStrain && SliceStrain <=
MasonryTensionStrainGrouted1
                SliceStressGrouted = SliceStrain*MasonryModulusGrouted ;
                elseif MasonryTensionStrainGrouted1 < SliceStrain && SliceStrain
<= MasonryTensionStrainGrouted2
                    SliceStressGrouted = TensionSlope1*SliceStrain +
TensionIntercept1;
                    elseif MasonryTensionStrainGrouted2 < SliceStrain && SliceStrain
<= MasonryTensionStrainGrouted3
                        SliceStressGrouted = TensionSlope2*SliceStrain +
TensionIntercept2;
                        else
                            SliceStressGrouted = 0;
                        end

                    SliceForceGrouted =
PhiM*SliceStressGrouted*ThicknessIncrement*GroutedLength;
                    SliceMomentGrouted = GroutedSlice*SliceForceGrouted;

                    TotalGroutedForce = TotalGroutedForce + SliceForceGrouted;
                    TotalGroutedMoment = TotalGroutedMoment + SliceMomentGrouted;

                    GroutedSlice = GroutedSlice + ThicknessIncrement;

end

UngrountedSlice = (ThicknessIncrement/2);
TotalUngrountedForce = 0;
TotalUngrountedMoment = 0;

if UngrountedLength ~= 0
for f = 1:NumberOfSlices

    SliceStrain = Strain*((UngrountedSlice-NeutralAxis)/NeutralAxis);

    if PeakStrainUngrounted <= SliceStrain && SliceStrain <= 0
        SliceStressUngrounted = (-
1)*UngrountedMasonryStrength*((2*abs(SliceStrain)/0.002)-
((abs(SliceStrain))/0.002)^2));
        elseif UltimateStrainUngrounted <= SliceStrain && SliceStrain <
PeakStrainUngrounted
            SliceStressUngrounted = (-1)*UngrountedMasonryStrength*(1-
UngrountedZ*(abs(SliceStrain)-abs(PeakStrainUngrounted)));

```

```

    elseif 0 < SliceStrain && SliceStrain <=
MasonryTensionStrainUngroued1
        SliceStressUngroued = SliceStrain*MasonryModulusGroued ;
        elseif MasonryTensionStrainGroued1 < SliceStrain && SliceStrain
<= MasonryTensionStrainUngroued2
            SliceStressUngroued = TensionSlope1*SliceStrain +
TensionIntercept1;
        elseif MasonryTensionStrainGroued2 < SliceStrain && SliceStrain
<= MasonryTensionStrainUngroued3
            SliceStressUngroued = TensionSlope2*SliceStrain +
TensionIntercept2;
        else
            SliceStressUngroued = 0;
        end

    if UngrouedSlice <= FaceShell
        SliceForceUngroued =
PhiM*SliceStressUngroued*ThicknessIncrement*UngrouedLength;
        elseif UngrouedSlice > FaceShell && UngrouedSlice <
(TotalThickness-FaceShell)
            SliceForceUngroued = 0;
        elseif UngrouedSlice >= (TotalThickness-FaceShell)
            SliceForceUngroued =
PhiM*SliceStressUngroued*ThicknessIncrement*UngrouedLength;
        end

    SliceMomentUngroued = UngrouedSlice*SliceForceUngroued;

    TotalUngrouedForce = TotalUngrouedForce + SliceForceUngroued;
    TotalUngrouedMoment = TotalUngrouedMoment +
SliceMomentUngroued;

    UngrouedSlice = UngrouedSlice + ThicknessIncrement;

end
end

TotalForceSteel = 0;
TotalMomentSteel = 0;

for s = 1:NumberOfRebar
    SteelStrain{s} = Strain*((SteelDistance{s}-
NeutralAxis)/NeutralAxis);

    if SteelStrain{s} < YieldStrain && SteelStrain{s} >= 0
        SteelForce{s} =
PhiS*AreaOfSteel{s}*SteelModulus*SteelStrain{s};
        elseif SteelStrain{s} >= YieldStrain && SteelStrain{s} <
StrainHardeningStrain
            SteelForce{s} = PhiS*AreaOfSteel{s}*SteelStrength;
        elseif SteelStrain{s} >= StrainHardeningStrain && SteelStrain{s} <
SteelRuptureStrain
            SteelForce{s} = PhiS*(StrainHardeningModulus*SteelStrain{s} +
StrainHardeningIntercept)*AreaOfSteel{s};

```

```

        elseif SteelStrain{s} > (-1)*YieldStrain && SteelStrain{s} < 0
            SteelForce{s} =
PhiS*AreaOfSteel{s}*SteelModulus*SteelStrain{s};
            elseif SteelStrain{s} <= (-1)*YieldStrain && SteelStrain{s} > (-
1)*StrainHardeningStrain
                SteelForce{s} = (-1)*PhiS*AreaOfSteel{s}*SteelStrength;
            elseif SteelStrain{s} <= (-1)*StrainHardeningStrain &&
SteelStrain{s} > (-1)*SteelRuptureStrain
                SteelForce{s} = (-
1)*PhiS*((StrainHardeningModulus*abs(SteelStrain{s})) +
StrainHardeningIntercept))*AreaOfSteel{s};
            else
                SteelForce{s} = 0;
            end

        SteelMoment{s} = SteelForce{s}*SteelDistance{s};

        TotalForceSteel = TotalForceSteel + SteelForce{s};
        TotalMomentSteel = TotalMomentSteel + SteelMoment{s};

end

Deviation(k) = TotalForceSteel + TotalGroutedForce +
TotalUngoutedForce + AxialLoad;

CompleteMoment = TotalMomentSteel + TotalUngoutedMoment +
TotalGroutedMoment + AxialLoad*(TotalThickness/2);
CompleteCurvature = Strain/NeutralAxis;

if Deviation(k) > 0.1
    NeutralAxis = NeutralAxis + DeviationChange;
elseif Deviation(k) < -0.1
    NeutralAxis = NeutralAxis - DeviationChange;
elseif Deviation(k) <= 0.1 && Deviation(k) >= -0.1
    break
end

if k >= 4 && Deviation(k-3) > 0.00001 && Deviation(k-2) < -0.00001 &&
Deviation(k-1) > 0.00001 && Deviation(k) < -0.00001
    DeviationChange = 0.1*DeviationChange;
end

if NeutralAxis <= 0;
    DeviationChange = ErrorChange;
    NeutralAxis = 150.0;
    ErrorChange = 0.1*ErrorChange;
end

if NeutralAxis > 9999 || (k > 5 && Deviation(k) == Deviation(k-1) &&
Deviation(k-1) == Deviation(k-2))
    NeutralAxis = (TotalThickness/2);
    CompleteMoment = 0;
    CompleteCurvature = 0;
    break
end

```



```

end

    Moment(j) = CompleteMoment;
    Curvature(j) = CompleteCurvature;
    CorrectNeutralAxis(j) = NeutralAxis;

    Strain = Strain + StrainIncrement;

end

MaxMoment = max(Moment/1000000);
MaxCurvature = max(Curvature);
CurvatureCut = [];
for d = 2:NumberOfStrains
    if Moment(d) < Moment(d-1)
        CurvatureCut(d) = d;
    end
end
StartD = (min(CurvatureCut(CurvatureCut>0)))-1;
MaxElasticMoment = Moment((min(CurvatureCut(CurvatureCut>0)))-1);
for d = 2:length(CurvatureCut)
    if CurvatureCut(d) > 0
        Moment(d) = 0;
        Curvature(d) = 0;
    end
end
for d = StartD:NumberOfStrains
    if Moment(d) < MaxElasticMoment
        Moment(d) = 0;
        Curvature(d) = 0;
    end
end
LastValue = length(Moment);
Moment(LastValue) = 0;
Curvature(LastValue) = 0;
Moment = Moment(Moment ~= 0);
Curvature = Curvature(Curvature ~= 0);

fprintf('The Moment Capacity of the Section is %0.2f kNm.
\n',MaxMoment)
fprintf('\n')

plot(Curvature, (Moment/1000000))
title('Moment Curvature Diagram')
xlabel('Curvature (1/mm)')
ylabel('Moment (kNm)')

for e = 1:(NumberOfElements+1)
    ElementMoment{e} = Moment;

```

```

    ElementCurvature{e} = Curvature;
end

end

% DEAD LOAD
if MasonryDeadLoad ~= 0

HeightIncrement = WallHeight/NumberOfElements;
NetArea = (GroutedLength*TotalThickness) + ((TotalWallLength-
GroutedLength)*FaceShell*2);
GrossArea = TotalThickness*TotalWallLength;
GroutingFactor = NetArea/GrossArea;
SelfWeight(1) =
MasonryDeadLoad*(TotalWallLength*WallHeight*TotalThickness)*GroutingFa
ctor;
TotalSelfWeight =
MasonryDeadLoad*(TotalWallLength*WallHeight*TotalThickness)*GroutingFa
ctor;

for w = 2:(NumberOfElements+1)
    SelfWeight(w) =
MasonryDeadLoad*(TotalWallLength*TotalThickness*(WallHeight - (w-
1)*HeightIncrement))*GroutingFactor;
end

for e = 1:(NumberOfElements+1)

Strain = 0;
NeutralAxis = TotalThickness/2;

for j = 1:(NumberOfStrains+1)

    DeviationChange = 100;
    ErrorChange = 100;

for k = 1:10000000

    GroutedSlice = (ThicknessIncrement/2);
    TotalGroutedForce = 0;
    TotalGroutedMoment = 0;

for f = 1:NumberOfSlices

    SliceStrain = Strain*((GroutedSlice-NeutralAxis)/NeutralAxis);

    if PeakStrainGrouted <= SliceStrain && SliceStrain <= 0
        SliceStressGrouted = (-
1)*GroutedMasonryStrength*((2*abs(SliceStrain)/0.002)-
((abs(SliceStrain))/0.002)^2));
    elseif UltimateStrainGrouted <= SliceStrain && SliceStrain <
PeakStrainGrouted
        SliceStressGrouted = (-1)*GroutedMasonryStrength*(1-
GroutedZ*(abs(SliceStrain)-abs(PeakStrainGrouted)));

```

```

        elseif 0 < SliceStrain && SliceStrain <=
MasonryTensionStrainGrouted1
            SliceStressGrouted = SliceStrain*MasonryModulusGrouted ;
            elseif MasonryTensionStrainGrouted1 < SliceStrain && SliceStrain
<= MasonryTensionStrainGrouted2
                SliceStressGrouted = TensionSlope1*SliceStrain +
TensionIntercept1;
            elseif MasonryTensionStrainGrouted2 < SliceStrain && SliceStrain
<= MasonryTensionStrainGrouted3
                SliceStressGrouted = TensionSlope2*SliceStrain +
TensionIntercept2;
            else
                SliceStressGrouted = 0;
            end

        SliceForceGrouted =
PhiM*SliceStressGrouted*ThicknessIncrement*GroutedLength;
        SliceMomentGrouted = GroutedSlice*SliceForceGrouted;

        TotalGroutedForce = TotalGroutedForce + SliceForceGrouted;
        TotalGroutedMoment = TotalGroutedMoment + SliceMomentGrouted;

        GroutedSlice = GroutedSlice + ThicknessIncrement;

end

        UngROUTEDSlice = (ThicknessIncrement/2);
        TotalUngROUTEDForce = 0;
        TotalUngROUTEDMoment = 0;

        if UngROUTEDLength ~= 0
for f = 1:NumberOfSlices

            SliceStrain = Strain*((UngROUTEDSlice-NeutralAxis)/NeutralAxis);

            if PeakStrainUngROUTED <= SliceStrain && SliceStrain <= 0
                SliceStressUngROUTED = (-
1)*UngROUTEDMasonryStrength*((2*abs(SliceStrain)/0.002) -
((abs(SliceStrain))/0.002)^2));
            elseif UltimateStrainUngROUTED <= SliceStrain && SliceStrain <
PeakStrainUngROUTED
                SliceStressUngROUTED = (-1)*UngROUTEDMasonryStrength*(1-
UngROUTEDZ*(abs(SliceStrain)-abs(PeakStrainUngROUTED)));
            elseif 0 < SliceStrain && SliceStrain <=
MasonryTensionStrainUngROUTED1
                SliceStressUngROUTED = SliceStrain*MasonryModulusGrouted ;
            elseif MasonryTensionStrainGrouted1 < SliceStrain && SliceStrain
<= MasonryTensionStrainUngROUTED2
                SliceStressUngROUTED = TensionSlope1*SliceStrain +
TensionIntercept1;
            elseif MasonryTensionStrainGrouted2 < SliceStrain && SliceStrain
<= MasonryTensionStrainUngROUTED3
                SliceStressUngROUTED = TensionSlope2*SliceStrain +
TensionIntercept2;
            else

```

```

        SliceStressUngrouped = 0;
    end

    if UngroupedSlice <= FaceShell
        SliceForceUngrouped =
PhiM*SliceStressUngrouped*ThicknessIncrement*UngroupedLength;
        elseif UngroupedSlice > FaceShell && UngroupedSlice <
(TotalThickness-FaceShell)
            SliceForceUngrouped = 0;
        elseif UngroupedSlice >= (TotalThickness-FaceShell)
            SliceForceUngrouped =
PhiM*SliceStressUngrouped*ThicknessIncrement*UngroupedLength;
        end

        SliceMomentUngrouped = UngroupedSlice*SliceForceUngrouped;

        TotalUngroupedForce = TotalUngroupedForce + SliceForceUngrouped;
        TotalUngroupedMoment = TotalUngroupedMoment +
SliceMomentUngrouped;

        UngroupedSlice = UngroupedSlice + ThicknessIncrement;
end
end

TotalForceSteel = 0;
TotalMomentSteel = 0;

for s = 1:NumberOfRebar
    SteelStrain{s} = Strain*((SteelDistance{s}-
NeutralAxis)/NeutralAxis);

    if SteelStrain{s} < YieldStrain && SteelStrain{s} >= 0
        SteelForce{s} =
PhiS*AreaOfSteel{s}*SteelModulus*SteelStrain{s};
    elseif SteelStrain{s} >= YieldStrain && SteelStrain{s} <
StrainHardeningStrain
        SteelForce{s} = PhiS*AreaOfSteel{s}*SteelStrength;
    elseif SteelStrain{s} >= StrainHardeningStrain && SteelStrain{s} <
SteelRuptureStrain
        SteelForce{s} = PhiS*(StrainHardeningModulus*SteelStrain{s} +
StrainHardeningIntercept)*AreaOfSteel{s};

        elseif SteelStrain{s} > (-1)*YieldStrain && SteelStrain{s} < 0
            SteelForce{s} =
PhiS*AreaOfSteel{s}*SteelModulus*SteelStrain{s};
        elseif SteelStrain{s} <= (-1)*YieldStrain && SteelStrain{s} > (-
1)*StrainHardeningStrain
            SteelForce{s} = (-1)*PhiS*AreaOfSteel{s}*SteelStrength;
        elseif SteelStrain{s} <= (-1)*StrainHardeningStrain &&
SteelStrain{s} > (-1)*SteelRuptureStrain
            SteelForce{s} = (-
1)*PhiS*((StrainHardeningModulus*abs(SteelStrain{s})) +
StrainHardeningIntercept))*AreaOfSteel{s};
        else

```

```

        SteelForce{s} = 0;
    end

    SteelMoment{s} = SteelForce{s}*SteelDistance{s};

    TotalForceSteel = TotalForceSteel + SteelForce{s};
    TotalMomentSteel = TotalMomentSteel + SteelMoment{s};

end

Deviation(k) = TotalForceSteel + TotalGroutedForce +
TotalUngoutedForce + AxialLoad + SelfWeight(e);

CompleteMoment = TotalMomentSteel + TotalUngoutedMoment +
TotalGroutedMoment + (AxialLoad+SelfWeight(e))*(TotalThickness/2);
CompleteCurvature = Strain/NeutralAxis;

if Deviation(k) > 0.1
    NeutralAxis = NeutralAxis + DeviationChange;
elseif Deviation(k) < -0.1
    NeutralAxis = NeutralAxis - DeviationChange;
elseif Deviation(k) <= 0.1 && Deviation(k) >= -0.1
    break
end

if k >= 4 && Deviation(k-3) > 0.00001 && Deviation(k-2) < -0.00001 &&
Deviation(k-1) > 0.00001 && Deviation(k) < -0.00001
    DeviationChange = 0.1*DeviationChange;
end

if NeutralAxis <= 0;
    DeviationChange = ErrorChange;
    NeutralAxis = 150.0;
    ErrorChange = 0.1*ErrorChange;
end

if NeutralAxis > 9999 || (k > 5 && Deviation(k) == Deviation(k-1) &&
Deviation(k-1) == Deviation(k-2))
    NeutralAxis = (TotalThickness/2);
    CompleteMoment = 0;
    CompleteCurvature = 0;
    break
end

end

end

Moment{e}(j) = CompleteMoment;
Curvature{e}(j) = CompleteCurvature;
CorrectNeutralAxis{e}(j) = NeutralAxis;

Strain = Strain + StrainIncrement;

end

for d = 2:NumberOfStrains

```

```

        if Moment{e}(d) < Moment{e}(d-1)
            CurvatureCut(d) = d;
        end
    end
end
StartD = (min(CurvatureCut(CurvatureCut>0)))-1;
MaxElasticMoment = Moment{e}((min(CurvatureCut(CurvatureCut>0)))-1);
for d = 2:length(CurvatureCut)
    if CurvatureCut(d) > 0
        Moment{e}(d) = 0;
        Curvature{e}(d) = 0;
    end
end
for d = StartD:length(CurvatureCut)
    if Moment{e}(d) < MaxElasticMoment
        Moment{e}(d) = 0;
        Curvature{e}(d) = 0;
    end
end
LastValue = length(Moment{e});
Moment{e}(LastValue) = 0;
Curvature{e}(LastValue) = 0;
Moment{e} = Moment{e}(Moment{e} ~= 0);
Curvature{e} = Curvature{e}(Curvature{e} ~= 0);

ElementMoment{e} = Moment{e};
ElementCurvature{e} = Curvature{e};

MaxMoment{e} = max(Moment{e}/1000000);
MaxCurvature{e} = max(Curvature{e});

fprintf('The Moment Capacity of the Section at Station %d is %0.2f
kNm. \n',e,MaxMoment{e})
fprintf('\n')

end

end

plot(ElementCurvature{1},(ElementMoment{1}/1000000))
title('Moment Curvature Diagram')
xlabel('Curvature (1/mm)')
ylabel('Moment (kNm)')

fprintf('Moment-Curvature Analysis Complete \n')
fprintf('\n')

end

%% ANALYSIS TYPE 2 - INTERACTION DIAGRAM

if AnalysisType == 2

fprintf('Analysis Started! \n')
fprintf('\n')

```

```

% MAX AXIAL LOAD
TotalRebarArea = 0;
UngrouedArea = 2*(TotalWallLength-GrouedLength)*FaceShell;
GrouedArea = GrouedLength*TotalThickness;
for s = 1:NumberOfRebar
    TotalRebarArea = TotalRebarArea + AreaOfSteel{s};
end
MaxAxialLoad =
((GrouedMasonryStrength*GrouedArea)+(UngrouedMasonryStrength*UngrouedArea)+(TotalRebarArea*SteelStrength))/1000;
fprintf('Max Axial Load (kN): %4.0f \n',MaxAxialLoad)
fprintf('\n')

fprintf('      Axial Load (kN)      |      Moment (kNm)      \n')
fprintf('      | \n')

% PRELIMINARY CALCULATIONS
StrainIncrement = abs(MasonryFailureStrain)/NumberOfStrains;
ThicknessIncrement = TotalThickness/NumberOfSlices;
YieldStrain = SteelStrength/SteelModulus;
StrainHardeningIntercept = SteelStrength -
(StrainHardeningModulus*StrainHardeningStrain);
UngrouedZ =
0.5/((3+0.29*UngrouedMasonryStrength)/(145*UngrouedMasonryStrength-1000))-0.002);
GrouedZ =
0.5/((3+0.29*GrouedMasonryStrength)/(145*GrouedMasonryStrength-1000))-0.002);
UltimateStrainGroued = MasonryFailureStrain-0.001;
UltimateStrainUngroued = MasonryFailureStrain-0.001;
UngrouedLength = TotalWallLength - GrouedLength;
SelfWeightAxialLoad =
(MasonryDeadLoad*WallHeight*TotalWallLength*TotalThickness)/2;

MasonryTensionStrainUngroued1 =
MasonryStrengthTension/MasonryModulusUngroued;
MasonryTensionStrainGroued1 =
MasonryStrengthTension/MasonryModulusGroued;
MasonryTensionStrainUngroued2 = 4*MasonryTensionStrainUngroued1;
MasonryTensionStrainGroued2 = 4*MasonryTensionStrainGroued1;
MasonryTensionStrainUngroued3 = 10*MasonryTensionStrainUngroued1;
MasonryTensionStrainGroued3 = 10*MasonryTensionStrainGroued1;
TensionSlope1 = (-0.35*MasonryStrengthTension)/3;
TensionSlope2 = (-0.45*MasonryStrengthTension)/6;
TensionIntercept1 = (0.8*MasonryStrengthTension)-(TensionSlope1);
TensionIntercept2 = (0.45*MasonryStrengthTension)-(TensionSlope2*4);

for p = 1:10000000
    AxialLoad = (p-1)*AxialLoadFactor;

Strain = 0;
NeutralAxis = TotalThickness/2;

for j = 1:(NumberOfStrains+1)

```

```

    DeviationChange = 100;
    ErrorChange = 100;

for k = 1:10000000

    GroutedSlice = (ThicknessIncrement/2);
    TotalGroutedForce = 0;
    TotalGroutedMoment = 0;

for f = 1:NumberOfSlices

    SliceStrain = Strain*((GroutedSlice-NeutralAxis)/NeutralAxis);

    if PeakStrainGrouted <= SliceStrain && SliceStrain <= 0
        SliceStressGrouted = (-
1)*GroutedMasonryStrength*((2*abs(SliceStrain)/0.002)-
((abs(SliceStrain))/0.002)^2));
        elseif UltimateStrainGrouted <= SliceStrain && SliceStrain <
PeakStrainGrouted
            SliceStressGrouted = (-1)*GroutedMasonryStrength*(1-
GroutedZ*(abs(SliceStrain)-abs(PeakStrainGrouted)));
        elseif 0 < SliceStrain && SliceStrain <=
MasonryTensionStrainGrouted1
            SliceStressGrouted = SliceStrain*MasonryModulusGrouted ;
        elseif MasonryTensionStrainGrouted1 < SliceStrain && SliceStrain
<= MasonryTensionStrainGrouted2
            SliceStressGrouted = TensionSlope1*SliceStrain +
TensionIntercept1;
        elseif MasonryTensionStrainGrouted2 < SliceStrain && SliceStrain
<= MasonryTensionStrainGrouted3
            SliceStressGrouted = TensionSlope2*SliceStrain +
TensionIntercept2;
        else
            SliceStressGrouted = 0;
        end

        SliceForceGrouted =
PhiM*SliceStressGrouted*ThicknessIncrement*GroutedLength;
        SliceMomentGrouted = GroutedSlice*SliceForceGrouted;

        TotalGroutedForce = TotalGroutedForce + SliceForceGrouted;
        TotalGroutedMoment = TotalGroutedMoment + SliceMomentGrouted;

        GroutedSlice = GroutedSlice + ThicknessIncrement;

end

    UngoutedSlice = (ThicknessIncrement/2);
    TotalUngoutedForce = 0;
    TotalUngoutedMoment = 0;

    if UngoutedLength ~= 0
for f = 1:NumberOfSlices

```



```

    SliceStrain = Strain*((UngrountedSlice-NeutralAxis)/NeutralAxis);

    if PeakStrainUngrounted <= SliceStrain && SliceStrain <= 0
        SliceStressUngrounted = (-
1)*UngrountedMasonryStrength*((2*abs(SliceStrain)/0.002)-
((abs(SliceStrain))/0.002)^2));
        elseif UltimateStrainUngrounted <= SliceStrain && SliceStrain <
PeakStrainUngrounted
            SliceStressUngrounted = (-1)*UngrountedMasonryStrength*(1-
UngrountedZ*(abs(SliceStrain)-abs(PeakStrainUngrounted)));
            elseif 0 < SliceStrain && SliceStrain <=
MasonryTensionStrainUngrounted1
                SliceStressUngrounted = SliceStrain*MasonryModulusGrounted ;
                elseif MasonryTensionStrainGrounted1 < SliceStrain && SliceStrain
<= MasonryTensionStrainUngrounted2
                    SliceStressUngrounted = TensionSlope1*SliceStrain +
TensionIntercept1;
                    elseif MasonryTensionStrainGrounted2 < SliceStrain && SliceStrain
<= MasonryTensionStrainUngrounted3
                        SliceStressUngrounted = TensionSlope2*SliceStrain +
TensionIntercept2;
                        else
                            SliceStressUngrounted = 0;
                        end

                    if UngrountedSlice <= FaceShell
                        SliceForceUngrounted =
PhiM*SliceStressUngrounted*ThicknessIncrement*UngrountedLength;
                        elseif UngrountedSlice > FaceShell && UngrountedSlice <
(TotalThickness-FaceShell)
                            SliceForceUngrounted = 0;
                            elseif UngrountedSlice >= (TotalThickness-FaceShell)
                                SliceForceUngrounted =
PhiM*SliceStressUngrounted*ThicknessIncrement*UngrountedLength;
                                end

                            SliceMomentUngrounted = UngrountedSlice*SliceForceUngrounted;

                            TotalUngrountedForce = TotalUngrountedForce + SliceForceUngrounted;
                            TotalUngrountedMoment = TotalUngrountedMoment +
SliceMomentUngrounted;

                            UngrountedSlice = UngrountedSlice + ThicknessIncrement;

end
end

TotalForceSteel = 0;
TotalMomentSteel = 0;

for s = 1:NumberOfRebar
    SteelStrain{s} = Strain*((SteelDistance{s}-
NeutralAxis)/NeutralAxis);

    if SteelStrain{s} < YieldStrain && SteelStrain{s} >= 0

```

```

        SteelForce{s} =
PhiS*AreaOfSteel{s}*SteelModulus*SteelStrain{s};
        elseif SteelStrain{s} >= YieldStrain && SteelStrain{s} <
StrainHardeningStrain
        SteelForce{s} = PhiS*AreaOfSteel{s}*SteelStrength;
        elseif SteelStrain{s} >= StrainHardeningStrain && SteelStrain{s} <
SteelRuptureStrain
        SteelForce{s} = PhiS*(StrainHardeningModulus*SteelStrain{s} +
StrainHardeningIntercept)*AreaOfSteel{s};

        elseif SteelStrain{s} > (-1)*YieldStrain && SteelStrain{s} < 0
        SteelForce{s} =
PhiS*AreaOfSteel{s}*SteelModulus*SteelStrain{s};
        elseif SteelStrain{s} <= (-1)*YieldStrain && SteelStrain{s} > (-
1)*StrainHardeningStrain
        SteelForce{s} = (-1)*PhiS*AreaOfSteel{s}*SteelStrength;
        elseif SteelStrain{s} <= (-1)*StrainHardeningStrain &&
SteelStrain{s} > (-1)*SteelRuptureStrain
        SteelForce{s} = (-
1)*PhiS*((StrainHardeningModulus*abs(SteelStrain{s})) +
StrainHardeningIntercept))*AreaOfSteel{s};
        else
        SteelForce{s} = 0;
        end

        SteelMoment{s} = SteelForce{s}*SteelDistance{s};

        TotalForceSteel = TotalForceSteel + SteelForce{s};
        TotalMomentSteel = TotalMomentSteel + SteelMoment{s};

end

Deviation(k) = TotalForceSteel + TotalGroutedForce +
TotalUngroupedForce + AxialLoad + SelfWeightAxialLoad;

CompleteMoment = TotalMomentSteel + TotalUngroupedMoment +
TotalGroutedMoment +
(AxialLoad+SelfWeightAxialLoad)*(TotalThickness/2);
CompleteCurvature = Strain/NeutralAxis;

if Deviation(k) > 0.1
        NeutralAxis = NeutralAxis + DeviationChange;
elseif Deviation(k) < -0.1
        NeutralAxis = NeutralAxis - DeviationChange;
elseif Deviation(k) <= 0.1 && Deviation(k) >= -0.1
        break
end

if k >= 4 && Deviation(k-3) > 0.00001 && Deviation(k-2) < -0.00001 &&
Deviation(k-1) > 0.00001 && Deviation(k) < -0.00001
        DeviationChange = 0.1*DeviationChange;
end

if NeutralAxis <= 0;
        DeviationChange = ErrorChange;

```

```

        NeutralAxis = 150.0;
        ErrorChange = 0.1*ErrorChange;
    end

    if NeutralAxis > 9999 || (k > 5 && Deviation(k) == Deviation(k-1) &&
Deviation(k-1) == Deviation(k-2))
        NeutralAxis = (TotalThickness/2);
        CompleteMoment = 0;
        CompleteCurvature = 0;
        break
    end
end

end

    Moment(j) = CompleteMoment;
    Curvature(j) = CompleteCurvature;
    CorrectNeutralAxis(j) = NeutralAxis;

    Strain = Strain + StrainIncrement;

end

if max(Moment) == 0
    break
end

PlotMoment(p) = max(Moment/1000000);
PlotAxialLoad(p) = (AxialLoad/1000);

fprintf('          %4.0f          | ',PlotAxialLoad(p));
fprintf('          %5.2f\n',PlotMoment(p));

end

plot(PlotMoment,PlotAxialLoad)
xlabel('Moment (kNm)')
ylabel('Axial Load (kN)')
title('Interaction Diagram')

end

%% ANALYSIS TYPE 3 - SLENDERNESS INTERACTION DIAGRAM

if AnalysisType == 3

    fprintf('Analysis Started! \n')
    fprintf('\n')
    fprintf('Slenderness Ratio: %2.0d \n', SlendernessRatio)
    fprintf('\n')

    % INITIAL MOMENT

    % PRELIMINARY CALCULATIONS
    StrainIncrement = abs(MasonryFailureStrain)/NumberOfStrains;
    ThicknessIncrement = TotalThickness/NumberOfSlices;

```

```

YieldStrain = SteelStrength/SteelModulus;
StrainHardeningIntercept = SteelStrength -
(StrainHardeningModulus*StrainHardeningStrain);
UngoutedZ =
0.5/(((3+0.29*UngoutedMasonryStrength)/(145*UngoutedMasonryStrength-
1000))-0.002);
GoutedZ =
0.5/(((3+0.29*GoutedMasonryStrength)/(145*GoutedMasonryStrength-
1000))-0.002);
UltimateStrainGouted = MasonryFailureStrain-0.001;
UltimateStrainUngouted = MasonryFailureStrain-0.001;
UngoutedLength = TotalWallLength - GoutedLength;
SelfWeightAxialLoad =
(MasonryDeadLoad*WallHeight*TotalWallLength*TotalThickness)/2;
CurvatureCut = [];

MasonryTensionStrainUngouted1 =
MasonryStrengthTension/MasonryModulusUngouted;
MasonryTensionStrainGouted1 =
MasonryStrengthTension/MasonryModulusGouted;
MasonryTensionStrainUngouted2 = 4*MasonryTensionStrainUngouted1;
MasonryTensionStrainGouted2 = 4*MasonryTensionStrainGouted1;
MasonryTensionStrainUngouted3 = 10*MasonryTensionStrainUngouted1;
MasonryTensionStrainGouted3 = 10*MasonryTensionStrainGouted1;
TensionSlope1 = (-0.35*MasonryStrengthTension)/3;
TensionSlope2 = (-0.45*MasonryStrengthTension)/6;
TensionIntercept1 = (0.8*MasonryStrengthTension)-(TensionSlope1);
TensionIntercept2 = (0.45*MasonryStrengthTension)-(TensionSlope2*4);

AxialLoad = 0;
Strain = 0;
NeutralAxis = TotalThickness/2;

for j = 1:(NumberOfStrains+1)

    DeviationChange = 100;
    ErrorChange = 100;

for k = 1:10000000

    GoutedSlice = (ThicknessIncrement/2);
    TotalGoutedForce = 0;
    TotalGoutedMoment = 0;

for f = 1:NumberOfSlices

    SliceStrain = Strain*((GoutedSlice-NeutralAxis)/NeutralAxis);

    if PeakStrainGouted <= SliceStrain && SliceStrain <= 0
        SliceStressGouted = (-
1)*GoutedMasonryStrength*((2*abs(SliceStrain)/0.002)-
((abs(SliceStrain))/0.002)^2);
    elseif UltimateStrainGouted <= SliceStrain && SliceStrain <
PeakStrainGouted

```

```

        SliceStressGrouted = (-1)*GroutedMasonryStrength*(1-
GroutedZ*(abs(SliceStrain)-abs(PeakStrainGrouted)));
        elseif 0 < SliceStrain && SliceStrain <=
MasonryTensionStrainGrouted1
            SliceStressGrouted = SliceStrain*MasonryModulusGrouted ;
            elseif MasonryTensionStrainGrouted1 < SliceStrain && SliceStrain
<= MasonryTensionStrainGrouted2
                SliceStressGrouted = TensionSlope1*SliceStrain +
TensionIntercept1;
            elseif MasonryTensionStrainGrouted2 < SliceStrain && SliceStrain
<= MasonryTensionStrainGrouted3
                SliceStressGrouted = TensionSlope2*SliceStrain +
TensionIntercept2;
            else
                SliceStressGrouted = 0;
            end

        SliceForceGrouted =
PhiM*SliceStressGrouted*ThicknessIncrement*GroutedLength;
        SliceMomentGrouted = GroutedSlice*SliceForceGrouted;

        TotalGroutedForce = TotalGroutedForce + SliceForceGrouted;
        TotalGroutedMoment = TotalGroutedMoment + SliceMomentGrouted;

        GroutedSlice = GroutedSlice + ThicknessIncrement;

end

    UngROUTEDSlice = (ThicknessIncrement/2);
    TotalUngROUTEDForce = 0;
    TotalUngROUTEDMoment = 0;

    if UngROUTEDLength ~= 0
for f = 1:NumberOfSlices

        SliceStrain = Strain*((UngROUTEDSlice-NeutralAxis)/NeutralAxis);

        if PeakStrainUngROUTED <= SliceStrain && SliceStrain <= 0
            SliceStressUngROUTED = (-
1)*UngROUTEDMasonryStrength*((2*abs(SliceStrain)/0.002)-
((abs(SliceStrain))/0.002)^2);
            elseif UltimateStrainUngROUTED <= SliceStrain && SliceStrain <
PeakStrainUngROUTED
                SliceStressUngROUTED = (-1)*UngROUTEDMasonryStrength*(1-
UngROUTEDZ*(abs(SliceStrain)-abs(PeakStrainUngROUTED)));
            elseif 0 < SliceStrain && SliceStrain <=
MasonryTensionStrainUngROUTED1
                SliceStressUngROUTED = SliceStrain*MasonryModulusGrouted ;
                elseif MasonryTensionStrainGrouted1 < SliceStrain && SliceStrain
<= MasonryTensionStrainUngROUTED2
                    SliceStressUngROUTED = TensionSlope1*SliceStrain +
TensionIntercept1;
                elseif MasonryTensionStrainGrouted2 < SliceStrain && SliceStrain
<= MasonryTensionStrainUngROUTED3

```

```

        SliceStressUngrounted = TensionSlope2*SliceStrain +
TensionIntercept2;
    else
        SliceStressUngrounted = 0;
    end

    if UngrountedSlice <= FaceShell
        SliceForceUngrounted =
PhiM*SliceStressUngrounted*ThicknessIncrement*UngrountedLength;
    elseif UngrountedSlice > FaceShell && UngrountedSlice <
(TotalThickness-FaceShell)
        SliceForceUngrounted = 0;
    elseif UngrountedSlice >= (TotalThickness-FaceShell)
        SliceForceUngrounted =
PhiM*SliceStressUngrounted*ThicknessIncrement*UngrountedLength;
    end

    SliceMomentUngrounted = UngrountedSlice*SliceForceUngrounted;

    TotalUngrountedForce = TotalUngrountedForce + SliceForceUngrounted;
    TotalUngrountedMoment = TotalUngrountedMoment +
SliceMomentUngrounted;

    UngrountedSlice = UngrountedSlice + ThicknessIncrement;

end
end

TotalForceSteel = 0;
TotalMomentSteel = 0;

for s = 1:NumberOfRebar
    SteelStrain{s} = Strain*((SteelDistance{s}-
NeutralAxis)/NeutralAxis);

    if SteelStrain{s} < YieldStrain && SteelStrain{s} >= 0
        SteelForce{s} =
PhiS*AreaOfSteel{s}*SteelModulus*SteelStrain{s};
    elseif SteelStrain{s} >= YieldStrain && SteelStrain{s} <
StrainHardeningStrain
        SteelForce{s} = PhiS*AreaOfSteel{s}*SteelStrength;
    elseif SteelStrain{s} >= StrainHardeningStrain && SteelStrain{s} <
SteelRuptureStrain
        SteelForce{s} = PhiS*(StrainHardeningModulus*SteelStrain{s} +
StrainHardeningIntercept)*AreaOfSteel{s};

    elseif SteelStrain{s} > (-1)*YieldStrain && SteelStrain{s} < 0
        SteelForce{s} =
PhiS*AreaOfSteel{s}*SteelModulus*SteelStrain{s};
    elseif SteelStrain{s} <= (-1)*YieldStrain && SteelStrain{s} > (-
1)*StrainHardeningStrain
        SteelForce{s} = (-1)*PhiS*AreaOfSteel{s}*SteelStrength;
    elseif SteelStrain{s} <= (-1)*StrainHardeningStrain &&
SteelStrain{s} > (-1)*SteelRuptureStrain

```

```

        SteelForce{s} = (-
1)*PhiS*((StrainHardeningModulus*abs(SteelStrain{s}) +
StrainHardeningIntercept))*AreaOfSteel{s};
        else
            SteelForce{s} = 0;
        end

        SteelMoment{s} = SteelForce{s}*SteelDistance{s};

        TotalForceSteel = TotalForceSteel + SteelForce{s};
        TotalMomentSteel = TotalMomentSteel + SteelMoment{s};

end

Deviation(k) = TotalForceSteel + TotalGroutedForce +
TotalUngoutedForce + AxialLoad + SelfWeightAxialLoad;

CompleteMoment = TotalMomentSteel + TotalUngoutedMoment +
TotalGroutedMoment +
(AxialLoad+SelfWeightAxialLoad)*(TotalThickness/2);
CompleteCurvature = Strain/NeutralAxis;

if Deviation(k) > 0.1
    NeutralAxis = NeutralAxis + DeviationChange;
elseif Deviation(k) < -0.1
    NeutralAxis = NeutralAxis - DeviationChange;
elseif Deviation(k) <= 0.1 && Deviation(k) >= -0.1
    break
end

if k >= 4 && Deviation(k-3) > 0.00001 && Deviation(k-2) < -0.00001 &&
Deviation(k-1) > 0.00001 && Deviation(k) < -0.00001
    DeviationChange = 0.1*DeviationChange;
end

if NeutralAxis <= 0;
    DeviationChange = ErrorChange;
    NeutralAxis = 150.0;
    ErrorChange = 0.1*ErrorChange;
end

if NeutralAxis > 9999 || (k > 5 && Deviation(k) == Deviation(k-1) &&
Deviation(k-1) == Deviation(k-2))
    NeutralAxis = (TotalThickness/2);
    CompleteMoment = 0;
    CompleteCurvature = 0;
    break
end

end

end

Moment(j) = CompleteMoment;
Curvature(j) = CompleteCurvature;
CorrectNeutralAxis(j) = NeutralAxis;

```

```

        Strain = Strain + StrainIncrement;

end

InitialMoment = max(Moment)/1000000;

% MAX AXIAL LOAD
TotalRebarArea = 0;
UngROUTEDArea = 2*(TotalWallLength-GroutedLength)*FaceShell;
GroutedArea = GroutedLength*TotalThickness;
for s = 1:NumberOfRebar
    TotalRebarArea = TotalRebarArea + AreaOfSteel{s};
end
MaxAxialLoad =
((GroutedMasonryStrength*GroutedArea)+(UngROUTEDMasonryStrength*UngROUTEDArea)+(TotalRebarArea*SteelStrength))/1000;

fprintf('        Axial Load (kN)      |        Moment (kNm) \n')
fprintf('                        | \n')
fprintf('            %3.0f            | ',0);
fprintf('            %5.2f\n',InitialMoment);

% CREATE FAIL CRITERION
Stop0 = 0;
Stop1 = 0;
Stop2 = 0;
Stop3 = 0;

% WALL HEIGHT
WallHeight = TotalThickness*SlendernessRatio;

% START INCREASING THE AXIAL LOAD
for p = 1:1000
    Stop2 = 0;
    AxialLoad = p*AxialLoadFactor;
    Eccentricity = 100;
    EccentricityFactor = 100;
    a = 0;
    Quit = 0;

% CYCLE THROUGH ECCENTRICITIES UNTIL FAILURE OCCURS
for r = 1:10000000

    if (AxialLoad/1000) > MaxAxialLoad
        Quit = 1;
        p = p - 1;
        break
    end

% CLEAR PREVIOUS VARIABLES FROM PRECEEDING AXIAL LOADS
clear Deflection
clear Slope
clear SlopeChange
clear PrimaryMoment

```



```

% MOMENT CURVATURE ANALYSIS

% PRELIMINARY CALCULATIONS
StrainIncrement = abs(MasonryFailureStrain)/NumberOfStrains;
ThicknessIncrement = TotalThickness/NumberOfSlices;
YieldStrain = SteelStrength/SteelModulus;
StrainHardeningIntercept = SteelStrength -
(StrainHardeningModulus*StrainHardeningStrain);
UngoutedZ =
0.5/(((3+0.29*UngoutedMasonryStrength)/(145*UngoutedMasonryStrength-
1000))-0.002);
GroutedZ =
0.5/(((3+0.29*GroutedMasonryStrength)/(145*GroutedMasonryStrength-
1000))-0.002);
UltimateStrainGrouted = MasonryFailureStrain-0.001;
MasonryTensionStrainGrouted =
MasonryStrengthTension/(GroutedMasonryStrength*(2/0.002));
UltimateStrainUngouted = MasonryFailureStrain-0.001;
MasonryTensionStrainUngouted =
MasonryStrengthTension/(UngoutedMasonryStrength*(2/0.002));
UngoutedLength = TotalWallLength - GroutedLength;

% NO DEAD LOAD
if MasonryDeadLoad == 0

Strain = 0;
NeutralAxis = TotalThickness/2;

for j = 1:(NumberOfStrains+1)

    DeviationChange = 100;
    ErrorChange = 100;

for k = 1:100000

    GroutedSlice = (ThicknessIncrement/2);
    TotalGroutedForce = 0;
    TotalGroutedMoment = 0;

for f = 1:NumberOfSlices

    SliceStrain = Strain*((GroutedSlice-NeutralAxis)/NeutralAxis);

    if PeakStrainGrouted <= SliceStrain && SliceStrain <= 0
        SliceStressGrouted = (-
1)*GroutedMasonryStrength*(((2*abs(SliceStrain)/0.002)-
(abs(SliceStrain))/0.002)^2));
        elseif UltimateStrainGrouted <= SliceStrain && SliceStrain <
PeakStrainGrouted
            SliceStressGrouted = (-1)*GroutedMasonryStrength*(1-
GroutedZ*(abs(SliceStrain)-abs(PeakStrainGrouted)));
        elseif 0 < SliceStrain && SliceStrain <=
MasonryTensionStrainGrouted

```

```

        SliceStressGrouted =
GroutedMasonryStrength*(2/0.002)*abs(SliceStrain);
        else
            SliceStressGrouted = 0;
        end

        SliceForceGrouted =
PhiM*SliceStressGrouted*ThicknessIncrement*GroutedLength;
        SliceMomentGrouted = GroutedSlice*SliceForceGrouted;

        TotalGroutedForce = TotalGroutedForce + SliceForceGrouted;
        TotalGroutedMoment = TotalGroutedMoment + SliceMomentGrouted;

        GroutedSlice = GroutedSlice + ThicknessIncrement;

end

        UngROUTedSlice = (ThicknessIncrement/2);
        TotalUngROUTedForce = 0;
        TotalUngROUTedMoment = 0;

        if UngROUTedLength ~= 0
for f = 1:NumberOfSlices

            SliceStrain = Strain*((UngROUTedSlice-NeutralAxis)/NeutralAxis);

            if PeakStrainUngROUTed <= SliceStrain && SliceStrain <= 0
                SliceStressUngROUTed = (-
1)*UngROUTedMasonryStrength*((2*abs(SliceStrain)/0.002)-
((abs(SliceStrain))/0.002)^2));
                elseif UltimateStrainUngROUTed <= SliceStrain && SliceStrain <
PeakStrainUngROUTed
                    SliceStressUngROUTed = (-1)*UngROUTedMasonryStrength*(1-
UngROUTedZ*(abs(SliceStrain)-abs(PeakStrainUngROUTed)));
                elseif 0 < SliceStrain && SliceStrain <=
MasonryTensionStrainUngROUTed
                    SliceStressUngROUTed =
UngROUTedMasonryStrength*(2/0.002)*abs(SliceStrain);
                else
                    SliceStressUngROUTed = 0;
                end

            if UngROUTedSlice <= FaceShell
                SliceForceUngROUTed =
PhiM*SliceStressUngROUTed*ThicknessIncrement*UngROUTedLength;
                elseif UngROUTedSlice > FaceShell && UngROUTedSlice <
(TotalThickness-FaceShell)
                    SliceForceUngROUTed = 0;
                elseif UngROUTedSlice >= (TotalThickness-FaceShell)
                    SliceForceUngROUTed =
PhiM*SliceStressUngROUTed*ThicknessIncrement*UngROUTedLength;
                end

            SliceMomentUngROUTed = UngROUTedSlice*SliceForceUngROUTed;

```

```

    TotalUngroupedForce = TotalUngroupedForce + SliceForceUngrouped;
    TotalUngroupedMoment = TotalUngroupedMoment +
SliceMomentUngrouped;

    UngroupedSlice = UngroupedSlice + ThicknessIncrement;

end
end

TotalForceSteel = 0;
TotalMomentSteel = 0;

for s = 1:NumberOfRebar
    SteelStrain{s} = Strain*((SteelDistance{s}-
NeutralAxis)/NeutralAxis);

    if SteelStrain{s} < YieldStrain && SteelStrain{s} >= 0
        SteelForce{s} =
PhiS*AreaOfSteel{s}*SteelModulus*SteelStrain{s};
    elseif SteelStrain{s} >= YieldStrain && SteelStrain{s} <
StrainHardeningStrain
        SteelForce{s} = PhiS*AreaOfSteel{s}*SteelStrength;
    elseif SteelStrain{s} >= StrainHardeningStrain && SteelStrain{s} <
SteelRuptureStrain
        SteelForce{s} = PhiS*(StrainHardeningModulus*SteelStrain{s} +
StrainHardeningIntercept)*AreaOfSteel{s};

        elseif SteelStrain{s} > (-1)*YieldStrain && SteelStrain{s} < 0
            SteelForce{s} =
PhiS*AreaOfSteel{s}*SteelModulus*SteelStrain{s};
        elseif SteelStrain{s} <= (-1)*YieldStrain && SteelStrain{s} > (-
1)*StrainHardeningStrain
            SteelForce{s} = (-1)*PhiS*AreaOfSteel{s}*SteelStrength;
        elseif SteelStrain{s} <= (-1)*StrainHardeningStrain &&
SteelStrain{s} > (-1)*SteelRuptureStrain
            SteelForce{s} = (-
1)*PhiS*((StrainHardeningModulus*abs(SteelStrain{s})) +
StrainHardeningIntercept))*AreaOfSteel{s};
        else
            SteelForce{s} = 0;
        end

        SteelMoment{s} = SteelForce{s}*SteelDistance{s};

        TotalForceSteel = TotalForceSteel + SteelForce{s};
        TotalMomentSteel = TotalMomentSteel + SteelMoment{s};

    end

Deviation(k) = TotalForceSteel + TotalGroutedForce +
TotalUngroupedForce + AxialLoad;

CompleteMoment = TotalMomentSteel + TotalUngroupedMoment +
TotalGroutedMoment + AxialLoad*(TotalThickness/2);
CompleteCurvature = Strain/NeutralAxis;

```

```

if Deviation(k) > 0.1
    NeutralAxis = NeutralAxis + DeviationChange;
elseif Deviation(k) < -0.1
    NeutralAxis = NeutralAxis - DeviationChange;
elseif Deviation(k) <= 0.1 && Deviation(k) >= -0.1
    break
end

if k >= 4 && Deviation(k-3) > 0.00001 && Deviation(k-2) < -0.00001 &&
Deviation(k-1) > 0.00001 && Deviation(k) < -0.00001
    DeviationChange = 0.1*DeviationChange;
end

if NeutralAxis <= 0;
    DeviationChange = ErrorChange;
    NeutralAxis = 150.0;
    ErrorChange = 0.1*ErrorChange;
end

if NeutralAxis > 5000 || (k > 5 && Deviation(k) == Deviation(k-1) &&
Deviation(k-1) == Deviation(k-2))
    NeutralAxis = (TotalThickness/2);
    CompleteMoment = 0;
    CompleteCurvature = 0;
    break
end

end

if CompleteMoment > 0
    Moment(j) = CompleteMoment;
    Curvature(j) = CompleteCurvature;
    CorrectNeutralAxis(j) = NeutralAxis;
else
    Moment(j) = 0;
    Curvature(j) = 0;
end

Strain = Strain + StrainIncrement;

end

for d = 2:NumberOfStrains
    if Moment(d) < Moment(d-1)
        CurvatureCut(d) = d;
    end
end

StartD = (min(CurvatureCut(CurvatureCut>0)))-1;
MaxElasticMoment = Moment((min(CurvatureCut(CurvatureCut>0)))-1);
for d = 2:length(CurvatureCut)
    if CurvatureCut(d) > 0
        Moment(d) = 0;
        Curvature(d) = 0;
    end
end

```

```

    end
end
for d = StartD:NumberOfStrains
    if Moment(d) < MaxElasticMoment
        Moment(d) = 0;
        Curvature(d) = 0;
    end
end
LastValue = length(Moment);
Moment(LastValue) = 0;
Curvature(LastValue) = 0;
Moment = Moment(Moment ~= 0);
Curvature = Curvature(Curvature ~= 0);

MaxMoment = max(Moment/1000000);
MaxCurvature = max(Curvature);

for e = 1:(NumberOfElements+1)
    ElementMoment{e} = Moment;
    ElementCurvature{e} = Curvature;
end

end

% DEAD LOAD
if MasonryDeadLoad ~= 0

HeightIncrement = WallHeight/NumberOfElements;
NetArea = (GroutedLength*TotalThickness) + ((TotalWallLength-
GroutedLength)*FaceShell*2);
GrossArea = TotalThickness*TotalWallLength;
GroutingFactor = NetArea/GrossArea;
SelfWeight(1) =
MasonryDeadLoad*(TotalWallLength*WallHeight*TotalThickness)*GroutingFactor;
TotalSelfWeight =
MasonryDeadLoad*(TotalWallLength*WallHeight*TotalThickness)*GroutingFactor;

for w = 2:(NumberOfElements+1)
    SelfWeight(w) =
MasonryDeadLoad*(TotalWallLength*TotalThickness*(WallHeight - (w-
1)*HeightIncrement))*GroutingFactor;
end

for e = 1:(NumberOfElements+1)

Strain = 0;
NeutralAxis = TotalThickness/2;

for j = 1:(NumberOfStrains+1)

    DeviationChange = 100;
    ErrorChange = 100;

```

```

for k = 1:10000000

    GroutedSlice = (ThicknessIncrement/2);
    TotalGroutedForce = 0;
    TotalGroutedMoment = 0;

for f = 1:NumberOfSlices

    SliceStrain = Strain*((GroutedSlice-NeutralAxis)/NeutralAxis);

    if PeakStrainGrouted <= SliceStrain && SliceStrain <= 0
        SliceStressGrouted = (-
1)*GroutedMasonryStrength*((2*abs(SliceStrain)/0.002)-
((abs(SliceStrain))/0.002)^2));
        elseif UltimateStrainGrouted <= SliceStrain && SliceStrain <
PeakStrainGrouted
            SliceStressGrouted = (-1)*GroutedMasonryStrength*(1-
GroutedZ*(abs(SliceStrain)-abs(PeakStrainGrouted)));
        elseif 0 < SliceStrain && SliceStrain <=
MasonryTensionStrainGrouted
            SliceStressGrouted =
GroutedMasonryStrength*(2/0.002)*abs(SliceStrain);
        else
            SliceStressGrouted = 0;
        end

    SliceForceGrouted =
PhiM*SliceStressGrouted*ThicknessIncrement*GroutedLength;
    SliceMomentGrouted = GroutedSlice*SliceForceGrouted;

    TotalGroutedForce = TotalGroutedForce + SliceForceGrouted;
    TotalGroutedMoment = TotalGroutedMoment + SliceMomentGrouted;

    GroutedSlice = GroutedSlice + ThicknessIncrement;

end

UngrountedSlice = (ThicknessIncrement/2);
TotalUngrountedForce = 0;
TotalUngrountedMoment = 0;

if UngrountedLength ~= 0
for f = 1:NumberOfSlices

    SliceStrain = Strain*((UngrountedSlice-NeutralAxis)/NeutralAxis);

    if PeakStrainUngrounted <= SliceStrain && SliceStrain <= 0
        SliceStressUngrounted = (-
1)*UngrountedMasonryStrength*((2*abs(SliceStrain)/0.002)-
((abs(SliceStrain))/0.002)^2));
        elseif UltimateStrainUngrounted <= SliceStrain && SliceStrain <
PeakStrainUngrounted
            SliceStressUngrounted = (-1)*UngrountedMasonryStrength*(1-
UngrountedZ*(abs(SliceStrain)-abs(PeakStrainUngrounted)));

```

```

elseif 0 < SliceStrain && SliceStrain <=
MasonryTensionStrainUngouted
    SliceStressUngouted =
UngoutedMasonryStrength*(2/0.002)*abs(SliceStrain);
else
    SliceStressUngouted = 0;
end

if UngoutedSlice <= FaceShell
    SliceForceUngouted =
PhiM*SliceStressUngouted*ThicknessIncrement*UngoutedLength;
elseif UngoutedSlice > FaceShell && UngoutedSlice <
(TotalThickness-FaceShell)
    SliceForceUngouted = 0;
elseif UngoutedSlice >= (TotalThickness-FaceShell)
    SliceForceUngouted =
PhiM*SliceStressUngouted*ThicknessIncrement*UngoutedLength;
end

SliceMomentUngouted = UngoutedSlice*SliceForceUngouted;

TotalUngoutedForce = TotalUngoutedForce + SliceForceUngouted;
TotalUngoutedMoment = TotalUngoutedMoment +
SliceMomentUngouted;

UngoutedSlice = UngoutedSlice + ThicknessIncrement;

end
end

TotalForceSteel = 0;
TotalMomentSteel = 0;

for s = 1:NumberOfRebar
    SteelStrain{s} = Strain*((SteelDistance{s}-
NeutralAxis)/NeutralAxis);

    if SteelStrain{s} < YieldStrain && SteelStrain{s} >= 0
        SteelForce{s} =
PhiS*AreaOfSteel{s}*SteelModulus*SteelStrain{s};
    elseif SteelStrain{s} >= YieldStrain && SteelStrain{s} <
StrainHardeningStrain
        SteelForce{s} = PhiS*AreaOfSteel{s}*SteelStrength;
    elseif SteelStrain{s} >= StrainHardeningStrain && SteelStrain{s} <
SteelRuptureStrain
        SteelForce{s} = PhiS*(StrainHardeningModulus*SteelStrain{s} +
StrainHardeningIntercept)*AreaOfSteel{s};

    elseif SteelStrain{s} > (-1)*YieldStrain && SteelStrain{s} < 0
        SteelForce{s} =
PhiS*AreaOfSteel{s}*SteelModulus*SteelStrain{s};
    elseif SteelStrain{s} <= (-1)*YieldStrain && SteelStrain{s} > (-
1)*StrainHardeningStrain
        SteelForce{s} = (-1)*PhiS*AreaOfSteel{s}*SteelStrength;

```

```

        elseif SteelStrain{s} <= (-1)*StrainHardeningStrain &&
SteelStrain{s} > (-1)*SteelRuptureStrain
            SteelForce{s} = (-
1)*PhiS*((StrainHardeningModulus*abs(SteelStrain{s}) +
StrainHardeningIntercept))*AreaOfSteel{s};
            else
                SteelForce{s} = 0;
            end

        SteelMoment{s} = SteelForce{s}*SteelDistance{s};

        TotalForceSteel = TotalForceSteel + SteelForce{s};
        TotalMomentSteel = TotalMomentSteel + SteelMoment{s};

    end

    Deviation(k) = TotalForceSteel + TotalGroutedForce +
TotalUngroupedForce + AxialLoad + SelfWeight(e);

    CompleteMoment = TotalMomentSteel + TotalUngroupedMoment +
TotalGroutedMoment + (AxialLoad+SelfWeight(e))*(TotalThickness/2);
    CompleteCurvature = Strain/NeutralAxis;

    if Deviation(k) > 0.1
        NeutralAxis = NeutralAxis + DeviationChange;
    elseif Deviation(k) < -0.1
        NeutralAxis = NeutralAxis - DeviationChange;
    elseif Deviation(k) <= 0.1 && Deviation(k) >= -0.1
        break
    end

    if k >= 4 && Deviation(k-3) > 0.00001 && Deviation(k-2) < -0.00001 &&
Deviation(k-1) > 0.00001 && Deviation(k) < -0.00001
        DeviationChange = 0.1*DeviationChange;
    end

    if NeutralAxis <= 0;
        DeviationChange = ErrorChange;
        NeutralAxis = 150.0;
        ErrorChange = 0.1*ErrorChange;
    end

    if NeutralAxis > 9999 || (k > 5 && Deviation(k) == Deviation(k-1) &&
Deviation(k-1) == Deviation(k-2))
        NeutralAxis = (TotalThickness/2);
        CompleteMoment = 0;
        CompleteCurvature = 0;
        break
    end

end

if CompleteMoment > 0
    Moment{e}(j) = CompleteMoment;
    Curvature{e}(j) = CompleteCurvature;
end

```



```

        CorrectNeutralAxis{e}(j) = NeutralAxis;
elseif CompleteMoment <= 0
    Moment{e}(j) = 0;
    Curvature{e}(j) = 0;
end

    Strain = Strain + StrainIncrement;

end

for d = 2:NumberOfStrains
    if Moment{e}(d) < Moment{e}(d-1)
        CurvatureCut(d) = d;
    end
end
StartD = (min(CurvatureCut(CurvatureCut>0)))-1;
MaxElasticMoment = Moment{e}((min(CurvatureCut(CurvatureCut>0)))-1);
for d = 2:length(CurvatureCut)
    if CurvatureCut(d) > 0
        Moment{e}(d) = 0;
        Curvature{e}(d) = 0;
    end
end
for d = StartD:NumberOfStrains
    if Moment{e}(d) < MaxElasticMoment
        Moment{e}(d) = 0;
        Curvature{e}(d) = 0;
    end
end
LastValue = length(Moment{e});
Moment{e}(LastValue) = 0;
Curvature{e}(LastValue) = 0;
Moment{e} = Moment{e}(Moment{e} ~= 0);
Curvature{e} = Curvature{e}(Curvature{e} ~= 0);

ElementMoment{e} = Moment{e};
ElementCurvature{e} = Curvature{e};

MaxMoment{e} = max(Moment{e}/1000000);
MaxCurvature{e} = max(Curvature{e});

end

end

% DEFINE INTERVALS %
DeltaHeight = WallHeight/NumberOfElements;
HeightIncrement = WallHeight/NumberOfElements;

% % SELF WEIGHT FORCE %
NetArea = (GroutedLength*TotalThickness) + ((TotalWallLength-
GroutedLength)*FaceShell*2);
GrossArea = TotalThickness*TotalWallLength;
GroutingFactor = NetArea/GrossArea;

```

```

SelfWeight(1) =
MasonryDeadLoad*(TotalWallLength*WallHeight*TotalThickness)*GroutingFactor;
TotalSelfWeight =
MasonryDeadLoad*(TotalWallLength*WallHeight*TotalThickness)*GroutingFactor;

% FOUNDATION SUPPORT STIFFNESS
if SupportStiffness == 1
    FoundationStiffness = RotationalStiffness*1000000;
elseif SupportStiffness == 2
    FoundationStiffness = SpecifiedSupportStiffness*1000000;
else
    FoundationStiffness = 0;
end

% INITIAL CONDITIONS %
Deflection(1) = 0;
SlopeChange = 0.0000001;
TopMoment = AxialLoad*Eccentricity;

if p == 1
    Slope(1) = -0.00001;
else
    Slope(1) = InitialSlope(p-1);
end

% CREATE A CHECK TO DETERMINE IF THE CORRECT VALUE OF SLOPE WAS USED %
for s = 1:100000000

BottomMoment = abs(Slope(1))*FoundationStiffness;

% CREATE THE LOOP TO GO THROUGH EACH ELEMENT %
for e = 2:(NumberOfElements + 1)

% CREATE THE EQUATION FOR THE PRIMARY MOMENT %
PrimaryMoment(e) = ((TopMoment+BottomMoment)/WallHeight)*DeltaHeight)
- BottomMoment;

% DETERMINE THE TOTAL MOMENT AT THE ELEMENT %
if SecondOrderEffects == 1
Moment(e) = PrimaryMoment(e) + AxialLoad*abs(Deflection(e-1));
else
Moment(e) = PrimaryMoment(e);
end

% DETERMINE MATERIAL FAILURE %
if abs(Moment(e)) > max(ElementMoment{e})
    if Stop1 == 0
        Stop0 = 1;
        Eccentricity = Eccentricity - EccentricityFactor;
        EccentricityFactor = 0.1*EccentricityFactor;
        Stop2 = 1;
        a = a + 1;
    end
end

```

```

        break
    end
end

% DETERMINE THE CURVATURE ASSOCIATED WITH THE TOTAL MOMENT %
Value1 = abs(ElementMoment{e} - abs(Moment(e)));
[Index Index] = min(Value1);
Closest = ElementMoment{e}(Index);
if abs(Moment(e)) < 0.00001
    SpecificCurvature(e) = 0;
elseif Index == 1
    SpecificCurvature(e) = ElementCurvature{e}(Index);
elseif Index == 501
    SpecificCurvature(e) = ElementCurvature{e}(Index);
elseif Closest > abs(Moment(e))
    SpecificCurvature(e) = ElementCurvature{e}(Index) -
    ((ElementMoment{e}(Index) - abs(Moment(e))) / (ElementMoment{e}(Index) -
    ElementMoment{e}(Index-1)) * (ElementCurvature{e}(Index) -
    ElementCurvature{e}(Index-1)));
elseif Closest < abs(Moment(e))
    SpecificCurvature(e) = ElementCurvature{e}(Index+1) -
    ((ElementMoment{e}(Index+1) -
    abs(Moment(e))) / (ElementMoment{e}(Index+1) -
    ElementMoment{e}(Index)) * (ElementCurvature{e}(Index+1) -
    ElementCurvature{e}(Index)));
end

% ACCOUNT FOR NEGATIVE MOMENTS %
if Moment(e) < 0
    SpecificCurvature(e) = (-1.0)*SpecificCurvature(e);
end

% DETERMINE THE SLOPE AT THE NEXT ELEMENT %
Slope(e) = Slope(e-1) + SpecificCurvature(e)*HeightIncrement;

% CALCULATE THE DEFLECTION AT THE END OF THE ELEMENT %
if SpecificCurvature(e) <= 0
    Deflection(e) = Deflection(e-1) + (Slope(e-1)*HeightIncrement) -
    ((0.5)*(SpecificCurvature(e))*(HeightIncrement^2));
elseif SpecificCurvature(e) > 0
    Deflection(e) = Deflection(e-1) + (Slope(e-1)*HeightIncrement) +
    ((0.5)*(SpecificCurvature(e))*(HeightIncrement^2));
end
% MUST FIX THE DELTA HEIGHT TO ADJUST THE PRIMARY MOMENT FOR THE NEXT
ITERATION %
DeltaHeight = DeltaHeight + HeightIncrement;

end

% CHECK THE SLOPE %

if Stop2 == 1
    break
end

```

```

DeflectionCheck(s) = Deflection(NumberOfElements+1);

if DeflectionCheck(s) > 0.1
    Slope(1) = Slope(1) - SlopeChange;
elseif DeflectionCheck(s) < -0.1
    Slope(1) = Slope(1) + SlopeChange;
elseif DeflectionCheck(s) <= 0.1 && DeflectionCheck(s) >= -0.1
    CompleteDeflection = Deflection;
    break
end

% CATCH THE ERROR IN SLOPE CHANGE %
if s >= 5 && DeflectionCheck(s-3) > 0.0001 && DeflectionCheck(s-2) < -
0.0001 && DeflectionCheck(s-1) > 0.0001 && DeflectionCheck(s) < -
0.0001
    SlopeChange = 0.1*SlopeChange;
end

% RESET THE DELTA HEIGHT
DeltaHeight = WallHeight/NumberOfElements;

end

if a == 7
    break
end

Eccentricity = Eccentricity + EccentricityFactor;

end

if Quit ~= 1
DiagramAxialLoad(p) = AxialLoad/1000;
DiagramMoment(p) = (AxialLoad*Eccentricity)/1000000;
end
if DiagramMoment(p) == 0
    Quit = 1;
end
if Quit == 1;
    fprintf('          %4.0f          |',MaxAxialLoad);
    fprintf('          %6.2f\n',0);
    break
end

fprintf('          %4.0f          |',DiagramAxialLoad(p));
fprintf('          %6.2f\n',DiagramMoment(p));

InitialSlope(p) = Slope(1);

end

% PLOT THE DIAGRAM
PlotAxialLoad(1) = 0;

```

```

PlotMoment(1) = InitialMoment;
for w = 1:p
    PlotAxialLoad(w+1) = DiagramAxialLoad(w);
    PlotMoment(w+1) = DiagramMoment(w);
end
PlotAxialLoad(p+1) = MaxAxialLoad;
PlotMoment(p+1) = 0;

plot(PlotMoment,PlotAxialLoad)
title('Slenderness Interaction Diagram')
xlabel('Moment (kNm)')
ylabel('Axial Load (kN)')

fprintf('\n')
fprintf('Analysis Complete! \n')
end

%% ANALYSIS TYPE 4 - ECCENTRIC AXIAL LOAD %

if AnalysisType == 4

fprintf('Analysis Started! \n')
fprintf('\n')

% MAX AXIAL LOAD
TotalRebarArea = 0;
UngroupedArea = 2*(TotalWallLength-GroutedLength)*FaceShell;
GroutedArea = GroutedLength*TotalThickness;
for s = 1:NumberOfRebar
    TotalRebarArea = TotalRebarArea + AreaOfSteel{s};
end
MaxAxialLoad =
((GroutedMasonryStrength*GroutedArea)+(UngroupedMasonryStrength*Ungrou
tedArea)+(TotalRebarArea*SteelStrength))/1000;
fprintf('Max Axial Load (kN): %4.0f \n',MaxAxialLoad)
fprintf('\n')

fprintf('      Axial Load (kN) | Midspan Deflection (mm) | Flexural
Rigidity (x10^12) (Nmm^2) \n')
fprintf('      | \n')
fprintf('      %3.1f |',0);
fprintf('      %5.2f |',0);
fprintf('      INF \n');

% CREATE FAIL CRITERION
Stop0 = 0;
Stop1 = 0;
Stop2 = 0;
Stop3 = 0;
b = 0;

% START INCREASING THE AXIAL LOAD
for p = 1:1000
    Stop2 = 0;

```

```

% START AT INCREMENTS OF 25 kN
if Stop1 ~= 1
    AxialLoad = p*AxialLoadFactor;
% SWITCH TO INCREMENTS OF 1 kN WHEN FIRST FAILURE OCCURS
elseif Stop1 == 1
    AxialLoad = StopAxialLoad + (p-p1)*AxialLoadFactor2;
end

% CLEAR PREVIOUS VARIABLES FROM PRECEEDING AXIAL LOADS
clear Deflection
clear Slope
clear SlopeChange
clear PrimaryMoment

% MOMENT CURVATURE ANALYSIS

% PRELIMINARY CALCULATIONS
StrainIncrement = abs(MasonryFailureStrain)/NumberOfStrains;
ThicknessIncrement = TotalThickness/NumberOfSlices;
YieldStrain = SteelStrength/SteelModulus;
StrainHardeningIntercept = SteelStrength -
(StrainHardeningModulus*StrainHardeningStrain);
UngoutedZ =
0.5/((3+0.29*UngoutedMasonryStrength)/(145*UngoutedMasonryStrength-
1000))-0.002);
GoutedZ =
0.5/((3+0.29*GoutedMasonryStrength)/(145*GoutedMasonryStrength-
1000))-0.002);
UltimateStrainGouted = MasonryFailureStrain-0.001;
MasonryTensionStrainGouted =
MasonryStrengthTension/(GoutedMasonryStrength*(2/0.002));
UltimateStrainUngouted = MasonryFailureStrain-0.001;
MasonryTensionStrainUngouted =
MasonryStrengthTension/(UngoutedMasonryStrength*(2/0.002));
UngoutedLength = TotalWallLength - GoutedLength;
CurvatureCut = [];

% NO DEAD LOAD
if MasonryDeadLoad == 0

Strain = 0;
NeutralAxis = TotalThickness/2;

for j = 1:(NumberOfStrains+1)

    DeviationChange = 100;
    ErrorChange = 100;

for k = 1:100000

    GoutedSlice = (ThicknessIncrement/2);
    TotalGoutedForce = 0;
    TotalGoutedMoment = 0;

```

```

for f = 1:NumberOfSlices

    SliceStrain = Strain*((GroutedSlice-NeutralAxis)/NeutralAxis);

    if PeakStrainGrouted <= SliceStrain && SliceStrain <= 0
        SliceStressGrouted = (-
1)*GroutedMasonryStrength*((2*abs(SliceStrain)/0.002)-
((abs(SliceStrain))/0.002)^2));
        elseif UltimateStrainGrouted <= SliceStrain && SliceStrain <
PeakStrainGrouted
            SliceStressGrouted = (-1)*GroutedMasonryStrength*(1-
GroutedZ*(abs(SliceStrain)-abs(PeakStrainGrouted)));
            elseif 0 < SliceStrain && SliceStrain <=
MasonryTensionStrainGrouted
                SliceStressGrouted =
GroutedMasonryStrength*(2/0.002)*abs(SliceStrain);
            else
                SliceStressGrouted = 0;
            end

        SliceForceGrouted =
PhiM*SliceStressGrouted*ThicknessIncrement*GroutedLength;
        SliceMomentGrouted = GroutedSlice*SliceForceGrouted;

        TotalGroutedForce = TotalGroutedForce + SliceForceGrouted;
        TotalGroutedMoment = TotalGroutedMoment + SliceMomentGrouted;

        GroutedSlice = GroutedSlice + ThicknessIncrement;

end

    UngROUTEDSlice = (ThicknessIncrement/2);
    TotalUngROUTEDForce = 0;
    TotalUngROUTEDMoment = 0;

    if UngROUTEDLength ~= 0
for f = 1:NumberOfSlices

        SliceStrain = Strain*((UngROUTEDSlice-NeutralAxis)/NeutralAxis);

        if PeakStrainUngROUTED <= SliceStrain && SliceStrain <= 0
            SliceStressUngROUTED = (-
1)*UngROUTEDMasonryStrength*((2*abs(SliceStrain)/0.002)-
((abs(SliceStrain))/0.002)^2));
            elseif UltimateStrainUngROUTED <= SliceStrain && SliceStrain <
PeakStrainUngROUTED
                SliceStressUngROUTED = (-1)*UngROUTEDMasonryStrength*(1-
UngROUTEDZ*(abs(SliceStrain)-abs(PeakStrainUngROUTED)));
                elseif 0 < SliceStrain && SliceStrain <=
MasonryTensionStrainUngROUTED
                    SliceStressUngROUTED =
UngROUTEDMasonryStrength*(2/0.002)*abs(SliceStrain);
                else
                    SliceStressUngROUTED = 0;
                end
            end
        end
    end

```

```

        if UngroupedSlice <= FaceShell
            SliceForceUngrouped =
PhiM*SliceStressUngrouped*ThicknessIncrement*UngroupedLength;
            elseif UngroupedSlice > FaceShell && UngroupedSlice <
(TotalThickness-FaceShell)
                SliceForceUngrouped = 0;
            elseif UngroupedSlice >= (TotalThickness-FaceShell)
                SliceForceUngrouped =
PhiM*SliceStressUngrouped*ThicknessIncrement*UngroupedLength;
            end

            SliceMomentUngrouped = UngroupedSlice*SliceForceUngrouped;

            TotalUngroupedForce = TotalUngroupedForce + SliceForceUngrouped;
            TotalUngroupedMoment = TotalUngroupedMoment +
SliceMomentUngrouped;

            UngroupedSlice = UngroupedSlice + ThicknessIncrement;

end
end

TotalForceSteel = 0;
TotalMomentSteel = 0;

for s = 1:NumberOfRebar
    SteelStrain{s} = Strain*(SteelDistance{s}-
NeutralAxis)/NeutralAxis);

        if SteelStrain{s} < YieldStrain && SteelStrain{s} >= 0
            SteelForce{s} =
PhiS*AreaOfSteel{s}*SteelModulus*SteelStrain{s};
            elseif SteelStrain{s} >= YieldStrain && SteelStrain{s} <
StrainHardeningStrain
                SteelForce{s} = PhiS*AreaOfSteel{s}*SteelStrength;
            elseif SteelStrain{s} >= StrainHardeningStrain && SteelStrain{s} <
SteelRuptureStrain
                SteelForce{s} = PhiS*(StrainHardeningModulus*SteelStrain{s} +
StrainHardeningIntercept)*AreaOfSteel{s};

            elseif SteelStrain{s} > (-1)*YieldStrain && SteelStrain{s} < 0
                SteelForce{s} =
PhiS*AreaOfSteel{s}*SteelModulus*SteelStrain{s};
            elseif SteelStrain{s} <= (-1)*YieldStrain && SteelStrain{s} > (-
1)*StrainHardeningStrain
                SteelForce{s} = (-1)*PhiS*AreaOfSteel{s}*SteelStrength;
            elseif SteelStrain{s} <= (-1)*StrainHardeningStrain &&
SteelStrain{s} > (-1)*SteelRuptureStrain
                SteelForce{s} = (-
1)*PhiS*((StrainHardeningModulus*abs(SteelStrain{s}) +
StrainHardeningIntercept))*AreaOfSteel{s};
            else
                SteelForce{s} = 0;
            end
end

```



```

    SteelMoment{s} = SteelForce{s}*SteelDistance{s};

    TotalForceSteel = TotalForceSteel + SteelForce{s};
    TotalMomentSteel = TotalMomentSteel + SteelMoment{s};

end

Deviation(k) = TotalForceSteel + TotalGroutedForce +
TotalUngoutedForce + AxialLoad;

CompleteMoment = TotalMomentSteel + TotalUngoutedMoment +
TotalGroutedMoment + AxialLoad*(TotalThickness/2);
CompleteCurvature = Strain/NeutralAxis;

if Deviation(k) > 0.1
    NeutralAxis = NeutralAxis + DeviationChange;
elseif Deviation(k) < -0.1
    NeutralAxis = NeutralAxis - DeviationChange;
elseif Deviation(k) <= 0.1 && Deviation(k) >= -0.1
    break
end

if k >= 4 && Deviation(k-3) > 0.00001 && Deviation(k-2) < -0.00001 &&
Deviation(k-1) > 0.00001 && Deviation(k) < -0.00001
    DeviationChange = 0.1*DeviationChange;
end

if NeutralAxis <= 0;
    DeviationChange = ErrorChange;
    NeutralAxis = 150.0;
    ErrorChange = 0.1*ErrorChange;
end

if NeutralAxis > 9999 || (k > 5 && Deviation(k) == Deviation(k-1) &&
Deviation(k-1) == Deviation(k-2))
    NeutralAxis = (TotalThickness/2);
    CompleteMoment = 0;
    CompleteCurvature = 0;
    break
end

end

end

if CompleteMoment > 0
    Moment(j) = CompleteMoment;
    Curvature(j) = CompleteCurvature;
    CorrectNeutralAxis(j) = NeutralAxis;
else
    Moment(j) = 0;
    Curvature(j) = 0;
end

Strain = Strain + StrainIncrement;

```

```

end

for d = 2:NumberOfStrains
    if Moment(d) < Moment(d-1)
        CurvatureCut(d) = d;
    end
end

StartD = (min(CurvatureCut(CurvatureCut>0)))-1;
MaxElasticMoment = Moment((min(CurvatureCut(CurvatureCut>0)))-1);
for d = 2:length(CurvatureCut)
    if CurvatureCut(d) > 0
        Moment(d) = 0;
        Curvature(d) = 0;
    end
end
for d = StartD:NumberOfStrains
    if Moment(d) < MaxElasticMoment
        Moment(d) = 0;
        Curvature(d) = 0;
    end
end
end
LastValue = length(Moment);
Moment(LastValue) = 0;
Curvature(LastValue) = 0;
Moment = Moment(Moment ~= 0);
Curvature = Curvature(Curvature ~= 0);

MaxMoment = max(Moment/1000000);
MaxCurvature = max(Curvature);

for e = 1:(NumberOfElements+1)
    ElementMoment{e} = Moment;
    ElementCurvature{e} = Curvature;
end

end

% DEAD LOAD
if MasonryDeadLoad ~= 0

HeightIncrement = WallHeight/NumberOfElements;
NetArea = (GroutedLength*TotalThickness) + ((TotalWallLength-
GroutedLength)*FaceShell*2);
GrossArea = TotalThickness*TotalWallLength;
GroutingFactor = NetArea/GrossArea;
SelfWeight(1) =
MasonryDeadLoad*(TotalWallLength*WallHeight*TotalThickness)*GroutingFa
ctor;
TotalSelfWeight =
MasonryDeadLoad*(TotalWallLength*WallHeight*TotalThickness)*GroutingFa
ctor;

for w = 2:(NumberOfElements+1)

```

```

    SelfWeight(w) =
MasonryDeadLoad*(TotalWallLength*TotalThickness*(WallHeight - (w-
1)*HeightIncrement))*GroutingFactor;
end

for e = 1:(NumberOfElements+1)

Strain = 0;
NeutralAxis = TotalThickness/2;

for j = 1:(NumberOfStrains+1)

    DeviationChange = 100;
    ErrorChange = 100;

for k = 1:10000000

    GroutedSlice = (ThicknessIncrement/2);
    TotalGroutedForce = 0;
    TotalGroutedMoment = 0;

for f = 1:NumberOfSlices

    SliceStrain = Strain*((GroutedSlice-NeutralAxis)/NeutralAxis);

    if PeakStrainGrouted <= SliceStrain && SliceStrain <= 0
        SliceStressGrouted = (-
1)*GroutedMasonryStrength*((2*abs(SliceStrain)/0.002) -
((abs(SliceStrain))/0.002)^2));
        elseif UltimateStrainGrouted <= SliceStrain && SliceStrain <
PeakStrainGrouted
            SliceStressGrouted = (-1)*GroutedMasonryStrength*(1-
GroutedZ*(abs(SliceStrain)-abs(PeakStrainGrouted)));
        elseif 0 < SliceStrain && SliceStrain <=
MasonryTensionStrainGrouted
            SliceStressGrouted =
GroutedMasonryStrength*(2/0.002)*abs(SliceStrain);
        else
            SliceStressGrouted = 0;
        end

        SliceForceGrouted =
PhiM*SliceStressGrouted*ThicknessIncrement*GroutedLength;
        SliceMomentGrouted = GroutedSlice*SliceForceGrouted;

        TotalGroutedForce = TotalGroutedForce + SliceForceGrouted;
        TotalGroutedMoment = TotalGroutedMoment + SliceMomentGrouted;

        GroutedSlice = GroutedSlice + ThicknessIncrement;

end

    UngROUTedSlice = (ThicknessIncrement/2);
    TotalUngROUTedForce = 0;
    TotalUngROUTedMoment = 0;

```

```

    if UngROUTEDLength ~= 0
    for f = 1:NumberOfSlices

        SliceStrain = Strain*((UngROUTEDSlice-NeutralAxis)/NeutralAxis);

        if PeakStrainUngROUTED <= SliceStrain && SliceStrain <= 0
            SliceStressUngROUTED = (-
1)*UngROUTEDMasonryStrength*((2*abs(SliceStrain)/0.002)-
((abs(SliceStrain))/0.002)^2));
            elseif UltimateStrainUngROUTED <= SliceStrain && SliceStrain <
PeakStrainUngROUTED
                SliceStressUngROUTED = (-1)*UngROUTEDMasonryStrength*(1-
UngROUTEDZ*(abs(SliceStrain)-abs(PeakStrainUngROUTED)));
            elseif 0 < SliceStrain && SliceStrain <=
MasonryTensionStrainUngROUTED
                SliceStressUngROUTED =
UngROUTEDMasonryStrength*(2/0.002)*abs(SliceStrain);
            else
                SliceStressUngROUTED = 0;
            end

            if UngROUTEDSlice <= FaceShell
                SliceForceUngROUTED =
PhiM*SliceStressUngROUTED*ThicknessIncrement*UngROUTEDLength;
            elseif UngROUTEDSlice > FaceShell && UngROUTEDSlice <
(TotalThickness-FaceShell)
                SliceForceUngROUTED = 0;
            elseif UngROUTEDSlice >= (TotalThickness-FaceShell)
                SliceForceUngROUTED =
PhiM*SliceStressUngROUTED*ThicknessIncrement*UngROUTEDLength;
            end

            SliceMomentUngROUTED = UngROUTEDSlice*SliceForceUngROUTED;

            TotalUngROUTEDForce = TotalUngROUTEDForce + SliceForceUngROUTED;
            TotalUngROUTEDMoment = TotalUngROUTEDMoment +
SliceMomentUngROUTED;

            UngROUTEDSlice = UngROUTEDSlice + ThicknessIncrement;

        end
    end

    TotalForceSteel = 0;
    TotalMomentSteel = 0;

    for s = 1:NumberOfRebar
        SteelStrain{s} = Strain*((SteelDistance{s}-
NeutralAxis)/NeutralAxis);

        if SteelStrain{s} < YieldStrain && SteelStrain{s} >= 0
            SteelForce{s} =
PhiS*AreaOfSteel{s}*SteelModulus*SteelStrain{s};

```

```

        elseif SteelStrain{s} >= YieldStrain && SteelStrain{s} <
StrainHardeningStrain
            SteelForce{s} = PhiS*AreaOfSteel{s}*SteelStrength;
        elseif SteelStrain{s} >= StrainHardeningStrain && SteelStrain{s} <
SteelRuptureStrain
            SteelForce{s} = PhiS*(StrainHardeningModulus*SteelStrain{s} +
StrainHardeningIntercept)*AreaOfSteel{s};

            elseif SteelStrain{s} > (-1)*YieldStrain && SteelStrain{s} < 0
                SteelForce{s} =
PhiS*AreaOfSteel{s}*SteelModulus*SteelStrain{s};
            elseif SteelStrain{s} <= (-1)*YieldStrain && SteelStrain{s} > (-
1)*StrainHardeningStrain
                SteelForce{s} = (-1)*PhiS*AreaOfSteel{s}*SteelStrength;
            elseif SteelStrain{s} <= (-1)*StrainHardeningStrain &&
SteelStrain{s} > (-1)*SteelRuptureStrain
                SteelForce{s} = (-
1)*PhiS*((StrainHardeningModulus*abs(SteelStrain{s})) +
StrainHardeningIntercept)*AreaOfSteel{s};
            else
                SteelForce{s} = 0;
            end

        SteelMoment{s} = SteelForce{s}*SteelDistance{s};

        TotalForceSteel = TotalForceSteel + SteelForce{s};
        TotalMomentSteel = TotalMomentSteel + SteelMoment{s};

    end

    Deviation(k) = TotalForceSteel + TotalGroutedForce +
TotalUngroudedForce + AxialLoad + SelfWeight(e);

    CompleteMoment = TotalMomentSteel + TotalUngroudedMoment +
TotalGroutedMoment + (AxialLoad+SelfWeight(e))*(TotalThickness/2);
    CompleteCurvature = Strain/NeutralAxis;

    if Deviation(k) > 0.1
        NeutralAxis = NeutralAxis + DeviationChange;
    elseif Deviation(k) < -0.1
        NeutralAxis = NeutralAxis - DeviationChange;
    elseif Deviation(k) <= 0.1 && Deviation(k) >= -0.1
        break
    end

    if k >= 4 && Deviation(k-3) > 0.00001 && Deviation(k-2) < -0.00001 &&
Deviation(k-1) > 0.00001 && Deviation(k) < -0.00001
        DeviationChange = 0.1*DeviationChange;
    end

    if NeutralAxis <= 0;
        DeviationChange = ErrorChange;
        NeutralAxis = 150.0;
        ErrorChange = 0.1*ErrorChange;
    end
end

```

```

    if NeutralAxis > 9999 || (k > 5 && Deviation(k) == Deviation(k-1) &&
Deviation(k-1) == Deviation(k-2))
        NeutralAxis = (TotalThickness/2);
        CompleteMoment = 0;
        CompleteCurvature = 0;
        break
    end
end

if CompleteMoment > 0
    Moment{e}(j) = CompleteMoment;
    Curvature{e}(j) = CompleteCurvature;
    CorrectNeutralAxis{e}(j) = NeutralAxis;
elseif CompleteMoment <= 0
    Moment{e}(j) = 0;
    Curvature{e}(j) = 0;
end

    Strain = Strain + StrainIncrement;

end

for d = 2:NumberOfStrains
    if Moment{e}(d) < Moment{e}(d-1)
        CurvatureCut(d) = d;
    end
end
StartD = (min(CurvatureCut(CurvatureCut>0)))-1;
MaxElasticMoment = Moment{e}((min(CurvatureCut(CurvatureCut>0)))-1);
for d = 2:length(CurvatureCut)
    if CurvatureCut(d) > 0
        Moment{e}(d) = 0;
        Curvature{e}(d) = 0;
    end
end
for d = StartD:NumberOfStrains
    if Moment{e}(d) < MaxElasticMoment
        Moment{e}(d) = 0;
        Curvature{e}(d) = 0;
    end
end
LastValue = length(Moment{e});
Moment{e}(LastValue) = 0;
Curvature{e}(LastValue) = 0;
Moment{e} = Moment{e}(Moment{e} ~= 0);
Curvature{e} = Curvature{e}(Curvature{e} ~= 0);

ElementMoment{e} = Moment{e};
ElementCurvature{e} = Curvature{e};

MaxMoment{e} = max(Moment{e}/1000000);
MaxCurvature{e} = max(Curvature{e});

```

```

end

end

clear Moment
clear DeflectionCheck

% DEFINE INTERVALS %
DeltaHeight = WallHeight/NumberOfElements;
HeightIncrement = WallHeight/NumberOfElements;

% % SELF WEIGHT FORCE %
NetArea = (GroutedLength*TotalThickness) + ((TotalWallLength-
GroutedLength)*FaceShell*2);
GrossArea = TotalThickness*TotalWallLength;
GroutingFactor = NetArea/GrossArea;
SelfWeight(1) =
MasonryDeadLoad*(TotalWallLength*WallHeight*TotalThickness)*GroutingFactor;
TotalSelfWeight =
MasonryDeadLoad*(TotalWallLength*WallHeight*TotalThickness)*GroutingFactor;

% FOUNDATION SUPPORT STIFFNESS
if SupportStiffness == 1
    FoundationStiffness = RotationalStiffness*1000000;
elseif SupportStiffness == 2
    FoundationStiffness = SpecifiedSupportStiffness*1000000;
else
    FoundationStiffness = 0;
end

% INITIAL CONDITIONS %
Deflection(1) = 0;
SlopeChange = 0.0001;
TopMoment = AxialLoad*Eccentricity;

if p == 1
    if FoundationStiffness < 3000
        Slope(1) = -0.0001;
    elseif FoundationStiffness >= 3000 && FoundationStiffness < 7000
        Slope(1) = -0.0005;
    elseif FoundationStiffness >= 7000
        Slope(1) = -0.0005;
    end
elseif Stop0 == 0
    Slope(1) = (-1)*InitialSlope(p-1);
elseif Stop0 == 1 && p > 2
    Slope(1) = (-1)*InitialSlope(p-2);
    Stop0 = 0;
end
b = 1;
c = 1;

```

```

% CREATE A CHECK TO DETERMINE IF THE CORRECT VALUE OF SLOPE WAS USED %
for s = 1:100000000

BottomMoment = abs(Slope(1))*FoundationStiffness;
Moment(1) = (-1)*BottomMoment;

% CREATE THE LOOP TO GO THROUGH EACH ELEMENT %
for e = 2:(NumberOfElements + 1)

% CREATE THE EQUATION FOR THE PRIMARY MOMENT %
PrimaryMoment(e) = ((TopMoment+BottomMoment)/WallHeight)*DeltaHeight)
- BottomMoment;

% DETERMINE THE TOTAL MOMENT AT THE ELEMENT %
if SecondOrderEffects == 1
Moment(e) = PrimaryMoment(e) + AxialLoad*abs(Deflection(e-1));
else
Moment(e) = PrimaryMoment(e);
end

% DETERMINE MATERIAL FAILURE %
if abs(Moment(e)) > max(ElementMoment{e})
    if Stop1 == 0
        Stop0 = 1;
        StopAxialLoad = AxialLoad - 25000;
        Stop1 = 1;
        Stop2 = 1;
        p1 = p;
        p = p - 2;
        break
    elseif Stop1 == 1
        Stop2 = 1;
        Stop3 = 1;
        break
    end
end

% DETERMINE THE CURVATURE ASSOCIATED WITH THE TOTAL MOMENT %
Value1 = abs(ElementMoment{e} - abs(Moment(e)));
[Index Index] = min(Value1);
Closest = ElementMoment{e}(Index);
if abs(Moment(e)) < 0.00001
    SpecificCurvature(e) = 0;
elseif Index == 1
    SpecificCurvature(e) = ElementCurvature{e}(Index);
elseif Index == 501
    SpecificCurvature(e) = ElementCurvature{e}(Index);
elseif Closest > abs(Moment(e))
    SpecificCurvature(e) = ElementCurvature{e}(Index) -
((ElementMoment{e}(Index)-abs(Moment(e)))/(ElementMoment{e}(Index)-
ElementMoment{e}(Index-1))*ElementCurvature{e}(Index)-
ElementCurvature{e}(Index-1));
elseif Closest < abs(Moment(e))
    SpecificCurvature(e) = ElementCurvature{e}(Index+1) -
((ElementMoment{e}(Index+1)-

```



```

abs(Moment(e))/(ElementMoment{e}(Index+1) -
ElementMoment{e}(Index))* (ElementCurvature{e}(Index+1) -
ElementCurvature{e}(Index));
    end

% ACCOUNT FOR NEGATIVE MOMENTS %
if Moment(e) < 0
    SpecificCurvature(e) = (-1.0)*SpecificCurvature(e);
end

% DETERMINE THE SLOPE AT THE NEXT ELEMENT %
Slope(e) = Slope(e-1) + SpecificCurvature(e)*HeightIncrement;

% CALCULATE THE DEFLECTION AT THE END OF THE ELEMENT %
if SpecificCurvature(e) <= 0
Deflection(e) = Deflection(e-1) + (Slope(e-1)*HeightIncrement) -
((0.5)*(SpecificCurvature(e))*(HeightIncrement^2));
elseif SpecificCurvature(e) > 0
    Deflection(e) = Deflection(e-1) + (Slope(e-1)*HeightIncrement) +
((0.5)*(SpecificCurvature(e))*(HeightIncrement^2));
end
% MUST FIX THE DELTA HEIGHT TO ADJUST THE PRIMARY MOMENT FOR THE NEXT
ITERATION %
DeltaHeight = DeltaHeight + HeightIncrement;

end

% CHECK THE SLOPE %

if Stop2 == 1
    break
end

DeflectionCheck(s) = Deflection(NumberOfElements+1);

if DeflectionCheck(s) > Tolerance
    Slope(1) = Slope(1) - SlopeChange;
elseif DeflectionCheck(s) < (-1)*Tolerance
    Slope(1) = Slope(1) + SlopeChange;
elseif DeflectionCheck(s) <= Tolerance && DeflectionCheck(s) >= (-
1)*Tolerance
    DCheck = DeflectionCheck(s);
    CompleteDeflection = Deflection;
    EI_Moment = Moment(e);
    EI_Curvature = SpecificCurvature(e);
    break
end

% CATCH THE ERROR IN SLOPE CHANGE %
if s >= 5 && DeflectionCheck(s-3) > 0.0001 && DeflectionCheck(s-2) < -
0.0001 && DeflectionCheck(s-1) > 0.0001 && DeflectionCheck(s) < -
0.0001 && b > 5
    SlopeChange = 0.1*SlopeChange;

```

```

        b = 1;
        c = c + 1;
    end
    b = b + 1;

    if c >= 30
        Slope(1) = Slope(1) - 0.002;
        SlopeChange = 0.0001;
        c = 1;
    end

    % RESET THE DELTA HEIGHT
    DeltaHeight = WallHeight/NumberOfElements;

    end
    if Stop3 == 1
        fprintf('\n')
        fprintf('Failure Occured: Material \n')
        break
    end

    % TRACK THE DEFLECTION AT A SPECIFIC AXIAL LOAD
    if Stop2 ~= 1
        MidspanDeflection(p) = abs(Deflection(((NumberOfElements+1)/2)));
        InitialSlope(p) = abs(Slope(1));
        TotalAxialLoad(p) = (AxialLoad/1000);
        MidspanMoment(p) = abs(Moment(((NumberOfElements+1)/2)))/1000000;
        MomentMagnification(p) =
        abs(Moment(((NumberOfElements+1)/2)))/abs(PrimaryMoment(((NumberOfElements+1)/2)));

    % CAPTURE THE DEFLECTION AND BENDING MOMENT PROFILE
    MomentProfile{p} = transpose(Moment/1000000);
    DeflectionProfile{p} = transpose(abs(Deflection));
    CurvatureProfile{p} = transpose(SpecificCurvature);

    % CALCULATE THE FLEXURAL RIGIDITY

    if EI_Method == 1

        Midpoint = WallHeight/2;
        StiffnessDeflection(p) = (-1)*MidspanDeflection(p);
        Term2 = InitialSlope(p)*FoundationStiffness;
        Term4 = (Midpoint/WallHeight);
        Term5 = AxialLoad*Eccentricity;
        StiffnessChange = 1000000000;

        EffectiveStiffness = 1000000000000000;

        for i = 1:10000000

            k = sqrt(AxialLoad/EffectiveStiffness);

```

```

Term10 = 1/(WallHeight*AxialLoad);
Term11 = Eccentricity*AxialLoad*Midpoint;
Term12 = (WallHeight-Midpoint)*FoundationStiffness*InitialSlope(p);
Term13 = WallHeight*csc(k*WallHeight);
Term14 = FoundationStiffness*InitialSlope(p)*sin((Midpoint-
WallHeight)*k);
Term15 = Eccentricity*AxialLoad*sin(k*Midpoint);

EstDeflection = Term10*(Term11 + Term12 + (Term13*(Term14-Term15)));

if abs(EstDeflection) > 1000 || EstDeflection > 0
    EffectiveStiffness = EffectiveStiffness + 1000000000000;

else

Error = StiffnessDeflection(p) - EstDeflection;

if Error >= 0.00001
    EffectiveStiffness = EffectiveStiffness + StiffnessChange;
    ErrorSwitch(i) = 1;
elseif Error <= -0.00001
    EffectiveStiffness = EffectiveStiffness - StiffnessChange;
    ErrorSwitch(i) = 2;
else
    MidspanEffectiveStiffness = EffectiveStiffness;
    break
end
end

if i > 1000 && ErrorSwitch(i-4) == 1 && ErrorSwitch(i-3) == 2 &&
ErrorSwitch(i-2) == 1 && ErrorSwitch(i-1) == 2 && ErrorSwitch(i) == 1
    StiffnessChange = 0.1*StiffnessChange;
end
end

elseif EI_Method == 2

    for w = 16:(NumberOfElements+1)
        EI_Element{p}(w) = Moment(w)/SpecificCurvature(w);
    end
    MidspanEffectiveStiffness =
(Moment(((NumberOfElements+1)/2))/SpecificCurvature(((NumberOfElements
+1)/2)));
    EI_Element{p} = EI_Element{p}(EI_Element{p} ~= 0);
    MinEI(p) = min(EI_Element{p})/1000000000000;
    MinEI2(p) = EI_Element{p}(7)/1000000000000;

end

BucklingRigidity(p) = MidspanEffectiveStiffness;
FlexuralRigidity(p) = MidspanEffectiveStiffness/1000000000000;

if p >= 5
Pcritical(p) = ((pi^2)*BucklingRigidity(p))/(WallHeight^2);

```

```

if AxialLoad >= Pcritical(p)
    fprintf('\n')
    fprintf('Failure Occured: Buckling \n')
    break
end
end

fprintf('          %6.1f      |', TotalAxialLoad(p));
fprintf('          %6.2f      |', MidspanDeflection(p));
fprintf('          %5.2f \n', FlexuralRigidity(p));
end
end

DataMidspan = transpose(MidspanDeflection);
DataLoad = transpose(TotalAxialLoad);
DataMidspanMoment = transpose(MidspanMoment);
DataEI = transpose(BucklingRigidity);
MomentMagnification = transpose(MomentMagnification);

fprintf('\n')
fprintf('Analysis Complete! \n')
beep on
beep
end

%% ANALYSIS TYPE 5 - LATERAL LOAD WITH ECCENTRIC AXIAL LOAD

if AnalysisType == 5

fprintf('Analysis Started \n')
fprintf('\n')

% MAX AXIAL LOAD
TotalRebarArea = 0;
UngroudedArea = 2*(TotalWallLength-GroudedLength)*FaceShell;
GroudedArea = GroudedLength*TotalThickness;
for s = 1:NumberOfRebar
    TotalRebarArea = TotalRebarArea + AreaOfSteel{s};
end
MaxAxialLoad =
((GroudedMasonryStrength*GroudedArea)+(UngroudedMasonryStrength*Ungrou
tedArea)+(TotalRebarArea*SteelStrength))/1000;
fprintf('Max Axial Load (kN): %4.0f \n', MaxAxialLoad)
fprintf('\n')

fprintf('          Lateral Load (kN/m) | Midspan Deflection (mm) | Flexural
Rigidity (x10^12) (Nmm^2) \n')
fprintf('          |                                     | \n')
fprintf('          %3.2f      |', 0);
fprintf('          %5.2f      |', 0);
fprintf('          INF \n');

% MOMENT CURVATURE ANALYSIS

% PRELIMINARY CALCULATIONS

```

```

StrainIncrement = abs(MasonryFailureStrain)/NumberOfStrains;
ThicknessIncrement = TotalThickness/NumberOfSlices;
YieldStrain = SteelStrength/SteelModulus;
StrainHardeningIntercept = SteelStrength -
(StrainHardeningModulus*StrainHardeningStrain);
UngoutedZ =
0.5/(((3+0.29*UngoutedMasonryStrength)/(145*UngoutedMasonryStrength-
1000))-0.002);
GoutedZ =
0.5/(((3+0.29*GoutedMasonryStrength)/(145*GoutedMasonryStrength-
1000))-0.002);
UltimateStrainGouted = MasonryFailureStrain-0.001;
UltimateStrainUngouted = MasonryFailureStrain-0.001;
UngoutedLength = TotalWallLength - GoutedLength;

MasonryTensionStrainUngouted1 =
MasonryStrengthTension/MasonryModulusUngouted;
MasonryTensionStrainGouted1 =
MasonryStrengthTension/MasonryModulusGouted;
MasonryTensionStrainUngouted2 = 4*MasonryTensionStrainUngouted1;
MasonryTensionStrainGouted2 = 4*MasonryTensionStrainGouted1;
MasonryTensionStrainUngouted3 = 10*MasonryTensionStrainUngouted1;
MasonryTensionStrainGouted3 = 10*MasonryTensionStrainGouted1;
TensionSlope1 = (-0.35*MasonryStrengthTension)/3;
TensionSlope2 = (-0.45*MasonryStrengthTension)/6;
TensionIntercept1 = (0.8*MasonryStrengthTension)-(TensionSlope1);
TensionIntercept2 = (0.45*MasonryStrengthTension)-(TensionSlope2*4);

% NO DEAD LOAD
if MasonryDeadLoad == 0

Strain = 0;
NeutralAxis = TotalThickness/2;

for j = 1:(NumberOfStrains+1)

    DeviationChange = 100;
    ErrorChange = 100;

for k = 1:100000

    GoutedSlice = (ThicknessIncrement/2);
    TotalGoutedForce = 0;
    TotalGoutedMoment = 0;

for f = 1:NumberOfSlices

    SliceStrain = Strain*((GoutedSlice-NeutralAxis)/NeutralAxis);

    if PeakStrainGouted <= SliceStrain && SliceStrain <= 0
        SliceStressGouted = (-
1)*GoutedMasonryStrength*((2*abs(SliceStrain)/0.002)-
((abs(SliceStrain))/0.002)^2);
    elseif UltimateStrainGouted <= SliceStrain && SliceStrain <
PeakStrainGouted

```

```

        SliceStressGrouted = (-1)*GroutedMasonryStrength*(1-
GroutedZ*(abs(SliceStrain)-abs(PeakStrainGrouted)));
        elseif 0 < SliceStrain && SliceStrain <=
MasonryTensionStrainGrouted1
            SliceStressGrouted = SliceStrain*MasonryModulusGrouted ;
            elseif MasonryTensionStrainGrouted1 < SliceStrain && SliceStrain
<= MasonryTensionStrainGrouted2
                SliceStressGrouted = TensionSlope1*SliceStrain +
TensionIntercept1;
            elseif MasonryTensionStrainGrouted2 < SliceStrain && SliceStrain
<= MasonryTensionStrainGrouted3
                SliceStressGrouted = TensionSlope2*SliceStrain +
TensionIntercept2;
            else
                SliceStressGrouted = 0;
            end

        SliceForceGrouted =
PhiM*SliceStressGrouted*ThicknessIncrement*GroutedLength;
        SliceMomentGrouted = GroutedSlice*SliceForceGrouted;

        TotalGroutedForce = TotalGroutedForce + SliceForceGrouted;
        TotalGroutedMoment = TotalGroutedMoment + SliceMomentGrouted;

        GroutedSlice = GroutedSlice + ThicknessIncrement;

end

    UngROUTedSlice = (ThicknessIncrement/2);
    TotalUngROUTedForce = 0;
    TotalUngROUTedMoment = 0;

    if UngROUTedLength ~= 0
for f = 1:NumberOfSlices

        SliceStrain = Strain*((UngROUTedSlice-NeutralAxis)/NeutralAxis);

        if PeakStrainUngROUTed <= SliceStrain && SliceStrain <= 0
            SliceStressUngROUTed = (-
1)*UngROUTedMasonryStrength*((2*abs(SliceStrain)/0.002)-
((abs(SliceStrain))/0.002)^2);
            elseif UltimateStrainUngROUTed <= SliceStrain && SliceStrain <
PeakStrainUngROUTed
                SliceStressUngROUTed = (-1)*UngROUTedMasonryStrength*(1-
UngROUTedZ*(abs(SliceStrain)-abs(PeakStrainUngROUTed)));

            elseif 0 < SliceStrain && SliceStrain <=
MasonryTensionStrainUngROUTed1
                SliceStressUngROUTed = SliceStrain*MasonryModulusGrouted ;
                elseif MasonryTensionStrainGrouted1 < SliceStrain && SliceStrain
<= MasonryTensionStrainUngROUTed2
                    SliceStressUngROUTed = TensionSlope1*SliceStrain +
TensionIntercept1;
                elseif MasonryTensionStrainGrouted2 < SliceStrain && SliceStrain
<= MasonryTensionStrainUngROUTed3

```

```

        SliceStressUngroued = TensionSlope2*SliceStrain +
TensionIntercept2;

    else
        SliceStressUngroued = 0;
    end

    if UngrouedSlice <= FaceShell
        SliceForceUngroued =
PhiM*SliceStressUngroued*ThicknessIncrement*UngrouedLength;
    elseif UngrouedSlice > FaceShell && UngrouedSlice <
(TotalThickness-FaceShell)
        SliceForceUngroued = 0;
    elseif UngrouedSlice >= (TotalThickness-FaceShell)
        SliceForceUngroued =
PhiM*SliceStressUngroued*ThicknessIncrement*UngrouedLength;
    end

    SliceMomentUngroued = UngrouedSlice*SliceForceUngroued;

    TotalUngrouedForce = TotalUngrouedForce + SliceForceUngroued;
    TotalUngrouedMoment = TotalUngrouedMoment +
SliceMomentUngroued;

    UngrouedSlice = UngrouedSlice + ThicknessIncrement;

end
end

TotalForceSteel = 0;
TotalMomentSteel = 0;

if SEASC == 2
for s = 1:NumberOfRebar
    SteelStrain{s} = Strain*((SteelDistance{s}-
NeutralAxis)/NeutralAxis);

    if SteelStrain{s} < YieldStrain && SteelStrain{s} >= 0
        SteelForce{s} =
PhiS*AreaOfSteel{s}*SteelModulus*SteelStrain{s};
    elseif SteelStrain{s} >= YieldStrain && SteelStrain{s} <
StrainHardeningStrain
        SteelForce{s} = PhiS*AreaOfSteel{s}*SteelStrength;
    elseif SteelStrain{s} >= StrainHardeningStrain && SteelStrain{s} <
SteelRuptureStrain
        SteelForce{s} = PhiS*(StrainHardeningModulus*SteelStrain{s} +
StrainHardeningIntercept)*AreaOfSteel{s};

    elseif SteelStrain{s} > (-1)*YieldStrain && SteelStrain{s} < 0
        SteelForce{s} =
PhiS*AreaOfSteel{s}*SteelModulus*SteelStrain{s};
    elseif SteelStrain{s} <= (-1)*YieldStrain && SteelStrain{s} > (-
1)*StrainHardeningStrain
        SteelForce{s} = (-1)*PhiS*AreaOfSteel{s}*SteelStrength;

```

```

elseif SteelStrain{s} <= (-1)*StrainHardeningStrain &&
SteelStrain{s} > (-1)*SteelRuptureStrain
    SteelForce{s} = (-
1)*PhiS*((StrainHardeningModulus*abs(SteelStrain{s}) +
StrainHardeningIntercept))*AreaOfSteel{s};
    else
        SteelForce{s} = 0;
    end

    SteelMoment{s} = SteelForce{s}*SteelDistance{s};

    TotalForceSteel = TotalForceSteel + SteelForce{s};
    TotalMomentSteel = TotalMomentSteel + SteelMoment{s};

end
elseif SEASC == 1
for s = 1:NumberOfRebar
    SteelStrain{s} = Strain*((SteelDistance{s}-
NeutralAxis)/NeutralAxis);

    if SteelStrain{s} < YieldStrain && SteelStrain{s} >= 0
        SteelForce{s} = AreaOfSteel{s}*SteelModulus*SteelStrain{s};
    elseif SteelStrain{s} >= YieldStrain && SteelStrain{s} < 0.0032
        SteelForce{s} = AreaOfSteel{s}*SteelStrength;
    elseif SteelStrain{s} >= 0.0032 && SteelStrain{s} < 0.038
        SteelForce{s} =
6.89475908677537*((30/0.0348)*SteelStrain{s}+67.24137932)*AreaOfSteel{
s};
    elseif SteelStrain{s} >= 0.038 && SteelStrain{s} < 0.09
        SteelForce{s} =
6.89475908677537*((10/0.052)*SteelStrain{s}+92.69230769)*AreaOfSteel{
s};
    elseif SteelStrain{s} >= 0.09 && SteelStrain{s} < 0.125
        SteelForce{s} = 6.89475908677537*((-
5/0.035)*SteelStrain{s}+122.8571429)*AreaOfSteel{s};
    elseif SteelStrain{s} >= 0.125 && SteelStrain{s} <= 0.15
        SteelForce{s} = 6.89475908677537*((-
25/0.025)*SteelStrain{s}+230)*AreaOfSteel{s};

    elseif SteelStrain{s} > (-1)*YieldStrain && SteelStrain{s} < 0
        SteelForce{s} = AreaOfSteel{s}*SteelModulus*SteelStrain{s};
    elseif SteelStrain{s} <= (-1)*YieldStrain && SteelStrain{s} > -
0.0032
        SteelForce{s} = (-1)*AreaOfSteel{s}*SteelStrength;
    elseif SteelStrain{s} <= -0.0032 && SteelStrain{s} > -0.038
        SteelForce{s} = 6.89475908677537*((30/0.0348)*SteelStrain{s}-
67.24137932)*AreaOfSteel{s};
    elseif SteelStrain{s} <= -0.038 && SteelStrain{s} > -0.09
        SteelForce{s} = 6.89475908677537*((10/0.052)*SteelStrain{s}-
92.69230769)*AreaOfSteel{s};
    elseif SteelStrain{s} <= -0.09 && SteelStrain{s} > -0.125
        SteelForce{s} = 6.89475908677537*((-5/0.035)*SteelStrain{s}-
122.8571429)*AreaOfSteel{s};
    elseif SteelStrain{s} <= -0.125 && SteelStrain{s} >= -0.15

```



```

        SteelForce{s} = 6.89475908677537*((-25/0.025)*SteelStrain{s}-
230)*AreaOfSteel{s};
    else
        SteelForce{s} = 0;
    end

    SteelMoment{s} = SteelForce{s}*SteelDistance{s};

    TotalForceSteel = TotalForceSteel + SteelForce{s};
    TotalMomentSteel = TotalMomentSteel + SteelMoment{s};

end
end

Deviation(k) = TotalForceSteel + TotalGroutedForce +
TotalUngoutedForce + AxialLoad;

CompleteMoment = TotalMomentSteel + TotalUngoutedMoment +
TotalGroutedMoment + AxialLoad*(TotalThickness/2);
CompleteCurvature = Strain/NeutralAxis;

if Deviation(k) > 0.1
    NeutralAxis = NeutralAxis + DeviationChange;
elseif Deviation(k) < -0.1
    NeutralAxis = NeutralAxis - DeviationChange;
elseif Deviation(k) <= 0.1 && Deviation(k) >= -0.1
    break
end

if k >= 4 && Deviation(k-3) > 0.00001 && Deviation(k-2) < -0.00001 &&
Deviation(k-1) > 0.00001 && Deviation(k) < -0.00001
    DeviationChange = 0.1*DeviationChange;
end

if NeutralAxis <= 0;
    DeviationChange = ErrorChange;
    NeutralAxis = 150.0;
    ErrorChange = 0.1*ErrorChange;
end

if NeutralAxis > 9999 || (k > 5 && Deviation(k) == Deviation(k-1) &&
Deviation(k-1) == Deviation(k-2))
    NeutralAxis = (TotalThickness/2);
    CompleteMoment = 0;
    CompleteCurvature = 0;
    break
end

end

end

Moment(j) = CompleteMoment;
Curvature(j) = CompleteCurvature;
CorrectNeutralAxis(j) = NeutralAxis;

Strain = Strain + StrainIncrement;

```

```

end

for d = 2:NumberOfStrains
    if Moment(d) < Moment(d-1)
        CurvatureCut(d) = d;
    else
        CurvatureCut(d) = 0;
    end
end
StartD = (min(CurvatureCut(CurvatureCut>0)))-1;
MaxElasticMoment = Moment((min(CurvatureCut(CurvatureCut>0)))-1);
for d = 2:length(CurvatureCut)
    if CurvatureCut(d) > 0
        Moment(d) = 0;
        Curvature(d) = 0;
    end
end
for d = StartD:NumberOfStrains
    if Moment(d) < MaxElasticMoment
        Moment(d) = 0;
        Curvature(d) = 0;
    end
end
LastValue = length(Moment);
Moment(LastValue) = 0;
Curvature(LastValue) = 0;
Moment = Moment(Moment ~= 0);
Curvature = Curvature(Curvature ~= 0);

for e = 1:(NumberOfElements+1)
    ElementMoment{e} = Moment;
    ElementCurvature{e} = Curvature;
end

end

% DEAD LOAD
if MasonryDeadLoad ~= 0

HeightIncrement = WallHeight/NumberOfElements;
NetArea = (GroutedLength*TotalThickness) + ((TotalWallLength-
GroutedLength)*FaceShell*2);
GrossArea = TotalThickness*TotalWallLength;
GroutingFactor = NetArea/GrossArea;
SelfWeight(1) =
MasonryDeadLoad*(TotalWallLength*WallHeight*TotalThickness)*GroutingFactor;
TotalSelfWeight =
MasonryDeadLoad*(TotalWallLength*WallHeight*TotalThickness)*GroutingFactor;

for w = 2:(NumberOfElements+1)

```

```

    SelfWeight(w) =
MasonryDeadLoad*(TotalWallLength*TotalThickness*(WallHeight - (w-
1)*HeightIncrement))*GroutingFactor;
end

for e = 1:(NumberOfElements+1)

Strain = 0;
NeutralAxis = TotalThickness/2;

for j = 1:(NumberOfStrains+1)

    DeviationChange = 100;
    ErrorChange = 100;

for k = 1:10000000

    GroutedSlice = (ThicknessIncrement/2);
    TotalGroutedForce = 0;
    TotalGroutedMoment = 0;

for f = 1:NumberOfSlices

    SliceStrain = Strain*((GroutedSlice-NeutralAxis)/NeutralAxis);

    if PeakStrainGrouted <= SliceStrain && SliceStrain <= 0
        SliceStressGrouted = (-
1)*GroutedMasonryStrength*((2*abs(SliceStrain)/0.002) -
((abs(SliceStrain))/0.002)^2));
        elseif UltimateStrainGrouted <= SliceStrain && SliceStrain <
PeakStrainGrouted
            SliceStressGrouted = (-1)*GroutedMasonryStrength*(1-
GroutedZ*(abs(SliceStrain)-abs(PeakStrainGrouted)));
        elseif 0 < SliceStrain && SliceStrain <=
MasonryTensionStrainGrouted1
            SliceStressGrouted = SliceStrain*MasonryModulusGrouted ;
        elseif MasonryTensionStrainGrouted1 < SliceStrain && SliceStrain
<= MasonryTensionStrainGrouted2
            SliceStressGrouted = TensionSlope1*SliceStrain +
TensionIntercept1;
        elseif MasonryTensionStrainGrouted2 < SliceStrain && SliceStrain
<= MasonryTensionStrainGrouted3
            SliceStressGrouted = TensionSlope2*SliceStrain +
TensionIntercept2;
        else
            SliceStressGrouted = 0;
        end

    SliceForceGrouted =
PhiM*SliceStressGrouted*ThicknessIncrement*GroutedLength;
    SliceMomentGrouted = GroutedSlice*SliceForceGrouted;

    TotalGroutedForce = TotalGroutedForce + SliceForceGrouted;
    TotalGroutedMoment = TotalGroutedMoment + SliceMomentGrouted;

```

```

    GroutedSlice = GroutedSlice + ThicknessIncrement;

end

    UngROUTEDSlice = (ThicknessIncrement/2);
    TotalUngROUTEDForce = 0;
    TotalUngROUTEDMoment = 0;

    if UngROUTEDLength ~= 0
for f = 1:NumberOfSlices

    SliceStrain = Strain*((UngROUTEDSlice-NeutralAxis)/NeutralAxis);

    if PeakStrainUngROUTED <= SliceStrain && SliceStrain <= 0
        SliceStressUngROUTED = (-
1)*UngROUTEDMasonryStrength*((2*abs(SliceStrain)/0.002) -
((abs(SliceStrain))/0.002)^2);
        elseif UltimateStrainUngROUTED <= SliceStrain && SliceStrain <
PeakStrainUngROUTED
            SliceStressUngROUTED = (-1)*UngROUTEDMasonryStrength*(1-
UngROUTEDZ*(abs(SliceStrain)-abs(PeakStrainUngROUTED)));
        elseif 0 < SliceStrain && SliceStrain <=
MasonryTensionStrainUngROUTED1
            SliceStressUngROUTED = SliceStrain*MasonryModulusGrouted ;
        elseif MasonryTensionStrainGrouted1 < SliceStrain && SliceStrain
<= MasonryTensionStrainUngROUTED2
            SliceStressUngROUTED = TensionSlope1*SliceStrain +
TensionIntercept1;
        elseif MasonryTensionStrainGrouted2 < SliceStrain && SliceStrain
<= MasonryTensionStrainUngROUTED3
            SliceStressUngROUTED = TensionSlope2*SliceStrain +
TensionIntercept2;
        else
            SliceStressUngROUTED = 0;
        end

        if UngROUTEDSlice <= FaceShell
            SliceForceUngROUTED =
PhiM*SliceStressUngROUTED*ThicknessIncrement*UngROUTEDLength;
        elseif UngROUTEDSlice > FaceShell && UngROUTEDSlice <
(TotalThickness-FaceShell)
            SliceForceUngROUTED = 0;
        elseif UngROUTEDSlice >= (TotalThickness-FaceShell)
            SliceForceUngROUTED =
PhiM*SliceStressUngROUTED*ThicknessIncrement*UngROUTEDLength;
        end

        SliceMomentUngROUTED = UngROUTEDSlice*SliceForceUngROUTED;

        TotalUngROUTEDForce = TotalUngROUTEDForce + SliceForceUngROUTED;
        TotalUngROUTEDMoment = TotalUngROUTEDMoment +
SliceMomentUngROUTED;

        UngROUTEDSlice = UngROUTEDSlice + ThicknessIncrement;

```

```

end
    end

TotalForceSteel = 0;
TotalMomentSteel = 0;

if SEASC == 2
for s = 1:NumberOfRebar
    SteelStrain{s} = Strain*((SteelDistance{s}-
NeutralAxis)/NeutralAxis);

        if SteelStrain{s} < YieldStrain && SteelStrain{s} >= 0
            SteelForce{s} =
PhiS*AreaOfSteel{s}*SteelModulus*SteelStrain{s};
        elseif SteelStrain{s} >= YieldStrain && SteelStrain{s} <
StrainHardeningStrain
            SteelForce{s} = PhiS*AreaOfSteel{s}*SteelStrength;
        elseif SteelStrain{s} >= StrainHardeningStrain && SteelStrain{s} <
SteelRuptureStrain
            SteelForce{s} = PhiS*(StrainHardeningModulus*SteelStrain{s} +
StrainHardeningIntercept)*AreaOfSteel{s};

        elseif SteelStrain{s} > (-1)*YieldStrain && SteelStrain{s} < 0
            SteelForce{s} =
PhiS*AreaOfSteel{s}*SteelModulus*SteelStrain{s};
        elseif SteelStrain{s} <= (-1)*YieldStrain && SteelStrain{s} > (-
1)*StrainHardeningStrain
            SteelForce{s} = (-1)*PhiS*AreaOfSteel{s}*SteelStrength;
        elseif SteelStrain{s} <= (-1)*StrainHardeningStrain &&
SteelStrain{s} > (-1)*SteelRuptureStrain
            SteelForce{s} = (-
1)*PhiS*((StrainHardeningModulus*abs(SteelStrain{s}) +
StrainHardeningIntercept))*AreaOfSteel{s};
        else
            SteelForce{s} = 0;
        end

        SteelMoment{s} = SteelForce{s}*SteelDistance{s};

        TotalForceSteel = TotalForceSteel + SteelForce{s};
        TotalMomentSteel = TotalMomentSteel + SteelMoment{s};

end
elseif SEASC == 1
for s = 1:NumberOfRebar
    SteelStrain{s} = Strain*((SteelDistance{s}-
NeutralAxis)/NeutralAxis);

        if SteelStrain{s} < YieldStrain && SteelStrain{s} >= 0
            SteelForce{s} = AreaOfSteel{s}*SteelModulus*SteelStrain{s};
        elseif SteelStrain{s} >= YieldStrain && SteelStrain{s} < 0.0032
            SteelForce{s} = AreaOfSteel{s}*SteelStrength;
        elseif SteelStrain{s} >= 0.0032 && SteelStrain{s} < 0.038

```

```

        SteelForce{s} =
6.89475908677537*((30/0.0348)*SteelStrain{s}+67.24137932)*AreaOfSteel{
s};
        elseif SteelStrain{s} >= 0.038 && SteelStrain{s} < 0.09
                SteelForce{s} =
6.89475908677537*((10/0.052)*SteelStrain{s}+92.69230769)*AreaOfSteel{s
};
        elseif SteelStrain{s} >= 0.09 && SteelStrain{s} < 0.125
                SteelForce{s} = 6.89475908677537*((-
5/0.035)*SteelStrain{s}+122.8571429)*AreaOfSteel{s};
        elseif SteelStrain{s} >= 0.125 && SteelStrain{s} <= 0.15
                SteelForce{s} = 6.89475908677537*((-
25/0.025)*SteelStrain{s}+230)*AreaOfSteel{s};

        elseif SteelStrain{s} > (-1)*YieldStrain && SteelStrain{s} < 0
                SteelForce{s} = AreaOfSteel{s}*SteelModulus*SteelStrain{s};
        elseif SteelStrain{s} <= (-1)*YieldStrain && SteelStrain{s} > -
0.0032
                SteelForce{s} = (-1)*AreaOfSteel{s}*SteelStrength;
        elseif SteelStrain{s} <= -0.0032 && SteelStrain{s} > -0.038
                SteelForce{s} = 6.89475908677537*((30/0.0348)*SteelStrain{s}-
67.24137932)*AreaOfSteel{s};
        elseif SteelStrain{s} <= -0.038 && SteelStrain{s} > -0.09
                SteelForce{s} = 6.89475908677537*((10/0.052)*SteelStrain{s}-
92.69230769)*AreaOfSteel{s};
        elseif SteelStrain{s} <= -0.09 && SteelStrain{s} > -0.125
                SteelForce{s} = 6.89475908677537*((-5/0.035)*SteelStrain{s}-
122.8571429)*AreaOfSteel{s};
        elseif SteelStrain{s} <= -0.125 && SteelStrain{s} >= -0.15
                SteelForce{s} = 6.89475908677537*((-25/0.025)*SteelStrain{s}-
230)*AreaOfSteel{s};
        else
                SteelForce{s} = 0;
        end

        SteelMoment{s} = SteelForce{s}*SteelDistance{s};

        TotalForceSteel = TotalForceSteel + SteelForce{s};
        TotalMomentSteel = TotalMomentSteel + SteelMoment{s};

end
end

Deviation(k) = TotalForceSteel + TotalGroutedForce +
TotalUngroupedForce + AxialLoad + SelfWeight(e);

CompleteMoment = TotalMomentSteel + TotalUngroupedMoment +
TotalGroutedMoment + (AxialLoad+SelfWeight(e))*(TotalThickness/2);
CompleteCurvature = Strain/NeutralAxis;

if Deviation(k) > 0.1
        NeutralAxis = NeutralAxis + DeviationChange;
elseif Deviation(k) < -0.1
        NeutralAxis = NeutralAxis - DeviationChange;
elseif Deviation(k) <= 0.1 && Deviation(k) >= -0.1

```

```

        break
    end

    if k >= 4 && Deviation(k-3) > 0.00001 && Deviation(k-2) < -0.00001 &&
Deviation(k-1) > 0.00001 && Deviation(k) < -0.00001
        DeviationChange = 0.1*DeviationChange;
    end

    if NeutralAxis <= 0;
        DeviationChange = ErrorChange;
        NeutralAxis = 150.0;
        ErrorChange = 0.1*ErrorChange;
    end

    if NeutralAxis > 9999999 || (k > 5 && Deviation(k) == Deviation(k-1)
&& Deviation(k-1) == Deviation(k-2))
        NeutralAxis = (TotalThickness/2);
        CompleteMoment = 0;
        CompleteCurvature = 0;
        break
    end

end

end

if CompleteMoment > 0
    Moment{e}(j) = CompleteMoment;
    Curvature{e}(j) = CompleteCurvature;
    CorrectNeutralAxis{e}(j) = NeutralAxis;
elseif CompleteMoment <= 0
    Moment{e}(j) = 0;
    Curvature{e}(j) = 0;
end

    Strain = Strain + StrainIncrement;

end

for d = 2:NumberOfStrains
    if Moment{e}(d) < Moment{e}(d-1)
        CurvatureCut(d) = d;
    end
end
StartD = (min(CurvatureCut(CurvatureCut>0)))-1;
MaxElasticMoment = Moment{e}((min(CurvatureCut(CurvatureCut>0)))-1);
for d = 2:length(CurvatureCut)
    if CurvatureCut(d) > 0
        Moment{e}(d) = 0;
        Curvature{e}(d) = 0;
    end
end
for d = StartD:NumberOfStrains
    if Moment{e}(d) < MaxElasticMoment
        Moment{e}(d) = 0;
        Curvature{e}(d) = 0;
    end
end

```

```

end
LastValue = length(Moment{e});
Moment{e}(LastValue) = 0;
Curvature{e}(LastValue) = 0;
Moment{e} = Moment{e}(Moment{e} ~= 0);
Curvature{e} = Curvature{e}(Curvature{e} ~= 0);

ElementMoment{e} = Moment{e};
ElementCurvature{e} = Curvature{e};
MaxMoment{e} = max(Moment{e}/1000000);
MaxCurvature{e} = max(Curvature{e});

end
end

% DELFECTION ANALYSIS

clear Moment

Stop0 = 0;
for w = 1:10000000
    LateralLoad = LateralLoadFactor*w;

    % DEFINE INTERVALS %
    DeltaHeight = WallHeight/NumberOfElements;
    HeightIncrement = WallHeight/NumberOfElements;

    % % SELF WEIGHT FORCE %
    NetArea = (GroutedLength*TotalThickness) + ((TotalWallLength-
    GroutedLength)*FaceShell*2);
    GrossArea = TotalThickness*TotalWallLength;
    GroutingFactor = NetArea/GrossArea;
    SelfWeight(1) =
    MasonryDeadLoad*(TotalWallLength*WallHeight*TotalThickness)*GroutingFactor;
    TotalSelfWeight =
    MasonryDeadLoad*(TotalWallLength*WallHeight*TotalThickness)*GroutingFactor;

    % PRELIMINARY CALCULATIONS
    TopMoment = AxialLoad*Eccentricity;
    TopReaction = ((LateralLoad*(WallHeight/2)) - (TopMoment/WallHeight));
    BottomReactionX = ((TopMoment/WallHeight) +
    (LateralLoad*(WallHeight/2)));
    BottomReactionY = AxialLoad + TotalSelfWeight;

    % FOUNDATION SUPPORT STIFFNESS
    if SupportStiffness == 1
        FoundationStiffness = RotationalStiffness*1000000;
    elseif SupportStiffness == 2
        FoundationStiffness = SpecifiedSupportStiffness*1000000;
    else
        FoundationStiffness = 0;
    end
end

```



```

% INITIAL CONDITIONS %
Deflection(1) = 0;
SpecificCurvature(1) = 0;
SlopeChange = 0.000001;

if w == 1
    Slope(1) = -0.000001;
else
    Slope(1) = (-1)*InitialSlope(w-1);
end

% CREATE A CHECK TO DETERMINE IF THE CORRECT VALUE OF SLOPE WAS USED %
for s = 1:100000000
    BottomMoment = abs(Slope(1))*FoundationStiffness;

% CREATE THE LOOP TO GO THROUGH EACH ELEMENT %
for e = 2:(NumberOfElements + 1)

% CREATE THE EQUATION FOR THE PRIMARY MOMENT %
PrimaryMoment(e) = ((BottomReactionX*(DeltaHeight)) -
(LateralLoad*((DeltaHeight^2)/2))) - BottomMoment;

% DETERMINE THE TOTAL MOMENT AT THE ELEMENT %
if SecondOrderEffects == 1
Moment(e) = PrimaryMoment(e) + ((AxialLoad+(TotalSelfWeight*(1-
(DeltaHeight/WallHeight))))*abs(Deflection(e-1)));
else
Moment(e) = PrimaryMoment(e);
end

% DETERMINE MATERIAL FAILURE %
if abs(Moment(e)) > max(ElementMoment{e})
    Stop0 = 1;
    fprintf('\n')
    fprintf('Failure Occured: Material \n\n')
    break
end

% DETERMINE THE CURVATURE ASSOCIATED WITH THE TOTAL MOMENT %
Value1 = abs(ElementMoment{e} - abs(Moment(e)));
[Index Index] = min(Value1);
Closest = ElementMoment{e}(Index);
if abs(Moment(e)) < 0.00001
    SpecificCurvature(e) = 0;
    SpecificCurvature = max(ElementCurvature{e});
elseif Index == 1
    SpecificCurvature(e) = ElementCurvature{e}(Index);
elseif Index == 501
    SpecificCurvature(e) = ElementCurvature{e}(Index);
elseif Closest > abs(Moment(e))
    SpecificCurvature(e) = ElementCurvature{e}(Index) -
((ElementMoment{e}(Index)-abs(Moment(e)))/(ElementMoment{e}(Index)-
ElementMoment{e}(Index-1))*ElementCurvature{e}(Index)-
ElementCurvature{e}(Index-1)));

```

```

        elseif Closest < abs(Moment(e))
            SpecificCurvature(e) = ElementCurvature{e}(Index+1) -
            ((ElementMoment{e}(Index+1) -
            abs(Moment(e)))/(ElementMoment{e}(Index+1) -
            ElementMoment{e}(Index))*ElementCurvature{e}(Index+1) -
            ElementCurvature{e}(Index));
            end

% ACCOUNT FOR NEGATIVE MOMENTS %
if Moment(e) < 0
    SpecificCurvature(e) = (-1.0)*SpecificCurvature(e);
end

% DETERMINE THE SLOPE AT THE NEXT ELEMENT %
Slope(e) = Slope(e-1) + SpecificCurvature(e)*HeightIncrement;

% CALCULATE THE DEFLECTION AT THE END OF THE ELEMENT %
if SpecificCurvature(e) <= 0
    Deflection(e) = Deflection(e-1) + (Slope(e-1)*HeightIncrement) -
    ((0.5)*(SpecificCurvature(e))*(HeightIncrement^2));
elseif SpecificCurvature(e) > 0
    Deflection(e) = Deflection(e-1) + (Slope(e-1)*HeightIncrement) +
    ((0.5)*(SpecificCurvature(e))*(HeightIncrement^2));
end
% MUST FIX THE DELTA HEIGHT TO ADJUST THE PRIMARY MOMENT FOR THE NEXT
ITERATION %
DeltaHeight = DeltaHeight + HeightIncrement;

end
if Stop0 == 1
    break
end

% CHECK THE SLOPE %
DeflectionCheck(s) = Deflection(NumberOfElements+1);

if DeflectionCheck(s) > 0.1
    Slope(1) = Slope(1) - SlopeChange;
elseif DeflectionCheck(s) < -0.1
    Slope(1) = Slope(1) + SlopeChange;
elseif DeflectionCheck(s) <= 0.1 && DeflectionCheck(s) >= -0.1
    CompleteDeflection = Deflection;
    break
end

% CATCH THE ERROR IN SLOPE CHANGE %
if s >= 10 && DeflectionCheck(s-4) < -0.1 && DeflectionCheck(s-3) >
0.1 && DeflectionCheck(s-2) < -0.1 && DeflectionCheck(s-1) > 0.1 &&
DeflectionCheck(s) < -0.1
    SlopeChange = 0.1*SlopeChange;
end

% RESET THE DELTA HEIGHT
DeltaHeight = WallHeight/NumberOfElements;

```

```

end

if Stop0 == 1
    break
end

% TRACK THE DEFLECTION AT A SPECIFIC LATERAL LOAD
MidspanDeflection(w) = abs(Deflection(((NumberOfElements+1)/2)));
InitialSlope(w) = abs(Slope(1));
TotalLateralLoad(w) = LateralLoad;

% CAPTURE THE DEFLECTION AND BENDING MOMENT PROFILE
MomentProfile{w} = Moment;
DeflectionProfile{w} = Deflection;

% CALCULATE THE FLEXURAL RIGIDITY

FlexuralRigidity(w) =
(Moment(((NumberOfElements+1)/2))/SpecificCurvature(((NumberOfElements
+1)/2)));
EffectiveStiffness(w) = FlexuralRigidity(w)/(1e12);

if w >= 5
Pcritical(w) = ((pi^2)*FlexuralRigidity(w))/(WallHeight^2);
if AxialLoad >= Pcritical(w)
    fprintf('Failure Occured: Buckling \n')
    fprintf('\n')
    break
end
end

fprintf('          %6.2f          |',TotalLateralLoad(w));
fprintf('          %7.2f          |',MidspanDeflection(w));
fprintf('          %5.2f \n',EffectiveStiffness(w));
end

fprintf('Analysis Complete!\n')
end

%% ANALYSIS TYPE 6 - 3 POINT BEND WITH ECCENTRIC AXIAL LOAD

if AnalysisType == 6

fprintf('Analysis Started \n')
fprintf('\n')

% MAX AXIAL LOAD
TotalRebarArea = 0;
UngoutedArea = 2*(TotalWallLength-GroutedLength)*FaceShell;
GroutedArea = GroutedLength*TotalThickness;
for s = 1:NumberOfRebar
    TotalRebarArea = TotalRebarArea + AreaOfSteel{s};

```

```

end
MaxAxialLoad =
((GroutedMasonryStrength*GroutedArea)+(UngoutedMasonryStrength*Ungrou
tedArea)+(TotalRebarArea*SteelStrength))/1000;
fprintf('Max Axial Load (kN): %4.0f \n',MaxAxialLoad)
fprintf('\n')

fprintf('      Lateral Load (kN) | Midspan Deflection (mm) | Flexural
Rigidity (x10^12) (Nmm^2) \n')
fprintf('      |                                     |\n')
fprintf('      %3.2f          |',0);
fprintf('      %5.2f          |',0);
fprintf('      INF \n');

% MOMENT CURVATURE ANALYSIS

% PRELIMINARY CALCULATIONS
StrainIncrement = abs(MasonryFailureStrain)/NumberOfStrains;
ThicknessIncrement = TotalThickness/NumberOfSlices;
YieldStrain = SteelStrength/SteelModulus;
StrainHardeningIntercept = SteelStrength -
(StrainHardeningModulus*StrainHardeningStrain);
UngoutedZ =
0.5/(((3+0.29*UngoutedMasonryStrength)/(145*UngoutedMasonryStrength-
1000))-0.002);
GroutedZ =
0.5/(((3+0.29*GroutedMasonryStrength)/(145*GroutedMasonryStrength-
1000))-0.002);
UltimateStrainGrouted = MasonryFailureStrain-0.001;
UltimateStrainUngouted = MasonryFailureStrain-0.001;
UngoutedLength = TotalWallLength - GroutedLength;

MasonryTensionStrainUngouted1 =
MasonryStrengthTension/MasonryModulusUngouted;
MasonryTensionStrainGrouted1 =
MasonryStrengthTension/MasonryModulusGrouted;
MasonryTensionStrainUngouted2 = 4*MasonryTensionStrainUngouted1;
MasonryTensionStrainGrouted2 = 4*MasonryTensionStrainGrouted1;
MasonryTensionStrainUngouted3 = 10*MasonryTensionStrainUngouted1;
MasonryTensionStrainGrouted3 = 10*MasonryTensionStrainGrouted1;
TensionSlope1 = (-0.35*MasonryStrengthTension)/3;
TensionSlope2 = (-0.45*MasonryStrengthTension)/6;
TensionIntercept1 = (0.8*MasonryStrengthTension)-(TensionSlope1);
TensionIntercept2 = (0.45*MasonryStrengthTension)-(TensionSlope2*4);

% NO DEAD LOAD
if MasonryDeadLoad == 0

Strain = 0;
NeutralAxis = TotalThickness/2;

for j = 1:(NumberOfStrains+1)

    DeviationChange = 100;
    ErrorChange = 100;

```

```

for k = 1:100000

    GroutedSlice = (ThicknessIncrement/2);
    TotalGroutedForce = 0;
    TotalGroutedMoment = 0;

for f = 1:NumberOfSlices

    SliceStrain = Strain*((GroutedSlice-NeutralAxis)/NeutralAxis);

    if PeakStrainGrouted <= SliceStrain && SliceStrain <= 0
        SliceStressGrouted = (-
1)*GroutedMasonryStrength*((2*abs(SliceStrain)/0.002)-
((abs(SliceStrain))/0.002)^2);
        elseif UltimateStrainGrouted <= SliceStrain && SliceStrain <
PeakStrainGrouted
            SliceStressGrouted = (-1)*GroutedMasonryStrength*(1-
GroutedZ*(abs(SliceStrain)-abs(PeakStrainGrouted)));
        elseif 0 < SliceStrain && SliceStrain <=
MasonryTensionStrainGrouted1
            SliceStressGrouted = SliceStrain*MasonryModulusGrouted ;
        elseif MasonryTensionStrainGrouted1 < SliceStrain && SliceStrain
<= MasonryTensionStrainGrouted2
            SliceStressGrouted = TensionSlope1*SliceStrain +
TensionIntercept1;
        elseif MasonryTensionStrainGrouted2 < SliceStrain && SliceStrain
<= MasonryTensionStrainGrouted3
            SliceStressGrouted = TensionSlope2*SliceStrain +
TensionIntercept2;
        else
            SliceStressGrouted = 0;
        end

    SliceForceGrouted =
PhiM*SliceStressGrouted*ThicknessIncrement*GroutedLength;
    SliceMomentGrouted = GroutedSlice*SliceForceGrouted;

    TotalGroutedForce = TotalGroutedForce + SliceForceGrouted;
    TotalGroutedMoment = TotalGroutedMoment + SliceMomentGrouted;

    GroutedSlice = GroutedSlice + ThicknessIncrement;

end

    UngroatedSlice = (ThicknessIncrement/2);
    TotalUngroatedForce = 0;
    TotalUngroatedMoment = 0;

    if UngroatedLength ~= 0
for f = 1:NumberOfSlices

    SliceStrain = Strain*((UngroatedSlice-NeutralAxis)/NeutralAxis);

    if PeakStrainUngroated <= SliceStrain && SliceStrain <= 0

```

```

        SliceStressUngroued = (-
1)*UngrouedMasonryStrength*((2*abs(SliceStrain)/0.002)-
((abs(SliceStrain))/0.002)^2));
        elseif UltimateStrainUngroued <= SliceStrain && SliceStrain <
PeakStrainUngroued
            SliceStressUngroued = (-1)*UngrouedMasonryStrength*(1-
UngrouedZ*(abs(SliceStrain)-abs(PeakStrainUngroued)));

        elseif 0 < SliceStrain && SliceStrain <=
MasonryTensionStrainUngroued1
            SliceStressUngroued = SliceStrain*MasonryModulusGroued ;
            elseif MasonryTensionStrainGroued1 < SliceStrain && SliceStrain
<= MasonryTensionStrainUngroued2
                SliceStressUngroued = TensionSlope1*SliceStrain +
TensionIntercept1;
            elseif MasonryTensionStrainGroued2 < SliceStrain && SliceStrain
<= MasonryTensionStrainUngroued3
                SliceStressUngroued = TensionSlope2*SliceStrain +
TensionIntercept2;

        else
            SliceStressUngroued = 0;
        end

        if UngrouedSlice <= FaceShell
            SliceForceUngroued =
PhiM*SliceStressUngroued*ThicknessIncrement*UngrouedLength;
            elseif UngrouedSlice > FaceShell && UngrouedSlice <
(TotalThickness-FaceShell)
                SliceForceUngroued = 0;
            elseif UngrouedSlice >= (TotalThickness-FaceShell)
                SliceForceUngroued =
PhiM*SliceStressUngroued*ThicknessIncrement*UngrouedLength;
            end

        SliceMomentUngroued = UngrouedSlice*SliceForceUngroued;

        TotalUngrouedForce = TotalUngrouedForce + SliceForceUngroued;
        TotalUngrouedMoment = TotalUngrouedMoment +
SliceMomentUngroued;

        UngrouedSlice = UngrouedSlice + ThicknessIncrement;

end
end

TotalForceSteel = 0;
TotalMomentSteel = 0;

if SEASC == 2
for s = 1:NumberOfRebar
    SteelStrain{s} = Strain*((SteelDistance{s}-
NeutralAxis)/NeutralAxis);

    if SteelStrain{s} < YieldStrain && SteelStrain{s} >= 0

```

```

        SteelForce{s} =
PhiS*AreaOfSteel{s}*SteelModulus*SteelStrain{s};
        elseif SteelStrain{s} >= YieldStrain && SteelStrain{s} <
StrainHardeningStrain
        SteelForce{s} = PhiS*AreaOfSteel{s}*SteelStrength;
        elseif SteelStrain{s} >= StrainHardeningStrain && SteelStrain{s} <
SteelRuptureStrain
        SteelForce{s} = PhiS*(StrainHardeningModulus*SteelStrain{s} +
StrainHardeningIntercept)*AreaOfSteel{s};

        elseif SteelStrain{s} > (-1)*YieldStrain && SteelStrain{s} < 0
        SteelForce{s} =
PhiS*AreaOfSteel{s}*SteelModulus*SteelStrain{s};
        elseif SteelStrain{s} <= (-1)*YieldStrain && SteelStrain{s} > (-
1)*StrainHardeningStrain
        SteelForce{s} = (-1)*PhiS*AreaOfSteel{s}*SteelStrength;
        elseif SteelStrain{s} <= (-1)*StrainHardeningStrain &&
SteelStrain{s} > (-1)*SteelRuptureStrain
        SteelForce{s} = (-
1)*PhiS*((StrainHardeningModulus*abs(SteelStrain{s})) +
StrainHardeningIntercept))*AreaOfSteel{s};
        else
        SteelForce{s} = 0;
        end

        SteelMoment{s} = SteelForce{s}*SteelDistance{s};

        TotalForceSteel = TotalForceSteel + SteelForce{s};
        TotalMomentSteel = TotalMomentSteel + SteelMoment{s};

end
elseif SEASC == 1
for s = 1:NumberOfRebar
    SteelStrain{s} = Strain*((SteelDistance{s}-
NeutralAxis)/NeutralAxis);

    if SteelStrain{s} < YieldStrain && SteelStrain{s} >= 0
        SteelForce{s} = AreaOfSteel{s}*SteelModulus*SteelStrain{s};
    elseif SteelStrain{s} >= YieldStrain && SteelStrain{s} < 0.0032
        SteelForce{s} = AreaOfSteel{s}*SteelStrength;
    elseif SteelStrain{s} >= 0.0032 && SteelStrain{s} < 0.038
        SteelForce{s} =
6.89475908677537*((30/0.0348)*SteelStrain{s}+67.24137932)*AreaOfSteel{
s};
    elseif SteelStrain{s} >= 0.038 && SteelStrain{s} < 0.09
        SteelForce{s} =
6.89475908677537*((10/0.052)*SteelStrain{s}+92.69230769)*AreaOfSteel{s
};
    elseif SteelStrain{s} >= 0.09 && SteelStrain{s} < 0.125
        SteelForce{s} = 6.89475908677537*((-
5/0.035)*SteelStrain{s}+122.8571429)*AreaOfSteel{s};
    elseif SteelStrain{s} >= 0.125 && SteelStrain{s} <= 0.15
        SteelForce{s} = 6.89475908677537*((-
25/0.025)*SteelStrain{s}+230)*AreaOfSteel{s};

```

```

elseif SteelStrain{s} > (-1)*YieldStrain && SteelStrain{s} < 0
    SteelForce{s} = AreaOfSteel{s}*SteelModulus*SteelStrain{s};
elseif SteelStrain{s} <= (-1)*YieldStrain && SteelStrain{s} > -
0.0032
    SteelForce{s} = (-1)*AreaOfSteel{s}*SteelStrength;
elseif SteelStrain{s} <= -0.0032 && SteelStrain{s} > -0.038
    SteelForce{s} = 6.89475908677537*((30/0.0348)*SteelStrain{s}-
67.24137932)*AreaOfSteel{s};
elseif SteelStrain{s} <= -0.038 && SteelStrain{s} > -0.09
    SteelForce{s} = 6.89475908677537*((10/0.052)*SteelStrain{s}-
92.69230769)*AreaOfSteel{s};
elseif SteelStrain{s} <= -0.09 && SteelStrain{s} > -0.125
    SteelForce{s} = 6.89475908677537*((-5/0.035)*SteelStrain{s}-
122.8571429)*AreaOfSteel{s};
elseif SteelStrain{s} <= -0.125 && SteelStrain{s} >= -0.15
    SteelForce{s} = 6.89475908677537*((-25/0.025)*SteelStrain{s}-
230)*AreaOfSteel{s};
else
    SteelForce{s} = 0;
end

SteelMoment{s} = SteelForce{s}*SteelDistance{s};

TotalForceSteel = TotalForceSteel + SteelForce{s};
TotalMomentSteel = TotalMomentSteel + SteelMoment{s};

end
end

Deviation(k) = TotalForceSteel + TotalGroutedForce +
TotalUngoutedForce + AxialLoad;

CompleteMoment = TotalMomentSteel + TotalUngoutedMoment +
TotalGroutedMoment + AxialLoad*(TotalThickness/2);
CompleteCurvature = Strain/NeutralAxis;

if Deviation(k) > 0.1
    NeutralAxis = NeutralAxis + DeviationChange;
elseif Deviation(k) < -0.1
    NeutralAxis = NeutralAxis - DeviationChange;
elseif Deviation(k) <= 0.1 && Deviation(k) >= -0.1
    break
end

if k >= 4 && Deviation(k-3) > 0.00001 && Deviation(k-2) < -0.00001 &&
Deviation(k-1) > 0.00001 && Deviation(k) < -0.00001
    DeviationChange = 0.1*DeviationChange;
end

if NeutralAxis <= 0;
    DeviationChange = ErrorChange;
    NeutralAxis = 150.0;
    ErrorChange = 0.1*ErrorChange;
end

```



```

    if NeutralAxis > 9999 || (k > 5 && Deviation(k) == Deviation(k-1) &&
Deviation(k-1) == Deviation(k-2))
        NeutralAxis = (TotalThickness/2);
        CompleteMoment = 0;
        CompleteCurvature = 0;
        break
    end
end

    Moment(j) = CompleteMoment;
    Curvature(j) = CompleteCurvature;
    CorrectNeutralAxis(j) = NeutralAxis;

    Strain = Strain + StrainIncrement;

end

for d = 2:NumberOfStrains
    if Moment(d) < Moment(d-1)
        CurvatureCut(d) = d;
    else
        CurvatureCut(d) = 0;
    end
end
StartD = (min(CurvatureCut(CurvatureCut>0)))-1;
MaxElasticMoment = Moment((min(CurvatureCut(CurvatureCut>0)))-1);
for d = 2:length(CurvatureCut)
    if CurvatureCut(d) > 0
        Moment(d) = 0;
        Curvature(d) = 0;
    end
end
for d = StartD:NumberOfStrains
    if Moment(d) < MaxElasticMoment
        Moment(d) = 0;
        Curvature(d) = 0;
    end
end
LastValue = length(Moment);
Moment(LastValue) = 0;
Curvature(LastValue) = 0;
Moment = Moment(Moment ~= 0);
Curvature = Curvature(Curvature ~= 0);

for e = 1:(NumberOfElements+1)
    ElementMoment{e} = Moment;
    ElementCurvature{e} = Curvature;
end

end

% DEAD LOAD
if MasonryDeadLoad ~= 0

```

```

HeightIncrement = WallHeight/NumberOfElements;
NetArea = (GroutedLength*TotalThickness) + ((TotalWallLength-
GroutedLength)*FaceShell*2);
GrossArea = TotalThickness*TotalWallLength;
GroutingFactor = NetArea/GrossArea;
SelfWeight(1) =
MasonryDeadLoad*(TotalWallLength*WallHeight*TotalThickness)*GroutingFa
ctor;
TotalSelfWeight =
MasonryDeadLoad*(TotalWallLength*WallHeight*TotalThickness)*GroutingFa
ctor;

for w = 2:(NumberOfElements+1)
    SelfWeight(w) =
MasonryDeadLoad*(TotalWallLength*TotalThickness*(WallHeight - (w-
1)*HeightIncrement))*GroutingFactor;
end

for e = 1:(NumberOfElements+1)

Strain = 0;
NeutralAxis = TotalThickness/2;

for j = 1:(NumberOfStrains+1)

    DeviationChange = 100;
    ErrorChange = 100;

for k = 1:10000000

    GroutedSlice = (ThicknessIncrement/2);
    TotalGroutedForce = 0;
    TotalGroutedMoment = 0;

for f = 1:NumberOfSlices

    SliceStrain = Strain*((GroutedSlice-NeutralAxis)/NeutralAxis);

    if PeakStrainGrouted <= SliceStrain && SliceStrain <= 0
        SliceStressGrouted = (-
1)*GroutedMasonryStrength*((2*abs(SliceStrain)/0.002)-
((abs(SliceStrain))/0.002)^2));
    elseif UltimateStrainGrouted <= SliceStrain && SliceStrain <
PeakStrainGrouted
        SliceStressGrouted = (-1)*GroutedMasonryStrength*(1-
GroutedZ*(abs(SliceStrain)-abs(PeakStrainGrouted)));
    elseif 0 < SliceStrain && SliceStrain <=
MasonryTensionStrainGrouted1
        SliceStressGrouted = SliceStrain*MasonryModulusGrouted ;
    elseif MasonryTensionStrainGrouted1 < SliceStrain && SliceStrain
<= MasonryTensionStrainGrouted2
        SliceStressGrouted = TensionSlope1*SliceStrain +
TensionIntercept1;
    elseif MasonryTensionStrainGrouted2 < SliceStrain && SliceStrain
<= MasonryTensionStrainGrouted3

```

```

        SliceStressGrouted = TensionSlope2*SliceStrain +
TensionIntercept2;
    else
        SliceStressGrouted = 0;
    end

    SliceForceGrouted =
PhiM*SliceStressGrouted*ThicknessIncrement*GroutedLength;
    SliceMomentGrouted = GroutedSlice*SliceForceGrouted;

    TotalGroutedForce = TotalGroutedForce + SliceForceGrouted;
    TotalGroutedMoment = TotalGroutedMoment + SliceMomentGrouted;

    GroutedSlice = GroutedSlice + ThicknessIncrement;

end

    UngROUTedSlice = (ThicknessIncrement/2);
    TotalUngROUTedForce = 0;
    TotalUngROUTedMoment = 0;

    if UngROUTedLength ~= 0
for f = 1:NumberOfSlices

    SliceStrain = Strain*((UngROUTedSlice-NeutralAxis)/NeutralAxis);

    if PeakStrainUngROUTed <= SliceStrain && SliceStrain <= 0
        SliceStressUngROUTed = (-
1)*UngROUTedMasonryStrength*((2*abs(SliceStrain)/0.002)-
((abs(SliceStrain))/0.002)^2));
        elseif UltimateStrainUngROUTed <= SliceStrain && SliceStrain <
PeakStrainUngROUTed
            SliceStressUngROUTed = (-1)*UngROUTedMasonryStrength*(1-
UngROUTedZ*(abs(SliceStrain)-abs(PeakStrainUngROUTed)));
        elseif 0 < SliceStrain && SliceStrain <=
MasonryTensionStrainUngROUTed1
            SliceStressUngROUTed = SliceStrain*MasonryModulusGrouted ;
        elseif MasonryTensionStrainGrouted1 < SliceStrain && SliceStrain
<= MasonryTensionStrainUngROUTed2
            SliceStressUngROUTed = TensionSlope1*SliceStrain +
TensionIntercept1;
        elseif MasonryTensionStrainGrouted2 < SliceStrain && SliceStrain
<= MasonryTensionStrainUngROUTed3
            SliceStressUngROUTed = TensionSlope2*SliceStrain +
TensionIntercept2;
        else
            SliceStressUngROUTed = 0;
        end

        if UngROUTedSlice <= FaceShell
            SliceForceUngROUTed =
PhiM*SliceStressUngROUTed*ThicknessIncrement*UngROUTedLength;
        elseif UngROUTedSlice > FaceShell && UngROUTedSlice <
(TotalThickness-FaceShell)
            SliceForceUngROUTed = 0;

```

```

        elseif UngroupedSlice >= (TotalThickness-FaceShell)
            SliceForceUngrouped =
PhiM*SliceStressUngrouped*ThicknessIncrement*UngroupedLength;
        end

        SliceMomentUngrouped = UngroupedSlice*SliceForceUngrouped;

        TotalUngroupedForce = TotalUngroupedForce + SliceForceUngrouped;
        TotalUngroupedMoment = TotalUngroupedMoment +
SliceMomentUngrouped;

        UngroupedSlice = UngroupedSlice + ThicknessIncrement;

end
end

TotalForceSteel = 0;
TotalMomentSteel = 0;

if SEASC == 2
for s = 1:NumberOfRebar
    SteelStrain{s} = Strain*((SteelDistance{s}-
NeutralAxis)/NeutralAxis);

    if SteelStrain{s} < YieldStrain && SteelStrain{s} >= 0
        SteelForce{s} =
PhiS*AreaOfSteel{s}*SteelModulus*SteelStrain{s};
    elseif SteelStrain{s} >= YieldStrain && SteelStrain{s} <
StrainHardeningStrain
        SteelForce{s} = PhiS*AreaOfSteel{s}*SteelStrength;
    elseif SteelStrain{s} >= StrainHardeningStrain && SteelStrain{s} <
SteelRuptureStrain
        SteelForce{s} = PhiS*(StrainHardeningModulus*SteelStrain{s} +
StrainHardeningIntercept)*AreaOfSteel{s};

    elseif SteelStrain{s} > (-1)*YieldStrain && SteelStrain{s} < 0
        SteelForce{s} =
PhiS*AreaOfSteel{s}*SteelModulus*SteelStrain{s};
    elseif SteelStrain{s} <= (-1)*YieldStrain && SteelStrain{s} > (-
1)*StrainHardeningStrain
        SteelForce{s} = (-1)*PhiS*AreaOfSteel{s}*SteelStrength;
    elseif SteelStrain{s} <= (-1)*StrainHardeningStrain &&
SteelStrain{s} > (-1)*SteelRuptureStrain
        SteelForce{s} = (-
1)*PhiS*((StrainHardeningModulus*abs(SteelStrain{s})) +
StrainHardeningIntercept)*AreaOfSteel{s};
    else
        SteelForce{s} = 0;
    end

    SteelMoment{s} = SteelForce{s}*SteelDistance{s};

    TotalForceSteel = TotalForceSteel + SteelForce{s};
    TotalMomentSteel = TotalMomentSteel + SteelMoment{s};

```

```

end
elseif SEASC == 1
for s = 1:NumberOfRebar
    SteelStrain{s} = Strain*((SteelDistance{s}-
NeutralAxis)/NeutralAxis);

    if SteelStrain{s} < YieldStrain && SteelStrain{s} >= 0
        SteelForce{s} = AreaOfSteel{s}*SteelModulus*SteelStrain{s};
    elseif SteelStrain{s} >= YieldStrain && SteelStrain{s} < 0.0032
        SteelForce{s} = AreaOfSteel{s}*SteelStrength;
    elseif SteelStrain{s} >= 0.0032 && SteelStrain{s} < 0.038
        SteelForce{s} =
6.89475908677537*((30/0.0348)*SteelStrain{s}+67.24137932)*AreaOfSteel{
s};
    elseif SteelStrain{s} >= 0.038 && SteelStrain{s} < 0.09
        SteelForce{s} =
6.89475908677537*((10/0.052)*SteelStrain{s}+92.69230769)*AreaOfSteel{s
};
    elseif SteelStrain{s} >= 0.09 && SteelStrain{s} < 0.125
        SteelForce{s} = 6.89475908677537*((-
5/0.035)*SteelStrain{s}+122.8571429)*AreaOfSteel{s};
    elseif SteelStrain{s} >= 0.125 && SteelStrain{s} <= 0.15
        SteelForce{s} = 6.89475908677537*((-
25/0.025)*SteelStrain{s}+230)*AreaOfSteel{s};

    elseif SteelStrain{s} > (-1)*YieldStrain && SteelStrain{s} < 0
        SteelForce{s} = AreaOfSteel{s}*SteelModulus*SteelStrain{s};
    elseif SteelStrain{s} <= (-1)*YieldStrain && SteelStrain{s} > -
0.0032
        SteelForce{s} = (-1)*AreaOfSteel{s}*SteelStrength;
    elseif SteelStrain{s} <= -0.0032 && SteelStrain{s} > -0.038
        SteelForce{s} = 6.89475908677537*((30/0.0348)*SteelStrain{s}-
67.24137932)*AreaOfSteel{s};
    elseif SteelStrain{s} <= -0.038 && SteelStrain{s} > -0.09
        SteelForce{s} = 6.89475908677537*((10/0.052)*SteelStrain{s}-
92.69230769)*AreaOfSteel{s};
    elseif SteelStrain{s} <= -0.09 && SteelStrain{s} > -0.125
        SteelForce{s} = 6.89475908677537*((-5/0.035)*SteelStrain{s}-
122.8571429)*AreaOfSteel{s};
    elseif SteelStrain{s} <= -0.125 && SteelStrain{s} >= -0.15
        SteelForce{s} = 6.89475908677537*((-25/0.025)*SteelStrain{s}-
230)*AreaOfSteel{s};
    else
        SteelForce{s} = 0;
    end

    SteelMoment{s} = SteelForce{s}*SteelDistance{s};

    TotalForceSteel = TotalForceSteel + SteelForce{s};
    TotalMomentSteel = TotalMomentSteel + SteelMoment{s};

end
end

```

```

Deviation(k) = TotalForceSteel + TotalGroutedForce +
TotalUngroudedForce + AxialLoad + SelfWeight(e);

CompleteMoment = TotalMomentSteel + TotalUngroudedMoment +
TotalGroutedMoment + (AxialLoad+SelfWeight(e))*(TotalThickness/2);
CompleteCurvature = Strain/NeutralAxis;

if Deviation(k) > 0.1
    NeutralAxis = NeutralAxis + DeviationChange;
elseif Deviation(k) < -0.1
    NeutralAxis = NeutralAxis - DeviationChange;
elseif Deviation(k) <= 0.1 && Deviation(k) >= -0.1
    break
end

if k >= 4 && Deviation(k-3) > 0.00001 && Deviation(k-2) < -0.00001 &&
Deviation(k-1) > 0.00001 && Deviation(k) < -0.00001
    DeviationChange = 0.1*DeviationChange;
end

if NeutralAxis <= 0;
    DeviationChange = ErrorChange;
    NeutralAxis = 150.0;
    ErrorChange = 0.1*ErrorChange;
end

if NeutralAxis > 9999999 || (k > 5 && Deviation(k) == Deviation(k-1)
&& Deviation(k-1) == Deviation(k-2))
    NeutralAxis = (TotalThickness/2);
    CompleteMoment = 0;
    CompleteCurvature = 0;
    break
end

end

if CompleteMoment > 0
    Moment{e}(j) = CompleteMoment;
    Curvature{e}(j) = CompleteCurvature;
    CorrectNeutralAxis{e}(j) = NeutralAxis;
elseif CompleteMoment <= 0
    Moment{e}(j) = 0;
    Curvature{e}(j) = 0;
end

    Strain = Strain + StrainIncrement;

end

for d = 2:NumberOfStrains
    if Moment{e}(d) < Moment{e}(d-1)
        CurvatureCut(d) = d;
    end
end
StartD = (min(CurvatureCut(CurvatureCut>0)))-1;

```

```

MaxElasticMoment = Moment{e} ((min(CurvatureCut(CurvatureCut>0)))-1);
for d = 2:length(CurvatureCut)
    if CurvatureCut(d) > 0
        Moment{e}(d) = 0;
        Curvature{e}(d) = 0;
    end
end
for d = StartD:NumberOfStrains
    if Moment{e}(d) < MaxElasticMoment
        Moment{e}(d) = 0;
        Curvature{e}(d) = 0;
    end
end
LastValue = length(Moment{e});
Moment{e}(LastValue) = 0;
Curvature{e}(LastValue) = 0;
Moment{e} = Moment{e}(Moment{e} ~= 0);
Curvature{e} = Curvature{e}(Curvature{e} ~= 0);

ElementMoment{e} = Moment{e};
ElementCurvature{e} = Curvature{e};
MaxMoment{e} = max(Moment{e}/1000000);
MaxCurvature{e} = max(Curvature{e});

end
end

% DELFECTION ANALYSIS

clear Moment

Stop0 = 0;
for w = 1:10000
    LateralLoad = PointLateralLoadFactor*w;

% DEFINE INTERVALS %
DeltaHeight = WallHeight/NumberOfElements;
HeightIncrement = WallHeight/NumberOfElements;

% % SELF WEIGHT FORCE %
NetArea = (GroutedLength*TotalThickness) + ((TotalWallLength-
GroutedLength)*FaceShell*2);
GrossArea = TotalThickness*TotalWallLength;
GroutingFactor = NetArea/GrossArea;
SelfWeight(1) =
MasonryDeadLoad*(TotalWallLength*WallHeight*TotalThickness)*GroutingFactor;
TotalSelfWeight =
MasonryDeadLoad*(TotalWallLength*WallHeight*TotalThickness)*GroutingFactor;

% PRELIMINARY CALCULATIONS
TopMoment = AxialLoad*Eccentricity;
TopReaction = ((LateralLoad*(1/2))-(TopMoment/WallHeight));
BottomReactionX = LateralLoad - TopReaction;

```

```

BottomReactionY = AxialLoad + TotalSelfWeight;

% FOUNDATION SUPPORT STIFFNESS
if SupportStiffness == 1
    FoundationStiffness = RotationalStiffness*1000000;
elseif SupportStiffness == 2
    FoundationStiffness = SpecifiedSupportStiffness*1000000;
else
    FoundationStiffness = 0;
end

% INITIAL CONDITIONS %
Deflection(1) = 0;
SpecificCurvature(1) = 0;
SlopeChange = 0.000001;

if Debugging == 0
if w == 1
    Slope(1) = -0.000001;
else
    Slope(1) = (-1)*InitialSlope(w-1);
end
elseif Debugging == 1
    Slope(1) = TestSlope;
end

% CREATE A CHECK TO DETERMINE IF THE CORRECT VALUE OF SLOPE WAS USED %
for s = 1:100000000
BottomMoment = abs(Slope(1))*FoundationStiffness;

% CREATE THE LOOP TO GO THROUGH EACH ELEMENT %
for e = 2:(NumberOfElements + 1)

% CREATE THE EQUATION FOR THE PRIMARY MOMENT %
if DeltaHeight < 0.5*WallHeight
PrimaryMoment(e) = ((BottomReactionX*(DeltaHeight)));
elseif DeltaHeight > 0.5*WallHeight
PrimaryMoment(e) = ((BottomReactionX*(DeltaHeight)) -
(LateralLoad*(DeltaHeight-(0.5*WallHeight))));
elseif DeltaHeight == 0.5*WallHeight
PrimaryMoment(e) = (LateralLoad*(0.5*WallHeight));
end

% DETERMINE THE TOTAL MOMENT AT THE ELEMENT %
if SecondOrderEffects == 1
Moment(e) = PrimaryMoment(e) +
(((BottomMoment/WallHeight)*DeltaHeight)-BottomMoment) +
AxialLoad*abs(Deflection(e-1)) + (TotalSelfWeight*(1-
(DeltaHeight/WallHeight))*abs(Deflection(e-1)));
else
Moment(e) = PrimaryMoment(e) +
(((BottomMoment/WallHeight)*DeltaHeight)-BottomMoment);
end

```



```

% DETERMINE MATERIAL FAILURE %
if Moment(e) > max(ElementMoment{e})
    Stop0 = 1;
    fprintf('\n')
    fprintf('Failure Occured: Material \n\n')
    break
end

% DETERMINE THE CURVATURE ASSOCIATED WITH THE TOTAL MOMENT %
Value1 = abs(ElementMoment{e} - abs(Moment(e)));
[Index Index] = min(Value1);
Closest = ElementMoment{e}(Index);
if abs(Moment(e)) < 0.00001
    SpecificCurvature(e) = 0;
    SpecificCurvature = max(ElementCurvature{e});
elseif Index == 1
    SpecificCurvature(e) = ElementCurvature{e}(Index);
elseif Index == 501
    SpecificCurvature(e) = ElementCurvature{e}(Index);
elseif Closest > abs(Moment(e))
    SpecificCurvature(e) = ElementCurvature{e}(Index) -
    ((ElementMoment{e}(Index)-abs(Moment(e)))/(ElementMoment{e}(Index)-
    ElementMoment{e}(Index-1))*ElementCurvature{e}(Index)-
    ElementCurvature{e}(Index-1));
elseif Closest < abs(Moment(e))
    SpecificCurvature(e) = ElementCurvature{e}(Index+1) -
    ((ElementMoment{e}(Index+1)-
    abs(Moment(e)))/(ElementMoment{e}(Index+1)-
    ElementMoment{e}(Index))*ElementCurvature{e}(Index+1)-
    ElementCurvature{e}(Index));
end

% ACCOUNT FOR NEGATIVE MOMENTS %
if Moment(e) < 0
    SpecificCurvature(e) = (-1.0)*SpecificCurvature(e);
end

% DETERMINE THE SLOPE AT THE NEXT ELEMENT %
Slope(e) = Slope(e-1) + SpecificCurvature(e)*HeightIncrement;

% CALCULATE THE DEFLECTION AT THE END OF THE ELEMENT %
if SpecificCurvature(e) <= 0
    Deflection(e) = Deflection(e-1) + (Slope(e-1)*HeightIncrement) -
    ((0.5)*(SpecificCurvature(e))*(HeightIncrement^2));
elseif SpecificCurvature(e) > 0
    Deflection(e) = Deflection(e-1) + (Slope(e-1)*HeightIncrement) +
    ((0.5)*(SpecificCurvature(e))*(HeightIncrement^2));
end

% MUST FIX THE DELTA HEIGHT TO ADJUST THE PRIMARY MOMENT FOR THE NEXT
ITERATION %
DeltaHeight = DeltaHeight + HeightIncrement;

end
if Stop0 == 1
    break

```

```

end

% CHECK THE SLOPE %
DeflectionCheck(s) = Deflection(NumberOfElements+1);

if DeflectionCheck(s) > Tolerance
    Slope(1) = Slope(1) - SlopeChange;
elseif DeflectionCheck(s) < (-1)*Tolerance
    Slope(1) = Slope(1) + SlopeChange;
elseif DeflectionCheck(s) <= Tolerance && DeflectionCheck(s) >= (-
1)*Tolerance
    CompleteDeflection = Deflection;
    break
end

% CATCH THE ERROR IN SLOPE CHANGE %
if s >= 10 && DeflectionCheck(s-4) < -0.1 && DeflectionCheck(s-3) >
0.1 && DeflectionCheck(s-2) < -0.1 && DeflectionCheck(s-1) > 0.1 &&
DeflectionCheck(s) < -0.1
    SlopeChange = 0.1*SlopeChange;
end

% RESET THE DELTA HEIGHT
DeltaHeight = WallHeight/NumberOfElements;
end

if Stop0 == 1
    break
end

% TRACK THE DEFLECTION AT A SPECIFIC LATERAL LOAD
MidspanDeflection(w) = abs(Deflection(((NumberOfElements+1)/2)));
InitialSlope(w) = abs(Slope(1));
TotalLateralLoad(w) = LateralLoad;

% CAPTURE THE DEFLECTION AND BENDING MOMENT PROFILE
MomentProfile{w} = Moment;
DeflectionProfile{w} = Deflection;

% CALCULATE THE FLEXURAL RIGIDITY

FlexuralRigidity(w) =
(Moment(((NumberOfElements+1)/2))/SpecificCurvature(((NumberOfElements
+1)/2)));
EffectiveStiffness(w) = FlexuralRigidity(w)/(1e12);

if w >= 5
Pcritical(w) = ((pi^2)*FlexuralRigidity(w))/(WallHeight^2);
if AxialLoad >= Pcritical(w)
    fprintf('Failure Occured: Buckling \n')
    fprintf('\n')
    break
end
end
end

```

```
TrackedLateralLoad(w,1) = TotalLateralLoad(w)/1000;
TrackedMidspanDeflection(w,1) = MidspanDeflection(w);
TrackedBaseSlope(w,1) = InitialSlope(w);

fprintf('          %6.2f          |', (TotalLateralLoad(w)/1000));
fprintf('          %7.2f          |', MidspanDeflection(w));
fprintf('          %5.2f \n', EffectiveStiffness(w));
end

fprintf('Analysis Complete!\n')
% plot(InitialSlope*(180/3.1415), (TotalLateralLoad/1000))
end
```